

โพธิ์โอมิกส์ของหัวกวาวเครือแดง *Butea superba* Roxb.



บทคัดย่อและแฟ้มข้อมูลฉบับเต็มของวิทยานิพนธ์ตั้งแต่ปีการศึกษา 2554 ที่ให้บริการในคลังปัญญาจุฬาฯ (CUIR)
เป็นแฟ้มข้อมูลของนิสิตเจ้าของวิทยานิพนธ์ ที่ส่งผ่านทางบัณฑิตวิทยาลัย

The abstract and full text of theses from the academic year 2011 in Chulalongkorn University Intellectual Repository (CUIR)
are the thesis authors' files submitted through the University Graduate School.

วิทยานิพนธ์นี้เป็นส่วนหนึ่งของการศึกษาตามหลักสูตรปริญญาวิทยาศาสตรดุษฎีบัณฑิต
สาขาวิชาเทคโนโลยีชีวภาพ
คณะวิทยาศาสตร์ จุฬาลงกรณ์มหาวิทยาลัย
ปีการศึกษา 2558
ลิขสิทธิ์ของจุฬาลงกรณ์มหาวิทยาลัย

PROTEOMICS OF RED KWAO KRUA *Butea superba* Roxb. TUBERS

Miss Chonchanok Leelahawong



A Dissertation Submitted in Partial Fulfillment of the Requirements
for the Degree of Doctor of Philosophy Program in Biotechnology

Faculty of Science

Chulalongkorn University

Academic Year 2015

Copyright of Chulalongkorn University

Thesis Title	PROTEOMICS OF RED KWAO KRUA <i>Butea superba</i> Roxb. TUBERS
By	Miss Chonchanok Leelahawong
Field of Study	Biotechnology
Thesis Advisor	Associate Professor Polkit Sangvanich, Ph.D.
Thesis Co-Advisor	Associate Professor Wichai Cherdshewasart, Ph.D. Chantragan Phiphobmongkol, Ph.D.

Accepted by the Faculty of Science, Chulalongkorn University in Partial
Fulfillment of the Requirements for the Doctoral Degree

.....Dean of the Faculty of Science
(Associate Professor Polkit Sangvanich, Ph.D.)

THESIS COMMITTEE

.....Chairman
(Associate Professor Vudhichai Parasuk, Ph.D.)

.....Thesis Advisor
(Associate Professor Polkit Sangvanich, Ph.D.)

.....Thesis Co-Advisor
(Associate Professor Wichai Cherdshewasart, Ph.D.)

.....Thesis Co-Advisor
(Chantragan Phiphobmongkol, Ph.D.)

.....Examiner
(Associate Professor Chanpen Chanchao, Ph.D.)

.....Examiner
(Associate Professor Nattaya Ngamrojanavanich, Ph.D.)

.....External Examiner
(Associate Professor Kanokporn Sompornpailin, Ph.D.)

ชนชนก ลีฬหาวงศ์ : โพรทีโอเมอิกส์ของหัวกวาวเครือแดง *Butea superba* Roxb. (PROTEOMICS OF RED KWAO KRUA *Butea superba* Roxb. TUBERS) อ.ที่ปริกษาวิทยานิพนธ์หลัก: รศ. ดร. พลกฤษณ์ แสงวณิช, อ.ที่ปริกษาวิทยานิพนธ์ร่วม: รศ. ดร. วิชัย เชิดชูวิชาสตร์, ดร. จันทรกานต์ พิภพมงคล, 350 หน้า.

กวาวเครือแดง (*Butea superba* Roxb.) เป็นพืชสมุนไพรไทยใช้ในการแพทย์ทางเลือกเพื่อการชะลอวัยและเสริมสมรรถภาพทางเพศของเพศชาย การเปลี่ยนแปลงของฤดูกาลโดยเฉพาะการเปลี่ยนแปลงของอุณหภูมิและปริมาณน้ำฝนมีอิทธิพลต่อพืช โดยชักนำให้เกิดการสังเคราะห์โปรตีนหลายชนิดที่ตอบสนองต่อความเครียดที่เกิดขึ้นในพืช นำไปสู่การเปลี่ยนแปลงชนิดและปริมาณของโปรตีนในวิถีเมแทบอลิซึมของเซลล์พืช ในการทดลองนี้ได้มีการประยุกต์วิธีการทางโพรทีโอเมอิกส์ โดยใช้เทคนิคทางเจลอิเล็กโตรโฟรีซิสแบบสองมิติ เพื่อแยกชนิดของโปรตีนร่วมกับการหาลำดับกรดอะมิโนของโปรตีนด้วยเทคนิคทางแมสสเปคโตรเมทรี เพื่อศึกษาความแปรผันขององค์ประกอบของโปรตีนในหัวและใบที่มีการเก็บตัวอย่างในฤดูฝน ฤดูร้อน และฤดูหนาว จากผลของการแยกโปรตีน แสดงให้เห็นว่า จุดโปรตีนที่ระบุชนิดโปรตีนได้ในหัวและใบ มีจำนวน 224 จุด และ 112 จุด ตามลำดับ สามารถจำแนกกลุ่มโปรตีนตามหน้าที่ได้ทั้งหมด 12 กลุ่มเท่ากัน จากโปรตีนทั้งหมดที่จำแนกได้จำนวน 45 โปรตีน ในหัว และ 12 โปรตีนในใบ พบว่า มีความแตกต่างของระดับความอุดมสัมพันธ์ที่มีความเกี่ยวข้องกับความหลายหลายของวิถีเมแทบอลิซึมในฤดูกาลที่ต่างกัน ผลจากการวิเคราะห์โดยอาศัยความเข้มของจุดโปรตีนที่ปรากฏในภาพ ชี้ให้เห็นว่าความเครียดของพืชเนื่องมาจากอุณหภูมิที่เพิ่มสูงขึ้นร่วมกับการที่พืชขาดน้ำในระหว่างฤดูร้อน และความเครียดของพืชเนื่องมาจากอุณหภูมิที่ลดต่ำลงร่วมกับการที่พืชขาดน้ำในระหว่างฤดูหนาว อาจจะเป็นปัจจัยที่ชักนำให้เกิดการเปลี่ยนแปลงในระดับของความอุดมสัมพันธ์ของโปรตีน เป็นสาเหตุทำให้เกิดการเปลี่ยนแปลงในสถานภาพของสรีรวิทยาภายในหัวและใบของพืช รวมถึงการเปลี่ยนแปลงของลักษณะทางฟิโนไทป์ที่เกี่ยวข้องกับการดำรงอยู่ของพืช ผลการทดลองที่ได้อาจมีส่วนช่วยสร้างความเข้าใจเกี่ยวกับพันธุศาสตร์พื้นฐานของโปรตีนชนิดต่างๆที่อยู่ในหัวและใบ นอกจากนี้ความแตกต่างอย่างเป็นเอกลักษณ์ของโปรตีนบางชนิดที่พบอาจนำไปใช้ประโยชน์ในการพัฒนาเครื่องหมายโปรตีนที่เป็นดัชนีบ่งชี้การตอบสนองต่อปัจจัยทางกายภาพที่เกิดขึ้นในระหว่างการเปลี่ยนแปลงของฤดูกาลในพืชชนิดอื่นๆ และอาจนำไปใช้เป็นตัวช่วยในการกำหนดช่วงเวลาในการเก็บเกี่ยวหัวและใบกวาวเครือแดง เพื่อให้ได้วัตถุดิบที่เหมาะสมที่สุดสำหรับนำไปในการผลิตผลิตภัณฑ์

สาขาวิชา เทคโนโลยีชีวภาพ

ปีการศึกษา 2558

ลายมือชื่อนิสิต

ลายมือชื่อ อ.ที่ปริกษาหลัก

ลายมือชื่อ อ.ที่ปริกษาร่วม

ลายมือชื่อ อ.ที่ปริกษาร่วม

5373900523 : MAJOR BIOTECHNOLOGY

KEYWORDS: BUTEA SUPERBA, PROTEOMICS, TWO-DIMENSIONAL GEL ELECTROPHORESIS, MASS SPECTROMETRY, TEMPERATURE STRESS, WATER STRESS

CHONCHANOK LEELAHAWONG: PROTEOMICS OF RED KWAO KRUA *Butea superba* Roxb. TUBERS. ADVISOR: ASSOC. PROF. POLKIT SANGVANICH, Ph.D., CO-ADVISOR: ASSOC. PROF. WICHAJ CHERDSHEWASART, Ph.D., CHANTRAGAN PHIPHOBMONGKOL, Ph.D., 350 pp.

Red Kwao Krua (*Butea superba* Roxb.) is a Thai traditional medicinal plants used in alternative medicines for anti-aging and increased sex vigor in male. Seasonal changes especially changes in temperature and amount of rainfall are major influencing factors which results in induction of protein biosynthesis in response to plant stresses, leading to changes in protein relative abundance in metabolic pathways of plant cells. Proteomics was applied in this study using the two-dimensional polyacrylamide gel electrophoresis for protein identification coupled with mass spectrometry, to study the variations in proteome compositions of *B. superba* tubers and leaves collected during rainy season, winter and summer. The protein separation results demonstrated the identified 224 protein spots in tubers and 112 protein spots in leaves which were classified to be the same amount of 12 functional protein groups. The 45 and 12 identified proteins in tubers and leaves were involved in multiple metabolic pathways in different seasons. The analysis of the protein spot intensities indicated that the differential amount of expressed proteins might be induced from the increased temperature and water shortage stresses occurred during summer and the decreased temperature and water shortage stresses occurred during winter might induce the differential abundance levels. It might result in changes in the physiological status within plant tubers and leaves, including phenotypic changes related to plant survival. The results might help the molecular basis understanding in tuber and leaf proteomes. In addition, the distinct of some proteins could potentially be used as protein markers to indicate the responses to the physical factors occurred during seasonal changes in other plants. It might also applied for setting of harvest of *B. superba* tubers and leaves for manufacturing of products.

Field of Study: Biotechnology

Academic Year: 2015

Student's Signature

Advisor's Signature

Co-Advisor's Signature

Co-Advisor's Signature

ACKNOWLEDGEMENTS

I would like to express my deeply sincere gratitude to my advisor, Associate Professor Dr. Polkit Sangvanich, and my co-advisors, Associate Professor Dr. Wichai Cherdshewasart and Dr. Chantragan Phiphobmongkol for their professional guidance especially in laboratory works.

I would like to express my special thanks to Miss Daranee Chokchaichamnankit, Chulabhorn Research Institute for kindly training, technical assistance and specific guidance in the main procedures in the laboratory works.

Thanks to the staffs of the Laboratory of Biochemistry for friendly welcome and comments.

Thanks to Chulabhorn Research Institute for the laboratory facilities. Thanks to Program in Biotechnology, the Department of Biology and the Department of Chemistry, Faculty of Science, Chulalongkorn University for academic support.

Thanks to the research grants from the National Research University, the Science for Local Project under the Chulalongkorn University Centenary Academic Development Plan (2008-2012) and the 90th Anniversary of Chulalongkorn University fund (Ratchadaphiseksomphot Endowment Fund) (1/2014) for financial support.

CONTENTS

	Page
THAI ABSTRACT	iv
ENGLISH ABSTRACT	v
ACKNOWLEDGEMENTS	vi
CONTENTS.....	vii
LIST OF TABLES	1
LIST OF FIGURES.....	3
LIST OF ABBREVIATIONS	9
CHAPTER I	16
INTRODUCTION	16
CHAPTER II.....	20
LITERATURE REVIEWS	20
2.1 <i>Butea superba</i> Roxb.....	20
2.1.1 General background.....	20
2.2.2 Botanical characteristics.....	20
2.1.3 Chemical constituents and traditional uses.....	22
2.2 Protein preparation.....	26
2.3 Proteomics	26
2.4 Literature reviews of plant proteomics	31
2.4.1. Proteomics in tuberous plants.....	31
2.4.2. Proteomics in leaves.....	36
2.5 ROS Scavenging mechanisms	40
2.6 Temperature stress.....	42

	Page
2.7 Water stress	44
CHAPTER III.....	46
EXPERIMENTAL.....	46
3.1 Plant materials and tuber and leaf collections.....	46
3.2 Protein extraction and quantification.....	46
3.3 Two-dimensional Polyacrylamide Gel electrophoresis.....	47
3.4 Protein visualization and image analysis	48
3.5 In-gel digestion with trypsin.....	49
3.6 Protein identification	49
CHAPTER IV.....	51
RESULTS AND DISCUSSION.....	51
4.1 Sample collection.....	51
4.2 Sample extraction and separation of proteins by 2-DE technique.....	54
4.2.1 Proteomic patterns of tubers	54
4.2.2 Proteomic patterns of leaves	79
4.3 Protein identification and functional classification	94
4.3.1 Protein identification and functional classification in tubers.....	132
4.3.2 Protein identification and functional classification in leaves.....	135
4.4 Proteins with differential levels in different seasons	138
4.4.1 Proteins with differential levels in different seasons in tubers.....	138
4.4.2 Proteins with differential levels in different seasons in leaves.....	169
4.5 Proteins abundance in response to temperature stress and water stress ..	182

	Page
4.5.1 Proteins abundance in response to temperature stress and water stress in tubers.....	182
4.5.2 Proteins abundance in response to temperature stress and water stress in leaves.....	187
CHAPTER V.....	190
CONCLUSION.....	190
REFERENCES.....	192
APPENDIX A.....	218
APPENDIX B.....	225
VITA.....	350



LIST OF TABLES

Table 1 The summary of chemical constituents of <i>B. superba</i>	23
Table 2 Protein spot appearance isolated from <i>B. superba</i> tubers originated from Lampung, Saraburi and Chachengsao in 2-DE gels	64
Table 3 Protein spot appearance isolated from <i>B. superba</i> leaves originated from Lampung, Saraburi and Chachengsao in 2-DE gels	86
Table 4 Identified proteins of <i>B.superba</i> tubers originated from Lampung, Saraburi and Chachengsao were identified by two-dimensional Polyacrylamide Gel electrophoresis (2D-PAGE) coupled with LC/MS/MS.....	95
Table 5 Identified proteins of <i>B.superba</i> leaves originated from Lampung, Saraburi and Chachengsao were identified by two-dimensional Polyacrylamide Gel electrophoresis (2D-PAGE) coupled with LC/MS/MS.....	115
Table 6 A number of protein spots of <i>B. superba</i> tubers were identified using 2-DE coupled with LC/MS/MS	132
Table 7 A number of protein spots of <i>B. superba</i> leaves were identified using 2-DE gels coupled with LC/MS/MS.....	135
Table 8 Identified proteins of tubers were analyzed changes and differences using the Image Master 2-DE program.....	160

Table 9 Identified proteins of leaves were analyzed for changes and differences using the Image Master 2-DE program	178
Table 10 Solution for protein extraction	219
Table 11 Solution for 2D-PAGE.....	220
Table 12 Coomassies gel stain and destain solution.....	222
Table 13 Digestion solutions	223
Table 14 Climatological data for the period 2010-2010.....	226
Table 15 Climatological data for the period 2011-2011	227
Table 16 Identified protein and peptide sequences of <i>B.suberba</i> tubers originated from Lampung, Saraburi and Chachoengsao were identified by two-dimensional Polyacrylamide Gel electrophoresis (2D-PAGE) coupled with LC/MS/MS	228
Table 17 Protein sequences of leaves were identified by two-dimensional Polyacrylamide Gel electrophoresis (2D-PAGE) coupled with LC/MS/MS	303
Table 18 Changes and differences in tubers by Image Master 2-DE program.....	346
Table 19 Changes and differences in leaves by Image Master 2-DE program.....	349

LIST OF FIGURES

Figure 1 The botanical characteristics: tuberous roots (a), leaves (b), flowers (c) and pods (d) of <i>B. superba</i>	21
Figure 2 The kinds of proteomics and their applications to Graves and Haystead (2002).	27
Figure 3 Workflow of proteomic experiments	30
Figure 4 Isoelectric focusing on an immobilized pH gradients (IPG) focused a single protein (a) and a mixture of proteins (b).	31
Figure 5 Pathways related to carbon assimilation, protein biogenesis and storage in potato and source-sink transport during tuber development of potato.....	34
Figure 6 Generation of different ROS by energy transfer or sequential univalent reduction of ground state triplet oxygen.....	41
Figure 7 The crucial modes of enzymatic ROS scavenging.	42
Figure 8 A model for temperature sensing.....	43
Figure 9 Photosynthesis under drought stress.....	45

Figure 10 Climate distribution during sample collection in Banpong district, Ratchaburi province, Thailand from August, 2010 to April, 2011.53

Figure 11 Representative 2-DE profiles of the 150 µg protein isolated from *B. superba* tubers which were originated from Lampang (1) and harvested from Banpong district, Ratchaburi province in rainy season (TR) at pH 3-10 using non-linear IEF strips.....55

Figure 12 Representative 2-DE profiles of the 150 µg protein isolated from *B. superba* tubers which were originated from Lampang (1) and harvested from Banpong district, Ratchaburi province in winter (TW) at pH 3-10 using non-linear IEF strips.....56

Figure 13 Representative 2-DE profiles of the 150 µg protein isolated from *B. superba* tubers which were originated from Lampang (1) and harvested from Banpong district, Ratchaburi province in summer (TS) at pH 3-10 using non-linear IEF strips.57

Figure 14 Representative 2-DE profiles of the 150 µg protein isolated from *B. superba* tubers which were originated from Saraburi (2) and harvested from Banpong district, Ratchaburi province in rainy season (TR) at pH 3-10 using non-linear IEF strips.....58

Figure 15 Representative 2-DE profiles of the 150 µg protein isolated from *B. superba* tubers which were originated from Saraburi (2) and harvested from Banpong district, Ratchaburi province in winter (TW) at pH 3-10 using non-linear IEF strips.....59

Figure 16 Representative 2-DE profiles of the 150 μg protein isolated from *B. superba* tubers which were originated from Saraburi (2) and harvested from Banpong district, Ratchaburi province in summer (TS) at pH 3-10 using non-linear IEF strips.....60

Figure 17 Representative 2-DE profiles of the 150 μg protein isolated from *B. superba* tubers which were originated from Chachoengsao (3) and harvested from Banpong district, Ratchaburi province in rainy season (TR) at pH 3-10 using non-linear IEF strips.....61

Figure 18 Representative 2-DE profiles of the 150 μg protein isolated from *B. superba* tubers which were originated from Chachoengsao (3) and harvested from Banpong district, Ratchaburi province in winter (TW) at pH 3-10 using non-linear IEF strips.....62

Figure 19 Representative 2-DE profiles of the 150 μg protein isolated from *B. superba* tubers which were originated from Chachoengsao (3) and harvested from Banpong district, Ratchaburi province in summer (TS) at pH 3-10 using non-linear IEF strips.....63

Figure 20 Representative 2-DE profiles of the 150 μg protein isolated from *B. superba* leaves originated from Lampang (1) and collected from Banpong district, Ratchaburi province in rainy season (LR) at pH 3-10 using non-linear IEF strips.....80

Figure 21 Representative 2-DE profiles of the 150 μg protein isolated from *B. superba* leaves originated from Lampang (1) and collected from Banpong district, Ratchaburi province in winter (LW) at pH 3-10 using non-linear IEF strips.....81

Figure 22 Representative 2-DE profiles of the 150 μg protein isolated from *B. superba* leaves originated from Lampang (1) and collected from Banpong district, Ratchaburi province in summer (LS) at pH 3-10 using non-linear IEF strips.....82

Figure 23 Representative 2-DE profiles of the 150 μg protein isolated from *B. superba* leaves originated from Saraburi (2) and collected from Banpong district, Ratchaburi province in rainy season (LR) at pH 3-10 using non-linear IEF strips.....83

Figure 24 Representative 2-DE profiles of the 150 μg protein isolated from *B. superba* leaves originated from Saraburi (2) and collected from Banpong district, Ratchaburi province in summer (LS) at pH 3-10 using non-linear IEF strips.....84

Figure 25 Representative 2-DE profiles of the 150 μg protein isolated from *B. superba* leaves originated from Chachoengsao (3) and collected from Banpong district, Ratchaburi province in rainy season (LR) at pH 3-10 using non-linear IEF strips.....85

Figure 26 Functional distribution of 224 protein spots identified in *B. superba* tubers.....133

Figure 27 Functional classification of 112 protein spots identified in *B. superba* leaves.....136

Figure 28 Gel spots of 8 proteins in allergy, photosynthesis, cellular structure and defense with differentially abundances during summer-or rainy season- as compared with winter-harvested samples.....164

Figure 29 Gel spots of 9 proteins in ROS scavenging and detoxifying and stress with differentially abundances during summer-or rainy season- as compared with winter-harvested samples.....165

Figure 30 Gel spots of 15 proteins in carbohydrate and energy metabolism with differential abundances during summer-or rainy season- as compared with winter-harvested samples.....166

Figure 31 Gel spots of 7 proteins in amino-acid biosynthesis and signal transduction and homeostasis with differential abundances during summer-or rainy season- as compared with winter-harvested samples.....167

Figure 32 Gel spots of 6 proteins in protein biosynthesis and protein destination and storage with differential abundances during summer-or rainy season- as compared with winter-harvested samples.....168

Figure 33 Gel spots of 6 proteins in carbohydrate and energy metabolism and photosynthesis with differential abundances in summer- or rainy season-as compared with winter-harvested samples.....180

Figure 34 Gel spots of 6 proteins in defense and stress, ROS scavenging and detoxifying, RNA metabolism, protein destination and storage with differential abundances with differential abundances in summer- or rainy season-as compared with winter-harvested samples.181

Figure 35 A model of proteins abundance in response to temperature stress during summer with analyzing from fold change of the terms in the ratio summer/ winter of spot intensities in summer- as compared with winter-harvested samples.....184

Figure 36 A model of proteins abundance in response to water stress during winter with analyzing from fold change of the terms in the ratio summer/ winter of spot intensities in summer- as compared with winter-harvested samples.186

Figure 37 A model of proteins abundance in response to temperature stress during summer and water stress during winter with analyzing from fold change of the terms in the ratio summer/ winter of spot intensities in summer- as compared with winter-harvested samples.....188



LIST OF ABBREVIATIONS

2-DE/2D-PAGE	Two-dimensional electrophoresis/ two-dimensional polyacrylamide gel electrophoresis
LC	Liquid chromatography
ESI	Electrospray ionization
ESI-Q/TOF	Electrospray ionization Quadrupole-time-of-flight
LC-ESI- MS/MS	Liquid chromatography/ Tandem mass spectrometry
TQ	The triple Quadrupole
MALDI	Matrix-assisted laser desorption/ionization
MS	Mass spectrometry
AChE	Acetylcholinesterase
ER	Estrogen receptor
LH	Luteinizing hormone
IPG	Immobilized pH gradients
pI	Isoelectric point
IEF	Isoelectric focusing
Arg	Arginine
TCA	Trichloro acetic acid
ACN	Acetonitrile
APS	Ammonium persulfate

Bis	<i>N,N'</i> -methylenebisacrylamide
CHAPS	3-(3-cholamidopropyl)dimethylammonio-1-propane sulfonate
TEMED	<i>N,N,N',N'</i> -tetramethylethylenediamine
TFA	Trifluoroacetic acid
Tris	Tris (hydroxymethyl)-aminoethane
IAA	Iodoacetamide
SDS	Sodium dodecyl sulfate
DTT	Dithiothreitol
EDTA	Ethylenediaminetetraacetic acid
MeOH	Methanol
KCl	Potassium Chloride
API	Triseposphate isomerase
GAPDH	Glyceraldehyde-3-phosphate dehydrogenase
G3P	glyceraldehyde 3-P
UDP-G	UDP-Glc
ADP-G	ADP-Glc
G-1-P	Glc 1 phosphate
G-6-P	Glc 6 phosphate
F-6-P	Fru 6 phosphate
F-1,6-bis P	Fru 1,6 bis phosphate
1,3-bis PGA	1,3 bis phosphoglyceric acid

3-PGA	3 phosphoglyceric acid
2-PGA	2 phosphoglyceric acid
PEP	Phosphoenolpyruvate
M-6-P	Mannose 6 phosphate
R-KGA	R-keto glutaric acid
MA	Malic acid
OAA	Oxalo acetic acid
UGPase	UDP-Glc pyrophosphorylase
AGPase	AGP-Glc pyrophosphorylase
PFK	Pyrophosphate-dependent phosphofructokinase
FBA	Fru bisphosphate aldolase
PGK	Phosphoglycerate kinase
MDH	Malate dehydrogenase
NdhF	NADP dehydrogenase F subunit
M6PR	Mannose 6 phosphate reductase
ALDH	Aldehyde dehydrogenase
NDK	Nucleoside diphosphate kinase
LEA	Late embryogenesis abundant;
KTPI	Kunitz type protease inhibitor
API	Aspartate protease inhibitor
CPI	Cystein protease inhibitor

SPI	Serine protease inhibitor
DHAP	Dihydroxyacetone phosphate
ADH	Alcohol dehydrogenase
GSH	Glutathione
GST	Glutathione S-transferase
DHAR	Dehydroascorbate reductase
MDAR	Monodehydroascorbate reductase
MDHA	Monodehydroascorbate
CAT	Catalase
GR	Glutathione reductase
GPX	Glutathione peroxidase
GSSG	Oxidized glutathione
PEPCase	Phosphoenolpyruvate carboxylase
NADP-ME	NADP-malic enzyme
FBPase	Fructose-1,6-bisphosphatase
PPDK	Pyruvate orthophosphate dikinase
EF-Tu	Elongation factor
HSPs	Heat shock proteins
sHSPs	Small heat shock proteins
ADH-1	Alcohol dehydrogenase 1
SOD	Superoxide dismutase

Cu/Zn-SOD	The copper/zinc- Superoxide dismutase
AC101	Actin-101
IFR2	Isoflavone reductase homolog 2
TUBA3	α -tubulin-3 chain
MS	Methionine synthase
APX	Ascorbate peroxidase
GR	Glutathione reductase
RuBisCO	Ribulose-1,5-biphosphate carboxylase/oxygenase
NADPH	Nicotinamide adenine dinucleotide phosphate
ADP	Adenosine diphosphate
ATP	Adenosine triphosphate
acetyl-CoA	Acetylacetyl coenzyme A
V-ATPase	V-type proton ATPase
TCA cycle	The tricarboxylic acid (TCA) cycle
ROS	Reactive oxygen Species
HSP70	heat shock protein 70
cm	centimeters
Da	Dalton
kDa	kilo Dalton
Vh	volthours
g	gram

mg	milligram
min	minute
ml	milliliter
mM	millimolar
h	hour
µg	microgram
µl	microliter
l	liter
kg	kilogram
v/v	volume by volume
w/v	weight by volume
°C	degree Celsius
MW	Molecular weight
m/z	mass per charge ratio
NCBI	National Center of Biotchnology Information
NL	Non-Linear
No	Number
OD	Optical density
C	carbamidomethyl
M	Oxidation
MOWSE	Molecular weight Search Score

p -values

Calculated probability



CHAPTER I

INTRODUCTION

Butea superba Roxb. is a native Thai herbal plant with common name of “Red Kwao Krua”. A large twining wood belongs to the leguminosae subfamily, family Fabaceae. The plant is commonly found in Thai deciduous forest of the Northern, Eastern, North-eastern and Central regions. The tuberous roots and stems are used in the Thai traditional therapies as anti-aging and alternative medicines for the purposes of rejuvenation, promotion of sexual vigor and treatment of erectile dysfunction in mature males (Cherdshevasart et al., 2004). In tuberous roots, the chemical constituents, flavonoid (3,7,3'-Trihydroxy-4'-methoxyflavone) and flavonoid glycosides (3,3'-dihydroxy-4'-methoxyflavone-7-O- β -D-glucopyranoside), were found to harbour cAMP phosphodiesterase inhibitory activity (Roengsumran et al., 2000), whereas formononetin and prunetin showed moderate cytotoxic activity on human oral cavity carcinoma cells (KB) and breast cancer cells (BC) (Ngamrojanavanich et al., 2007). In addition, the plant crude extracts were also shown to act as antimicrobial agents (Yadava and Reddy, 1998), antioxidant (Chukeatirote and Saisavoey 2009), acetylcholinesterase (AChE) inhibitor for protection of Alzheimer's disease (Ingkaninan et al., 2003) and anti-proliferation agents of human breast adenocarcinoma cells (MCF-

7) (Cherdshewasart et al., 2004). The male potency benefits of the plant tubers were proven in the Thai human clinical trial in which the consumption of the tuberous powder could be used as the alternative treatment for erectile dysfunction (Cherdshewasart and Nimsakul, 2003). The mechanism of action of the tuberous chemical constituents might need endogenous testosterone to work synergistically to stimulate the accessory male sex organ of intact animals (Malaivijitnond et al., 2010). The tuberous powder initiates androgen disruption within the male body (Cherdshewasart et al., 2008). The tests in male rats confirmed the initiation of vasodilation and subsequently, enhance penile erection (Tocharus et al., 2006).

In plants, these beneficial chemical constituents are biosynthesized with the aid of various enzymes in multiple biosynthetic pathways. Seasonal changes might influence temperature and amount of rainfall in the plant environment (Porter and Semenov, 2005) and thus initiate stresses in plants and affect levels of certain proteins, leading to changes in protein relative abundance in the complex cellular plant metabolic pathways.

Plant proteins are major components in biological systems which are the main structural or mechanical role and the functional molecules to involve in signal transductions, biochemical reactions, metabolic pathways, developmental/ differential stages, abiotic and biotic stress defenses and plant-pathogen interactions (Rossignol et

al., 2006). For example, plants such as roots of sugar beet, wheat, wild watermelon, and sugarcane were responded to drought stress by increasing the levels of heat shock proteins as molecular chaperones (Ghosh and Xu, 2014). In potato (*Solanum tuberosum* L.), differential abundances of 219 proteins during its tuber development were exhibited (Agrawal et al., 2008). Multiple signaling pathways and environmental factors were related to tuber development, physiology, dormancy and signal transductions were found (Agrawal et al., 2008; Lehesranta et al., 2006).

In addition, leaves are specialized organ involved a primary role in photosynthesis (Komatsu and Hossain, 2013). The leaves produce specific tuberization stimuli and transmit into the underground part to control the tuberization process during photosynthesis. The metabolic stresses in leaf lead to change in profile of proteins related to physiological processes in storage root initiation and growth (Mitprasat et al., 2011). While these stimuli range from proteins to small-molecule hormones, most were found to be proteins and were related to energy production, metabolism and photosynthesis as well as stress response, detoxification and defense. Major identified proteins were related to energy production, metabolism and photosynthesis as well as stress response, detoxification and defense (Donnelly et al., 2005).

Proteomics is a high-throughput technology used for identifying and measuring the levels of multiple proteins. The study applied two-dimensional polyacrylamide gel electrophoresis coupled with a nanoflow liquid chromatography coupled to electrospray ionization quadrupole-time-of-flight tandem mass spectrometry to determine the proteomic patterns of *B. superba* tubers and leaves collected in varied seasons. The outcome should allow better understanding of the plant proteomes, especially those relating to growth, development, tuberization, biosynthesis, allergy, stress tolerance, antioxidant defense system and signaling pathway in *B. superba* tubers and leaves.

The objectives of this study are:

1. To determine the proteomic patterns of *B. superba* tubers and leaves
2. To analyse *B. superba* tubers and leaves differential protein relative abundance under the influence of seasons and varieties

CHAPTER II

LITERATURE REVIEWS

2.1 *Butea superba* Roxb.

2.1.1 General background

One of the well-known Thai plants in sub-family Leguminosae, family Fabaceae is *Butea superba* Roxb., which is commonly called “red kwao krua”. The plant is widely found in the Central, Northern, North-Eastern, and Eastern regions of Thailand. Its tuberous roots and stems have been traditionally used as alternative medicine with anti-aging properties for rejuvenation, stimulation of male sexual strength and also for treatment of erectile dysfunction (Suntara, 1931). The plant potential for treatment of erectile dysfunction was proofed in the clinical trial in Thai males (Cherdshewasart and Nimsakul, 2003).

2.2.2 Botanical characteristics

B. superba is a strong twinning plant. The tuberous roots are budded underground. The mature roots are elongate tuberous shape. On cutting, the tuberous

roots release the red sap. One branch has three leaves, smooth ventral and nap dorsal leaves, acuminate leaflet and five to seven in each veinlet. Flowers are yellowish orange colors which are perfect flower and indeterminate inflorescence with blooming period during late winter to early summer. Pods are 10 to 15 centimeters long to cover sprouting short hair and inside only one seed (Loontaisong, 2005). The pictures of tuberous roots, leaves, flowers and pods are shown in Figure 1.

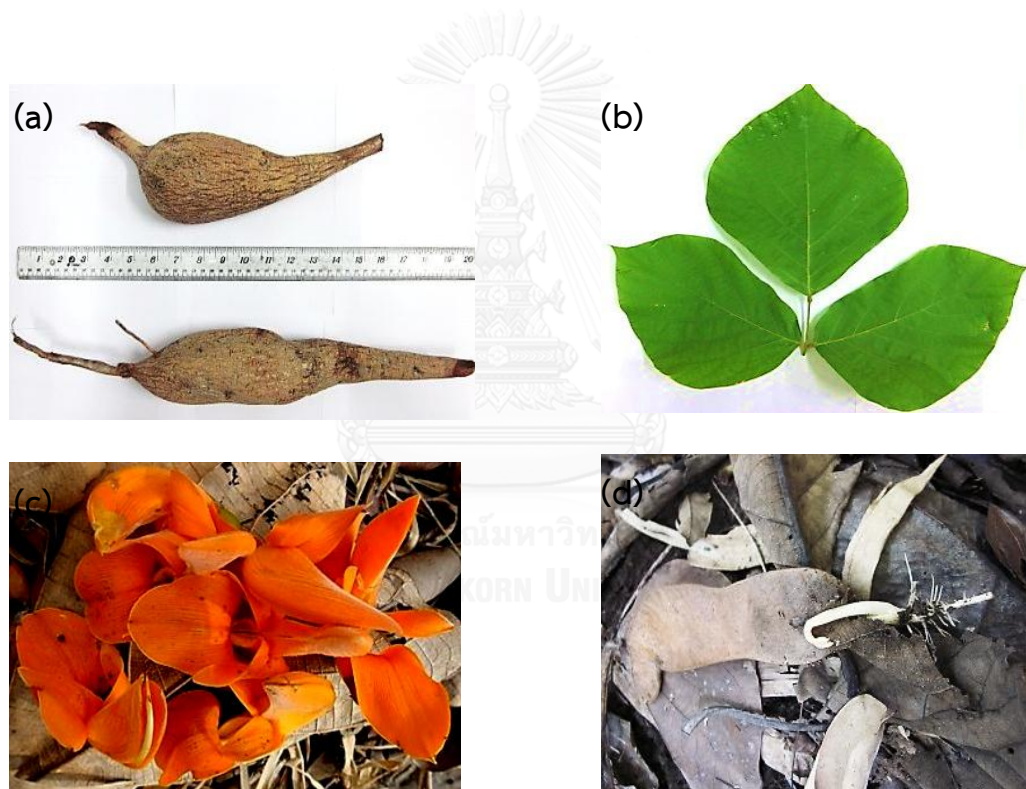


Figure 1 The botanical characteristics: tuberous roots (a), leaves (b), flowers (c) and pods (d) of *B. superba*.

2.1.3 Chemical constituents and traditional uses

B. superba tubers harbor six categories of chemical constituents namely; carboxylic acid, steroid, steroid glycoside, flavonoid, flavonoid glycoside and coumestain, isoflavones and others. The summary of chemical constituents are shown in Table 1. Flavonoid (3,7,3'-Trihydroxy-4'-methoxyflavone) and flavonoid glycosides (3,3'-dihydroxy-4'-methoxyflavone-7-O- β -D-glucopyranoside) isolated from tuberous roots had an inhibiting effect upon cAMP phosphodiesterase (Roengsumran et al., 2000). The tuberous formononetin and prunetin exhibited moderate cytotoxicity on human oral cavity carcinoma cells (KB) and breast cancer cells (BC) (Ngamrojanavanich et al., 2007), especially that formononetin exhibited estrogenic activity via ER α and ER β and sympathy between progesterone receptor and androgen receptor. Medicarpin exhibited cytotoxic activity on tumor cells. 7, 4'-dimethoxyisoflavone exhibited an effective cancer-chemoprevention in mouse mammary organ culture (Cherdshewasart et al., 2008). The plant crude extracts were shown to exhibit antioxidant activities (Chukeatirote and Saisavoey 2009), antimicrobial agents (Yadava and Reddy, 1998), acetylcholinesterase (AChE) inhibitory properties for preventing of Alzheimer's disease (Ingkaninan et al., 2003), and anti-proliferation activity on the growth of human breast adenocarcinoma cells (MCF-7) (Cherdshewasart et al., 2004). The male potency benefits of the plant tubers were proven in the Thai clinical trial in which the consumption of the tuberous powder could be the alternative treatment for erectile

dysfunction (Cherdshewasart and Nimsakul, 2003). The mechanism of action of the tuberous chemical constituents might need endogenous testosterone to work synergistically to stimulate the accessory male sex organ of intact animals (Malaivijitnond et al., 2010). The plant powder had an androgenic effect in the reproductive organs and anti-estrogenic activity on luteinizing hormone (LH) in ovariectomized rats but it exhibited the other mechanism of the initiation of androgen disruption within the male body by decreasing in blood testosterone level (Cherdshewasart et al., 2008). The tests in male rats confirmed the initiation of vasodilation and subsequently enhance penile erection (Tocharus et al., 2006).

Table 1 The summary of chemical constituents of *B. superba*

Categories	Chemical constituents	References
Carboxylic acid	docosanoic acid (C ₂₂ H ₄₄ O ₂)	Ruksilp (1995)
	tricosanoic acid (C ₂₃ H ₄₆ O ₂)	
	tetracosanoic acid (C ₂₄ H ₄₈ O ₂)	
	pentacosanoic acid (C ₂₅ H ₅₀ O ₂)	
	hexacosanoic acid (C ₂₆ H ₅₂ O ₂)	
		3-hexacosanoloxy-propane-1,2-diol

Table 1 (Continued)

Categories	Chemical constituents	References
Phytosterols and sterol glycosides	campesterol β -sitosterol stigmasterol β -sitosteryl-3-O- β -D-glucopyranoside stigmasteryl-3-O- β -D-glucopyranoside	Ngamrojanavanich et al. (2007)
Flavonoids, flavonoid glycosides and coumestans	7-hydroxy-6,4'-dimethoxyisoflavone 3,5,7,3',4'-pentahydroxy-8-methoxy flavonol-3-O- β -D-xylopyranosyl- α -L-rhamnopyranoside 3,7-dihydroxy-8-methoxyflavone-7-O- α -L-rhamnopyranoside 3,7,3'-Trihydroxy-4'-methoxyflavone 3,3'-dihydroxy-4'-methoxyflavone-7-O- β -D-glucopyranoside coumestrol	Yadava and Reddy (1998) Roengsumran et al. (2000) Ma et al. (2005)

Table 1 (Continued)

Categories	Chemical constituents	References
Isoflavones	medicarpin (3-hydroxy-9-methoxypterocarpan) formononetin (7-hydroxy-4'-methoxy-isoflavone) daidzein genistein biochanin A (5,7-dihydroxy-4'-methoxyisoflavone) prunetin (5,4'-dihydroxy-7-methoxy-isoflavone) butesuperins A butesuperins B	Ma et al. (2005); Ngamrojanavanich et al. (2007) Ma et al. (2005) Ngamrojanavanich et al. (2007) Ma et al. (2005)
Others	calycosin pseubaptigenin	Ma et al. (2005)

* Modified from Kaewmuangmoon (2006) and Sangkapong (2005).

2.2 Protein preparation

Phenol extraction is a powerful procedure for protein preparation. Sucrose is added to the buffer to inverse phase. The buffer forms consist of the aqueous lower phase containing carbohydrates, nucleic acids and insoluble cell debris and the upper phenol containing cytosolic and membrane proteins, lipids and pigments were high pH to inhibit proteases, followed by KCl to extract proteins, EDTA to restrain polyphenol oxidase and metalloproteases, DTT to prevent the oxidation of plant (poly)-phenols (quinines) and protease inhibitor to irreversibly inactivated proteases (Carpentier et al., 2005).

2.3 Proteomics

Proteomics is the multidimensional protein identification technology for measuring comparative levels of proteins. The technique is the completely protein complement of the whole genomes. The proteins are significant components of cells in virtually biological systems which are the major structural or mechanical role and the functional molecules to involve in signal transductions, biochemical reactions, metabolic pathways, developmental/ differential stages, abiotic and biotic stress defenses and plant-pathogen interactions (Graves and Haystead, 2002). The proteome is dynamic response to access in cells both intracellular and extracellular signal

molecules to change the levels and activities of its proteins and environmental condition. The functional characterization of individual proteins in the pathways, networks and complexes are based on its regulation, stability, structure, localization, modification and interactions. The proteomics is a range of technological approaches to directly apply on study of differential protein expressions, subcellular localization, biochemical activities and regulation (Twyman, 2004). In previous times, In previous times, the kinds of proteomics and their applications to biology were categorized under the heading of proteomics (Graves and Haystead, 2002) as shown in Figure 2

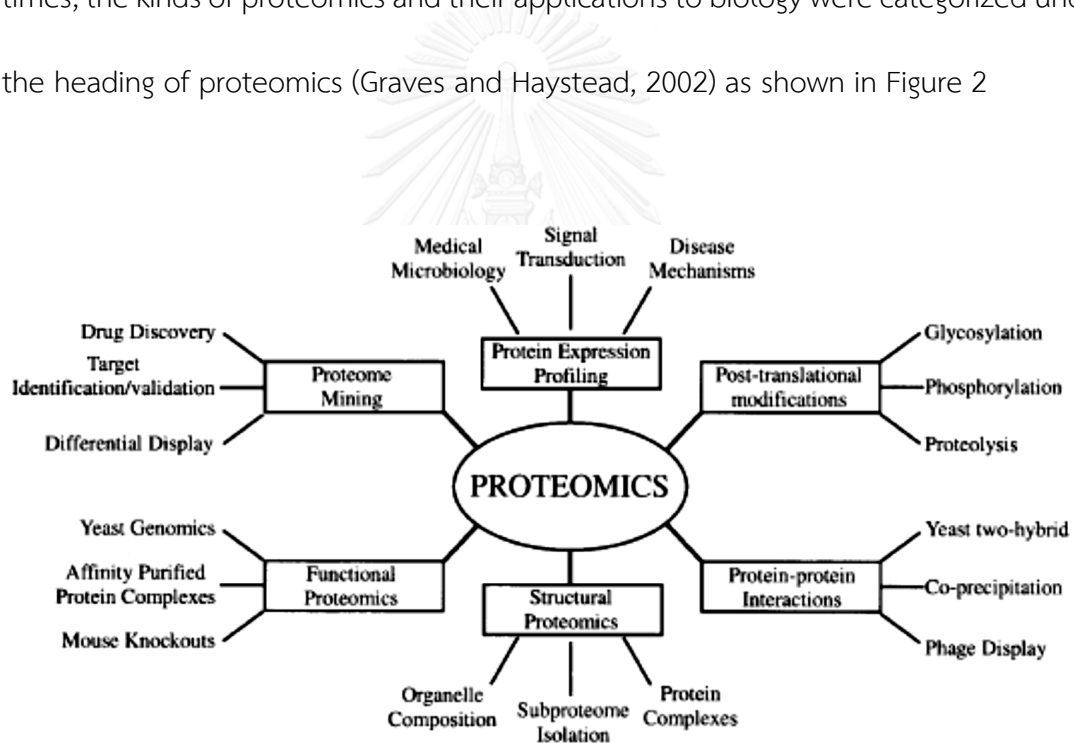


Figure 2 The kinds of proteomics and their applications to Graves and Haystead (2002).

According to Twyman (2004), the functional proteomics is concerned with the investigation of binary interactions between individual proteins and higher-order

interactions of protein complexes including biochemical, cellular and systemic functions. The initial step of proteomic procedures are protein separation for resolving all the individual proteins in cell (Figure 3). Many methods used to separate complex protein mixtures are depended on charge, size, hydrophobicity and ligand specificity. Two-dimensional gel electrophoresis (2-DE) is a high-resolution for protein fractionation which provides effectively resolving power in each dimension. Polyacrylamide gels are generally used for electrophoresis, which are from the polymerization reaction of acrylamide monomer and N,N' -methylene-bis-acrylamide to be catalyzed by N,N,N',N'' -tetramethylethylenediamine (TEMED) and ammonium persulfate (Sawasdi-putka, 2008). The experiment relates tolerated proteins, which combines two steps of separation according to their charge and molecular weight. The first-dimension step is isoelectrically focused in pH gradient to separate proteins on the foundation of net charge based on isoelectric points (pI) across the x-axis which is equal to the surrounding pH and the net charge on the protein is zero (neutral charge). Proteins represent the differences of the pI values and types of smaller more acidic proteins and larger more basic proteins (Figure 4). Then, the second-dimension step is protein separation according to molecular mass across the y-axis with sodium dodecylsulfate polyacrylamide gel electrophoresis (SDS-PAGE). The proteins are denatured with SDS detergent which binds protein stoichiometrically to the polypeptide backbone to be negatively charged. The protein-SDS complexes carry the same charge density and difference in mass. Larger molecules move slowly in gel

whereas smaller molecules move quickly in gel. After that the analysis of all proteins is measured mass/charge ratio (m/z) of ions in a vacuum using mass spectrometry (MS). Molecular masses are analyzed with efficiently high degree of accuracy depend on digestion with specific protease such as trypsin (cleavage site Arg-amino acid side of Y residue and Lys-amino acid side of Y residue) or a similar reagent to intact peptide ions and fragmented ions. Three principle components of mass spectrometers consist of ion source, mass analyzer and ion detector. Two common methods have been widely used for ionization of peptide mixtures are matrix-assisted laser desorption/ionization (MALDI) which is utilized to analyze simple peptide mixtures and electrospray ionization (ESI) which is combined capillary electrophoresis, liquid chromatography (LC) or tandem MS (LC/MS/MS) to analyze complex peptide mixtures. The gas phase ions in a vacuum are converted by the ion source. The ions are increased speed in an electric field from the ion source to the mass analyzer and then the ions are separated mass/charge ratio (m/z). Different types of mass analyzer are applied to separate the ions with determination of the required time to pass through the length of a flight tube such as time-of-flight (TOF), tandem TOF-TOF, the triple quadrupole (TQ), and hybrid quadrupole-TOF. Later, the ion detector recorded to detect the collision of individual ions. The amino acid sequences are contrasted by expected values of theoretical peptide masses from the term of database sequencing algorithms. Calculation of the score is reflected the match between the theoretically and experimentally established masses with the peptide mass mapping search program by MASCOT, profound, or MS-

FIT comparing other amino acid sequences based on the significant degree of sequence similarity in GenBank database or SWISS-PROT database. The identified proteins are categorized functional annotation.

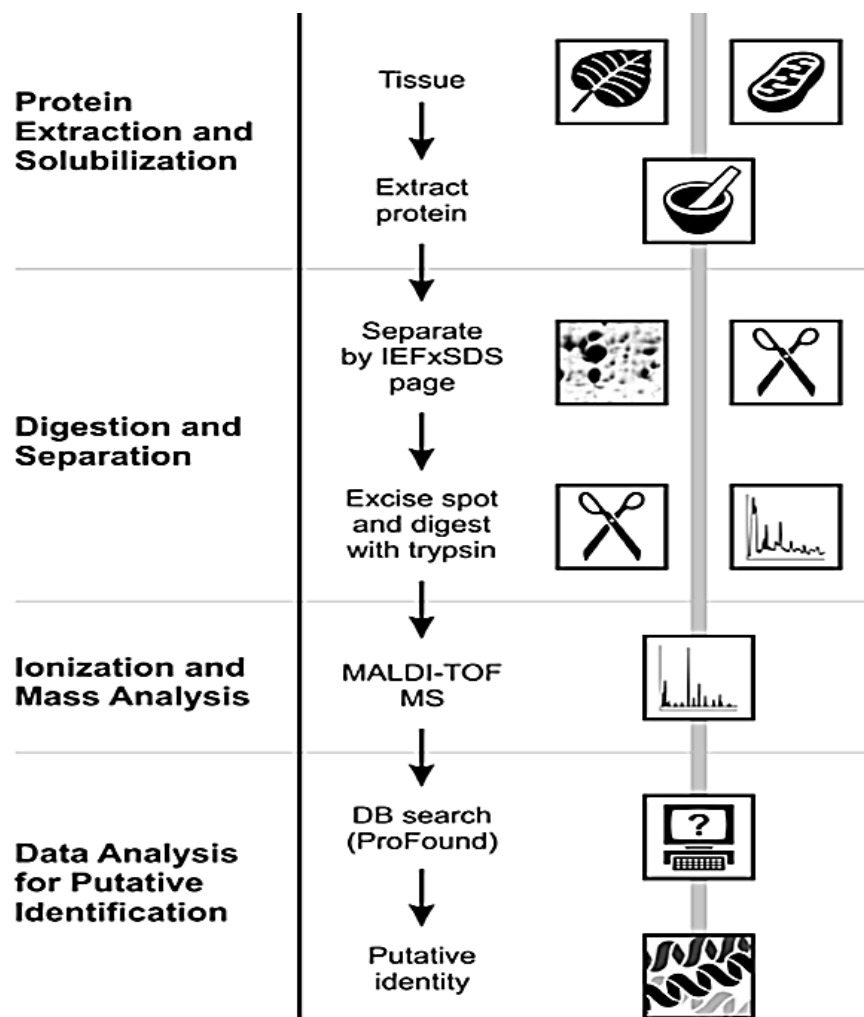


Figure 3 Workflow of proteomic experiments (Rampitsch and Srinivasan, 2006).

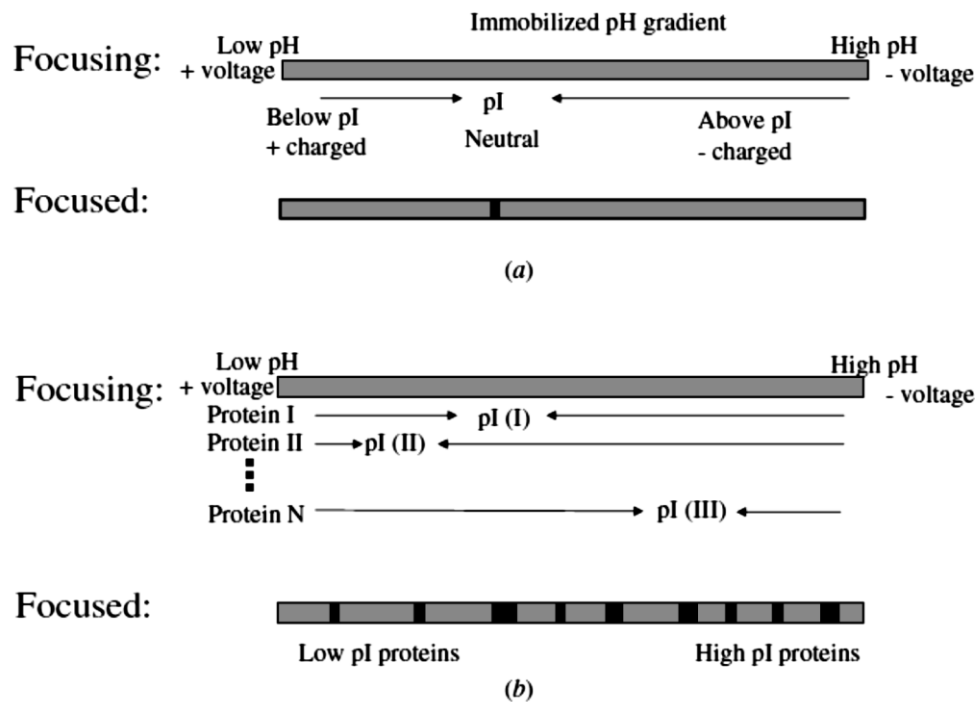


Figure 4 Isoelectric focusing on an immobilized pH gradients (IPG) focused a single protein (a) and a mixture of proteins (b) (Figeys, 2005).

2.4 Literature reviews of plant proteomics

2.4.1. Proteomics in tuberous plants

Agrawal et al. (2008) studied the differential development stages during tuberization in potato (*Solanum tuberosum* L.) by two-dimensional polyacrylamide gel electrophoresis (2-D PAGE) and coupled with electrospray ionization time-of-flight mass spectrometry (ESI-TOF/MS). A total of 219 protein spots were differentially expressed

to change their intensities more than 2.5-fold. The functional classification of proteins related to the various metabolic pathways such as glycolysis, sucrose and starch synthesis, and defense and rescue. The majority group of identified proteins was found in biogenesis storage (29%), bioenergy and metabolism (21%), and cell defense and rescue (12%). Glyceraldehyde-3-phosphate dehydrogenase (GAPDH) and alcohol dehydrogenase (ADH) were increased in initial tubers. GAPDH and UDP-glucose pyrophosphorylase (UGPase) were high-level expression in synthesis of sucrose during tuber developmental stages. The UGPase plays an important role in cell wall biogenesis, which catalyzes in biosynthesis of cell wall polysaccharides. Although fructokinase could increase during tuber development and maturation, fructose bisphosphate aldolase increased the catalyze conversion of the aldol cleavage of Fructose-1,6-bisphosphate (Fru 1,6-bisP) to glyceraldehyde 3-P (G3P) and dihydroxyacetone phosphate (DHAP) during tuber maturation. ATPase was expressed to accumulate starch during tuber maturation, whereas malate dehydrogenase and NADP dehydrogenase were increased during tuber development. Superoxide dismutase (SOD), ascorbate peroxidase (APX) and catalase were directly found to involve reactive oxygen species catabolizing enzymes that proteins could transit from stolons into tubers during tuberization. Heat shock proteins (HSPs) were found during late expressions of tuberization. In addition, low temperature or short day conditions might induce reactive oxygen species levels. The activities of proteins play a significant role in cell defense and rescue mechanism. Multiple signaling pathways and

environmental factors were related to tuber development, physiology, dormancy and signal transductions were found. In additional, dynamics of the protein networks during tuberization of potato were found to involve in pathways of carbon assimilation, protein biogenesis and storage and source-sink transport. Proteins related to sugar breakdown, ROS mechanism, and tuberous storages were exhibited in metabolic pathways. The graphs were represented the profile-expression of individual protein and number given below in individual graph point to the protein identification number (Figure 5).



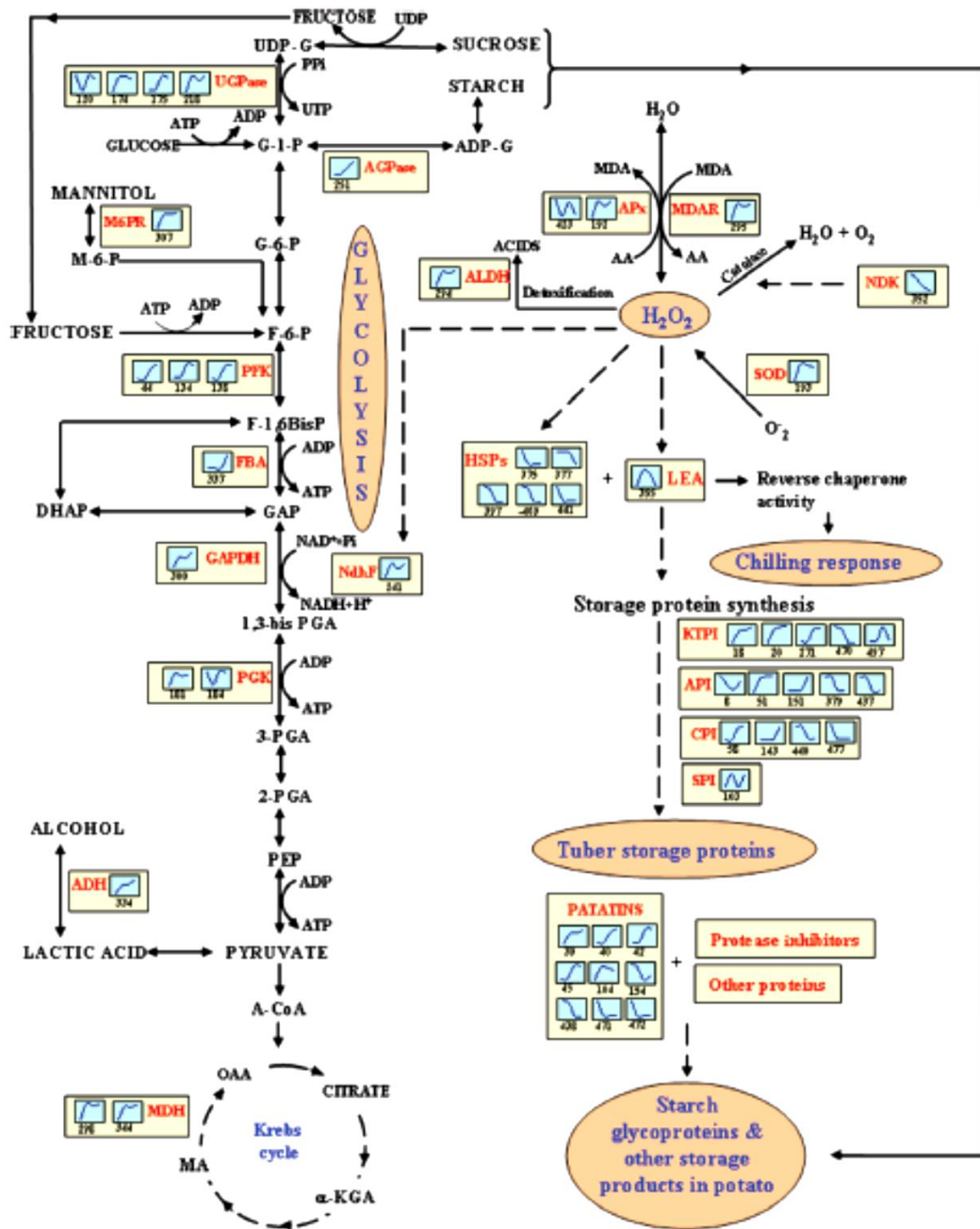


Figure 5 Pathways related to carbon assimilation, protein biogenesis and storage in potato and source-sink transport during tuber development of potato (Agrawal et al., 2008).

Li et al. (2011b) identified 102 proteins in tuberous roots of cassava (*Manihot esculenta* Crantz). Major proteins were found during physiological and developmental stages of tuberous roots. For example, 1,4-alpha-glucan branching enzyme precursor, starch branching enzyme I, starch phosphorylase precursor, ADP-glucose pyrophosphorylase exhibited the key proteins in starch metabolism which were unique to be metabolically active in tuberous roots. For group of cell structure, alpha-tubulin (α -tubulin) was high-level expression in fiber development of tuberous roots.

Du et al. (2011) studied the protein expression during early stage of tuberization in taro (*Colocasia esculenta* var. *antiquorum*) by 2-DE and coupled with electrospray ionization mass spectrometry (ESI/MS). GAPDH, ADH, chloroplast protein synthesis elongation factor (EF-Tu) and ankyrin repeat protein HBP1 were found involved in tuberization in taro. GAPDH was increased under dehydration to involve in sucrose metabolism in *in vitro* tuberization. Some important metabolic changes including sucrose metabolism, signal transductions and cell defenses was found in early stage.

Jungsukcharoen et al. (2016) reported the major proteins including isoflavone synthase, chalcone isomerase, UDP-glycosyltransferase, isoflavone reductase, and cytochrome P450 were related to isoflavonoid pathways in *Pueraria mirifica* tubers.

2.4.2. Proteomics in leaves

Donnelly et al. (2005) studied leaf proteome of wheat (*Triticum aestivum* L.) by 2-DE and coupled with matrix-assisted laser desorption/ionization-time of flight mass spectrometry (MALDI-TOF/MS). The results showed that the majority of functional protein group involved in energy production, primary and secondary metabolism. The proteins in energy production related to metabolic pathways such as glycolysis, gluconeogenesis, pentose phosphate pathway, TCA cycle, respiration, fermentation, electron transport, and photosynthesis, whereas the proteins in primary and secondary metabolism were related to the metabolism of amino acids, nitrogen and sulfur nucleotides, phosphate, sugars and polysaccharides, lipids, sterols, and cofactors.

Xu et al. (2006) studied soybean leaf proteins by 2-DE and mass spectrometry. Fifty-three protein spots were analyzed by MALDI-TOF/MS, whereas 67 protein spots were not identified. MALDI-TOF/MS were allowed to analyze by liquid chromatography tandem mass spectrometry (LC-MS/MS). The largest identified proteins were related to energy metabolism. Energy harvesting, conversion, and storage were found the important functions of plant leaf. The proteins was found to involve in photosynthetic electronic transport such as subunits of PSI and PSII, Rieske FeS protein, plastocyanin, and ferredoxin. Seven proteins, namely, RuBisCO, matate dehydrogenase, sedoheptulose-1,7-biphosphatase, phosphoglycerate kinase, glyceraldehyde-3-

phosphate dehydrogenase, triosephosphate isomerase and transketolase were found in carbohydrate metabolism. Glutamine synthetase, serine hydroxymethyltransferase, alanine aminotransferase, methionine synthase, aspartate transaminase, P-, H- and T protein of the glycine cleavage system were associated with amino acid metabolism. In addition, chaperonin, heat shock proteins/heat shock cognate 70, co-chaperones, cyclophilin, endopeptidase Clp and polyubiquitin play the important roles in protein folding, protein translocation across membranes, assembly of oligomeric proteins, modulation of receptor activities, mRNA protection, prevention of enzyme denaturation and stress-induced aggregation and with post-stress ubiquitin and chaperonin-aided repair.

Lee et al. (2007) studied rice leaf proteome in response to heat stress in temperature of 42°C by 2-DE and coupled with MALDI-TOF/MS. Forty-eight proteins were identified and grouped into heat shock proteins, energy and metabolism, redox homeostasis, and regulatory proteins. Due to heat stress might increase ROS, HSPs such as HSP 70, HSP 100, dnaK-type molecular chaperone BiP, and small heat shock proteins (sHSPs), they were primarily induced in response to heat stress. HSP 70 and dnaK-type molecular chaperone BiP related to folding and synthesis of new polypeptides. HSP 100 could be found to protect protein aggregation and protein degradation. The proteins such as transketolase, UDP-glucose pyrophosphorylase (UGPase), putative thiamine biosynthesis protein, and pyruvate dehydrogenase were

increased to involve in tri-carboxylic-acid (TCA) cycle in energy metabolism. RuBisCO and RuBisCO activase were decreased under heat temperature. Therefore, the plant might retrieve in the state with up-regulation of transketolase to increase precursor of Rubisco by catalyzing reversible conversion a two-carbon ketol unit from a 5-carbon keto sugar to a 5-carbon aldo sugar. ATP synthase was decreased under heat stress which might influence energy-dependent processes. Heat stress might result to change energy production systems. In redox homostasis, GST isoenzymes was increased in response to heat stress because of detoxification of ROS-induced lipid peroxidation products. Dehydroascorbate reductase (DHAR) might increase under heat stress to protect against oxidative stress.

Rasineni et al. (2009) studied leaf proteins of a fast-growing tree *Gmelina arborea* Linn. Roxb. Sixty-four protein spots were identified by 2-DE and coupled with MALDI-TOF-TOF/MS. The identified proteins were involved in photosynthesis, amino acid metabolism, cytoskeleton, cell wall metabolism, stress-related proteins, redox maintenance, electron transport chain, phytohormone metabolism and protein translation and folding. The major proteins in *G. arborea* leaf tissues such as RuBisCO large subunit, RuBisCO activase, carbonic anhydrase, glyceraldehyde-3-phosphate dehydrogenase, trisphosphate isomerase and ferredoxin NADP reductase were categorized in photosynthesis and energy metabolism. One of the low-potential iron-

sulfur proteins was ferredoxin, which plays a role in reduction of NADP⁺ cyclic photophosphorylation and thioredoxin systems.

Mitprasat et al. (2011) studied leaf proteins in cassava (*Manihot esculenta*, Crantz) by 2-DE and coupled with LC/MS/MS machine model Finnigan LTQ Linear Ion trap mass spectrometry. The results demonstrated that the leaves produced specific tuberization stimuli, and transmit into the underground part to control the tuberization process. The signaling pathway between leaves and roots might contribute physiological changes. The metabolic switches lead physiological changes, development including storage tuber.

Zhang et al. (2012) studied heat stress response in leaves of radish (*Raphanus sativus* L.) by 2-DE and coupled with MALDI-TOF/MS. Eleven proteins were differentially expressed and divided into four groups such as HSPs, redox-related protein, energy and metabolism-related protein, and signal transduction-related protein. HSPs CPN 10, HSP17.4, HSP17.6II and putHs42 was highly induced under heat stress. The key enzyme in the ascorbate-glutathione pathway was L-ascorbate peroxidase (APX). It was found in response to reactive oxygen, salt stress, heat and low temperature stress. In addition, oxygen-evolving enhancer protein 2 was found to relate to photosynthesis and light reaction to maintain stability of Photosystem II.

2.5 ROS Scavenging mechanisms

Glutathione (γ -glutamylcysteinylglycine) is multiple functional metabolites to interact via thiol-disulphide exchange of the ascorbate-glutathione pathway for scavenging of hydrogen peroxide that is a ubiquitous low-molecular-weight consisted of tripeptides (γ -glu-cys-gly). It plays a key role in in maintaining cellular signaling and homeostasis processes and redox balance of plants during development, growth, redox homeostasis, antioxidant defense system and plant-pathogen interaction (Gill et al., 2013).

Enzymatic ROS scavenging mechanisms of plants are regulated via the ascorbate-glutathione pathway, including monodehydroascorbate reductase (MDAR), catalase (CAT), glutathione reductase (GR), dehydroascorbate reductase (DHAR), ascorbate peroxidase (APX), glutathione-S-transferase (GST), guaiacol peroxidase, glutathione peroxidase (GPX) and non-enzymes such as glutathione, ascorbic acid and antioxidants. In addition, superoxide anion radicals ($O_2^{\cdot-}$) can be dismutated to hydrogen peroxide (H_2O_2) and oxygen (O_2) by superoxide dismutases (SODs) which is antioxidant metalloenzymes defense in biological systems against ROS (Apel and Hirt, 2004), as shown in Figure 6.

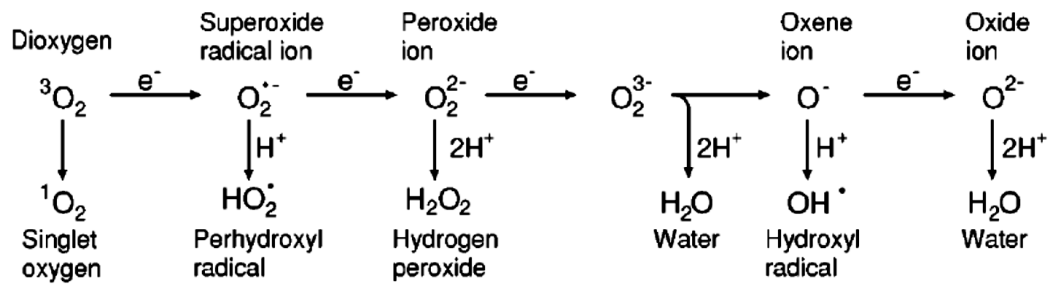


Figure 6 Generation of different ROS by energy transfer or sequential univalent reduction of ground state triplet oxygen (Apel and Hirt, 2004).

The crucial modes of enzymatic ROS scavenging by SOD and CAT, which are involved in the ascorbate-glutathione cycle, and the glutathione GPX cycle to perform the first line for defense against ROS. Hydrogen superoxide into hydrogen peroxide (H_2O_2) was converted by SOD (Figure 7a). Hydrogen peroxide (H_2O_2) into water (H_2O) was converted by CAT (Figure 7b), the ascorbate-glutathione cycle also converts from hydrogen peroxide to water. Ascorbate peroxidase (APX) needs ascorbate and GSH regeneration system (Figure 7c). APX appears by oxidation of ascorbate to MDA. MDA is reduced into ascorbate by MDA reductase (MDAR) with the aid of NAD(P)H as reducing equivalents. MDA can naturally dismutate into Dehydroascorbate (DHA). For ascorbate regeneration, DHA reductase (DHAR) can mediate in the oxidation of glutathione (GSH). By the end of cycle, GSH was regenerated with converting from oxidized glutathione (GSSG) by glutathione reductase (GR) with the aid of NAD(P)H. Hydrogen peroxide into water was converted by the GPX cycle by reducing equivalents from GSH Oxidized

GSSG, is replicated to be converted into GSH by GR including the reducing agent NAD(P)H (Figure 7d).

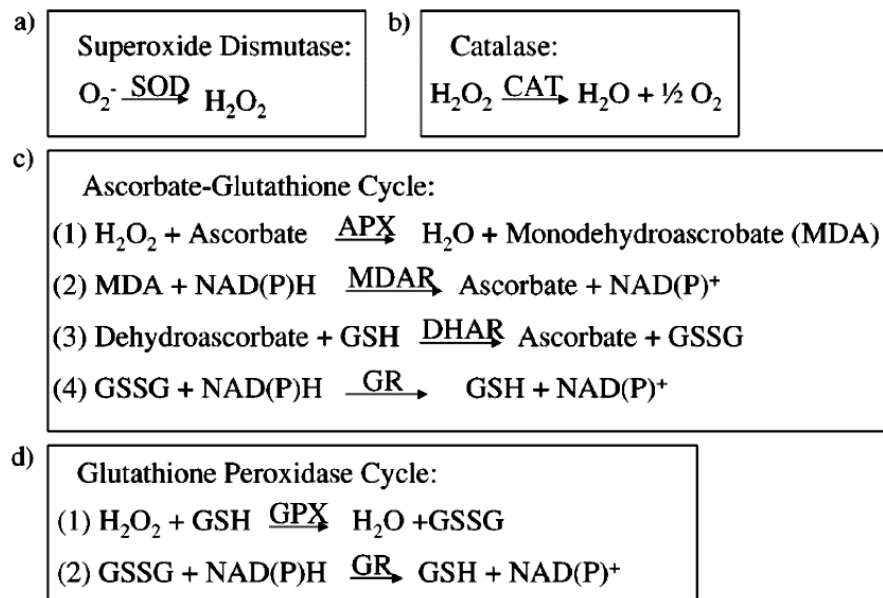


Figure 7 The crucial modes of enzymatic ROS scavenging (Apel and Hirt, 2004).

2.6 Temperature stress

Temperature stress might be related to either higher or lower temperature changes and are environment factors influencing growth and development as well as induction of the physiology, biochemical and morphological alterations in plants. A temperature of $\leq 40^\circ\text{C}$ can induce high temperatures stress and resulted in leaf abscission and senescence, fruit discoloration, sunburns on stems, branches and leaves, shoot growth inhibition, and scorching of twigs and leaves (Waraich et al., 2012).

The primary heat sensing mechanism of plants initiates from the increases of temperature, which is effect on the fluidity of membrane properties, the combination of glycolipids and activation of ion channels (Ca^{2+}). Subsequently, calcium interrupt signal transduction events and changes in transcriptome, proteome and metabolome including changes in protein stability and revelation of hydrophobic residues of proteins might alter the reaction of enzymes and the accumulation of ROS to include modification of cellular energy levels, and RNA unfolding. However, the increased temperature might activate prograded cell death of plants (Mittler et al., 2012) as shown in Figure 8

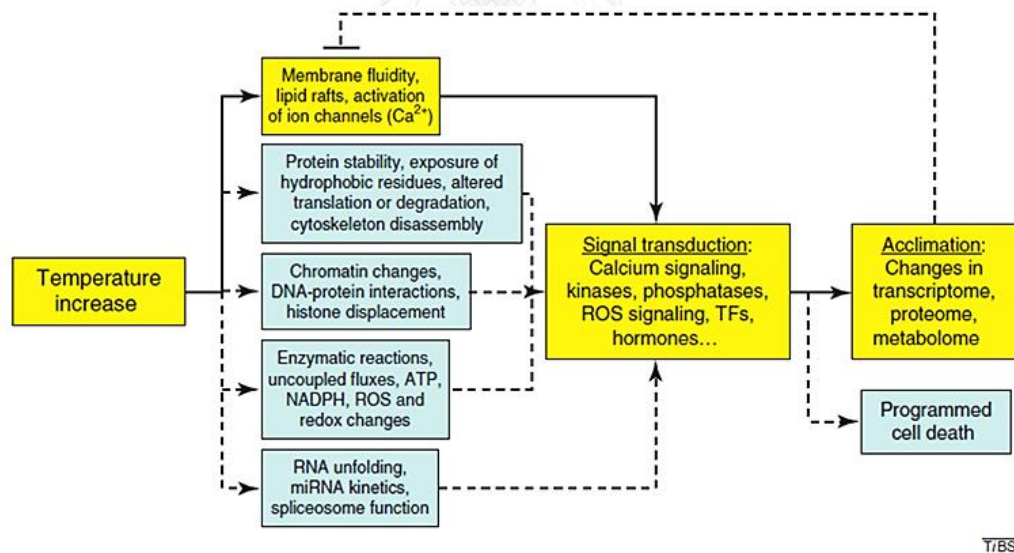


Figure 8 A model for temperature sensing (Mittler et al., 2012).

2.7 Water stress

Water stresses is one of the environmental factors initiating water deficit and drought, which impacts on plant growth and development, physiological process, photosynthetic ability and productivity (Boutraa et al., 2010). Drought and water deficit might inhibit cell elongation and reduce the photo assimilation and required metabolites of cell division (Farooq et al., 2009).

A main influence of drought is failure in photosynthesis, which is represented the possible mechanisms under stress. Drought stress or reduced water availability induces the loss of balance between ROS's and the antioxidant defense, affecting ROS accumulation, which persuades oxidative stress. A stomata is closed throughout ABA signaling, which reduces the CO₂ influx. Reduced CO₂ affects the decreases of carboxylation and the stimulated ROS production. The reduction of activities of ribulose-1,5-bisphosphate carboxylase/oxygenase (RuBisCO), phosphoenolpyruvate carboxylase (PEPCase), NADP-malic enzyme (NADP-ME), fructose-1, 6-bisphosphatase (FBPase) and pyruvate orthophosphate dikinase (PPDK) affects photosynthetic limitation. The activity of RuBisCo binding inhibitors is increased by the decreased tissue water contents. The decreased non-cyclic electron transport corresponds the decreased obligations of Nicotinamide adenine dinucleotide phosphate (NADPH)

production and the reduction of ATP synthesis leading to declined photosynthesis as shown in Figure 9 (Farooq et al., 2009).

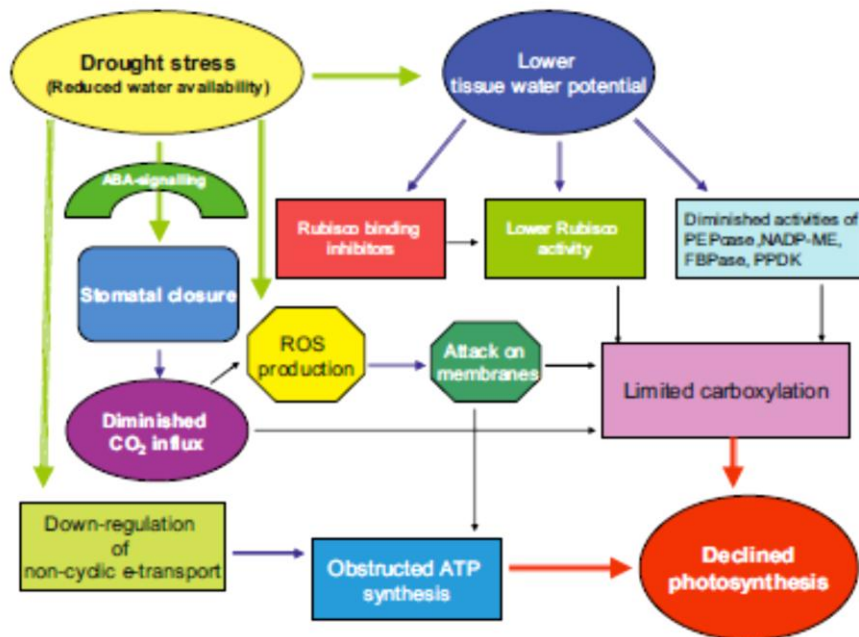


Figure 9 Photosynthesis under drought stress (Farooq et al., 2009).

CHAPTER III

EXPERIMENTAL

3.1 Plant materials and tuber and leaf collections

B. superba originated from Lampang, Saraburi and Chachoengsao provinces, Thailand, was grown to the age of at least 3 years old in a farm located in Banpong district, Ratchaburi province, Thailand. The tubers and leaves were then harvested during rainy season (August, 2010), winter (January, 2011) and summer (April, 2011) and were stored at -80°C. All collected tuber samples had diameter sizes of not less than 7 centimeter in their annual rings that exhibited clearly of the secondary growth of xylem and phloem in the root vascular cambium.

3.2 Protein extraction and quantification

B. superba tissues (20 grams) were extracted by soaking in the extraction buffer [0.7 M sucrose, 0.5M Tris, 30 mM HCl, 50mM EDTA, 0.1 M KCl, 2% (v/v) β -mercaptoethanol and 2mM PMSF] for 30 min at 4°C and centrifuged at 8000 g_{\max} for 10 min at 4°C to aid collection of supernatant. The process was repeated 2-3 times;

before one volume of water-saturated phenol was added to the harvested supernatant. The phenolic mixture was homogenized and kept on ice for 30 min. After centrifugation ($8000 g_{\max}$ for 10 min at 4°C), the upper phenol phase was transferred to another tube. Proteins in the phenol phase were precipitated at -20°C overnight by adding 5 volumes of 0.1 M ammonium acetate in methanol. The mixture was centrifuged at $4000 g_{\max}$ for 10 min at 4°C . The supernatant was discarded and the pellet was dissolved immediately with 1 volume of cold water and subsequently sonicated for 3 min. The precipitate was washed once with 9 volumes of cold acetone, kept at -20°C for at least 4 hours and then centrifuged at $4000 g_{\max}$ for 10 min at 4°C . The washed pellet was air-dried to remove acetone before the dried pellet was solubilized in lysis buffer [7 M urea, 2 M thiourea, 4% (w/v) CHAPS, 2% (w/v) dithiothreitol (DTT) and 5% (v/v) ampholine, pH 3–10]. The protein concentration was determined by Bradford's method (Bradford, 1976).

CHULALONGKORN UNIVERSITY

3.3 Two-dimensional Polyacrylamide Gel electrophoresis

150 μg protein sample was solubilized in rehydration buffer [8 M urea, 2% (w/v) CHAPS, 0.28% (w/v) DTT and 0.5% (v/v) IPG buffer pH 3–10, non-linear (NL)] and 1% (v/v) bromophenol blue was added and subsequently dehydrated overnight in immobilized drystrip pH 3-10 NL, 7 cm (GE Healthcare, Inc.). The first dimension was performed on Ettan IPGphor II Isoelectric Focusing System (Amersham Biosciences,

USA) in steps, which held at 300 V for 200 Vh, followed by at the gradient of 1,000 V for 300 Vh, 5,000 V for 4500 Vh and finally at 5000V for 2000 Vh. In the second dimension, the IPG strips were equilibrated for 2x10 minutes with gentle shaking in 1.5 ml of a solution containing 6 M urea, 50 mM Tris-HCl (pH 6.8), 30% (v/v) glycerol, 2% (w/v) SDS. One percent (w/v) of DTT was added to the first equilibration step, and 2.5% (w/v) iodoacetamide was added to the second equilibration step. After equilibration, the IPG strips were applied to the 14% SDS-PAGE and separated by Hoefer system (Hoefer, Inc.).

3.4 Protein visualization and image analysis

To aid visualization of protein spots, the gels were stained overnight using Coomassie Blue R-250 with gentle shaking. The gels were destained with 40% (v/v) methanol and 10% (v/v) acetic acid for 2 hours, followed by 10% (v/v) methanol and 5% (v/v) acetic acid overnight, until the clear backgrounds were observed. The destained gels were scanned by image scanner (Amersham Biosciences, USA). The experiments were performed in triplicate. The results were aligned, matched and analyzed using the Image Master 2-DE platinum 7.0 (GE Healthcare, UK).

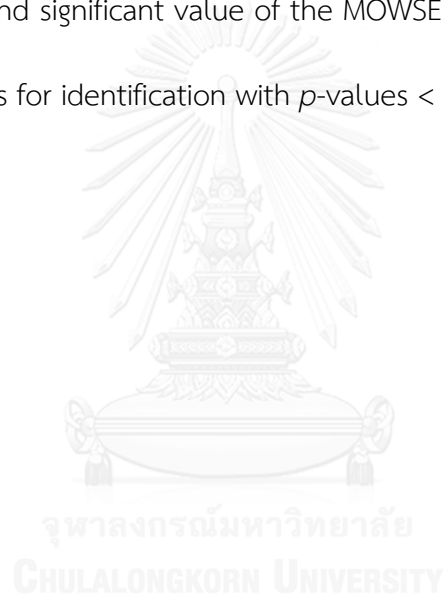
3.5 In-gel digestion with trypsin

Protein spots were cut and sliced into pieces, followed by destaining with 0.1 mM ammonium bicarbonate (NH_4HCO_3) and 50% (v/v) acetonitrile (ACN) for 20 min at 30°C. They were dried in vacuo for 5 min and subsequently swelled in 0.1 mM NH_4HCO_3 , 10 mM DTT and 1 mM EDTA for 45 min at 60°C to reduce the disulfide bonds. 100 mM iodoacetamide and 0.1 mM NH_4HCO_3 were added and incubated for 30 min at 25°C in the dark for alkylation of the proteins. The samples were then washed with 0.05 M Tris-HCl, pH 8.5 and 50% (v/v) ACN, dried in vacuo for 5 min, and then lysed with digestion buffer [0.05 M Tris-HCl, pH 8.5, 10% (v/v) ACN and 1 mM CaCl_2] and trypsin (10% acetic acid and 0.2 mg/ml trypsin) (9:1, v/v) at 37°C overnight. In the final step, the samples were completely eluted with 2% (v/v) trifluoroacetic acid (TFA), 0.05 M Tris-HCl, pH 8.5 and 1 mM CaCl_2 , ACN and 5% (v/v) formic acid and ACN, respectively, and the solutions were completely dried in *vacuo*.

3.6 Protein identification

Protein samples were analyzed using a nanoflow liquid chromatography coupled to electrospray ionization quadruple-time-of-flight tandem mass spectrometer (Micromass; Wythenshaw, Manchester, United Kingdom) working mode (Srisomsap et al., 2010). The database search was performed with ProteinLynx

screening NCBI nr using MASCOT (Matrix Science Ltd., London, UK) during 2012-2014. The database search parameters were set as follows: Viridiplantae (Green Plants); enzyme, trypsin; variable modification, carbamidomethyl (C) and oxidation (M); peptide tolerance, ± 1 Da; MS/MS ion mass tolerance, ± 0.6 kDa; peptide charges, 1+, 2+ and 3+ and maximum allowed missed cleavage, 1. The confidence of peptide matches were based on the experimental M_r , pI , number of peptide matches, percentage of sequence coverage and significant value of the MOWSE score (> 35) as promising hits and matched proteins for identification with p -values < 0.05 .



CHAPTER IV

RESULTS AND DISCUSSION

4.1 Sample collection

The tubers and leaves of *B. superba* were harvested during August, 2010 to represent rainy season samples, January, 2011 to represent winter samples and April, 2011 to represent summer samples. According to the Thai Meteorological Department data during the harvested period, these months were fixed based on temperature, the amount of rainfall and sunshine hours at Banpong district, Ratchaburi province, Thailand (Figure 10). Such physical factors could induce major effects on protein relative abundances and cellular functions in plants. For example, high temperature is able to disrupt photosynthesis (Wahid et al., 2007), whereas low temperature can inhibit growth stages, photosynthesis, pollination, fruit set, and fruit development (Lurie and Sabehat, 1997). Short-term ultimate temperature can decrease crop yields during developmental period (Hashiguchi et al., 2010). In addition, day and night temperature cycles are the important factors on the growth of *Agave deserti*, *Carnegiea gigantean* and *Ferocactus acanthodes* (Mohamed and Al-Whaibi., 2011). In terms of rainfall, temporal variations result in differences in water resources across

years, signal germination and competitive suppression (Levine et al., 2008), which might affect annual plant population dynamics. Plants receive radiant energy from sunshine that influences plant growth and reproduction (Khan et al., 2012).

Rainy season was August to October with a wide range of sunshine and high rainfall. August had the lowest sunshine duration of 117.8 hours/month along with moderate temperature. Shortage of sunshine causes numerous diseases and low growth (Khan et al., 2012). Winter was from November to February with the low level of rainfall. January was the coldest month with minimum temperature of 20.2°C. Low temperature might regulate cold-stress responsive proteins associated with membrane repair (Hossain et al., 2012). Summer was in March and April. April was the hottest period with maximum temperature of 34.5°C and the highest sunshine duration of 235.6 hours/month. During these months, plants might respond to high temperatures by stimulating synthesis of heat shock proteins (Sebehat et al., 1998).

For leaf sample collected in winter, *B. superba* originated from Chachoengsao and Saraburi shed their leaves to keep reducing water loss. In some plants, this kind of response is to aid plant survival under low temperature and drought stress (Mahajan and Tuteja, 2005). Unfortunately, *B. superba* leaf originated from Chachoengsao lacked of sample in collection of summer because the plant might be sensitive to high temperature and also grew slowly resulting in rare amount of presence leaves.

Elevated temperature can regulate multi-seasonal life cycle to reset physiological and molecular mechanism including homeostasis and survival (Ahuja et al., 2010). *B. superba* originated from Lampang occurred faster growth during summer. The rates of growth and maturity can increase rapidly and reach maturity over a short period during the season (Khan et al., 2012).

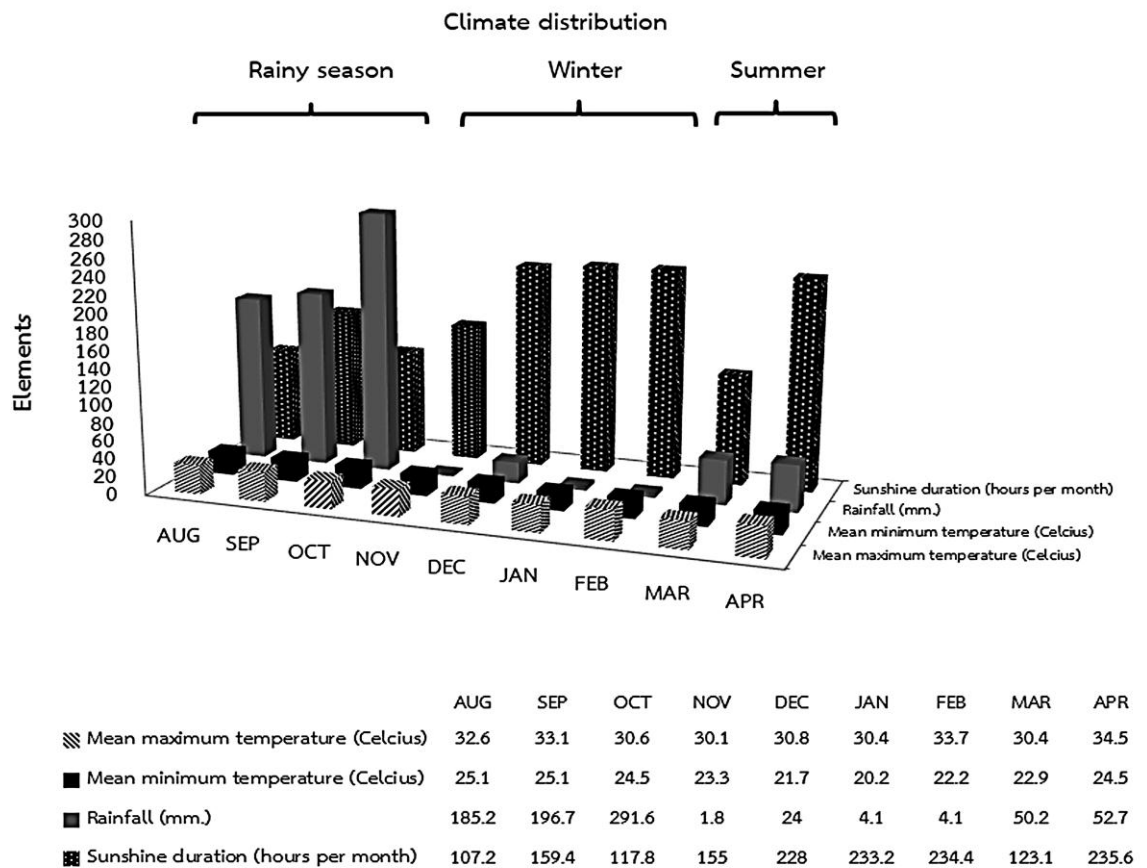


Figure 10 Climate distribution during sample collection in Banpong district, Ratchaburi province, Thailand from August, 2010 to April, 2011.

4.2 Sample extraction and separation of proteins by 2-DE technique

Comparative proteomic analysis of *B. superba* tubers and leaves was achieved by comparing intensities of spots on 2-DE gels. Although the phenol extraction (Faurobert et al., 2007) technique is more protocol-extensive and time consuming than another method such as TCA-acetone and TCA-acetone/Phenol (Carpentier et al., 2005), It was applied in the sample preparation process to inhibit protease and remove the interferences in the analysis from tannins, lignins, polysaccharides, lipids, phenolic compounds, pigments and high content of secondary metabolites in the plant extract (Boonmee et al., 2011; Chokchaichamnankit et al., 2009). Subsequently, the 150 µg protein samples were subjected to protein analysis on 2D-PAGE consisting of pH 3-10, non-linear IEF strips.

4.2.1 Proteomic patterns of tubers

Under the pH gradient, the individual proteomic patterns showed the high intensity of resolved spots within broader and narrower pH gradients with a large number of proteins found in the acidic to basic regions (pH 4-8). Overall, despite the large similarities, the proteome abundance patterns among samples from different

seasons and varieties were visually distinguishable on the 2-DE gels (Figure 11-19 and Table 2).

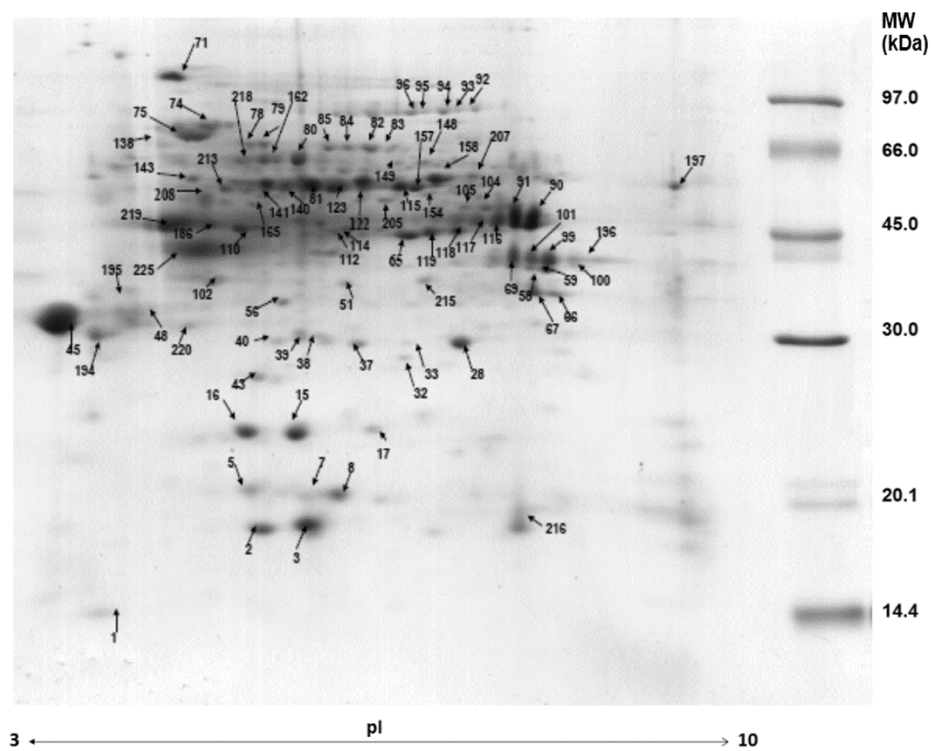


Figure 11 Representative 2-DE profiles of the 150 µg protein isolated from *B. superba* tubers which were originated from Lampang (1) and harvested from Banpong district, Ratchaburi province in rainy season (TR) at pH 3-10 using non-linear IEF strips.

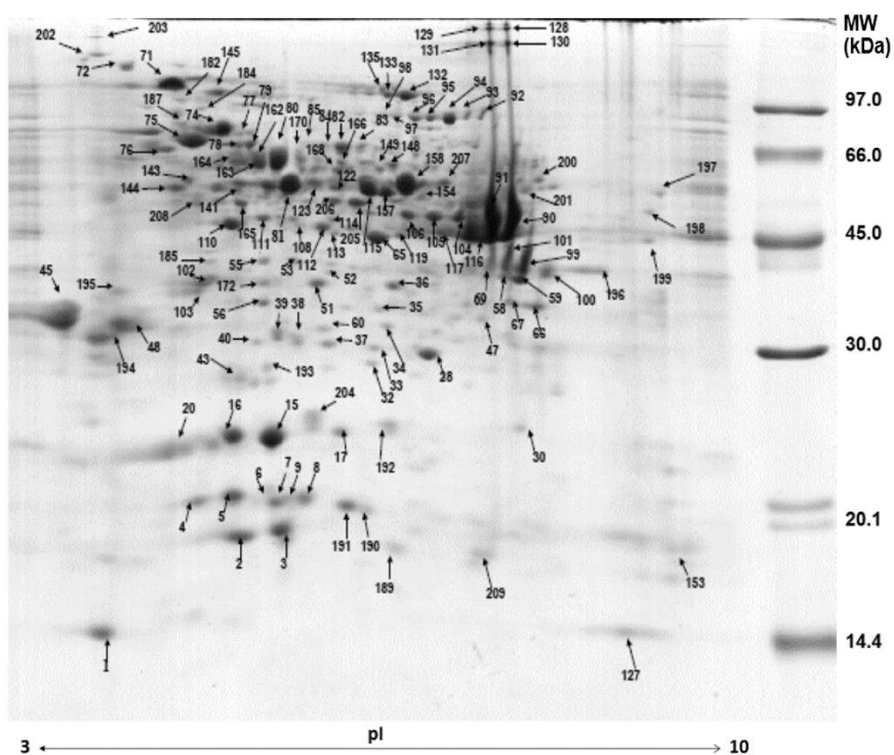


Figure 12 Representative 2-DE profiles of the 150 μ g protein isolated from *B. superba* tubers which were originated from Lampang (1) and harvested from Banpong district, Ratchaburi province in winter (TW) at pH 3-10 using non-linear IEF strips.

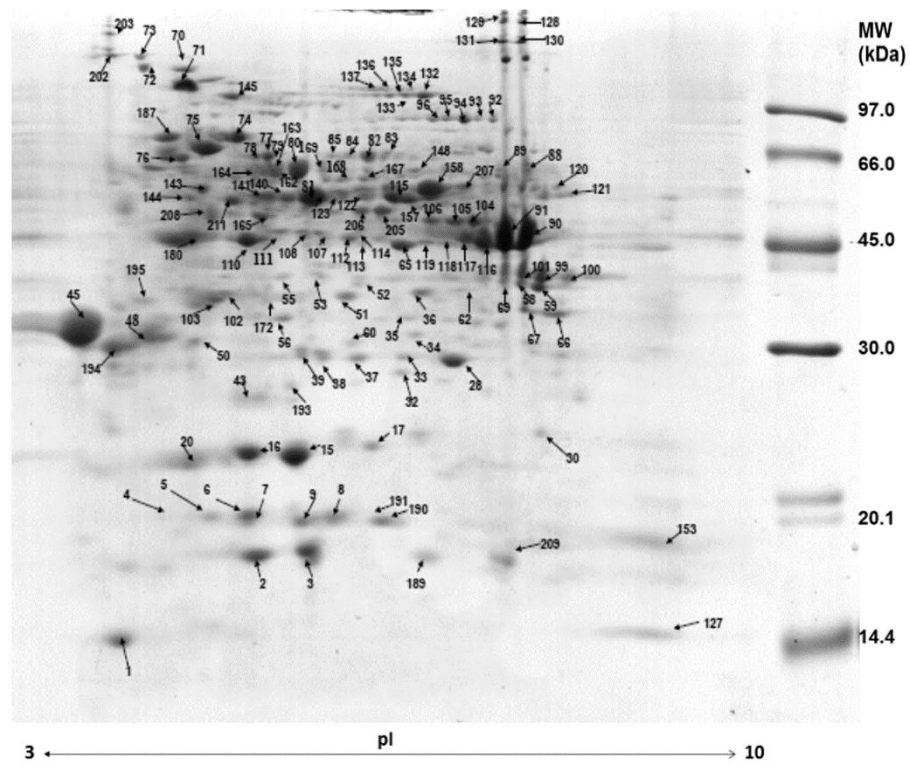


Figure 13 Representative 2-DE profiles of the 150 μ g protein isolated from *B. superba* tubers which were originated from Lampang (1) and harvested from Banpong district, Ratchaburi province in summer (TS) at pH 3-10 using non-linear IEF strips.

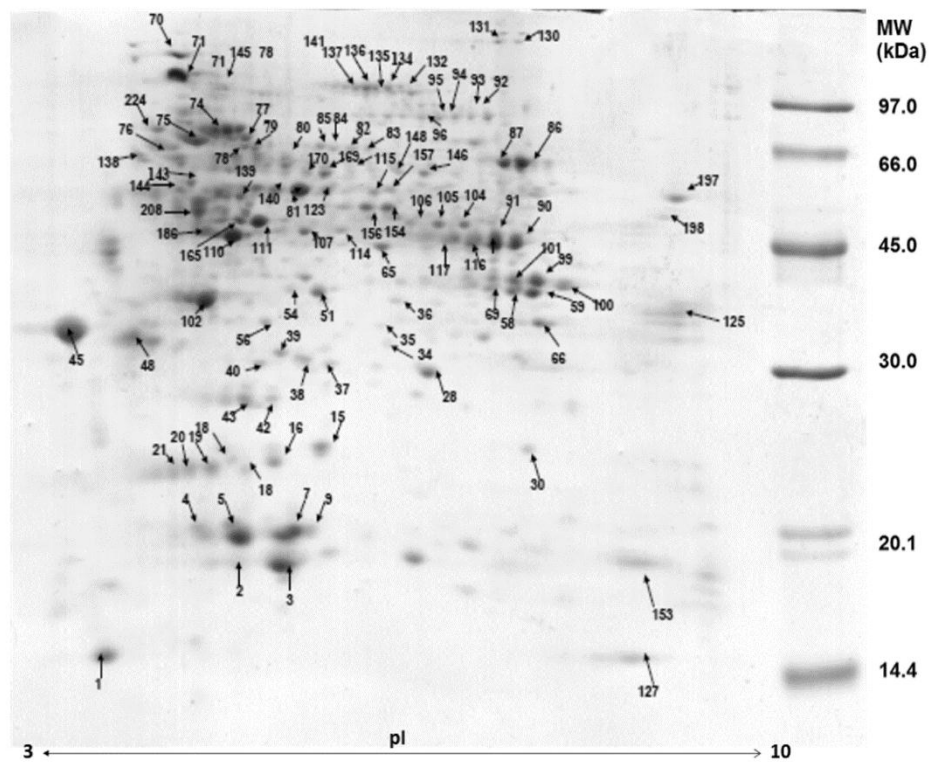


Figure 14 Representative 2-DE profiles of the 150 μ g protein isolated from *B. superba* tubers which were originated from Saraburi (2) and harvested from Banpong district, Ratchaburi province in rainy season (TR) at pH 3-10 using non-linear IEF strips.

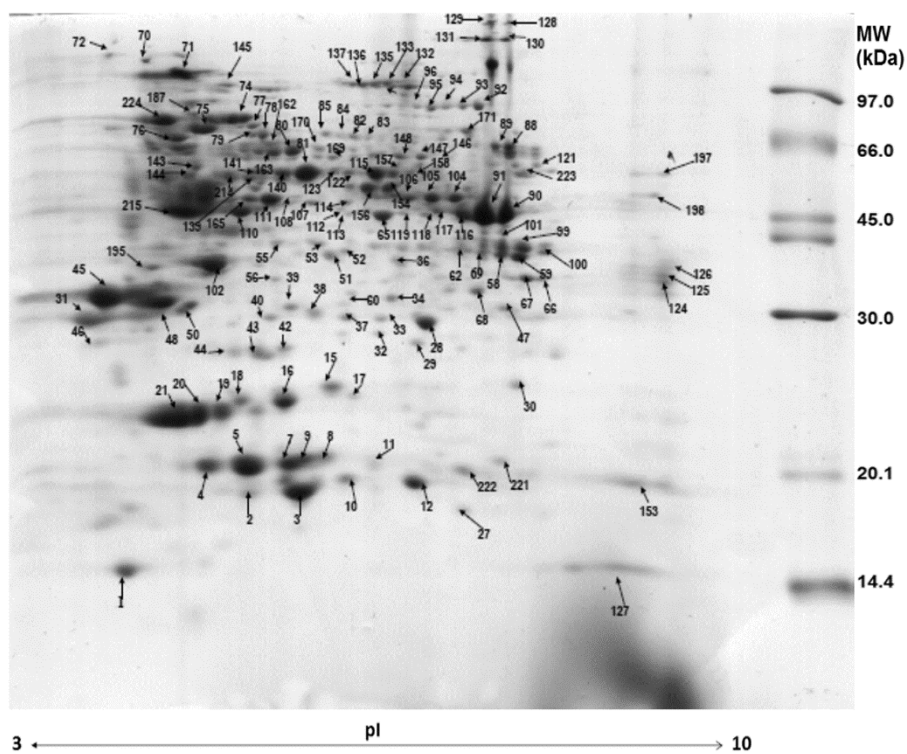


Figure 15 Representative 2-DE profiles of the 150 μ g protein isolated from *B. superba* tubers which were originated from Saraburi (2) and harvested from Banpong district, Ratchaburi province in winter (TW) at pH 3-10 using non-linear IEF strips.

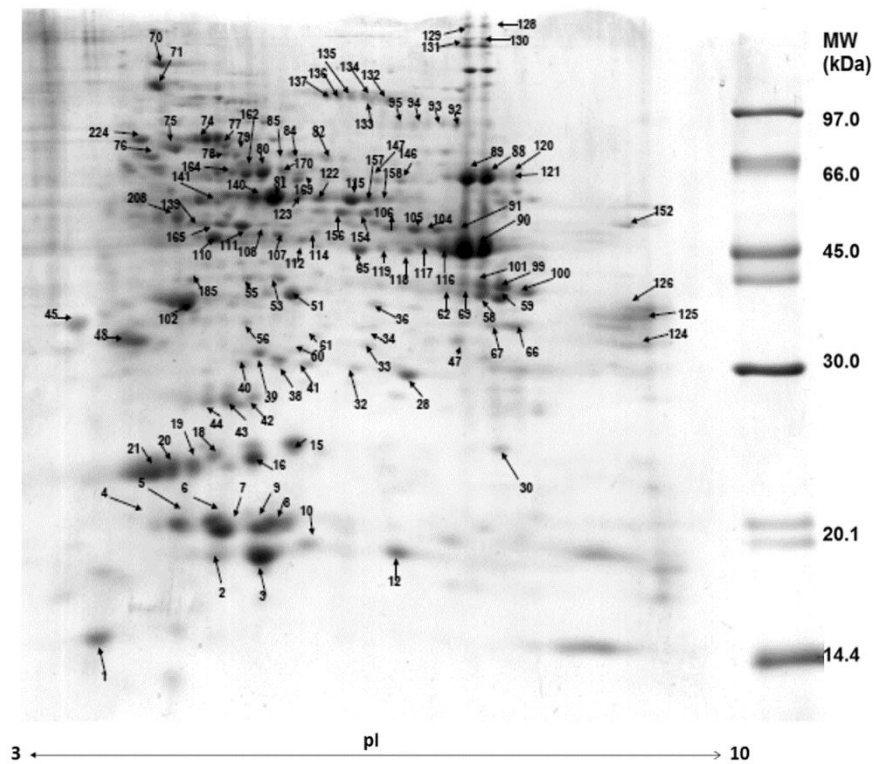


Figure 16 Representative 2-DE profiles of the 150 μ g protein isolated from *B. superba* tubers which were originated from Saraburi (2) and harvested from Banpong district, Ratchaburi province in summer (TS) at pH 3-10 using non-linear IEF strips.

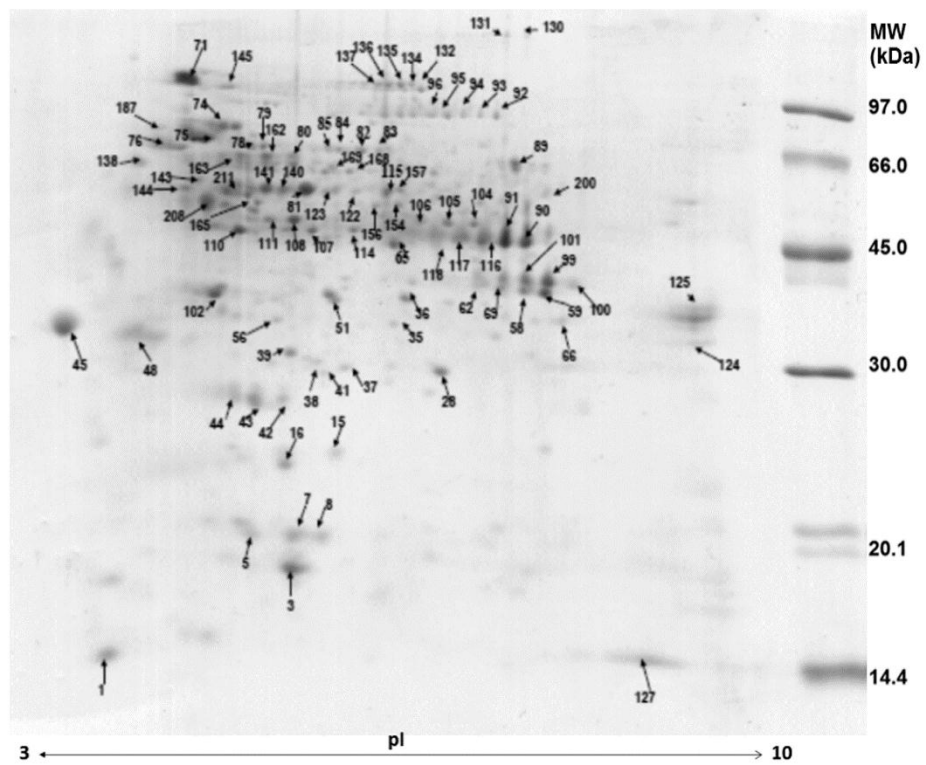


Figure 17 Representative 2-DE profiles of the 150 µg protein isolated from *B. superba* tubers which were originated from Chachoengsao (3) and harvested from Banpong district, Ratchaburi province in rainy season (TR) at pH 3-10 using non-linear IEF strips.

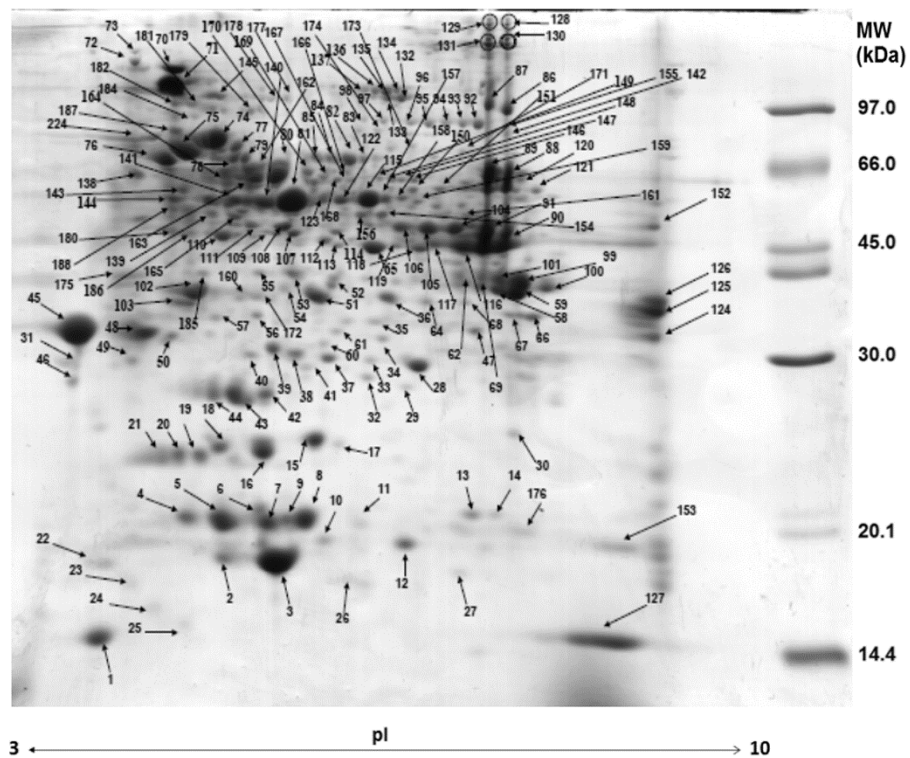


Figure 18 Representative 2-DE profiles of the 150 μg protein isolated from *B. superba* tubers which were originated from Chachoengsao (3) and harvested from Banpong district, Ratchaburi province in winter (TW) at pH 3-10 using non-linear IEF strips.

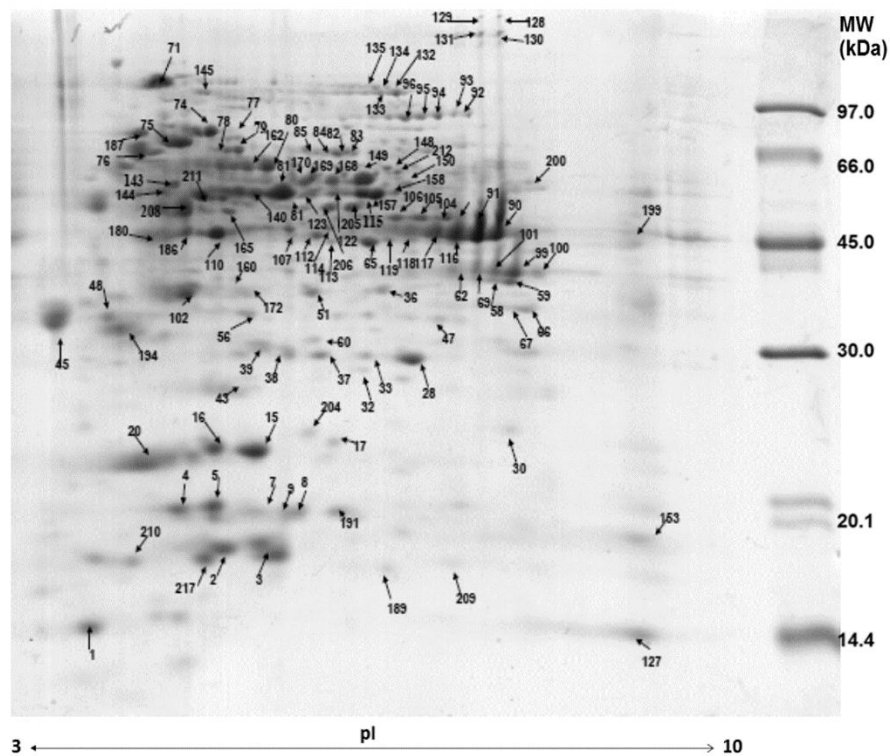


Figure 19 Representative 2-DE profiles of the 150 μ g protein isolated from *B. superba* tubers which were originated from Chachoengsao (3) and harvested from Banpong district, Ratchaburi province in summer (TS) at pH 3-10 using non-linear IEF strips.

Table 2 (Continued)

Spot no.	Accession number ^{a)}	Protein name	TR1	TW1	TS1	TR2	TW2	TS2	TR3	TW3	TS3
Functional group 2: Carbohydrate and energy metabolism											
106	gij342851387	Alcohol dehydrogenase, putative	-	✓	✓	✓	✓	✓	✓	✓	✓
112	gij356509324	Alcohol dehydrogenase 1	-	✓	✓	-	✓	✓	✓	✓	✓
113	gij356525744	Phosphoglycerate kinase, cytosolic	-	✓	✓	-	✓	-	-	✓	✓
115	gij344190186	Enolase	✓	✓	✓	✓	✓	✓	✓	✓	✓
116	gij445589	Alcohol dehydrogenase	✓	✓	✓	✓	✓	✓	✓	✓	✓
117	gij445589	Alcohol dehydrogenase	✓	✓	✓	✓	✓	✓	✓	✓	✓
118	gij445589	Alcohol dehydrogenase	✓	-	✓	-	✓	✓	✓	✓	✓
119	gij445589	Alcohol dehydrogenase	✓	✓	✓	-	✓	✓	-	✓	✓
120	gij22296818	Pyruvate kinase	-	-	✓	-	✓	✓	-	✓	-
121	gij356521618	Pyruvate kinase	-	-	✓	-	-	✓	-	✓	-
122	gij1169534	Enolase	✓	✓	✓	-	✓	✓	✓	✓	✓
123	gij356530953	Enolase	✓	✓	✓	✓	✓	✓	✓	✓	✓
128	gij22597178	Alcohol dehydrogenase 1	-	✓	✓	-	✓	✓	-	✓	✓
129	gij22597178	Alcohol dehydrogenase 1	-	✓	✓	-	✓	✓	-	✓	✓
130	gij470108526	Alcohol dehydrogenase 1	-	✓	✓	✓	✓	✓	✓	✓	✓
131	gij22597178	Alcohol dehydrogenase 1	-	✓	✓	✓	✓	✓	✓	✓	✓
138	gij255538186	D-3-phosphoglycerate dehydrogenase, putative	-	-	-	✓	-	-	✓	✓	-
139	gij356536246	ATP synthase subunit beta	-	-	-	-	-	-	-	✓	-
140	gij351724891	Enolase	✓	✓	✓	✓	✓	✓	✓	✓	✓
141	gij1169534	Enolase	✓	✓	✓	-	✓	✓	✓	✓	-
143	gij226492645	Vacuolar ATP synthase subunit B	✓	✓	✓	✓	✓		✓	✓	✓
166	gij33149681	Pyruvate decarboxylase	-	✓	-	-	-	-	-	-	-

Table 2 (Continued)

Spot no.	Accession number ^{a)}	Protein name	TR1	TW1	TS1	TR2	TW2	TS2	TR3	TW3	TS3
Functional group 2: Carbohydrate and energy metabolism											
171	gij22597178	Alcohol dehydrogenase1	-	✓	-	-	✓	-	-	-	-
172	gij125662890	Glyceraldehyde -3-phosphate dehydrogenase UDP- sugar	-	✓	✓	-	-	-	-	✓	✓
173	gij75110834	pyrophospharylase UDP- sugar	-	-	-	-	-	-	-	✓	-
174	gij351727947	pyrophospharylase 1	-	-	-	-	-	-	-	✓	-
175	gij3023814	Glyceraldehyde -3-phosphate dehydrogenase,	-	-	-	-	-	-	-	✓	-
176	gij120666	Glyceraldehyde -3-phosphate dehydrogenase ATP synthase subunit	-	-	-	-	-	-	-	✓	-
183	gij356536246	beta	-	-	-	-	-	-	-	✓	-
186	gij22597178	Alcohol dehydrogenase1	✓	-	✓	-	-	✓	-	✓	✓
196	gij149391151	Glyceraldehyde -3-phosphate dehydrogenase	✓	✓	-	-	-	-	-	✓	-
200	gij22296818	Pyruvate kinase	-	✓	-	-	-	-	✓	-	✓
202	gij22597178	Alcohol dehydrogenase1	-	✓	✓	-	-	-	-	-	-
203	gij502117964	Enolase-phosphatase E1	-	✓	✓	-	-	-	-	-	-
205	gij1169534	Enolase	✓	✓	✓	-	-	-	-	-	✓
207	gij1169534	Enolase ATP synthase subunit	✓	✓	-	-	-	-	-	-	-
211	gij356536246	beta	-	-	✓	-	-	-	✓	✓	✓
214	gij356561923	Glucan endo-1,3-beta-glucosidase 5	-	-	-	-	✓	-	-	-	-

Table 2 (Continued)

Spot no.	Accession number ^{a)}	Protein name	TR1	TW1	TS1	TR2	TW2	TS2	TR3	TW3	TS3
Functional group 2: Carbohydrate and energy metabolism											
		Alcohol									
216	gij543176666	dehydrogenase1	✓	-	-	-	-	-	-	-	-
		Alcohol									
219	gij71793966	dehydrogenase	✓	-	-	-	-	-	-	-	-
220	gij356552857	Pyruvate	✓	-	-	-	-	-	-	-	-
		dehydrogenase									
		E1									
		component									
		subunit beta									
Functional group 3: Photosynthesis											
		Ribulose 1,5-									
157	gij18157251	bisphosphate	✓	✓	✓	✓	✓	✓	✓	✓	✓
		carboxylase-									
		oxygenase									
		Ribulose-1,5-									
158	gij229464442	bisphosphate	✓	✓	✓	-	✓	✓	-	✓	✓
		carboxylase/									
		oxygenase									
		Ribulose-1,5-									
159	gij229464442	bisphosphate	-	-	-	-	-	-	-	✓	-
		carboxylase/									
		oxygenase									
Functional group 4: Cellular structure											
		Stem-specific									
60	gij356549751	protein	-	✓	✓	-	✓	-	-	✓	✓
		TSJT1 isoform 1									
110	gij356558578	Actin-101	✓	✓	✓	✓	✓	✓	✓	✓	✓
		Tubulin beta									
144	gij1351202	chain	-	✓	✓	✓	✓	-	✓	✓	✓
180	gij356558578	Actin-101	-	-	✓	-	-	-	-	✓	✓
		Tubulin alpha-3									
208	gij356560917	chain	-	✓	✓	✓	-	✓	✓	-	✓

Table 2 (Continued)

Spot no.	Accession number ^{a)}	Protein name	TR1	TW1	TS1	TR2	TW2	TS2	TR3	TW3	TS3
Functional group 6: ROS scavenging and detoxifying											
4	gij134684	Cu/Zn-SOD	-	✓	✓	✓	✓	✓	-	✓	✓
32	gij356526968	GST F10	✓	✓	✓	-	✓	✓	-	✓	✓
34	gij225448353	Hydroxyglutathione hydrolase	-	✓	✓	✓	✓	✓	-	✓	✓
37	gij120969450	Cytosolic APX	✓	-	✓	✓	✓	-	✓	✓	✓
47	gij15227376	S- formylglutathione hydrolase	✓	✓	-	✓	✓	✓	✓	✓	-
56	gij356531939	Putative lactoylglutathione lyase	✓	✓	✓	✓	✓	✓	✓	✓	✓
61	gij225448353	Hydroxyacylglutathione hydrolase cytoplasmic	-	-	-	-	-	-	-	✓	-
107	gij356577825	MDAR	-	-	✓	✓	✓	✓	✓	✓	✓
109	gij356533631	MDAR isoform 1	-	-	-	-	-	-	-	✓	-
114	gij356577825	MDAR	✓	✓	✓	✓	✓	✓	✓	✓	✓
124	gij356509058	Peroxidase 52 isoform1	-	-	-	-	✓	✓	-	✓	-
125	gij356496705	Peroxidase 72 isoform1	-	-	-	-	✓	✓	-	✓	-
126	gij449457510	Peroxidase 72	-	-	-	-	✓	✓	-	✓	-
150	gij6714837	GR, cytosolic	-	-	-	-	-	-	-	✓	✓
151	gij224133228	GR	-	-	-	-	-	-	-	✓	-
154	gij356559573	GR	✓	✓	-	✓	✓	✓	✓	✓	-
161	gij50058096	GR	-	-	-	-	-	-	-	✓	-
199	gij62909961	Peroxidase	-	✓	-	-	-	-	-	-	✓
Functional group 7: Amino-acid biosynthesis											
27	gij26245395	Nucleoside diphosphate kinase	-	✓	-	-	✓	-	-	✓	-
50	gij15235282	D-3-phosphoglycerate dehydrogenase	-	-	-	✓	✓	-	-	✓	-

Table 2 (Continued)

Spot no.	Accession number ^{a)}	Protein name	TR1	TW1	TS1	TR2	TW2	TS2	TR3	TW3	TS3
Functional group 7: Amino-acid biosynthesis											
53	gij4255689399	Branched-chain-amino- acid aminotransferase	-	✓	✓	✓	✓	✓	-	✓	-
55	gij42568800	Branched-chain-amino-acid aminotransferase 5	-	✓	✓	-	✓	✓	-	✓	-
70	gij356536156	D-3-phosphoglycerate dehydrogenase	-	-	✓	✓	-	✓	-	✓	-
80	gij356536156	D-3-phosphoglycerate dehydrogenase	✓	✓	✓	✓	✓	✓	✓	✓	✓
93	gij356547867	5-methyltetrahydro pteroyltriglutamate -homocysteine methyltransferase	✓	✓	✓	✓	-	✓	✓	✓	✓
94	gij356508448	5-methyltetrahydro pteroyltriglutamate -homocysteine methyltransferase	✓	✓	✓	✓	-	✓	✓	✓	✓
95	gij356508448	5-methyltetrahydro pteroyltriglutamate -homocysteine methyltransferase	✓	✓	✓	✓	-	✓	✓	✓	✓
102	gij134142075	Serine hydroxymethyltransferase Chloroplast	✓	✓	✓	✓	✓	✓	✓	✓	✓
146	gij341958461	acetohydroxy acid isomeroreductase	-	-	-	✓	-	✓	-	✓	-

Table 2 (Continued)

Spot no.	Accession number ^{a)}	Protein name	TR1	TW1	TS1	TR2	TW2	TS2	TR3	TW3	TS3
Functional group 7: Amino-acid biosynthesis											
138	gij255538186	D-3-phosphoglycerate dehydrogenase	✓	-	-	✓	-	-	-	✓	-
147	gij341958461	Chloroplast acetohydroxy acid isomeroreductase	-	-	-	✓	✓	✓	✓	✓	-
148	gij341958461	Chloroplast acetohydroxy acid isomeroreductase	✓	✓	-	✓	✓	-	-	✓	✓
149	gij341958461	Chloroplast acetohydroxy acid isomeroreductase	✓	✓	-	-	-	-	-	✓	✓
162	gij356536156	D-3-phosphoglycerate dehydrogenase	✓	✓	✓	-	✓	✓	✓	✓	✓
163	gij356536156	D-3-phosphoglycerate dehydrogenase	-	✓	✓	-	✓	-	-	✓	-
164	gij356536156	D-3-phosphoglycerate dehydrogenase	-	✓	✓	-	-	✓	-	✓	-
167	gij341958461	Chloroplast acetohydroxy acid isomeroreductase	-	-	✓	-	-	-	-	✓	-
168	gij341958461	Chloroplast acetohydroxy acid isomeroreductase	-	✓	✓	-	✓	-	✓	✓	✓
169	gij6225542	Chloroplast acetohydroxy acid isomeroreductase	-	-	✓	✓	✓	✓	✓	✓	✓

Table 2 (Continued)

Spot no.	Accession number ^{a)}	Protein name	TR1	TW1	TS1	TR2	TW2	TS2	TR3	TW3	TS3
Functional group 10: Protein destination and storage											
29	gij356526807	Proteasome subunit beta type-1	-	-	-	-	✓	-	-	✓	-
30	gij227937349	20S proteasome beta subunit 5	-	✓	✓	✓	✓	✓	-	✓	✓
38	gij356496249	Proteasome subunit alpha type-4 isoform 1	✓	✓	✓	✓	✓	✓	✓	✓	✓
40	gij356496096	Proteasome subunit alpha type-2-A	✓	✓	✓	✓	✓	✓	-	✓	-
Functional group 11: Cell cycle and division											
46	gij413916456	Cyclin superfamily protein	-	-	-	-	✓	-	-	✓	-
127	gij413916456	Cyclin superfamily protein	-	✓	✓	✓	✓	✓	✓	✓	✓
145	gij356508699	Cell division cycle protein 48 homolog	-	✓	✓	-	✓	-	✓	✓	✓
152	gij356539207	Apoptosis-inducing factor homolog A	-	-	-	-	-	✓	✓	✓	-
156	gij356496197	Proliferation-associated protein 2G4	-	-	-	✓	✓	✓	✓	✓	-
Functional group 12: Others											
Fatty acid metabolism											
17	gij363808072	Allene oxide cyclase 4	✓	✓	✓	✓	✓	-	-	✓	✓

Table 2 (Continued)

Spot no.	Accession number ^{a)}	Protein name	TR1	TW1	TS1	TR2	TW2	TS2	TR3	TW3
Fatty acid metabolism										
18	gij358345896	Allene-oxide cyclase	-	-	-	-	✓	✓	-	✓
217	gij502140113	Lipoxygenase homology	-	-	-	-	-	-	-	✓
Plant hormone metabolism										
31	gij84579412	9-cis-epoxycarotenoid dioxygenase 4	-	-	-	-	✓	-	-	✓
Secondary metabolism										
52	gij356538206	Isoflavone reductase homolog A622	-	✓	✓	-	✓	-	-	✓
Protein transport										
72	gij255561582	Patellin-3	-	✓	✓	-	✓	-	-	✓
Translation										
153	gij223469633	S18 ribosomal protein	-	✓	✓	-	✓	-	-	✓
Protein translocation										
184	gij460378451	Luminal-binding protein 5	-	✓	-	-	-	-	-	✓
Unknown										
21	gij363807526	Uncharacterized protein LOC100798019 precursor	-	-	-	✓	✓	✓	-	✓

Table 2 (Continued)

Spot no.	Accession number ^{a)}	Protein name	TR1	TW1	TS1	TR2	TW2	TS2	TR3	TW3	TS3
Unknown											
23	gij351723665	Uncharacterized protein	-	-	-	-	-	-	-	✓	-
		LOC100306050 precursor									
24	gij351723665	Uncharacterized protein	-	-	-	-	-	-	-	✓	-
		LOC100306050 precursor									
42	gij255637227	Unknown	-	-	-	-	✓	✓	-	✓	-
35	gij300392456	SEC 13 family	✓	✓	✓	✓		✓	✓	✓	✓
39	gij255647220	Unknown	✓	✓	✓	✓	✓	✓	✓	✓	✓
44	gij255637227	Unknown	-	-	-	-	✓	✓	✓	✓	-
71	gij8894548	Hypothetical protein	✓	✓	✓	✓	✓	✓	✓	✓	✓
73	gij358348031	Gene X-like protein									
103	gij356525790	Nitrile-specifier protein-5	✓	-	✓	-	-	-	-	✓	-
108	gij255636611	Unknown	-	✓	✓	-	-	✓	-	✓	-
142	gij357520365	Protein tolB	-	-	-	-	-	-	-	✓	-
155	gij357520365	Protein tolB	-	-	-	-	-	-	-	✓	-
160	gij255580564	Nutrient reservoir, putative	-	-	-	-	✓	-	-	✓	✓
		Uncharacterized protein									
198	gij359807022	Uncharacterized protein	-	✓	-	✓	✓	-	-	-	-
		LOC100813980									
		Uncharacterized protein									
213	gij502120564	Uncharacterized protein	✓	-	-	-	-	-	-	-	-
		LOC101500213									

a) The protein's NCBI accession number

Most protein spots belonging to carbohydrate and energy metabolism, photosynthesis, cellular structure, amino-acid biosynthesis, signal transduction and homeostasis, protein biosynthesis and protein destination and storage were similarly appeared in 3 seasons, whereas other protein spots were differentially expressed in proteomic abundance patterns among samples from different seasons and varieties involving in allergy, defense and stress ROS scavenging and detoxifying, cell cycle and division (Table 2).

4.2.2 Proteomic patterns of leaves

Under the pH gradient, the individual 2-DE patterns in each sample exhibited high intensity of resolved spots in the acidic region and weak intensity in basic region. Most protein spots were scattered in the range of pH 4-7. Overall, despite the large similarities, the proteome abundance patterns among samples from different seasons and varieties were visually distinguishable on the 2-DE gels (Figure 20-25 and Table 3).

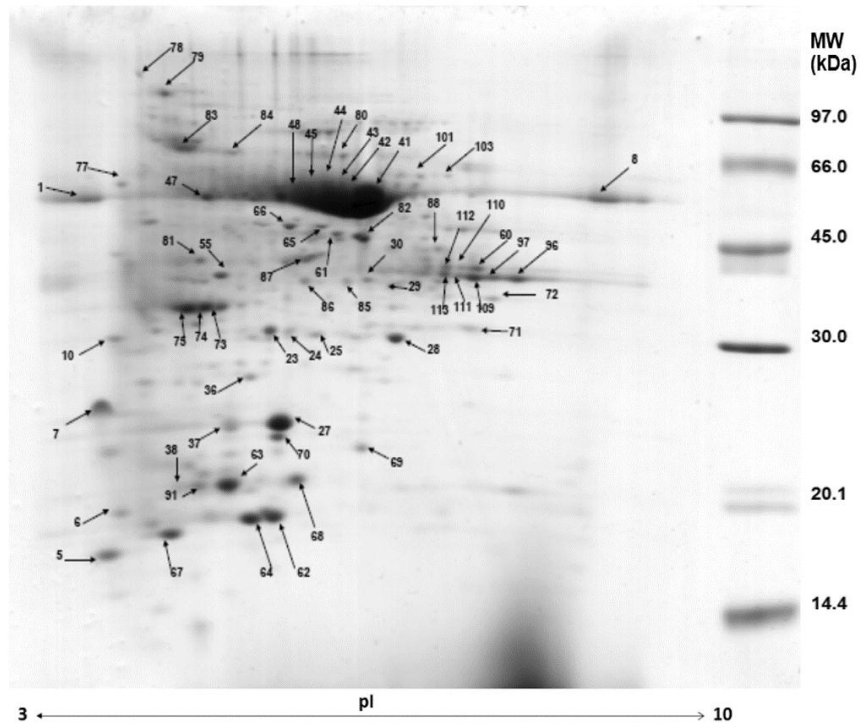


Figure 20 Representative 2-DE profiles of the 150 μ g protein isolated from *B. superba* leaves originated from Lampang (1) and collected from Banpong district, Ratchaburi province in rainy season (LR) at pH 3-10 using non-linear IEF strips.

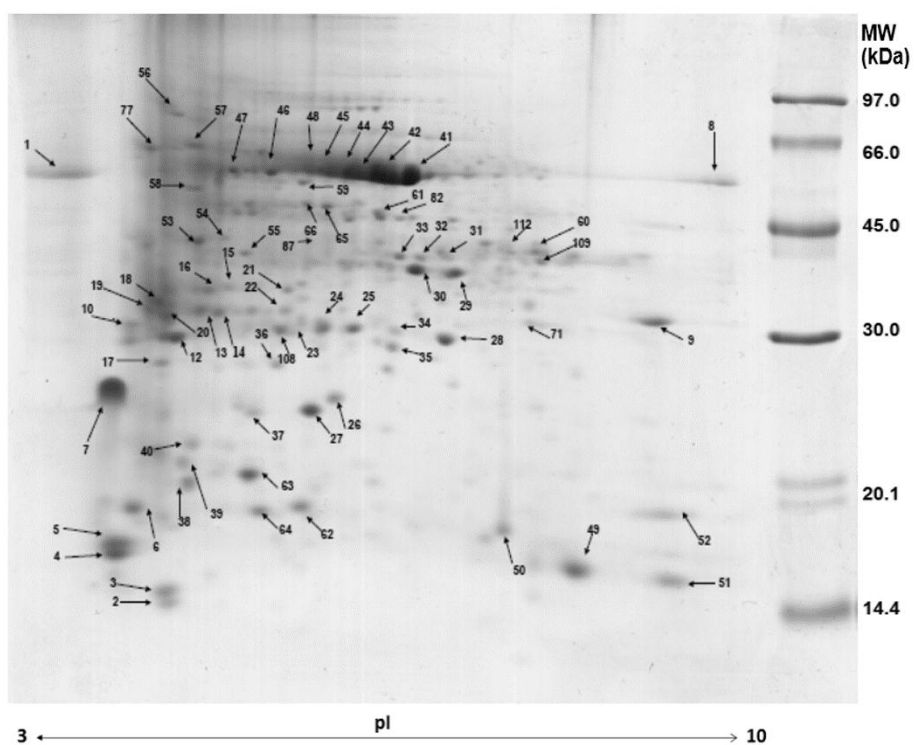


Figure 21 Representative 2-DE profiles of the 150 μ g protein isolated from *B. superba* leaves originated from Lampang (1) and collected from Banpong district, Ratchaburi province in winter (LW) at pH 3-10 using non-linear IEF strips.

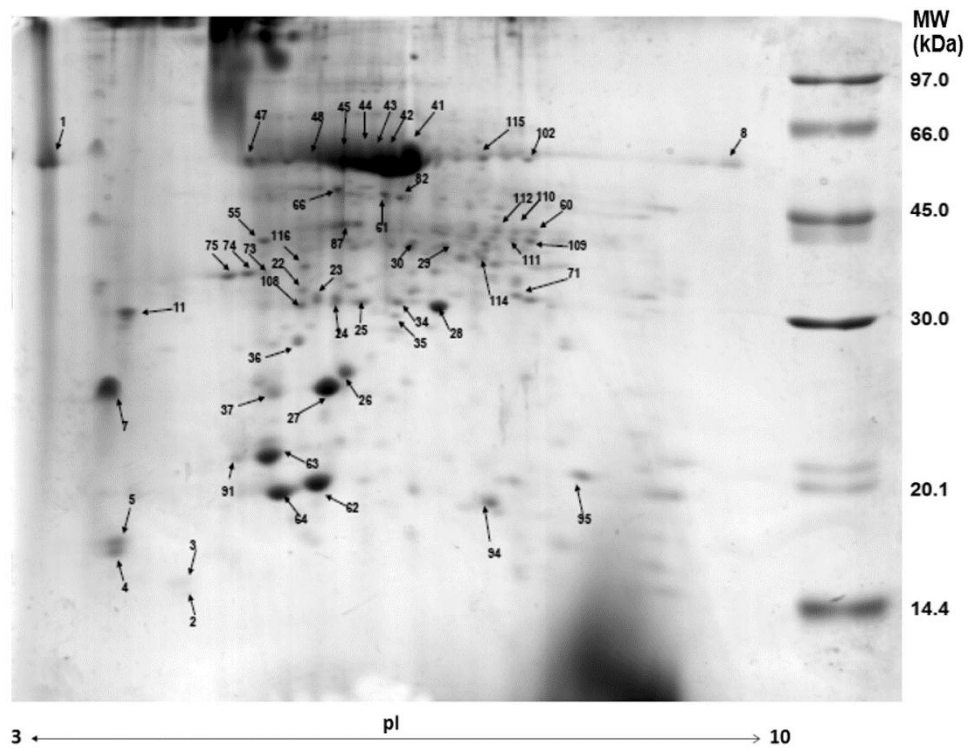


Figure 22 Representative 2-DE profiles of the 150 μg protein isolated from *B. superba* leaves originated from Lampang (1) and collected from Banpong district, Ratchaburi province in summer (LS) at pH 3-10 using non-linear IEF strips.

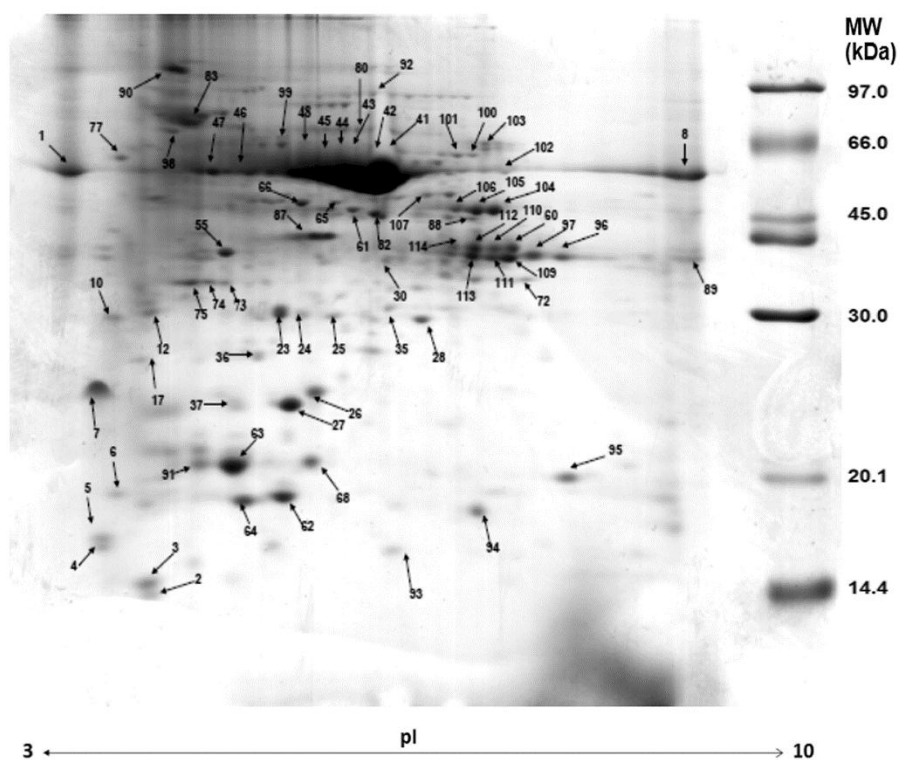


Figure 23 Representative 2-DE profiles of the 150 μg protein isolated from *B. superba* leaves originated from Saraburi (2) and collected from Banpong district, Ratchaburi province in rainy season (LR) at pH 3-10 using non-linear IEF strips.

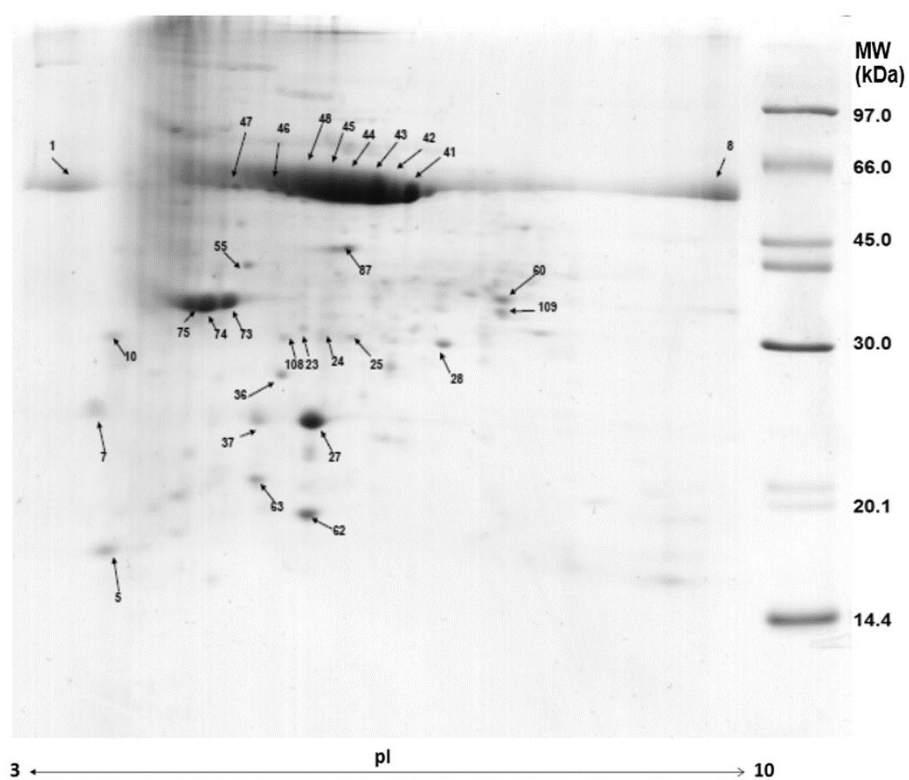


Figure 24 Representative 2-DE profiles of the 150 μg protein isolated from *B. superba* leaves originated from Saraburi (2) and collected from Banpong district, Ratchaburi province in summer (LS) at pH 3-10 using non-linear IEF strips.

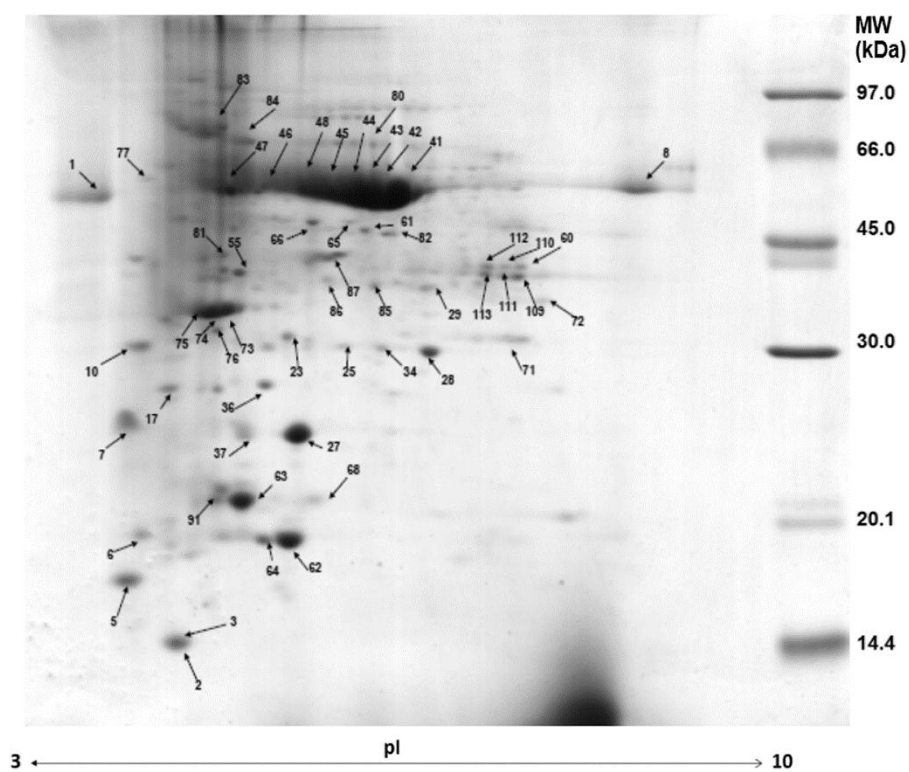


Figure 25 Representative 2-DE profiles of the 150 μg protein isolated from *B. superba* leaves originated from Chachoengsao (3) and collected from Banpong district, Ratchaburi province in rainy season (LR) at pH 3-10 using non-linear IEF strips.

Table 3 Protein spot appearance isolated from *B. superba* leaves originated from Lampang, Saraburi and Chachengsao in 2-DE gels

Spot no.	Accession number ^{a)}	Protein name	LW1	LS1	LR1	LS2	LR2	LR3
Functional group 1: Carbohydrate and energy metabolism								
13	gi 357507859	Phosphoglycolate phosphatase	✓	-	-	-	-	-
14	gi 357507859	Phosphoglycolate phosphatase	✓	-	-	-	-	-
24	gi 15226479	Triosephosphate isomerase	✓	✓	✓	-	✓	-
25	gi 57283985	Triosephosphate isomerase	✓	✓	✓	✓	✓	✓
28	gi 77540216	Triosephosphate isomerase	✓	-	✓	✓	-	✓
31	gi 83283965	Malate dehydrogenase-like protein	✓	✓	-	-	-	-
34	gi 77540216	Triosephosphate isomerase	✓	✓	✓	-	✓	-
46	gi 904085	Adenosine triphosphatase, partial (chloroplast)	✓	✓	-	✓	✓	✓
47	gi 91214148	ATP synthase CF1-alpha subunit	✓	✓	✓	✓	✓	✓
54	gi 357484753	Phosphoribulokinase	✓	-	-	-	-	-
60	gi 255543455	Glyceraldehyde -3-phosphate dehydrogenase	✓	✓	✓	-	✓	✓
61	gi 356525742	Phosphoglycerate kinase, chloroplastic-like	✓	✓	✓	-	✓	✓
79	gi 543176666	Alcohol dehydrogenase 1	-	-	✓	-	-	-
81	gi 5881134	Phosphoribulokinase	-	-	✓	-	-	✓
82	gi 351726690	Glyceraldehyde-3-phosphate dehydrogenase B	-	✓	✓	✓	-	✓
87	gi 120661	Glyceraldehyde-3-phosphate dehydrogenase A	-	✓	✓	✓	✓	✓
89	gi 120658	Glyceraldehyde-3-phosphate dehydrogenase A	-	-	-	-	✓	-
96	gi 255543455	Glyceraldehyde-3-phosphate dehydrogenase	-	-	✓	-	✓	-

Table 3 (Continued)

Spot no.	Accession number ^{a)}	Protein name	LW1	LS1	LR1	LS2	LR2	LR3
Functional group 1: Carbohydrate and energy metabolism								
97	gi 255543455	Glyceraldehyde-3-phosphate dehydrogenase	-	-	✓	-	✓	-
102	gi 356500643	NADP-dependent glyceraldehyde-3-phosphate dehydrogenase	-	✓	✓	-	✓	-
107	gi 255585914	Alcohol dehydrogenase, putative	-	-	-	-	✓	-
109	gi 255543455	Glyceraldehyde-3-phosphate dehydrogenase	-	✓	✓	✓	-	✓
110	gi 255543455	Glyceraldehyde-3-phosphate dehydrogenase	-	✓	✓	✓	-	✓
111	gi 255543455	Glyceraldehyde-3-phosphate dehydrogenase	-	✓	✓	✓	-	✓
112	gi 3023814	Glyceraldehyde-3-phosphate dehydrogenase	-	✓	✓	✓	-	✓
113	gi 255543455	Glyceraldehyde-3-phosphate dehydrogenase	-	✓	✓	✓	-	✓
114	gi 556796254	Glyceraldehyde-3-phosphate dehydrogenase	-	✓	✓	✓	-	✓
115	gi 357437219	NADP-dependent glyceraldehyde-3-phosphate dehydrogenase	-	✓	-	-	-	-
Functional group 2: Photosynthesis								
1	gi 3980231	Ribulose 1,5 biphosphate carboxylase-oxygenase large subunit	✓	✓	✓	✓	✓	✓
8	gi 18157251	Ribulose 1,5 biphosphate carboxylase-oxygenase large subunit Chloroplast photosynthetic water	✓	✓	✓	✓	✓	✓
15	gi 152143640	oxidation complex 33kDa subunit precursor	✓	-	-	-	-	-

Table 3 (Continued)

Spot no.	Accession number ^{a)}	Protein name	LW1	LS1	LR1	LS2	LR2	LR3
Functional group 2: Photosynthesis								
16	gij152143640	Chloroplast photosynthetic water oxidation complex 33kDa subunit precursor	✓	-	-	-	-	-
17	gij1079736	Ribulose 1,5-bisphosphate carboxylase small subunit	✓	-	✓	-	✓	✓
27	gij356501429	Oxygen-evolving enhancer protein 2						
37	gij356526942	Oxygen-evolving enhancer protein 2	✓	✓	✓	✓	✓	✓
39	gij1079736	Ribulose 1,5-bisphosphate carboxylase small subunit	✓	-	-	-	-	-
40	gij1079736	Ribulose 1,5-bisphosphate carboxylase small subunit	✓	-	-	-	-	-
41	gij2961268	Ribulose 1,5-bisphosphate carboxylase small subunit	✓	✓	✓	✓	✓	✓
42	gij1881501	Ribulose 1,5 bisphosphate carboxylase/oxygenase large subunit	✓	✓	✓	✓	✓	✓
43	gij2808617	Ribulose 1,5 bisphosphate carboxylase/oxygenase large subunit	✓	✓	✓	✓	✓	✓
44	gij1771817	Ribulose 1,5 bisphosphate carboxylase/oxygenase large subunit	✓	✓	✓	✓	✓	✓
45	gij1769935	Ribulose 1,5 bisphosphate carboxylase/oxygenase large subunit	✓	✓	✓	✓	✓	✓
48	gij11990290	Ribulose 1,5 bisphosphate carboxylase/oxygenase large subunit	✓	✓	✓	✓	✓	✓
49	gij77157637	Ribulose 1,5-bisphosphate carboxylase small subunit	✓	-	-	-	-	-

Table 3 (Continued)

Spot no.	Accession number ^{a)}	Protein name	LW1	LS1	LR1	LS2	LR2	LR3
Functional group 2: Photosynthesis								
50	gij132150	Ribulose 1,5-bisphosphate carboxylase small subunit	✓	-	-	-	-	-
51	gij1079736	Ribulose 1,5-bisphosphate carboxylase small subunit	✓	-	-	✓	-	-
55	gij356544404	Photosynthesis II stability/assembly factor HCF136	✓	✓	✓	✓	✓	✓
58	gij508726180	Ribulose 1,5 bisphosphate carboxylase/oxygenase large subunit	✓	-	-	-	-	-
73	gij356526942	Oxygen-evolving enhancer protein 1	-	✓	✓	✓	✓	✓
74	gij326467059	Oxygen-evolving enhancer protein 1	-	✓	✓	✓	✓	✓
75	gij326467059	Oxygen-evolving enhancer protein 1	-	✓	✓	✓	✓	✓
76	gij357507859	Phosphoglycolate phosphatase	-	-	✓	-	-	✓
80	gij671611	Ribulose 1,5 bisphosphate carboxylase-oxygenase large subunit	-	-	✓	-	✓	✓
94	gij20341	Ribulose bisphosphate carboxylase	-	✓	-	-	✓	-
99	gij1771248	Ribulose 1,5 bisphosphate carboxylase-oxygenase large subunit	-	-	-	-	✓	-
Functional group 3: Secondary metabolism								
20	gij508777952	NAD(P)-binding Rossmann-fold superfamily protein isoform 1	✓	-	-	-	-	-
29	gij351726399	Isoflavone reductase homolog 2	✓	✓	✓	-	-	✓
30	gij351726399	Isoflavone reductase homolog 2	✓	✓	✓	-	✓	-
32	gij351726399	Isoflavone reductase homolog 2	✓	✓	-	-	-	-
33	gij356518030	Isoflavone reductase homolog	✓	-	-	-	-	-
88	gij356549501	Probable cinnamyl alcohol dehydrogenase 1-like	-	-	✓	-	✓	-

Table 3 (Continued)

Spot no.	Accession number ^{a)}	Protein name	LW1	LS1	LR1	LS2	LR2	LR3
Functional group 4: Defense and Stress								
Defense								
93	gij632736	Pathogen- and wound-inducible antifungal protein CBP20 precursor	-	-	-	-	✓	-
Stress								
36	gij356556406	20 kDa chaperonin	✓	✓	✓	✓	✓	✓
56	gij356559803	Stromal 70 kDa heat shock-related protein	✓	-	-	✓	-	✓
57	gij171854980	Protein disulfide isomerase chloroplastic-like	✓	-	-	-	-	✓
83	gij502145084	Heat shock cognate 70kDa protein 2-like	-	-	✓	-	✓	✓
84	gij356549495	Heat shock 70 kDa protein, mitochondrial-like	-	-	✓	-	-	✓
Functional group 5: ROS scavenging and detoxifying								
21	gij502079139	Putative lactoylglutathione lyase-like isoform X1	✓	-	-	-	-	-
35	gij356526968	Glutathione S-transferase F10-like	✓	-	✓	-	-	-
64	gij134684	Superoxide dismutase [Cu-Zn], chloroplastic	✓	✓	✓	-	✓	✓
65	gij356577825	Monodehydroascorbate reductase	✓	-	✓	-	✓	✓
66	gij356533631	Monodehydroascorbate reductase -like isoform 1	✓	✓	✓	-	✓	✓
91	gij12230569	Superoxide dismutase [Cu-Zn]	-	✓	✓	-	✓	✓
116	gij356531939	Putative lactoylglutathione lyase-like	-	✓	-	-	-	-
Functional group 6: RNA metabolism								
10	gij21309	28kD RNA binding protein	✓	✓	✓	✓	✓	-
11	gij21309	28kD RNA binding protein	✓	✓	✓	-	✓	-

Table 3 (Continued)

Spot no.	Accession number ^{a)}	Protein name	LW1	LS1	LR1	LS2	LR2	LR3
Functional group 6: RNA metabolism								
52	gi 131772	40S ribosomal protein S14						
62	gi 359475330	Glycine-rich RNA-binding protein GRP1A-like	✓	✓	✓	✓	✓	✓
72	gi 351727433	Guanine nucleotide -binding protein subunit beta-like protein	-	-	✓	-	✓	✓
Functional group 7: Protein destination and storage								
23	gi 255544626	Proteasome subunit alpha type, putative	✓	✓	✓	✓	✓	✓
71	gi 356502736	Proteasome subunit alpha type- 7-like isoform 1	✓	✓	✓	✓	-	✓
108	gi 255544626	Proteasome subunit alpha type, putative	-	✓	-	-	-	-
Functional group 8: Amino-acid biosynthesis								
59	gi 351724777	Alanine aminotransferase 3 protein	✓	-	-	-	-	-
Functional group 9: Signal transduction and homeostasis								
18	gi 302122828	14-3-3g protein	✓	-	-	-	-	-
19	gi 1345588	14-3-3-like protein GF14-12	✓	-	-	-	-	-
69	gi 159470791	Exostosin-like glycosyltransferase	-	-	✓	-	-	-
77	gi 351726214	Calreticulin I precursor	-	✓	✓	✓	✓	✓
85	gi 294095	Ferredoxin NADP+ reductase, patial	-	✓	✓	-	-	✓
86	gi 356504476	NADP-dependent alkenal double bond reductase P1-like	-	-	✓	-	-	✓
95	gi 28380082	Maturase K	-	✓	✓	-	✓	-
100	gi 75207006	Ferric leghemoglobin reductase	-	-	-	-	✓	-
101	gi 75207006	Ferric leghemoglobin reductase	-	-	✓	-	-	✓
Functional group 10: Allergy								
9	gi 2921320	Beta-1,3-glucanase 5	✓	-	-	-	✓	-

Table 3 (Continued)

Spot no.	Accession number ^{a)}	Protein name	LW1	LS1	LR1	LS2	LR2	LR3
Functional group 10: Allergy								
12	gij25091405	Thaumatococcus protein 1	✓	-	-	-	-	-
Functional group 11: Protein biosynthesis								
68	gij124230	Eukaryotic translation initiation factor 5A-1	-	-	✓	-	✓	✓
Functional group 12: Others								
Fatty metabolism								
6	gij15236014	Lipase/lipoxygenase, PLAT/LH2 family protein	-	-	✓	-	✓	✓
Transcription								
63	gij62734702	Retrotransposon	✓	✓	✓	✓	✓	✓
Unknown								
2	gij527200637	Hypothetical protein M569_06763	✓	-	-	-	✓	✓
3	gij527200637	Hypothetical protein M569_06763	✓	-	-	-	✓	✓
22	gij557532497	Hypothetical protein CICLE_v10012559mg	✓	-	-	-	-	-
26	gij129320	Protein P21	✓	-	✓	-	✓	✓
38	gij502158725	Disease resistance response protein 206-like	✓	-	-	-	-	-
53	gij561036976	Hypothetical protein PHAVU_001G240200g	✓	-	-	-	-	-
67	gij38123356	Pathogenesis-related class 10 protein SPE-16	-	-	✓	-	-	-
70	gij217072770	Unknown	-	-	✓	-	-	-
78	gij356544363	Uncharacterized protein LOC100792883	-	-	✓	-	-	-
90	gij84453208	Putative cytosolic factor	-	-	-	-	✓	-
103	gij147797552	Hypothetical protein VITISV_037210	-	-	✓	✓	-	-

Table 3 (Continued)

Spot no.	Accession number ^{a)}	Protein name	LW1	LS1	LR1	LS2	LR2	LR3
Unknown								
104	gij363807510	Uncharacterized protein LOC100775490	-	-	-	-	✓	-
105	gij363807510	Uncharacterized protein LOC100775490	-	-	-	-	✓	-
106	gij363807510	Uncharacterized protein LOC100775490	-	-	-	-	✓	-
117	gij557532497	Hypothetical protein CICLE_v10012559mg	-	✓	-	-	-	-
^{a)} The protein's NCBI accession number								

Majority of protein spots in carbohydrate and energy metabolism, photosynthesis, RNA metabolism and protein destination and storage were similarly appeared in 3 seasons, while the differences of protein spots in proteomic abundance patterns among samples from different seasons and varieties were found to be involved in defense and stress, amino-acid biosynthesis, signal transduction and homeostasis, protein biosynthesis and allergy (Table 3).

4.3 Protein identification and functional classification

For protein identification, each protein spot on the 2-DE gels was subsequently analyzed using a nanoflow liquid chromatography coupled to electrospray ionization quadrupole-time-of-flight tandem mass spectrometry, followed by database search using MASCOT. The tuber results revealed the highest numbers of protein spots and a variety of proteins in winter-harvested samples from the 3 plant samples, whereas the leaves demonstrated the various protein spots in winter samples originated from Lampang. Fold changes were calculated by comparing the intensities of each individual protein spot in summer- and rainy season- harvested samples with these of the corresponding spot in winter- harvested samples. The matched peptides allowed identification of a total of 224 protein spots in tubers (Table 4) and 112 protein spots in leaves (Table 5) from different seasons, arranged according to their theoretical pI and molecular weight, respectively.

Table 4 Identified proteins of *B. superba* tubers originated from Lampang, Saraburi and Chachengsao were identified by

two-dimensional Polyacrylamide Gel electrophoresis (2D-PAGE) coupled with LC/MS/MS

Spot no.	Accession number ^{a)}	Protein name	Organism	Theoretical ^{b)} MW (Da)	pI	Score ^{c)}	Peptide match ^{d)}	% Coverage ^{e)}
Functional group 1: Allergy								
1	gi 3914435	Profilin-1	<i>Glycine max</i>	14091	4.58	46	13	16
41	gi 25091405	Thaumatin protein 1	<i>Prunus persica</i>	25748	8.29	64	1	4
57	gi 1619903	Thiol protease isoform B, partial	<i>Glycine max</i>	34946	7.60	44	1	2
111	gi 113781	Alpha-amylase	<i>Vigna mungo</i>	46859	5.45	73	6	5
Functional group 2: Carbohydrate and energy metabolism								
15	gi 1675394	Alcohol dehydrogenase 3	<i>Oryza sativa</i>	40802	6.78	54	12	13
22	gi 15235282	Glyceraldehyde -3-phosphate dehydrogenase	<i>Solms-laubachia</i>	13267	6.81	41	5	23
26	gi 2746513	Alcohol dehydrogenase 1,partial	<i>Leavenworthia uniflora</i>	36520	6.01	78	2	5
28	gi 77540216	Triosephosphate isomerase	<i>Glycine max</i>	27187	5.87	206	15	23
33	gi 57283985	Triosephosphate isomerase	<i>Phaseolus vulgaris</i> var. nanus	27183	5.87	144	3	10
58	gi 48508784	Glyceraldehyde -3-phosphate dehydrogenase	<i>Triticum aestivum</i>	36626	7.08	157	4	7

Table 4 (Continued)

Spot no.	Accession number ^{a)}	Protein name	Organism	Theoretical ^{b)} MW (Da)	pI	Score ^{c)}	Peptide match ^{d)}	% Coverage ^{e)}
Functional group 2: Carbohydrate and energy metabolism								
59	gi 351723699	Glyceraldehyde -3-phosphate dehydrogenase C subunit	<i>Glycine max</i>	36701	6.72	224	6	14
62	gi 307136111	Glyceraldehyde -3-phosphate dehydrogenase	<i>Cucumis melo</i>	36640	6.62	92	4	11
63	gi 211906450	Phosphoglycerate kinase,	<i>Gossypium hirsutum</i>	42237	5.97	77	28	20
65	gi 356525744	Phosphoglycerate kinase, cytosolic	<i>Glycine max</i>	42366	6.28	448	11	30
69	gi 418731090	Glyceraldehyde -3-phosphate dehydrogenase	<i>Solanum tuberosum</i>	36701	7.03	155	3	15
79	gi 363806992	V-type proton ATPase catalytic subunit A	<i>Glycine max</i>	68736	5.41	476	11	17
81	gi 356505318	Enolase	<i>Glycine max</i>	47628	5.92	350	10	18
82	gi 356513072	Phosphoglucomutase, cytoplasmic	<i>Glycine max</i>	63474	5.33	448	10	17
83	gi 357483399	Succinate dehydrogenase	<i>Medicago truncatula</i>	68879	6.10	314	4	6
84	gi 13467795	2,3-bisphosphoglycerate independent phosphoglycerate mutase	<i>Ricinus communis</i>	60780	5.52	201	4	6
85	gi 356524354	Phosphoglucomutase,cytoplasmic	<i>Glycine max</i>	63351	5.35	522	10	15
86	gi 22597178	Alcohol dehydrogenase 1	<i>Glycine max</i>	39981	6.19	212	4	9

Table 4 (Continued)

Spot no.	Accession number ^{a)}	Protein name	Organism	Theoretical ^{b)} MW (Da)	pI	Score ^{c)}	Peptide match ^{d)}	% Coverage ^{e)}
Functional group 2: Carbohydrate and energy metabolism								
87	gi 22597178	Alcohol dehydrogenase 1	<i>Glycine max</i>	39981	6.19	218	4	9
88	gi 22597178	Alcohol dehydrogenase 1	<i>Glycine max</i>	39981	6.19	227	6	11
89	gi 22597178	Alcohol dehydrogenase 1	<i>Glycine max</i>	39981	6.19	192	6	9
90	gi 22597178	Alcohol dehydrogenase 1	<i>Glycine max</i>	39981	6.19	73	19	7
91	gi 1351887	Alcohol dehydrogenase	<i>Malus x domestica</i>	41382	6.48	60	10	7
99	gi 351723699	Glyceraldehyde -3-phosphate dehydrogenase C subunit	<i>Glycine max</i>	36701	6.72	220	6	14
100	gi 380746853	Glyceraldehyde -3-phosphate dehydrogenase	<i>Cuscuta pentagona</i>	32268	6.97	141	7	24
101	gi 48508784	Glyceraldehyde -3-phosphate dehydrogenase	<i>Triticum aestivum</i>	36626	7.08	182	6	10
104	gi 71793966	Alcohol dehydrogenase	<i>Alnus glutinosa</i>	40971	6.28	161	4	10
105	gi 255585914	Alcohol dehydrogenase,putative	<i>Ricinus communis</i>	40718	6.37	66	5	5
106	gi 342851387	Alcohol dehydrogenase,putative	<i>Malus rockii</i>	35862	6.21	87	2	5
112	gi 356509324	Alcohol dehydrogenase 1	<i>Glycine max</i>	40897	5.97	232	6	10
113	gi 356525744	Phosphoglycerate kinase, cytosolic	<i>Glycine max</i>	42366	6.28	342	9	28

Table 4 (Continued)

Spot no.	Accession number ^{a)}	Protein name	Organism	Theoretical ^{b)}		Score ^{c)}	Peptide match ^{d)}	Peptide % Coverage ^{e)}
				MW (Da)	pI			
Functional group 2: Carbohydrate and energy metabolism								
115	gi 344190186	Enolase	<i>Corylus heterophylla</i>	49091	5.62	334	36	21
116	gi 445589	Alcohol dehydrogenase	<i>Glycine max</i>	34404	6.14	277	5	12
117	gi 445589	Alcohol dehydrogenase	<i>Glycine max</i>	34404	6.14	281	5	12
118	gi 445589	Alcohol dehydrogenase	<i>Glycine max</i>	34404	6.14	220	4	9
119	gi 445589	Alcohol dehydrogenase	<i>Glycine max</i>	34404	6.14	232	4	11
120	gi 22296818	Pyruvate kinase	<i>Glycine max</i>	55282	7.89	367	6	10
121	gi 356521618	Pyruvate kinase	<i>Glycine max</i>	54251	7.53	408	8	11
122	gi 1169534	Enolase	<i>Ricinus communis</i>	47883	5.56	411	7	18
123	gi 356530953	Enolase	<i>Glycine max</i>	47989	5.92	295	7	16
128	gi 22597178	Alcohol dehydrogenase 1	<i>Glycine max</i>	39981	6.19	189	3	7
129	gi 22597178	Alcohol dehydrogenase 1	<i>Glycine max</i>	39981	6.19	197	4	9
130	gi 470108526	Alcohol dehydrogenase 1	<i>Fragaria vesca</i>	41304	6.33	159	4	10
131	gi 22597178	Alcohol dehydrogenase 1	<i>Glycine max</i>	39981	6.19	231	5	9
138	gi 255538186	D-3-phosphoglycerate dehydrogenase, putative	<i>Ricinus communis</i>	63396	5.81	140	3	4

Table 4 (Continued)

Spot no.	Accession number ^{a)}	Protein name	Organism	Theoretical ^{b)} MW (Da)	pI	Score ^{c)}	Peptide match ^{d)}	Peptide % Coverage ^{e)}
Functional group 2: Carbohydrate and energy metabolism								
139	gi 356536246	ATP synthase subunit beta , mitochondrial	<i>Glycine max</i>	59799	5.80	50	5	6
140	gi 351724891	Enolase	<i>Glycine max</i>	47689	5.31	237	6	9
141	gi 1169534	Enolase	<i>Ricinus communis</i>	47883	5.56	403	9	18
143	gi 226492645	Vacuolar ATP synthase subunit B	<i>Zea mays</i>	54028	5.07	422	11	13
166	gi 33149681	Pyruvate decarboxylase	<i>Dianthus caryophyllus</i>	65401	5.99	196	6	9
171	gi 22597178	Alcohol dehydrogenase 1	<i>Glycine max</i>	39981	6.19	180	4	9
172	gi 125662890	Glyceraldehyde -3-phosphate dehydrogenase	<i>Beta vulgaris</i>	36650	6.77	70	3	11
173	gi 75110834	UDP- sugar pyrophosphorylase	<i>Pisum sativum</i>	66136	5.87	219	4	6
174	gi 351727947	UDP- sugar pyrophosphorylase 1	<i>Glycine max</i>	66085	5.70	215	5	7
175	gi 3023814	Glyceraldehyde -3-phosphate dehydrogenase,	<i>Craterostigma plantagineum</i>	36454	7.06	147	4	7
176	gi 120666	Glyceraldehyde -3-phosphate dehydrogenase	<i>Antirrhinum majur</i>	36662	8.30	111	3	5
183	gi 356536246	ATP synthase subunit beta , mitochondrial	<i>Glycine max</i>	59799	5.80	50	5	6

Table 4 (Continued)

Spot no.	Accession number ^{a)}	Protein name	Organism	Theoretical ^{b)} MW (Da)	pI	Score ^{c)}	Peptide match ^{d)}	% Coverage ^{e)}
Functional group 2: Carbohydrate and energy metabolism								
186	gi 22597178	Alcohol dehydrogenase 1	<i>Glycine max</i>	39981	6.19	187	3	7
196	gi 149391151	Glyceraldehyde -3-phosphate dehydrogenase	<i>Oryza sativa</i>	28297	8.62	370	9	23
			Indica Group					
200	gi 22296818	Pyruvate kinase	<i>Glycine max</i>	55282	7.89	692	16	24
202	gi 22597178	Alcohol dehydrogenase 1	<i>Glycine max</i>	39981	6.19	189	3	7
203	gi 502117964	Enolase-phosphatase E1	<i>Cicer arietinum</i>	53391	4.38	41	1	1
205	gi 1169534	Enolase	<i>Ricinus communis</i>	47883	5.56	112	3	5
207	gi 1169534	Enolase	<i>Glycine max</i>	47883	5.56	257	6	10
211	gi 356536246	ATP synthase subunit beta	<i>Glycine max</i>	59799	5.80	423	9	15
214	gi 356561923	Glucan endo-1,3-beta-glucosidase 5	<i>Glycine max</i>	84337	5.61	95	2	2
216	gi 543176666	Alcohol dehydrogenase 1	<i>Phaseolus vulgaris</i>	41328	6.39	94	2	4
219	gi 71793966	Alcohol dehydrogenase	<i>Alnus glutinosa</i>	40971	6.28	149	4	11
220	gi 356552857	Pyruvate dehydrogenase E1 component subunit beta, mitochondrial	<i>Glycine max</i>	38751	5.80	144	3	8

Table 4 (Continued)

Spot no.	Accession number ^{a)}	Protein name	Organism	Theoretical ^{b)} MW (Da)	pI	Score ^{c)}	Peptide match ^{d)}	Peptide % Coverage ^{e)}
Functional group 3: Photosynthesis								
157	gi 18157251	Ribulose 1,5-bisphosphate carboxylase-oxygenase	<i>Butea minor</i>	51578	6.04	470	10	20
158	gi 229464442	Ribulose-1,5-bisphosphate carboxylase/oxygenase	<i>Hylomecon japonica</i>	51502	6.00	370	8	18
159	gi 229464442	Ribulose-1,5-bisphosphate carboxylase/oxygenase	<i>Hylomecon japonica</i>	51502	6.00	316	6	13
Functional group 4: Cellular structure								
60	gi 356549751	Stern-specific protein TSJT1 isoform 1	<i>Glycine max</i>	28029	6.30	136	3	14
110	gi 356558578	Actin-101	<i>Glycine max</i>	41626	5.31	228	12	16
144	gi 1351202	Tubulin beta chain	<i>Glycine max</i>	45721	5.63	533	12	28
180	gi 356558578	Actin-101	<i>Glycine max</i>	41626	5.31	189	5	12
208	gi 356560917	Tubulin alpha-3 chain	<i>Glycine max</i>	49053	5.10	209	5	11
215	gi 1498330	Actin,partial	<i>Glycine max</i>	37150	5.38	243	5	18
Functional group 5: Defense and Stress								
Defense								
36	gi 357465811	Omega-amidase NIT2	<i>Medicago truncatula</i>	39012	7.11	77	5	9
51	gi 974782	Cobalamine-independent methionine synthase	<i>Solenostemon</i>	86717	6.17	121	2	3

Table 4 (Continued)

Spot no.	Accession number ^{a)}	Protein name	Organism	Theoretical ^{b)} MW (Da)	pI	Score ^{c)}	Peptide match ^{d)}	Peptide % Coverage ^{e)}
Functional group 5: Defense and Stress								
Defense								
64	gij356514703	Omega-amidase, NIT2	<i>Glycine max</i>	38534	7.68	317	6	14
68	gij356514703	Omega-amidase, NIT2	<i>Glycine max</i>	38534	7.68	226	6	10
92	gij351724907	Methionine synthase	<i>Glycine max</i>	84230	5.93	79	12	8
96	gij351724907	Methionine synthase	<i>Glycine max</i>	84230	5.93	297	5	8
97	gij351724907	Methionine synthase	<i>Glycine max</i>	84230	5.93	331	6	9
98	gij351724907	Methionine synthase	<i>Glycine max</i>	84230	5.93	236	5	9
195	gij359807014	Desiccation-related protein At2g46140	<i>Glycine max</i>	34343	4.74	172	7	16
Stress								
5	gij349591294	Class I small heat shock protein 20.1	<i>Solanum lycopersicum</i>	17628	5.82	123	5	17
7	gij351721881	18.5 kDa class I heat shock protein	<i>Glycine max</i>	18491	5.82	238	6	26
9	gij351721881	18.5 kDa class I heat shock protein	<i>Glycine max</i>	18491	5.82	312	8	32
10	gij41059801	Small heat shock protein	<i>Prunus persica</i>	17380	5.98	55	1	5

Table 4 (Continued)

Spot no.	Accession number ^{a)}	Protein name	Organism	Theoretical ^{b)} MW (Da)	pI	Score ^{c)}	Peptide match ^{d)}	% Coverage ^{e)}
Functional group 5: Defense and Stress								
Stress								
11	gi 123556	18.2 kDa class I heat shock protein	<i>Medicago sativa</i>	18154	5.81	132	3	15
12	gi 356496106	18.2 kDa class I heat shock protein	<i>Glycine max</i>	16362	5.56	88	7	16
13	gi 38639431	17.5 kDa class I heat shock protein	<i>Carica papaya</i>	17471	5.31	76	6	12
14	gi 356559136	17.4 kDa class III heat shock protein	<i>Glycine max</i>	17959	6.17	97	2	14
19	gi 255582541	Heat shock protein, putative	<i>Ricinus communis</i>	26082	8.59	161	4	11
20	gi 161291483	Heat shock protein	<i>Ammopiptanthus</i>	26082	7.66	165	3	12
74	gi 356500683	Heat shock protein 70 kDa protein	<i>Glycine max</i>	71582	5.20	343	38	24
75	gi 211906504	Heat shock protein 70 kDa protein	<i>Gossypium hirsutum</i>	70952	5.11	304	31	27
77	gi 186898205	Heat shock protein 70 kDa protein	<i>Hevea brasiliensis</i>	71694	5.27	52	14	16
78	gi 356549495	Heat shock 70 kDa protein, mitochondrial	<i>Glycine max</i>	72383	5.68	317	7	9
134	gi 449439307	Chaperone protein ClpB1	<i>Cucumis sativus</i>	100877	5.99	182	5	4
135	gi 356519114	Chaperone protein ClpB1	<i>Glycine max</i>	84629	6.18	288	6	9

Table 4 (Continued)

Spot no.	Accession number ^{a)}	Protein name	Organism	Theoretical ^{b)} MW (Da)	pI	Score ^{c)}	Peptide match ^{d)}	% Coverage ^{e)}
Functional group 5: Defense and Stress								
Stress								
136	gi 449439307	Chaperone protein ClpB1	<i>Cucumis sativus</i>	100877	5.99	182	5	5
137	gi 449439307	Chaperone protein ClpB1	<i>Cucumis sativus</i>	100877	5.99	104	2	1
177	gi 356516495	Chaperone protein ClpC_chloroplastic	<i>Glycine max</i>	102434	6.09	588	13	11
178	gi 356508861	Chaperone protein ClpC_chloroplastic	<i>Glycine max</i>	102490	6.16	108	4	4
179	gi 356501703	Heat shock protein 90	<i>Glycine max</i>	89661	5.25	290	8	8
181	gi 20559	Heat shock protein 70 (AA 6-651)	<i>Petunia x hybrida</i>	70738	5.07	103	3	6
182	gi 356501703	Heat shock protein 90	<i>Glycine max</i>	89661	5.25	275	7	7
189	gi 21807	Heat shock protein 17.3	<i>Triticum aestivum</i>	17342	5.58	49	1	6
190	gi 351721881	18.5 kDa class I heat shock protein	<i>Glycine max</i>	18491	5.82	146	4	19
191	gi 99033689	Chaperone	<i>Agave tequilana</i>	18325	6.19	150	4	16
192	gi 356519335	26.5 kDa heat shock	<i>Glycine max</i>	24584	9.11	142	3	11
204	gi 356519335	26.5 kDa heat shock protein, mitochondrial	<i>Glycine max</i>	24584	9.11	166	4	11
221	gi 356559136	17.4 kDa class III heat shock protein	<i>Glycine max</i>	17959	6.17	155	3	14

Table 4 (Continued)

Spot no.	Accession number ^{a)}	Protein name	Organism	Theoretical ^{b)} MW (Da)	pI	Score ^{c)}	Peptide match ^{d)}	Peptide % Coverage ^{e)}
Functional group 5: Defense and Stress								
Stress								
222	gi 16930753	Small heat shock protein	<i>Retama raetam</i>	17880	5.82	161	4	18
223	gi 543177195	CHP-rich zinc finger protein	<i>Phaseolus vulgaris</i>	26411	5.81	165	4	12
224	gi 508712741	Chloroplast heat shock protein 70 isoform 3	<i>Theobroma cacao</i>	75464	5.40	465	10	15
Functional group 6: ROS scavenging and detoxifying								
2	gi 13274150	Putative cytosolic CuZn-superoxide	<i>Populus tremula</i> x <i>Populus tremuloides</i>	15186	5.47	63	3	13
3	gi 225451120	Superoxide dismutase [Cu-Zn] isoform 2	<i>Vitis vinifera</i>	15272	5.49	159	7	26
4	gi 134684	Superoxide dismutase [Cu-Zn] chloroplastic	<i>Petunia hybrida</i>	22302	6.17	58	5	12
32	gi 355626968	Glutathione S- transferase F10	<i>Glycine max</i>	25708	6.12	148	4	12
34	gi 225448353	Hydroxyglutathione hydrolase cytoplasmic	<i>Vitis vinifera</i>	28651	5.53	67	1	3
37	gi 120969450	Cytosolic ascorbate peroxidase	<i>Arachis hypogaea</i>	27034	5.52	47	9	28
47	gi 152227376	S- formylglutathione hydrolase	<i>Arabidopsis thaliana</i>	31635	5.91	124	4	9
56	gi 3556531939	Putative lactoylglutathione lyase	<i>Glycine max</i>	33451	6.14	263	6	18

Table 4 (Continued)

Spot no.	Accession number ^{a)}	Protein name	Organism	Theoretical ^{b)} MW (Da)	pI	Score ^{c)}	Peptide match ^{d)}	Peptide % Coverage ^{e)}
Functional group 6: ROS scavenging and detoxifying								
61	gi 225448353	Hydroxyacylglutathione hydrolase cytoplasmic	<i>Vitis vinifera</i>	28651	5.53	56	1	3
107	gi 356577825	Monodehydroascorbate reductase	<i>Glycine max</i>	47011	5.49	202	4	9
109	gi 356533631	Monodehydroascorbate reductase isoform 1	<i>Glycine max</i>	46822	5.73	159	4	10
114	gi 356577825	Monodehydroascorbate reductase	<i>Glycine max</i>	47011	5.49	257	6	13
124	gi 356509058	Peroxidase 52 isoform 1	<i>Glycine max</i>	34503	9.14	46	3	7
125	gi 356496705	Peroxidase 72 isoform 1	<i>Glycine max</i>	36417	9.23	66	3	7
126	gi 449457510	Peroxidase 72	<i>Cucumis sativus</i>	37424	9.18	208	4	11
150	gi 6714837	Glutathione reductase, cytosolic	<i>Glycine max</i> <i>Populus</i>	58703	8.12	274	7	14
151	gi 224133228	Glutathione reductase	<i>trichocarpa</i>	60545	7.69	205	4	6
154	gi 356559573	Glutathione reductase	<i>Glycine max</i>	53958	5.63	141	4	6
161	gi 50058096	Glutathione reductase	<i>Zinnia violacea</i>	60947	8.75	185	4	6
199	gi 62909961	Peroxidase	<i>Pisum sativum</i>	38032	5.84	188	5	9

Table 4 (Continued)

Spot no.	Accession number ^{a)}	Protein name	Organism	Theoretical ^{b)} MW (Da)	pI	Score ^{c)}	Peptide match ^{d)}	Peptide %	Coverage ^{e)}
Functional group 7: Amino-acid biosynthesis									
27	gi 26245395	Nucleoside diphosphate kinase	<i>Glycine max</i>	16344	6.91	114	2	12	
50	gi 15235282	D-3-phosphoglycerate dehydrogenase	<i>Arabidopsis thaliana</i>	63286	8.54	83	1	2	
53	gi 4255689399	Branched-chain-amino- acid aminotransferase,	<i>Glycine max</i>	35948	6.28	243	5	13	
55	gi 42568800	Branched-chain-amino-acid aminotransferase 5	<i>Arabidopsis thaliana</i>	45552	8.03	125	3	6	
70	gi 356536156	D-3-phosphoglycerate dehydrogenase, chloroplastic	<i>Glycine max</i>	63573	6.32	654	10	18	
80	gi 356536156	D-3-phosphoglycerate dehydrogenase	<i>Glycine max</i>	62573	6.32	632	11	18	
93	gi 356547867	5-methyltetrahydro pteroyltriglutamate -homocysteine methyltransferase	<i>Glycine max</i>	89014	6.33	473	9	11	
94	gi 356508448	5-methyltetrahydro pteroyltriglutamate -homocysteine methyltransferase	<i>Glycine max</i>	88609	6.41	420	7	10	
95	gi 356508448	5-methyltetrahydro pteroyltriglutamate -homocysteine methyltransferase	<i>Glycine max</i>	88609	6.41	474	10	13	

Table 4 (Continued)

Spot no.	Accession number ^{a)}	Protein name	Organism	Theoretical ^{b)} MW (Da)	pI	Score ^{c)}	Peptide match ^{d)}	% Coverage ^{e)}
Functional group 7: Amino-acid biosynthesis								
<i>Populus</i>								
102	g 134142075	Serine hydroxymethyltransferase	<i>tremuloides</i>	51944	7.18	228	5	8
138	g 255538186	D-3-phosphoglycerate dehydrogenase,putative	<i>Ricinus communis</i>	63396	5.81	140	3	4
146	g 341958461	Chloroplast acetohydroxy acid isomeroeductase	<i>Glycine max</i>	63569	7.14	170	3	4
147	g 341958461	Chloroplast acetohydroxy acid isomeroeductase	<i>Glycine max</i>	63569	7.14	204	4	6
148	g 341958461	Chloroplast acetohydroxy acid isomeroeductase	<i>Glycine max</i>	63569	7.14	189	3	6
149	g 341958461	Chloroplast acetohydroxy acid isomeroeductase	<i>Glycine max</i>	63569	7.14	209	5	8
162	g 356536156	D-3-phosphoglycerate dehydrogenase	<i>Glycine max</i>	62573	6.32	765	12	21
163	g 356536156	D-3-phosphoglycerate dehydrogenase	<i>Glycine max</i>	62573	6.32	539	8	14
164	g 356536156	D-3-phosphoglycerate dehydrogenase	<i>Glycine max</i>	62573	6.32	705	12	20
167	g 341958461	Chloroplast acetohydroxy acid isomeroeductase	<i>Glycine max</i>	63569	7.14	234	5	8
168	g 341958461	Chloroplast acetohydroxy acid isomeroeductase	<i>Glycine max</i>	63569	7.14	205	4	7
169	g 6225542	Chloroplast acetohydroxy acid isomeroeductase	<i>Glycine max</i>	62812	6.62	162	5	5
170	g 356536156	D-3-phosphoglycerate dehydrogenase	<i>Glycine max</i>	62573	6.32	387	6	10
185	g 113204693	Homocystein S-methyltransferase	<i>Medicago sativa</i>	32607	4.97	53	1	3

Table 4 (Continued)

Spot no.	Accession number ^{a)}	Protein name	Organism	Theoretical ^{b)} MW (Da)	pI	Score ^{c)}	Peptide match ^{d)}	% Coverage ^{e)}
Functional group 7: Amino-acid biosynthesis								
201	gi 389548688	Serine hydroxymethyl-transferase	<i>Glycine max</i>	51733	7.59	418	9	17
212	gi 502082432	Ketol-acid reductoisomerase	<i>Cicer arietinum</i>	63532	6.18	170	4	5
218	gi 356536156	D-3-phosphoglycerate dehydrogenase	<i>Glycine max</i>	62573	6.32	644	10	19
Functional group 8: Signal transduction and homeostasis								
8	gi 151347490	Translation initiation factor	<i>Carica papaya</i>	17421	5.60	159	5	17
27	gi 26245395	Nucleoside diphosphate kinase	<i>Glycine max</i>	16344	6.91	114	2	12
43	gi 1052778	Ferritin	<i>Pisum sativum</i>	28629	6.01	109	7	9
45	gi 3023194	14-3-3 protein A	<i>Glycine max</i>	29031	4.72	160	4	15
48	gi 67107029	14-3-3 protein	<i>Manihot esculenta</i>	29813	4.75	295	7	21
54	gi 356504476	NADP-dependent alkenal double bond reductase P1	<i>Glycine max</i>	37905	5.81	170	4	11
66	gi 3023847	Guanine nucleotide-binding protein subunit beta protein	<i>Medicago sativa</i>	35644	7.07	46	7	19
67	gi 212292267	Rack	<i>Phaseolus vulgaris</i>	35580	7.60	53	16	36
76	gi 356526803	Probable nucleoredoxin 1	<i>Glycine max</i>	64172	4.86	277	8	8

Table 4 (Continued)

Spot no.	Accession number ^{a)}	Protein name	Organism	Theoretical ^{b)} MW (Da)	pI	Score ^{c)}	Peptide match ^{d)}	% Coverage ^{e)}
Functional group 8: Signal transduction and homeostasis								
193	gi 1052778	Ferritin-3, chloroplastic	<i>Vigna unguiculata</i>	28426	5.54	84	1	3
194	gi 67107029	14-3-3 protein	<i>Manihot esculenta</i>	29813	4.75	240	7	18
206	gi 159470791	Exostosin-like glycosyltransferase	<i>Chlamydomonas reinhardtii</i>	56018	8.95	41	1	1
209	gi 26245395	Nucleoside diphosphate kinase	<i>Glycine max</i>	16344	6.91	105	2	12
210	gi 302847713	Acetylglucosaminyltransferase	<i>Volvox carteri</i>	29019	4.74	54	1	2
Functional group 9: Protein biosynthesis								
6	gi 33325131	Eukaryotic translation initiation factor 5A isoform VIII	<i>Hevea brasiliensis</i>	17344	5.60	55	10	31
8	gi 151347490	Translation initiation factor	<i>Carica papaya</i>	17421	5.60	159	5	17
49	gi 225438420	Eukaryotic translation initiation factor 6-2 isoform 1	<i>Vitis vinifera</i>	26473	4.77	97	6	17
132	gi 356525774	Elongation factor 2	<i>Glycine max</i>	93982	5.80	291	7	7
133	gi 356556977	Elongation factor 2	<i>Glycine max</i>	93996	5.80	316	9	9
165	gi 1170509	Eukaryotic translation initiation factor 4A	<i>Hevea brasiliensis</i>	46898	5.31	553	12	23
197	gi 399414	Elongation factor 1- alpha	<i>Triticum aestivum</i>	49138	9.20	257	6	12

Table 4 (Continued)

Spot no.	Accession number ^{a)}	Protein name	Organism	Theoretical ^{b)} MW (Da)	pI	Score ^{c)}	Peptide match ^{d)}	% Coverage ^{e)}
Functional group 10: Protein destination and storage								
16	gi 502132065	Proteasome subunit beta type	<i>Cicer arietinum</i>	25110	5.12	207	4	16
29	gi 356526807	Proteasome subunit beta type-1	<i>Glycine max</i>	24573	6.20	144	4	15
30	gi 227937349	20S proteasome beta subunit 5	<i>Citrus maxima</i>	29244	5.89	166	5	13
38	gi 356496249	Proteasome subunit alpha type-4 isoform 1	<i>Glycine max</i>	27294	5.96	59	8	29
40	gi 356496096	Proteasome subunit alpha type-2-A	<i>Glycine max</i>	25608	5.51	266	6	23
Functional group 11: Cell cycle and division								
46	gi 413916456	Cyclin superfamily protein,putative	<i>Zea mays</i>	44233	8.88	41	1	1
127	gi 413916456	Cyclin superfamily protein,putative	<i>Zea mays</i>	44233	8.88	36	1	1
145	gi 356508699	Cell division cycle protein 48 homolog	<i>Glycine max</i>	90826	5.11	311	8	7
152	gi 356539207	Apoptosis-inducing factor homolog A	<i>Glycine max</i>	39271	9.43	81	2	4
156	gi 356496197	Proliferation-associated protein 2G4	<i>Glycine max</i>	42946	6.30	290	6	15

Table 4 (Continued)

Spot no.	Accession number ^{a)}	Protein name	Organism	Theoretical ^{b)} MW (Da)	pI	Score ^{c)}	Peptide match ^{d)}	% Coverage ^{e)}
Functional group 12: Others								
Fatty acid metabolism								
17	gi 363808072	Allene oxide cyclase 4, chloroplastic	<i>Glycine max</i>	28394	8.75	68	2	6
18	gi 358345896	Allene-oxide cyclase	<i>Medicago truncatula</i>	27932	8.54	87	4	5
217	gi 502140113	Lipoxygenase homology	<i>Cicer arietinum</i>	21310	6.05	112	2	8
Plant hormone metabolism								
31	gi 84579412	9-cis-epoxycarotenoid dioxygenase 4	<i>Lactuca sativa</i>	64049	7.65	37	1	1
Secondary metabolism								
52	gi 356538206	Isoflavone reductase homolog A622	<i>Glycine max</i>	33973	6.12	130	2	7
Protein transport								
72	gi 255561582	Patellin-3, putative	<i>Ricinus communis</i>	69576	4.76	108	3	3
Translation								
153	gi 223469633	S18 ribosomal protein	<i>Jatropha curcas</i>	17599	10.46	178	4	21
Protein translocation								
184	gi 460378451	Luminal-binding protein 5	<i>Solanum lycopersicum</i>	73444	5.07	188	4	5

Table 4 (Continued)

Spot no.	Accession number ^{a)}	Protein name	Organism	Theoretical ^{b)} MW (Da)	pI	Score ^{c)}	Peptide match ^{d)}	Peptide % Coverage ^{e)}
Functional group 12: Others								
Unknown								
21	gi 363807526	Uncharacterized protein LOC100798019 precursor	<i>Glycine max</i>	26013	7.77	70	13	17
23	gi 351723665	Uncharacterized protein LOC100306050 precursor	<i>Glycine max</i>	16723	5.16	54	1	7
24	gi 351723665	Uncharacterized protein LOC100306050 precursor	<i>Glycine max</i>	16723	5.16	54	1	7
35	gi 300392456	SEC 13 family	<i>Lotus japonicus</i>	32598	5.59	130	3	9
39	gi 255647220	Unknown	<i>Glycine max</i>	27162	5.60	300	38	54
42	gi 255637227	Unknown	<i>Glycine max</i>	29152	5.94	57	12	11
44	gi 255637227	Unknown	<i>Glycine max</i>	29152	5.94	52	12	17
71	gi 8894548	Hypothetical protein	<i>Cicer arietinum</i> <i>Medicago</i>	54901	4.87	89	6	5
73	gi 358348031	Gene X-like protein	<i>truncatula</i>	77534	8.25	58	2	2
103	gi 356525790	Nitrile-specifier protein-5	<i>Glycine max</i>	35707	5.59	113	2	7
108	gi 255636611	Unknown	<i>Glycine max</i>	47417	5.76	120	15	14

Table 4 (Continued)

Spot no.	Accession number ^{a)}	Protein name	Organism	Theoretical ^{b)} MW (Da)	pI	Score ^{c)}	Peptide match ^{d)}	% Coverage ^{e)}
Functional group 12: Others								
Unknown								
142	gi 357520365	Protein toIB	<i>Medicago truncatula</i>	76488	6.52	191	4	5
155	gi 357520365	Protein toIB	<i>Medicago truncatula</i>	76488	6.52	191	4	5
160	gi 255580564	Nutrient reservoir, putative	<i>Ricinus communis</i>	38947	6.97	102	2	5
198	gi 359807022	Uncharacterized protein LOC100813980	<i>moellendorffii</i>	39118	9.39	79	2	4
213	gi 502120564	Uncharacterized protein LOC101500213	<i>Cicer arietinum</i>	120841	5.79	543	11	10

^{a)} The protein's NCBI accession number

^{b)} Theoretical molecular mass (Da) and pI of the protein spot found in database

^{c)} The protein's score from MS/MS ion-search

^{d)} Peptide fragments submitted to the database matched the protein identified

^{e)} The percentage of the protein's sequence those peptide fragments.

Table 5 Identified proteins of *B.superba* leaves originated from Lampang, Saraburi and Chachengsao were identified by two-dimensional Polyacrylamide Gel electrophoresis (2D-PAGE) coupled with LC/MS/MS

Spot no.	Accession number ^{a)}	Protein name	Organism	Theoretical ^{b)} MW (Da)	Score ^{c)}	Peptide match ^{d)}	Peptide % Coverage ^{e)}	
Functional group 1: Carbohydrate and energy metabolism								
13	gi 357507859	Phosphoglycolate phosphatase	<i>Medicago truncatula</i>	40307	6.90	178	5	10
14	gi 357507859	Phosphoglycolate phosphatase	<i>Medicago truncatula</i>	40307	6.90	195	5	10
24	gi 15226479	Triosephosphate isomerase	<i>Arabidopsis thaliana</i>	33325	7.67	47	1	4
25	gi 57283985	Triosephosphate isomerase	<i>Phaseolus vulgaris var. nanus</i>	27183	5.87	146	2	8
28	gi 77540216	Triosephosphate isomerase	<i>Glycine max</i>	27187	7.67	393	8	31
31	gi 83283965	Malate dehydrogenase-like protein	<i>Solanum tuberosum</i>	35463	5.74	176	4	9

Table 5 (Continued)

Spot no.	Accession number ^{a)}	Protein name	Organism	Theoretical ^{b)} MW (Da)	pI	Score ^{c)}	Peptide match ^{d)}	Peptide % Coverage ^{e)}
Functional group 1: Carbohydrate and energy metabolism								
34	gi 77540216	Triosephosphate isomerase	<i>Glycine max</i>	27187	5.87	126	4	13
46	gi 904085	Adenosine triphosphatase, partial (chloroplast)	<i>Boquila trifoliolata</i>	53577	4.97	370	7	16
47	gi 91214148	ATP synthase CF1-alpha subunit	<i>Glycine max</i>	55719	5.15	265	6	10
54	gi 357484753	Phosphoribulokinase	<i>Medicago truncatula</i>	45661	6.68	165	5	12
60	gi 255543455	Glyceraldehyde -3-phosphate dehydrogenase	<i>Ricinus communis</i>	43087	8.14	495	10	25
61	gi 356525742	Phosphoglycerate kinase, chloroplastic-like	<i>Glycine max</i>	50236	7.79	454	8	18
79	gi 543176666	Alcohol dehydrogenase 1	<i>Phaseolus vulgaris</i>	41328	6.39	250	5	11
81	gi 5881134	Phosphoribulokinase	<i>Beta vulgaris</i>	30596	5.15	189	4	11
82	gi 351726690	Glyceraldehyde-3-phosphate dehydrogenase B	<i>Glycine max</i>	48199	7.10	394	7	15

Table 5 (Continued)

Spot no.	Accession number ^{a)}	Protein name	Organism	Theoretical ^{b)} MW (Da)	pI	Score ^{c)}	Peptide match ^{d)}	Peptide % Coverage ^{e)}
Functional group 1: Carbohydrate and energy metabolism								
87	gij120661	Glyceraldehyde-3-phosphate dehydrogenase A	<i>Nicotiana tabacum</i>	41837	6.60	91	3	10
89	gij120658	Glyceraldehyde-3-phosphate dehydrogenase A	<i>Pisum sativum</i>	43312	8.80	72	2	6
96	gij255543455	Glyceraldehyde-3-phosphate dehydrogenase	<i>Ricinus communis</i>	43087	8.14	621	15	31
97	gij255543455	Glyceraldehyde-3-phosphate dehydrogenase	<i>Ricinus communis</i>	43087	8.14	495	10	25
102	gij356500643	NADP-dependent glyceraldehyde-3-phosphate dehydrogenase	<i>Glycine max</i>	53217	6.76	167	5	11
107	gij255585914	Alcohol dehydrogenase, putative	<i>Ricinus communis</i>	40718	6.37	93	2	4
109	gij255543455	Glyceraldehyde-3-phosphate dehydrogenase	<i>Ricinus communis</i>	43087	8.14	677	16	35

Table 5 (Continued)

Spot no.	Accession number ^{a)}	Protein name	Organism	Theoretical ^{b)} MW (Da)	Score ^{c)} pl	Peptide match ^{d)}	% Coverage ^{e)}	
Functional group 1: Carbohydrate and energy metabolism								
110	gi 255543455	Glyceraldehyde-3-phosphate dehydrogenase	<i>Ricinus communis</i>	43087	8.14	495	10	25
111	gi 255543455	Glyceraldehyde-3-phosphate dehydrogenase	<i>Ricinus communis</i>	43087	8.14	677	16	35
112	gi 3023814	Glyceraldehyde-3-phosphate dehydrogenase	<i>Craterostigma plantagineum</i>	36454	7.06	93	1	4
113	gi 255543455	Glyceraldehyde-3-phosphate dehydrogenase	<i>Ricinus communis</i>	43087	8.14	395	9	25
114	gi 556796254	Glyceraldehyde-3-phosphate dehydrogenase	<i>Phaseolus vulgaris</i>	5668	4.31	58	1	39
115	gi 357437219	NADP-dependent glyceraldehyde-3-phosphate dehydrogenase	<i>Medicago truncatula</i>	53275	8.12	256	8	15

Table 5 (Continued)

Spot no.	Accession number ^{a)}	Protein name	Organism	Theoretical ^{b)} MW (Da)	Score ^{c)} pl	Peptide match ^{d)}	Peptide % Coverage ^{e)}
Functional group 2: Photosynthesis							
1	gi 3980231	Ribulose 1,5 biphosphate carboxylase-oxygenase large subunit	<i>Stewartia pseudocamellia</i>	51268	6.46	400 9	20
8	gi 18157251	Ribulose 1,5 biphosphate carboxylase-oxygenase large subunit	<i>Butea minor</i>	51578	6.04	450 10	23
15	gi 152143640	Chloroplast photosynthetic water oxidation complex 33kDa subunit precursor	<i>Morus nigra</i>	28249	5.48	173 4	10
16	gi 152143640	Chloroplast photosynthetic water oxidation complex 33kDa subunit precursor	<i>Morus nigra</i>	28249	5.48	74 6	10
17	gi 1079736	Ribulose 1,5-biphosphate carboxylase small subunit	<i>Glycine soja</i>	19962	8.80	87 2	8

Table 5 (Continued)

Spot no.	Accession number ^{a)}	Protein name	Organism	Theoretical ^{b)} MW (Da)	pI	Score ^{c)}	Peptide match ^{d)}	% Coverage ^{e)}
Functional group 2: Photosynthesis								
27	gi 356501429	Oxygen-evolving enhancer protein 2	<i>Glycine max</i>	28000	7.68	134	5	13
37	gi 356526942	Oxygen-evolving enhancer protein 2	<i>Glycine max</i>	28212	6.96	126	3	8
39	gi 1079736	Ribulose 1,5-bisphosphate carboxylase small subunit	<i>Glycine soja</i>	19962	8.80	120	3	12
40	gi 1079736	Ribulose 1,5-bisphosphate carboxylase small subunit	<i>Glycine soja</i>	19962	8.80	98	2	8
41	gi 2961268	Ribulose 1,5-bisphosphate carboxylase small subunit	<i>Iserfia pittieri</i>	52641	6.10	234	5	7
42	gi 1881501	Ribulose 1,5 bisphosphate carboxylase/oxygenase large subunit	<i>Psychotria peteri</i>	52000	6.32	364	8	15
43	gi 2808617	Ribulose 1,5 bisphosphate carboxylase/oxygenase large subunit	<i>Phylloglossum</i>	50190	6.90	335	8	12
44	gi 1771817	Ribulose 1,5 bisphosphate carboxylase/oxygenase large subunit	<i>Touroulia guianensis</i>	51662	6.13	371	8	18

Table 5 (Continued)

Spot no.	Accession number ^{a)}	Protein name	Organism	Theoretical ^{b)} MW (Da)	Score ^{c)}	Peptide match ^{d)}	% Coverage ^{e)}	
Functional group 2: Photosynthesis								
45	gi 1769935	Ribulose 1,5 biphosphate carboxylase/oxygenase large subunit	<i>Burchellia bubalina</i>	51911	6.12	312	6	12
48	gi 11990290	Ribulose 1,5 biphosphate carboxylase/oxygenase large subunit	<i>Prismatomeris beccariana</i>	51742	6.04	201	4	8
49	gi 77157637	Ribulose 1,5-biphosphate carboxylase small subunit	<i>Panax ginseng</i>	20534	8.57	126	3	9
50	gi 132150	Ribulose 1,5-biphosphate carboxylase small subunit	<i>Pinus thunbergii</i>	19300	8.80	65	2	8
51	gi 1079736	Ribulose 1,5-biphosphate carboxylase small subunit	<i>Glycine soja</i>	19962	8.80	193	4	20
55	gi 356544404	Photosynthesis II stability/assembly factor HCF136	<i>Oryza sativa</i> subsp. <i>japonica</i>	43281	6.79	655	16	37
58	gi 508726180	Ribulose 1,5 biphosphate carboxylase/oxygenase large subunit	<i>Theobroma cacao</i>	48338	5.56	137	3	6

Table 5 (Continued)

Spot no.	Accession number ^{a)}	Protein name	Organism	Theoretical ^{b)} MW (Da)	Score ^{c)}	Peptide match ^{d)}	% Coverage ^{e)}
Functional group 2: Photosynthesis							
73	gij356526942	Oxygen-evolving enhancer protein 1	<i>Litchi chinensis</i>	35165	6.96	132	3
74	gij326467059	Oxygen-evolving enhancer protein 1	<i>Litchi chinensis</i>	35165	5.86	175	4
75	gij326467059	Oxygen-evolving enhancer protein 1	<i>Litchi chinensis</i>	35165	5.86	98	5
76	gij357507859	Phosphoglycolate phosphatase	<i>Medicago truncatula</i>	40307	5.15	199	6
80	gij671611	Ribulose 1,5 bisphosphate carboxylase-oxygenase large subunit	<i>Prostanthera nivea</i>	52365	6.33	283	5
94	gij20341	Ribulose bisphosphate	<i>Oryza sativa</i>	19456	8.26	49	1
99	gij1771248	carboxylase large subunit	<i>Maackia amurensis</i>	50367	6.33	101	3

Table 5 (Continued)

Spot no.	Accession number ^{a)}	Protein name	Organism	Theoretical ^{b)} MW (Da)	Score ^{c)}	Peptide match ^{d)}	% Coverage ^{e)}
Functional group 3: Secondary metabolism							
20	gi 508777952	NAD(P)-binding Rossmann-fold superfamily protein isoform 1	<i>Theobroma cacao</i>	31979	7.62	151	3 6
29	gi 351726399	Isoflavone reductase homolog 2	<i>Glycine max</i>	33919	5.60	190	4 12
30	gi 351726399	Isoflavone reductase homolog 2	<i>Glycine max</i>	33919	5.60	206	5 16
32	gi 351726399	Isoflavone reductase homolog 2	<i>Glycine max</i>	33919	5.60	171	4 11
33	gi 356518030	Isoflavone reductase homolog	<i>Glycine max</i>	43079	6.10	239	5 12
88	gi 356549501	Probable cinnamyl alcohol dehydrogenase 1-like	<i>Glycine max</i>	38616	6.88	148	4 7
Functional group 4: Defense and Stress							
Defense							
93	gi 632736	Pathogen- and wound-inducible antifungal protein CBP20 precursor	<i>Nicotiana tabacum</i>	21907	8.40	54	1 6

Table 5 (Continued)

Spot no.	Accession number ^{a)}	Protein name	Organism	Theoretical ^{b)} MW (Da)	pI	Score ^{c)}	Peptide match ^{d)}	% Coverage ^{e)}
Functional group 4: Stress								
36	gi 356556406	20 kDa chaperonin	<i>Glycine max</i>	26653	7.79	235	5	16
56	gi 356559803	Stromal 70 kDa heat shock-related protein	<i>Glycine max</i>	73709	5.20	267	5	6
57	gi 171854980	Protein disulfide isomerase chloroplastic-like	<i>Glycine max</i>	58554	5.13	191	5	10
83	gi 502145084	Heat shock cognate 70kDa protein 2-like	<i>Cicer arietinum</i>	71128	5.11	445	10	15
84	gi 356549495	Heat shock 70 kDa protein, mitochondrial-like	<i>Glycine max</i>	72383	5.68	370	8	10
Functional group 5: ROS scavenging and detoxifying								
21	gi 502079139	Putative lactoylglutathione lyase-like isoform X1	<i>Cicer arietinum</i>	37148	6.04	153	4	10

Table 5 (Continued)

Spot no.	Accession number ^{a)}	Protein name	Organism	Theoretical ^{b)} MW (Da)	Score ^{c)} pI	Peptide match ^{d)}	Peptide % Coverage ^{e)}
Functional group 5: ROS scavenging and detoxifying							
35	gij 356526968	Glutathione S-transferase F10-like	<i>Glycine max</i>	25708	6.15 277	7	16
64	gij 134684	Superoxide dismutase [Cu-Zn], chloroplastic	<i>Petunia x hybrida</i>	22302	6.17 139	4	12
65	gij 356577825	Monodehydroascorbate reductase	<i>Glycine max</i>	47011	5.49 192	3	8
66	gij 356533631	Monodehydroascorbate reductase - like isoform 1	<i>Glycine max</i>	46822	5.73 137	3	6
91	gij 12230569	Superoxide dismutase [Cu-Zn]	<i>Medicago sativa</i>	20813	6.02 38	1	6
116	gij 356531939	Putative lactoylglutathione lyase-like	<i>Glycine max</i>	33451	6.14 259	7	23
Functional group 6: RNA metabolism							
10	gij 21309	28kD RNA binding protein	<i>Spinacia oleracea</i>	24498	4.42 90	2	8

Table 5 (Continued)

Spot no.	Accession number ^{a)}	Protein name	Organism	Theoretical ^{b)} MW (Da)	pI	Score ^{c)}	Peptide match ^{d)}	Peptide % Coverage ^{e)}
Functional group 6: RNA metabolism								
11	gi 21309	28kD RNA binding protein	<i>Spinacia oleracea</i>	24498	4.42	92	2	8
52	gi 131772	40S ribosomal protein S14	<i>Zea mays</i>	16248	10.70	57	1	7
62	gi 359475330	Glycine-rich RNA-binding protein GRP1A-like	<i>Vitis vinifera</i>	16319	6.32	112	3	23
72	gi 351727433	Guanine nucleotide-binding protein subunit beta-like protein	<i>Glycine max</i>	35586	7.62	156	6	20
Functional group 7: Protein destination and storage								
23	gi 255544626	Proteasome subunit alpha type, putative	<i>Ricinus communis</i>	25582	5.73	219	4	17
71	gi 356502736	Proteasome subunit alpha type-7-like isoform 1	<i>Glycine max</i>	27085	5.82	242	4	15
108	gi 255544626	Proteasome subunit alpha type, putative	<i>Ricinus communis</i>	25582	5.73	219	4	17

Table 5 (Continued)

Spot no.	Accession number ^{a)}	Protein name	Organism	Theoretical ^{b)} MW (Da)	Score ^{c)}	Peptide match ^{d)}	% Coverage ^{e)}
Functional group 8: Amino-acid biosynthesis							
59	gi 351724777	Alanine aminotransferase 3 protein	<i>Glycine max</i>	53390	239	5	10
Functional group 9: Signal transduction and homeostasis							
18	gi 302122828	14-3-3g protein	<i>Gossypium hirsutum</i>	29405	332	9	23
19	gi 1345588	14-3-3-like protein GF14-12	<i>Zea mays</i>	29618	122	3	9
69	gi 159470791	Exostosin-like glycosyltransferase	<i>Chlamydomonas reinhardtii</i>	56018	49	2	1
77	gi 351726214	Calreticulin I precursor	<i>Glycine max</i>	48114	79	2	7
85	gi 294095	Ferredoxin NADP+ reductase, partial	<i>Pisum sativum</i>	10721	151	3	27
86	gi 356504476	NADP-dependent alkenal double bond reductase P1-like	<i>Glycine max</i>	37905	261	6	17
95	gi 28380082	Maturase K	<i>Adesmia lanata</i>	60976	52	1	3

Table 5 (Continued)

Spot no.	Accession number ^{a)}	Protein name	Organism	Theoretical ^{b)} MW (Da)	pI	Score ^{c)}	Peptide match ^{d)}	% Coverage ^{e)}
Functional group 9: Signal transduction and homeostasis								
100	gi 75207006	Ferric leghemoglobin reductase	<i>Vigna unguiculata</i>	55745	8.08	81	2	4
101	gi 75207006	Ferric leghemoglobin reductase	<i>Vigna unguiculata</i>	55745	8.08	164	5	10
Functional group 10: Allergy								
9	gi 2921320	Beta-1,3- β -glucanase 5	<i>Glycine max</i>	25522	8.42	47	1	7
12	gi 25091405	Thaumatococcus-like protein 1	<i>Prunus persica</i>	25748	8.29	62	1	4
Functional group 11: Protein biosynthesis								
68	gi 124230	Eukaryotic translation initiation factor 5A-1	<i>Medicago sativa</i>	17648	5.48	73	2	9
Functional group 12: Others								
Fatty metabolism								
6	gi 15236014	Lipase/lipoxygenase,PLAT/LH2 family protein	<i>Arabidopsis thaliana</i>	20123	4.97	61	1	4

Table 5 (Continued)

Spot no.	Accession number ^{a)}	Protein name	Organism	Theoretical ^{b)} MW (Da)	pI	Score ^{c)}	Peptide match ^{d)}	Peptide % Coverage ^{e)}
Functional group 12: Others								
Transcription								
63	gi 62734702	Retrotransposon	<i>Pseudotsuga</i>	138642	8.77	40	1	0
Unknown								
2	gi 527200637	Hypothetical protein M569_06763	<i>Gentisea aurea</i>	13163	4.60	48	1	5
3	gi 527200637	Hypothetical protein M569_06763	<i>Gentisea aurea</i>	13163	4.60	37	1	5
22	gi 557532497	Hypothetical protein CICLE_v10012559mg	<i>Citrus clementina</i>	27352	6.11	111	2	7
26	gi 129320	Protein P21	<i>Glycine max</i>	21449	7.68	125	2	10
38	gi 502158725	Disease resistance response protein 206-like	<i>Cicer ariletinum</i>	20849	5.10	127	2	11

Table 5 (Continued)

Spot no.	Accession number ^{a)}	Protein name	Organism	Theoretical ^{b)} MW (Da)	pI	Score ^{c)}	Peptide match ^{d)}	% Coverage ^{e)}
Functional group 12: Others								
Unknown								
53	gi 561036976	Hypothetical protein PHAVU_001G240200g	<i>Phaseolus vulgaris</i>	41634	5.94	367	6	15
67	gi 38123356	Pathogenesis-related class 10 protein SPE-16	<i>Pachyrhizus erosus</i>	15798	5.02	58	1	6
70	gi 217072770	Unknown	<i>Medicago truncatula</i>	28143	7.66	80	2	6
78	gi 356544363	Uncharacterized protein LOC100792883	<i>Glycine max</i>	149573	4.69	421	10	6
90	gi 84453208	Putative cytosolic factor	<i>Trifolium pretense</i>	67827	4.72	130	4	7
103	gi 147797552	Hydrothermal protein VITISV_037210	<i>Vitis vinifera</i>	78877	6.01	36	1	1

Table 5 (Continued)

Spot no.	Accession number ^{a)}	Protein name	Organism	Theoretical ^{b)} MW (Da)	Score ^{c)}	Peptide match ^{d)}	% Coverage ^{e)}
Functional group 12: Others							
Unknown							
104	gi 363807510	Uncharacterized protein LOC100775490	<i>Glycine max</i>	44109	157	5	12
105	gi 363807510	Uncharacterized protein LOC100775490	<i>Glycine max</i>	44109	189	4	12
106	gi 363807510	Uncharacterized protein LOC100775490	<i>Glycine max</i>	44109	81	3	10
117	gi 57532497	Hypothetical protein CICLE_v10012559mg	<i>Citrus clementina</i>	27352	111	2	7

^{a)} The protein's NCBI accession number ^{b)} Theoretical molecular mass (Da) and pI of the protein spot found in database

^{c)} The protein's score from MS/MS ion-search ^{d)} Peptide fragments submitted to the database matched the protein identified

^{e)} The percentage of the protein's sequence those peptide fragments.

4.3.1 Protein identification and functional classification in tubers

Out of the 224 proteins spots, 87 were found in rainy season-, 131 in summer-, and 136 in winter-collected samples originated from Lampang, 124 were found in rainy season-, 130 in summer-, and 141 in winter- collected samples originated from Saraburi and 94 were found in rainy season-, 120 in summer, and 184 in winter-collected samples originated from Chachoengsao, respectively (Table 6). Remarkably, the winter-collected samples exhibited higher numbers and more diverse protein spots than other seasons. Plants might respond to cold by inducing responsive gene expression, stress-inducible genes expression and combination of other stresses (Shinozaki and Yamaguchi-Shinozaki, 2000).

Table 6 A number of protein spots of *B. superba* tubers were identified using 2-DE coupled with LC/MS/MS

Originated source	Rainy season (TR)	Summer (TS)	Winter (TW)
Lampang (1)	87	131	136
Saraburi (2)	124	130	141
Chachoengsao (3)	94	120	184

The found proteins could be categorized into 12 functional groups (Figure 26), including carbohydrate and energy metabolism (30.80%), amino-acid biosynthesis (11.61%), reactive oxygen species (ROS) scavenging and detoxifying (8.93%), signal transduction and homeostasis (6.25%), cellular structure (2.68%), protein destination and storage (2.23%), protein biosynthesis (3.13%), allergy (1.79%), cell cycle and division (2.23%), photosynthesis (1.34%) and others: fatty acid metabolism, plant hormone metabolism, secondary metabolism, protein transport, translation, and unknown (10.71%).

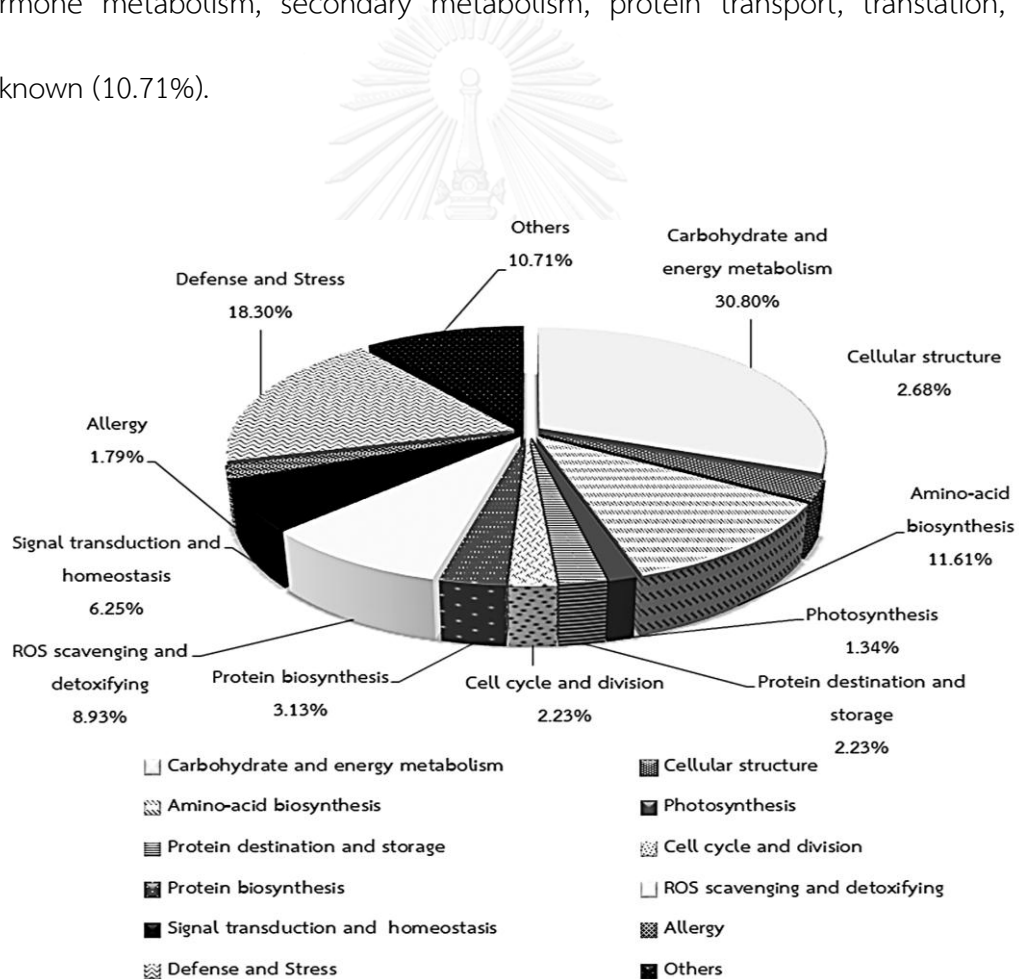


Figure 26 Functional distribution of 224 protein spots identified in *B. superba* tubers.

The largest functional group of identified proteins was associated with carbohydrate and energy metabolism which appeared directly related to diverse biological processes during growth and development. For examples, triosephosphate isomerase (spot no. 28) and glyceraldehyde-3-phosphate dehydrogenase (spot no. 58, 59, 62, 69, 99, 100, 101, 172) were involved in glycolysis. Protein spots associated with gluconeogenesis process such as alcohol dehydrogenase (spot no. 91, 104, 105, 106, 116, 117) alcohol dehydrogenase I (spot no. 90, 186) and alcohol dehydrogenase III (spot no. 15) and succinate dehydrogenase (spot no. 83) were also involved in cellular respiration. Yet, other groups of identified proteins allowed plants to adapt to various environments, including heat shock protein in HSP families, small heat shock in sHSP families, methionine synthase (spot no. 96) and cobalamine-independent methionine synthase (spot no. 51). Furthermore, eight protein spots were associated with ROS scavenging and detoxifying, namely, the copper/zinc-like isoform 2 of superoxide dismutase (spot no. 3, 4), glutathione S-transferase F10 (spot no. 32), cytosolic ascorbate peroxidase (spot no. 37), S-formylglutathione hydrolase (spot no. 47), lactoylglutathione lyase (spot no. 56), monodehydroascorbate reductase (spot no. 107, 114), and glutathione reductase (spot no. 150). Because of the occurrence of isoforms from post-translational modifications, it might result in the similar protein in several spots (Jungsukcharoen et al., 2016).

4.3.2 Protein identification and functional classification in leaves

Out of the 112 proteins spots, 60 were found in rainy season, 50 in summer, and 69 in winter originated from Lampang, 69 were found in rainy season and 28 in summer originated from Saraburi and 53 were found in rainy season originated from Chachoengsao, respectively (Table 7).

Table 7 A number of protein spots of *B. superba* leaves were identified using 2-DE gels coupled with LC/MS/MS

Originated source	Rainy season (LR)	Summer (LS)	Winter (LW)
Lampang (1)	60	50	69
Saraburi (2)	69	28	-
Chachoengsao (3)	53	-	-

The results exhibited the winter-harvested samples originated from Lampang exhibited a number of protein spots equal to the rainy season-harvested samples originated from Saraburi, however, the winter-harvested samples originated from Lampang were more diverse protein spots than rainy season-harvested samples originated from Saraburi and the other seasons. The identified proteins could be classified into 12 major functional classes (Figure 27).

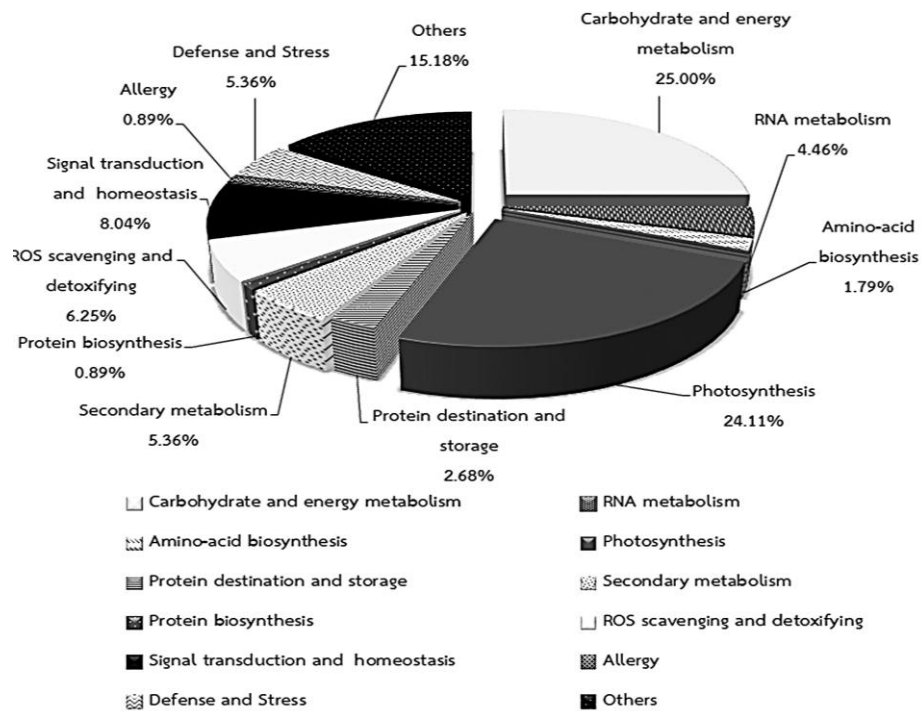


Figure 27 Functional classification of 112 protein spots identified in *B. superba* leaves.

As expected in plant leaf tissues, more than half of proteins were in the groups of carbohydrate and energy metabolism (25%) and photosynthesis (24.11%). The largest functional group of identified proteins was associated with carbohydrate and energy metabolism which appeared directly related to diverse biological processes during growth and development. For example, triosephosphate isomerase (spot no. 24, 25, 28, 34), ATP synthase CF1-alpha subunit (spot no. 47) and glyceraldehyde-3-phosphate dehydrogenase (spot no. 60, 82, 87, 96-97, 109-115) were involved in glycolysis. Then, other groups of identifiable proteins allowed plants to involve

photosynthesis such as ribulose-1,5-bisphosphate carboxylase/oxygenase large subunit (spot no. 1, 8, 42-48, 58, 80) and oxygen-evolving enhancer protein 2 (spot no. 27, 37). The rest of the proteins were found in the following categories: secondary metabolism (5.36%), defense and stress (5.36%), reactive oxygen species (ROS) scavenging and detoxifying (6.25%), RNA metabolism (4.46%), protein destination and storage (2.68%), signal transduction and homeostasis (8.04%), allergy (0.89%), amino-acid biosynthesis (1.79%), protein biosynthesis (0.89%) and others (15.18%); transferase, fatty acid metabolism, plant hormone metabolism, protein transport, transcription, RNA metabolism and unknown. Due to the occurrence of isoforms from post-translational modifications, it might result in the similar protein in several spots (Jungsukcharoen et al., 2016).

During seasonal changes, functional groups of proteins from tubers and leaves were similarities or differences, which were related to changes in protein relative abundances because temperature-protein interactions might influence on protein expression, multiple changes of the amino acid sequence, adaptable changes of structural, kinetic and stable properties among homologues of proteins, protein folding including interspecific variations in the thermal stability of protein, acclimation of enzymatic activities with compensation for temperature alterations, and efficiency of catalytic rates (Jaenicke et al., 1990; Somera, 1995). In addition, the stability of proteins could be limited under low or high temperatures (Jaenicke et al., 1990).

4.4 Proteins with differential levels in different seasons

4.4.1 Proteins with differential levels in different seasons in tubers

All categorized proteins were analyzed for changes and differences using the Image Master 2-DE program. Since our results from previous section showed the highest numbers of proteins in the winter-harvested samples originated from Chachoengsao, thus fold changes were calculated by dividing the intensity of each protein spot in summer- and rainy season- with that in winter-harvested sample. The exhibited 17 and 12 protein spots were statistically-significantly increased, and 14 and 8 protein spots were statistically-significantly decreased in summer- and rainy season-harvested samples, respectively.

Among the identified differentially-abundant proteins, 45 proteins belonging to 10 functional groups were found involving in important metabolic pathways and therefore picked for further discussion (Table 8 and Figure 28-32).

Functional group 1: Allergy. Allergy is initiated from hypersensitivity reactions of immune system. In plants, allergen was derived from defense response system to fight against pathogen (Sinha et al., 2014). Some allergic proteins were also used as basic regulator in cell structure. One of the well-known allergic-response proteins is

profilin-1, which belongs to families of profilin. Proteins in profilin families are small actin-binding proteins, which serve as key regulators to stimulate actin polymerization in various signaling pathways such as cell movement, cytokinesis, cell elongation, signaling and the growth of pollen tubes and root hairs (Hauser et al., 2008), (Radauer and Breiteneder, 2007). Recent studies demonstrated that expression of the allergenic profilins derived from monocot and dicots pollens in flowering plants, plant-derived foods and latexes. Thus profilins were considered as pan-allergens, which moderate the highly conserved structure and cross-reactivity of immunoglobulin E antibodies. Previous immunoblot analysis showed that when profilin bound to immunoglobulin E, a higher frequency of sensitization in pollen-allergic patients and plant food allergens could be observed (Santos and Van Ree, 2011).

In the study, the identified for spot 1 was matched well with the peptide sequence profilin-1 from *Glycine max* (% sequence coverage=16; protein score=46). Further comparative analysis indicated that profilin-1 level was statistically-significantly increased by 1.31-fold in rainy season- as compared with the winter-harvested samples (Table 8 and Figure 28). The varied level of profilin can be induced by climate changes, environmental conditions and abiotic stresses that may play significant roles of pathogen defense responses and modification of the actin filaments (Songnuan, 2013). Profilin-1 expression can be stimulated, whereas dehydrated weather was shown to increase in expression of the allergenic transcripts and proteins and protein-ligand

interactions for the regulation of biological functions in Ragweed (*Ambrosia artemisiifolia*) (Kelish et al., 2014), (Shinozaki and Yamaguchi-Shinozaki, 2000).

Functional group 2: Carbohydrate and energy metabolism. Carbohydrates provide essential sources of energy in plants. Their synthesis and catabolism therefore often involves multiple biochemical reactions, which are tightly regulated. In the study, the six enzymes in this functional group whose abundant levels were altered among different seasons were triosephosphate isomerase (spot 28) alcohol dehydrogenase (spot 105, 116, 117), alcohol dehydrogenase I (spot 186), glyceraldehyde-3-phosphate dehydrogenase (spot no. 58, 62, 69) and enolase (spot no. 81, 115, 122, 123, 140). Specifically, triosephosphate isomerase (spot 28) was statistically-significantly increased by 1.89-fold in summer- as compared with winter-harvested samples, nevertheless; glyceraldehyde-3-phosphate dehydrogenase (spot 58) and alcohol dehydrogenase (spot 116) were statistically-significantly decreased by 1.64-fold and 1.52-fold in summer- as compared with winter-harvested samples, respectively. The spot 81 and 115 of enolase were statistically-significantly decreased by 1.59-fold, 1.85-fold, 1.75-fold, and 2.22-fold in summer-and rainy season- as compared with winter-harvested samples, respectively, whereas the spot 122 was statistically-significantly decreased by 1.39-fold in rainy season- as compared with winter-harvested samples.

The spot 105 with significant sequence similarity to alcohol dehydrogenase from *Ricinus communis* (% sequence coverage =5; protein score = 66) was statistically-significantly decreased by 1.72-fold and 1.64-fold in summer-and rainy season- as compared with winter-harvested samples, whereas the spot 62 and 69 of glyceraldehyde-3-phosphate dehydrogenase were statistically-significantly increased by 1.77-fold and 1.88-fold in rainy season- as compared with winter-harvested samples, respectively. The spot 123 and 140 of enolase was statistically-significantly increased by 1.68-fold and 2.06-fold in rainy season- as compared with winter-harvested samples. Moreover, alcohol dehydrogenase (spot 117) was statistically-significantly increased by 1.92-fold and 2.72-fold in summer-and rainy season- as compared with winter-harvested samples, respectively, while and alcohol dehydrogenase I (spot 186) was statistically-significantly increased by 1.99-fold and 4.88-fold in summer-and rainy season- as compared with winter-harvested samples, respectively (Table 8 and Figure 30). Most proteins showed high scores in our protein identification process, which were potentially due to the structural conservation of these important proteins among different species.

Coincidentally with the seasonal changes, triosephosphate isomerase is involved in glycolysis and catalyzes the interconversion between D-glyceraldehyde-3-phosphate and dihydroxyacetone phosphate. The process mediated energy, which is extensively needed in summer for photosynthesis (Janmohammadi et al., 2015). In

addition, some glycolytic enzymes are also involved in cellular energy production needed for growth and development including tuber maturation and tuberization (Boonmee et al., 2011), which highly occurs during summer under high temperature. For glyceraldehyde-3-phosphate dehydrogenase, the enzyme converts D-glyceraldehyde-3-phosphate into 1,3-bisphosphoglycerate. Also, enolase catalyzes the formation of phosphoenolpyruvate from 2-phosphoglycerate. Because of metabolic flexibility to enable plant response to environmental stresses (Ma et al., 2013), the results of densitometric analysis of the proteins were variable during summer and rainy season.

Another proteins, alcohol dehydrogenase and alcohol dehydrogenase I are associated with gluconeogenesis (Chokchaichamnankit et al., 2009). By facilitating the interconversion between alcohols and aldehydes, alcohol dehydrogenase initiates a pyruvate decarboxylase bypass by converting acetaldehyde into ethanol and NAD^+ in anaerobic glycolysis or ethanolic fermentation instead of metabolizes into pyruvate and acetyl-CoA (Bolton, 2009). Moreover, the enzyme accelerates energy production in pollen tube growth and development (Gass et al., 2005). Pollen tube growth occurs during spring and early summer before winter dormancy, appearing as conifer (Fernando et al., 2005). The enzymes are actively used for shoot growth in rhizome and storage roots during dormancy, which was shown in *Curcuma alimatifolia* (Chokchaichamnankit et al., 2009). Because this leads to energy storage instead of

turning it into energy, either decrease or increase were found in summer and rainy season.

One of the electrogenic H⁺-pump proteins was V-type proton ATPase, which is the central H⁺-pump occurring at the side of endomembrane of plants. It is directly involved in energizing of the secondary transport, solute homeostasis and enabling vesicle fusion within cells (Dietz et al., 2001). The V-type proton ATPase catalytic subunit A (spot 79) was statistically-significantly increased by 1.48-fold in summer- as compared with winter-harvested samples, respectively (Table 8 and Figure 23). It might be regulated by gene expression in response to various stress conditions during severed seasonal changes with adaption of the V-ATPase (Dietz et al., 2001) whose activity tends to be increased during summer and rainy season.

From the densitometric analysis, the last appeared proteins in carbohydrate and energy metabolism with differential abundance levels was vacuolar ATP synthase subunit B from spot 143 with sequence significant similar to vacuolar ATP synthase subunit B from *Zea mays* (% sequence coverage = 13; protein score = 422). Its level was statistically-significantly increased by 2.02-fold and 3.11-fold in summer-and rainy season- as compared with winter-harvested samples, respectively (Table 8 and Figure 30). ATP synthase is a key enzyme directly involved in ATP synthesis in anabolism of ATP. The enzyme is involved in the crucial energy source in individual cellular

processes such as glycolysis, the citric acid (TCA) cycle and the oxidative phosphorylation (Li et al., 2011b). Vacuolar ATP synthase subunit B is a catalytic subunit in ATP-binding site (Arechaga and Jones, 2001). The regulation of energy level within cells to utilize multiple cellular processes might cause changes of vacuolar ATP synthase subunit B levels (Nakanishi-Matsui et al., 2010), which tends to be increased during summer and rainy season.

Functional group 3: Photosynthesis. Photosynthesis is one of a key process to initiate plant growth and development. Ribulose-1,5-bisphosphate carboxylase/oxygenase (RuBisCO) is one of the key photosynthetic enzymes which catalyzed the carboxylation or oxygenation reactions in photosynthetic CO₂ fixation (Ashida et al., 2008). The results demonstrated that the spots 157 and 158 of RuBisCO were statistically-significantly increased by 5.02-fold and 1.62-fold in summer- as compared with winter-harvested samples, respectively (Table 8 and Figure 28). Raised temperature might affect the induction of the reversible activation of RuBisCO (Feller et al., 1998). A factor of high temperature could lead to decreased RuBisCO and thus a decline in the photosynthetic CO₂ fixation (Han et al., 2009), However, the decreased RuBisCO activities might be happened under moderate heat stress (Song et al., 2014). Moreover, the moderately elevated temperatures could inhibit the light-dependent activation of Rubisco, as shown in spinach (*Spinacia oleracea* L.) (Feller et al., 1998).

Functional group 4: Cellular structure. Multiple proteins are not only used to maintain cellular structures in plants but also affect plant morphology of the individual cells as well as of the whole plants. From the densitometric analysis, two of the proteins with statistically significant differential levels were actin-101 and α -tubulin-3. Actin-101 was detected in spot 110 and was matched with actin-101 from *G. max* with percent sequence coverage of 16 and protein score of 228. Actin-101 was statistically-significantly increased by 2.07-fold in summer- as compared with winter-harvested samples (Table 8 and Figure 28), supporting the role of actin-101 as a regulator of cell polarity, cell division and cell wall synthesis (Mccurdy et al., 2001) whose activities were increased during summer.

Another protein with differential abundance levels was α -tubulin-3. α -tubulin-3 was identified at the spot 208 with significant sequence similarity to α -tubulin from *G. max* (% sequence coverage = 11; protein score = 209). Its level was statistically-significantly increased by 5.05-fold in summer- as compared with the winter-harvested samples (Table 8 and Figure 28). α -tubulin is one of the main components and the building block of microtubules (Aman et al., 2013) whose shapes give rise to plant morphology through cellular division planes, axes of cellular elongation and the deposition of cellulose microfibrils within the cell walls (Dixon et al., 1994). In rice and *Arabidopsis*, the expressed α -tubulin is also involved in polymerization of the

microtubules in a variety of dynamic activities in plant cells and is likely needed in high temperature of summer to induce α -tubulin phosphorylation as the process becomes more vital. However, temperature stress might affect polymerization of the microtubules (Ban et al., 2013).

Functional group 5: Defense and Stress. Well-studied protein relating to defense mechanism is cobalamine-independent methionine synthase and methionine synthase. The first enzyme catalyzes the synthesis of methionine by with transferring a methyl group from methyltetrahydrofolate to L-homocysteine without the aid of intermediate methyl carrier. It requires zinc dependent enzyme to activate zinc for binding to L-homocysteine substrate. The process is dependent on the association growth, pathogen interactions, and plant defense in response to abiotic stress (Ravanel et al., 1998). The second enzyme catalyzes methylation reactions of the thiol group of homocysteine to form methionine, transferring methyl group from 5-methyltetrahydrofolate to homocysteine in the last step of methionine synthesis in the aspartate pathway.

The first enzyme was statistically-significantly decreased by 2.27-fold in summer- as compared with winter-harvested samples (Table 8 and Figure 28). It might be limited with combined oxidative and heat stress in summer (Job et al., 2005), (Leichert and Jakob, 2006). For methionine synthase (spot 96), the enzyme level was

statistically-significantly increased by 3.22-fold in summer- as compared with winter-harvested samples (Table 8 and Figure 28), suggesting that methionine synthase level might be induced under high temperature. Because the process of germination and seedling growth of plants was previously shown to slow down during elevated temperature (Chakraborty and Pradhan, 2011), this could generate oxidative stress in plants, leading to up-regulation of ROS-catabolizing enzymes, such as superoxide dismutase, ascorbate peroxidase and other antioxidant responses, which was shown in *Ucaria tomentosa* roots to stimulate methionine synthase expression (Chakraborty and Pradhan, 2011), (Vera-Reyes et al., 2015).

The spot 36 was identified as omega-amidase NIT2 from *Medicago truncatula* (% sequence coverage = 9; protein score = 77) and showed that the enzyme level was statistically-significantly decreased by 1.52-fold in summer- as compared with winter-harvested samples (Table 8 and Figure 28). It is the member of nitrilase superfamily amidase, which is involved in the removal of toxic intermediates in nitrogen compound metabolic processes by catalyzing the deamination of alpha- ketoglutaramate and alpha-ketosuccinamate to alpha-ketoglutarate and oxaloacetate, respectively (Krasnikov et al., 2009). The level of omega-amidase NIT2 was decreased during summer thus it might be predominant components involved in cellular and biological processes of metabolism in response to elevated temperature (Huang et al., 2012).

Due to the variable changes in environments, plants have created several mechanisms to protect themselves from such stresses. One of the known mechanisms is the induced level of heat shock protein 70 (HSP70) and small heat shock proteins (sHSPs) to ensure correct folding of other proteins under stresses, such as severe temperature changes or oxidative stresses (Mohamed and Al-Whaibi., 2011). In line with the previous report, the level of class I small heat shock protein 20.1 was statistically-significantly decreased by 1.39-fold in summer- as compared with the winter-harvested samples, whereas that of 18.5 kDa class I heat shock protein was statistically-significantly increased by 2.86-fold in summer- as compared with winter-harvested samples (Table 8 and Figure 29). It was noteworthy that the varied results of densitometric analysis of sHSP was not correlated with induction of thermotolerance. It was possible that the sHSP level might depend on cellular localization and developmental periods as well as embryogenesis, germination, pollen development, and fruit maturation (Mohamed and Al-Whaibi., 2011).

In addition, HSP70 (spot 77) might be influenced by temperature changes. The level was statistically-significantly decreased by 4.76-fold and 1.79-fold in summer-and rainy season- as compared with winter-harvested samples, respectively, whereas HSP70 (spot 74) level was statistically-significantly decreased by 1.75-fold in summer- as compared with winter-harvested samples (Table 8 and Figure 29). The results demonstrated the effect of seasons rather than sole temperature, it was thus possible

that changes in HSP70 levels might result from water delicacy and drought during winter, which leads to osmotic stress instead (Timperio et al., 2008).

Functional group 6: ROS scavenging and detoxifying. ROS's are essential signal proteins for polymerization of cell wall constituents, biosynthesis of complex organic molecules, and defense against abiotic and biotic stresses (Zhang et al., 2012). However, ROS's are highly oxidative and poisonous, causing damage to carbohydrates, lipids, proteins, and DNA including plant programmed cell death (Gill and Tuteja, 2010). Superoxide dismutase is one of the found ROS-related enzymes to be differentially regulated in different seasons. In plants, superoxide dismutase is found in chloroplast and cytosol, and acts as an intracellular metalloenzyme antioxidant, catalyzing dismutation of superoxide anions in plant stress tolerance. The enzyme converts superoxide anion radicals (O_2^-) to hydrogen peroxide (H_2O_2) and oxygen (O_2). Nowadays, superoxide dismutase, e.g. from *Curcuma comasa*, has also been applied in cosmetic products for reducing free radical levels which causes skin damage (Boonmee et al., 2011). In the study, the spot 3 was identified as the copper/zinc-like isoform 2 of superoxide dismutase from *Vitis vinifera* (% sequence coverage = 26; protein score = 159). The enzyme was statistically-significantly decreased by 1.61-fold in rainy season-harvested samples but expressed at lower level in summer-as compared with winter-harvested samples (Table 8 and Figure 29). It was possible that superoxide dismutase

activity could be an efficient drought stress response mechanism, which was shown in *Allium ascalonicum* (Csiszar et al., 2007).

The second ROS-related enzyme exhibited differential levels in varying seasons was Glutathione S-transferase. Glutathione S-transferase play major roles in herbicide detoxification and hormone homeostasis. It is known to be involved in ascorbate-glutathione pathway, catalyzing the conjugation between electrophilic xenobiotic substrates and the tripeptide glutathione. From the densitometric analysis, glutathione S-transferase (spot 32) was statistically-significantly increased by 1.50-fold in rainy season- as compared with winter-harvested samples (Table 8 and Figure 29). However glutathione S-transferase appearance was not significant in summer- as compared with winter-harvested samples. The enzymatic activity was changed in relation to the water content, which was shown in *Allium* roots (Csiszar et al., 2007). It was possible that change in glutathione S-transferase levels might result from the enhanced ROS's or oxidizing the increased glutathione levels to induce the protective mechanisms of plants (Csiszar et al., 2007), which leads to connection with elevated abiotic stress resistance during rainy season.

Yet, despite the unchanging levels of superoxide dismutase and glutathione S-transferase in summer-harvested samples compared with winter-harvested samples, the other three important ROS-related enzymes, cytosolic ascorbate peroxidase (spot

37) and putative lactoylglutathione lyase-like (spot 56) were statistically-significantly increased by 1.88-fold and 2.13-fold in summer- as compared with winter-harvested samples and glutathione reductase (spot 150) was statistically-significantly increased by 1.88-fold and 1.32-fold in summer- and rainy season- as compared with winter-harvested samples, respectively (Table 8 and Figure 29).

Ascorbate peroxidase acts as a hydrogen peroxide detoxifying enzyme, which controls the removal of the toxic hydrogen peroxide (H_2O_2) (Boonmee et al., 2011). For lactoylglutathione lyase or glyoxalase I, the enzyme is associated with glyoxalase system which catalyzes the conversion of methylglyoxal into S-D-lactoylglutathione by utilizing glutathione (Yadav et al., 2008), while glutathione reductase catalyzes the NADPH-dependent reduction of the disulfide bond of oxidized glutathione (Noctor et al., 2012). The detected increasing levels of ascorbate peroxidase, lactoylglutathione lyase and glutathione reductase in summer-harvested samples could be explained partially by temperature stress where it was reported that in *Ficus concinna* seedlings, ascorbate peroxidase, lactoylglutathione lyase and glutathione reductase were increasingly expressed at high and moderate temperature, respectively (Jin et al., 2015). Both ROS's and methylglyoxal could be induced under abiotic stresses. Moreover, the responses to abiotic and biotic stresses in higher plants were increased in ascorbate peroxidase activity (Lee et al., 2015). However, the same study also reported the increases in levels of superoxide dismutase and glutathione S-transferase

at high temperature as well while the levels of these enzymes was unaltered in summer- compared to winter-harvested samples. It was possible that factors rather than temperature could also be involved in regulating these enzymes.

Functional group 7: Amino-acid biosynthesis. Three proteins including D-3-phosphoglycerate dehydrogenase, chloroplast acetohydroxy acid isomeroreductase, and 5-methyltetrahydropteroyltriglutamate-homocysteine methyltransferase were detected to have differential relative abundances. D-3-phosphoglycerate dehydrogenase is involved in serine biosynthesis pathway (Cramer et al., 2013). D-3-phosphoglycerate dehydrogenase was identified from spot 80 with significant sequence similarity to D-3-phosphoglycerate dehydrogenase from *G. max* (% sequence coverage = 18; protein score = 632), which was statistically-significantly decreased by 1.64-fold and 1.69- fold in summer-and rainy season- as compared with winter-harvested samples, respectively (Table 8 and Figure 29).

Acetohydroxy acid isomeroreductase is required in biosynthetic pathway of the branched-chain amino acids valine, leucine and isoleucine. It is cobalamin-dependent enzymes, which requires metal ions such as Mg^{2+} , Mn^{2+} or Co^{2+} for initiating NADPH-dependent reduction and alkyl migration (isomerization) 2-acetolactate (AL) or 2-aceto-2-hydroxybutyrate (AHB), which are precursors of valine and leucine, or isoleucine, respectively (Dumas et al., 2001). The enzyme might influence cell division,

mitochondria DNA stabilization (Xu, 2003) and mechanism to inhibit the potential herbicides (Dumas et al., 2001). In the study, chloroplast acetohydroxy acid isomeroeductase from spot 148 was statistically-significantly increased by 10.78-fold in summer- and rainy season- as compared with winter-harvested samples, whereas spot 168 was statistically-significantly increased by 8.07-fold and 2.06-fold in summer- and rainy season- as compared with winter-harvested samples, respectively (Table 8 and Figure 31). The findings suggest that heat stress, drought stress and high light and other light stresses might influence another biosynthetic pathway, thereby requiring more chloroplast acetohydroxy acid isomeroeductase to perform the activities (Galili et al., 2016).

The spot 93 of 5-methyltetrahydropteroyltriglutamate-homocysteine methyltransferase, the enzyme acts as a methionine synthase in the methionine metabolism and regulate levels of regenerated methionine (Wu et al., 2013). In the study, its level was found to be statistically-significantly decreased by 1.75-fold in summer- and rainy season- as compared with winter-harvested samples (Table 8 and Figure 31). The decreases in the level of this enzyme might affect the cytoskeleton of plants, as well as the induction of ethylene metabolism as shown in *Agrostis capillaris* L. (Hego et al., 2014).

Functional group 8: Signal transduction and homeostasis. Iron is an essential element for both productivity and nutritional quality of plants. Ferritin is a major iron storage protein, which regulates plant physiology by responding to excess iron at the transcriptional level (Briat et al., 2010). The levels of ferritin (spot 43) was statistically-significantly decreased by 1.82-fold in summer- as compared with winter-harvested samples (Table 8 and Figure 31). The change might result from modulation of ferritin to create a balance between availability of iron for metabolism and sequestration of the metal to ensure protection of ROS-related damages (Briat et al., 2010), the process that could increase the protection ability against oxidative stress during summer.

The 14-3-3 proteins play major roles in regulating nitrogen and carbon metabolism, especially those involving in controlling the tricarboxylic acid (TCA) cycle and the Shikimate pathway (Diaz et al., 2011). In addition, the protein underpins regulation of H⁺-ATPase that controls the electrochemical gradient across the plasma membrane, including ion transport and cytosolic pH, relates to regulation of transcription factors, hormone signaling, positive regulators, metabolism, adhesion, cellular proliferation, differentiation, survival, apoptosis and ion homeostasis as well as signal transduction pathways of plasma membrane H⁺-ATPase and ions channels; and interactions with a number of proteins in ethylene biosynthesis (Hego et al., 2014). 14-3-3- like protein (spot 48) was statistically-significantly decreased by 1.85-fold in summer- as compared with winter-harvested samples (Table 8 and Figure 31). The activity of 14-3-3- like protein might depend on the levels of sugars and nitrogen-

containing-compounds as well as the levels of aromatic compounds. The result supports the report of overexpression of 14-3-3 proteins in *Arabidopsis* which is related to the reduction of the levels of nitrogen-containing-compounds and sugars, including citrate and malate as the major intermediate compounds of the tricarboxylic acid (TCA) cycle. In addition, such changes might decrease the activities of isocitrate dehydrogenase and malate dehydrogenase and involve in the levels of aromatic compounds as well as the activities of Shikimate dehydrogenase linked to aromatic compound biosynthesis (Diaz et al., 2011).

Nucleoredoxin found in maize (*Zea mays* L.), belonging to thioredoxin superfamily (Laughner et al., 1998), is a thiol oxidoreductase. It is needed for DNA synthesis via ribonucleotide reductase and for abundant redox signaling pathways including scavenger ROS's in response to oxidative stress (Hanschmann et al., 2013). From the densitometric analysis, nucleoredoxin 1 was identified from spot 76 with significant sequence similarity to probable nucleoredoxin 1 from *G. max* (% sequence coverage = 8; protein score = 277), which was statistically-significantly increased by 1.94-fold in rainy season- as compared with winter-harvested samples (Table 8 and Figure 31). It was possible that nucleoredoxin 1 might act as redox-sensor in the metabolite detoxification with glutathione as a hydrogen donor and is regulated by ROS-signaling activation (Funato and Miki, 2007).

Functional group 9: Protein biosynthesis. Three proteins including translation initiation factor, eukaryotic translation initiation factor 4A and elongation factor 2 were found to have differential seasonal relative abundances. The spot 8 was identified as an analog protein of translation initiation factor from *Carica papaya* (% sequence coverage = 17; protein score = 159) and appeared to be statistically-significantly decreased by 2.27-fold in summer- as compared with winter-harvested samples. The eukaryotic translation initiation factor 4A (spot 165) was statistically-significantly increased by 1.86-fold and 2.12-fold in summer-and rainy season- as compared with winter-harvested samples, respectively (Table 8 and Figure 32). Translation initiation factor is a member of DEAD box-protein family involving in RNA metabolism. Eukaryotic translation initiation factors 4A is one of the DEAD box helicases; the 46 kDa polypeptide involves in the first step of RNA dependent ATPase and bidirectional RNA helicase activities in cap-dependent translation initiation. Changes in levels of the two proteins might influence the promotion or inhibition of the translation of specific mRNAs. Moreover, some protein is active in processes rather than translation in relevant of specific expression of tissues and developmental stages and subsequently plays important roles of plant tolerance in response to abiotic stress (Hernandez and Vazquez-Pianzola, 2005). Elongation factor 2 involves in the regulation of translational activities by modulating specific Ca^{2+} /calmodulin-dependent kinase (Gallie et al., 1998). Its level was statistically-significantly decreased by 1.39-fold in rainy season- as compared with winter-harvested samples (Table 8 and Figure 32). It was possible that

the level of elongation factor 2 might be to be positively correlated with that of heat shock proteins (Gallie et al., 1998).

Functional group 10: Protein destination and storage. One of the multicatalytic complex proteins is proteasome subunits, which is related to extralysosomal energy- and ubiquitin-dependent proteolytic pathway and degradation of proteins (Genschik et al., 1994; Huang et al., 2012). The different subunits depend on cleavage of peptide bonds on the carboxyl side of basic, hydrophobic or acidic residues. Particularly, the proteolytic activities can be carried out by beta-type subunits (Genschik et al., 1994), including proteasome subunit beta type-6-like (spot 16), proteasome subunit beta type-1-like (spot 29) and 20S proteasome beta subunit 5 (spot 30) which were statistically-significantly increased by 1.89-fold, 2.32-fold and 1.93-fold in summer- as compared with winter-harvested samples, respectively (Table 8 and Figure 32).

In total, the proteomic analysis identified 45 proteins in tubers with statistically-significantly changing levels. Compared to detected levels in winter-harvested samples, proteins with the increased levels in summer-harvested samples were triphosphate isomerase (spot 28), V-type proton ATPase catalytic subunit A (spot 79), RuBisCO (spot 157 and 158), actin-101-like (spot 110), α -tubulin-3 chain-like (spot 208), methionine synthase (spot 96), cytosolic ascorbate peroxidase (spot 37), putative

lactoylglutathione lyase-like (spot 56), chloroplast acetoxy acid isomeroreductase (spot 148), proteasome subunit beta type-6-like (spot 16), proteasome subunit beta type-1-like (spot 29) and 20S proteasome beta subunit 5 (spot 30), while those with the decreased levels were glyceraldehyde-3-phosphate dehydrogenase (spot 58), enolase (spot 81 and 115), alcohol dehydrogenase (spot 105), omega-amidase NIT 2 (spot 36), cobalamine-independent methionine synthase (spot 51), class I small heat shock protein 20.1 (spot 5), heat shock protein 70 (spot 74 and 77), 5-methyltetrahydropteroyltriglutamate-homocysteine methyltransferase (spot 93), D-3-phosphoglycerate dehydrogenase (spot 80), ferritin (spot 43), 14-3-3-like (spot 48) and translation initiation factor (spot 8).

For rainy season- as compared with winter-harvested samples, proteins with the increased levels in rainy season-harvested samples were profilin-1 (spot 1), glyceraldehyde-3-phosphate dehydrogenase (spot 62 and 69), enolase (spot 140), 18.5 kDa class I heat shock protein (spot 7) and probable nucleoredoxin 1, while those with the decreased levels were enolase (spot 81, 115 and 122), alcohol dehydrogenase (spot 105), heat shock protein 70 (spot 77), CU/Zn-SOD-like isoform 2 (spot 3), D-3-phosphoglycerate dehydrogenase (spot 80) and elongation factor 2 (spot 132).

Three proteins in carbohydrate and energy metabolism, one protein in amino acid biosynthesis, one protein in ROS scavenging and detoxifying and one protein in

protein biosynthesis including alcohol dehydrogenase (spot 117), vascular ATP synthase subunit B (spot 143), alcohol dehydrogenase 1 (spot 186), chloroplast acetohydroxy acid isomeroreductase (spot 168), glutathione reductase, cytosolic (spot 150) and eukaryotic transition initiation factor 4A (spot 165) were statistically-significantly increased in summer and rainy season- as compared with winter-harvested samples, whereas four proteins were statistically-significantly in winter-harvested samples were enolase (spot 81 and 115), alcohol dehydrogenase (spot 105) and heat shock protein 70 (spot 77).



Table 8 Identified proteins of tubers were analyzed changes and differences using the Image Master 2-DE program

Spot no.	Accession number ^{a)}	Protein Name	Between						% Coverage ^{f)}
			summer and winter p-value ^{b)}	Fold ^{c)}	rainy season and winter p-value ^{b)}	Fold ^{d)}	Score ^{e)}		
Functional group 1: Allergy									
1	gi 3914435	Profilin-1	0.69	1.08	0.04	↑	1.31	46	16
Functional group 2: Carbohydrate and energy metabolism									
28	gi 77540216	Triosephosphate isomerase	0.01	↑	1.89		1.09	206	23
58	gi 48508784	Glyceraldehyde -3-phosphate dehydrogenase	0.02	↓	1.64		1.29	157	7
62	gi 307136111	Glyceraldehyde -3-phosphate dehydrogenase	0.45		1.33	↑	1.77	92	11
69	gi 418731090	Glyceraldehyde -3-phosphate dehydrogenase	0.70	↑	0.94		1.88	155	15
79	gi 363806992	V-type proton ATPase catalytic subunit A	0.04	↑	1.48		1.77	476	17
81	gi 356505318	Enolase	0.01	↓	1.59		1.75	350	18
105	gi 255585914	Alcohol dehydrogenase	0.02	↓	1.72		1.64	66	5
115	gi 344190186	Enolase	0.01	↓	1.85		2.22	334	21
116	gi 445589	Alcohol dehydrogenase	0.04	↓	1.52		0.76	277	12
122	gi 1169534	Enolase	0.58		1.12	↓	1.39	411	18
123	gi 356530953	Enolase	0.94		1.02	↑	1.68	295	16
117	gi 445589	Alcohol dehydrogenase	0.01	↑	1.92		2.72	281	12
140	gi 351724891	Enolase	0.27		0.86	↑	2.06	237	9
143	gi 226492645	Vacuolar ATP synthase subunit B	0.02	↑	2.02		3.11	422	13
186	gi 22597178	Alcohol dehydrogenase 1	0.01	↑	1.99		4.88	187	7

Table 8 (Continued)

Spot no.	Accession number ^{a)}	Protein Name	Between						
			summer and winter p-value ^{b)}	Fold ^{c)}	rainy season and winter p-value ^{b)}	Fold ^{d)}	Score ^{e)}	% Coverage ^{f)}	
Functional group 3: Photosynthesis									
157	gi 18157251	RuBisCO large subunit	0.01	↑ 5.02	0.50	1.23	470	20	
158	gi 229464442	RuBisCO large subunit	0.01	↑ 1.62	0.05	0.62	370	18	
Functional group 4: Cellular structure									
110	gi 356558578	Actin-101-like	0.00	↑ 2.07	0.08	2.17	228	16	
208	gi 356560917	Tubulin alpha-3 chain-like	0.00	↑ 5.05	0.14	4.39	209	11	
Functional group 5: Defense and Stress									
Defense									
36	gi 357465811	Omega-amidase NIT2	0.01	↓ 1.52	0.97	1.01	77	9	
Cobalamine-independent methionine synthase									
51	gi 974782	synthase	0.01	↓ 2.27	0.08	1.36	121	3	
96	gi 351724907	Methionine synthase	0.01	↑ 3.22	0.12	2.53	297	8	
Stress									
5	gi 349591294	Class I small heat shock protein 20.1	0.04	↓ 1.39	0.54	0.91	123	17	
7	gi 351721881	18.5 kDa class I heat shock protein	0.18	1.54	0.02	↑ 2.86	238	26	
74	gi 356500683	Heat shock protein 70	0.01	↓ 1.75	0.44	0.80	343	24	
77	gi 186898205	Heat shock protein 70	0.00	↓ 4.76	0.01	↓ 1.79	52	16	

Table 8 (Continued)

Spot no.	Accession number ^{a)}	Protein Name	Between						% Coverage ^{f)}
			summer and winter p-value ^{b)}	Fold ^{c)}	rainy season and winter p-value ^{b)}	Fold ^{d)}	Score ^{e)}		
Functional group 6: ROS scavenging and detoxifying									
3	g 225451120	Superoxide dismutase [Cu-Zn]-like isoform 2	0.40	0.87	0.02	↓ 1.61	159	26	
32	g 356526968	GST F10-like	0.11	1.18	0.00	↑ 1.50	148	12	
37	g 120969450	Cytosolic APX	0.00	1.88	0.07	1.61	47	28	
56	g 356531939	Putative lactoylglutathione lyase-like	0.00	2.13	0.11	2.05	263	18	
150	g 6714837	GR, cytosolic	0.00	1.88	0.01	↑ 1.32	274	14	
Functional group 7: Amino-acid biosynthesis									
80	g 356536156	D-3-phosphoglycerate dehydrogenase	0.01	1.64	0.00	↓ 1.69	632	18	
93	g 356547867	5-methyltetrahydropteroyltriglutamate-homocysteine methyltransferase	0.04	1.75	0.96	0.98	473	11	
148	g 341958461	Chloroplast acetoxy acid isomerase	0.00	10.78	0.74	0.87	189	6	
168	g 341958461	Chloroplast acetoxy acid isomerase	0.01	8.07	0.01	↑ 2.06	205	7	
Functional group 8: Signal transduction and homeostasis									
43	g 1052778	Ferritin	0.01	1.82	0.50	1.08	109	9	
48	g 67107029	14-3-3-like	0.04	1.85	0.26	1.31	295	21	
76	g 356526803	Probable nucleoredoxin 1	0.15	1.36	0.01	↑ 1.94	277	8	

Table 8 (Continued)

Spot no.	Accession number ^{a)}	Protein Name	Between					% Coverage ^{f)}
			summer and winter p-value ^{b)}	Fold ^{c)}	rainy season and winter p-value ^{b)}	Fold ^{d)}	Score ^{e)}	
Functional group 9: Protein biosynthesis								
8	gjl151347490	Translation initiation factor	0.02	↓ 2.27	0.19	0.71	159	17
132	gjl356525774	Elongation factor 2	0.06	0.71	0.03	↓ 1.39	291	7
165	gjl1170509	Eukaryotic translation initiation factor 4A	0.01	↑ 1.86	0.01	↑ 2.12	553	23
Functional group 10: Protein destination and storage								
16	gjl502132065	Proteasome subunit beta type-6-like	0.01	↑ 1.89	0.54	0.84	207	16
29	gjl356526807	Proteasome subunit beta type-1-like	0.00	↑ 2.32	0.07	2.00	144	15
30	gjl227937349	20S proteasome beta subunit 5	0.03	↑ 1.93	0.06	2.49	166	13

^{a)}The protein's NCBI accession number ^{b)} p-value following Student's t-test of means of protein abundances in seasonal comparison ^{c)} Fold change of the terms in the ratio summer/ winter of spot intensities in summer- as compared with winter-harvested samples ^{d)} Fold change of the terms in the ratio rainy season/ winter of spot intensities in rainy season- as compared with winter-harvested samples ^{e)} The protein scores from MS/MS ion-search ^{f)} The percentage of the protein's sequence those peptide fragments

↑ A significant increase in fold changes, ↓ A significant decrease in fold changes

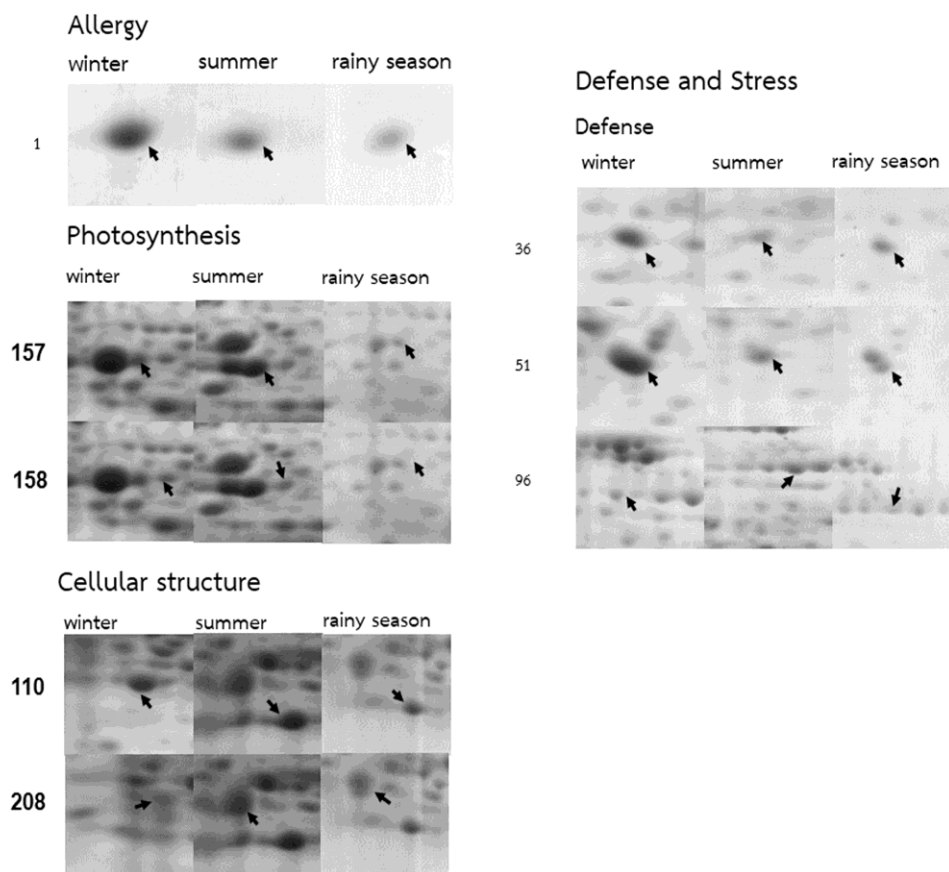


Figure 28 Gel spots of 8 proteins in allergy, photosynthesis, cellular structure and defense with differentially abundances during summer-or rainy season- as compared with winter-harvested samples.

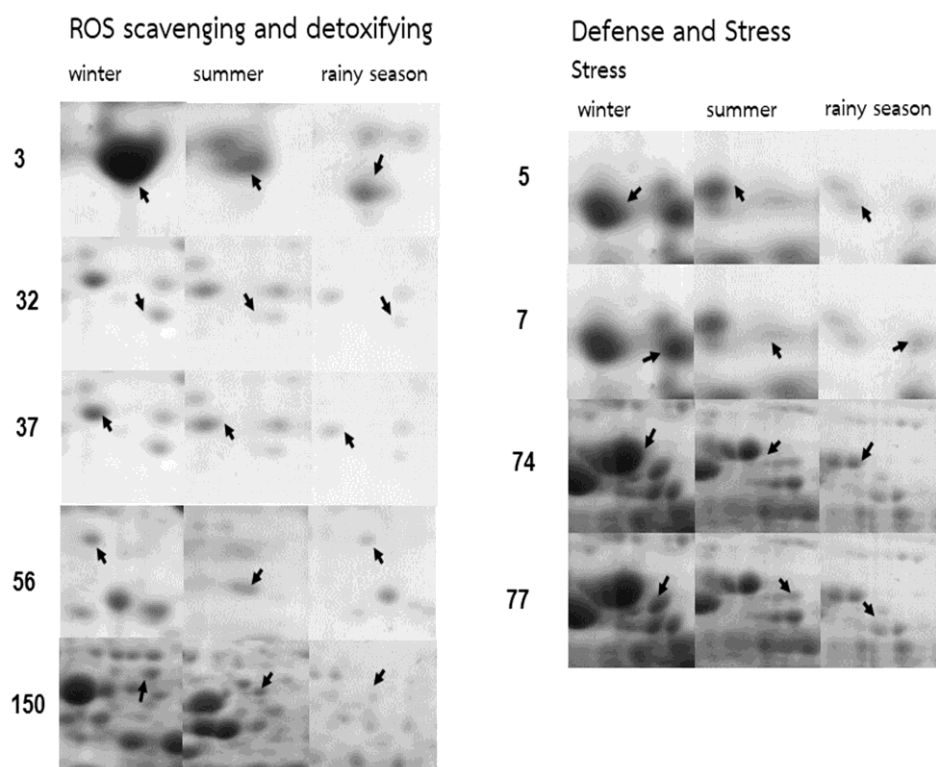


Figure 29 Gel spots of 9 proteins in ROS scavenging and detoxifying and stress with differentially abundances during summer-or rainy season- as compared with winter-harvested samples.

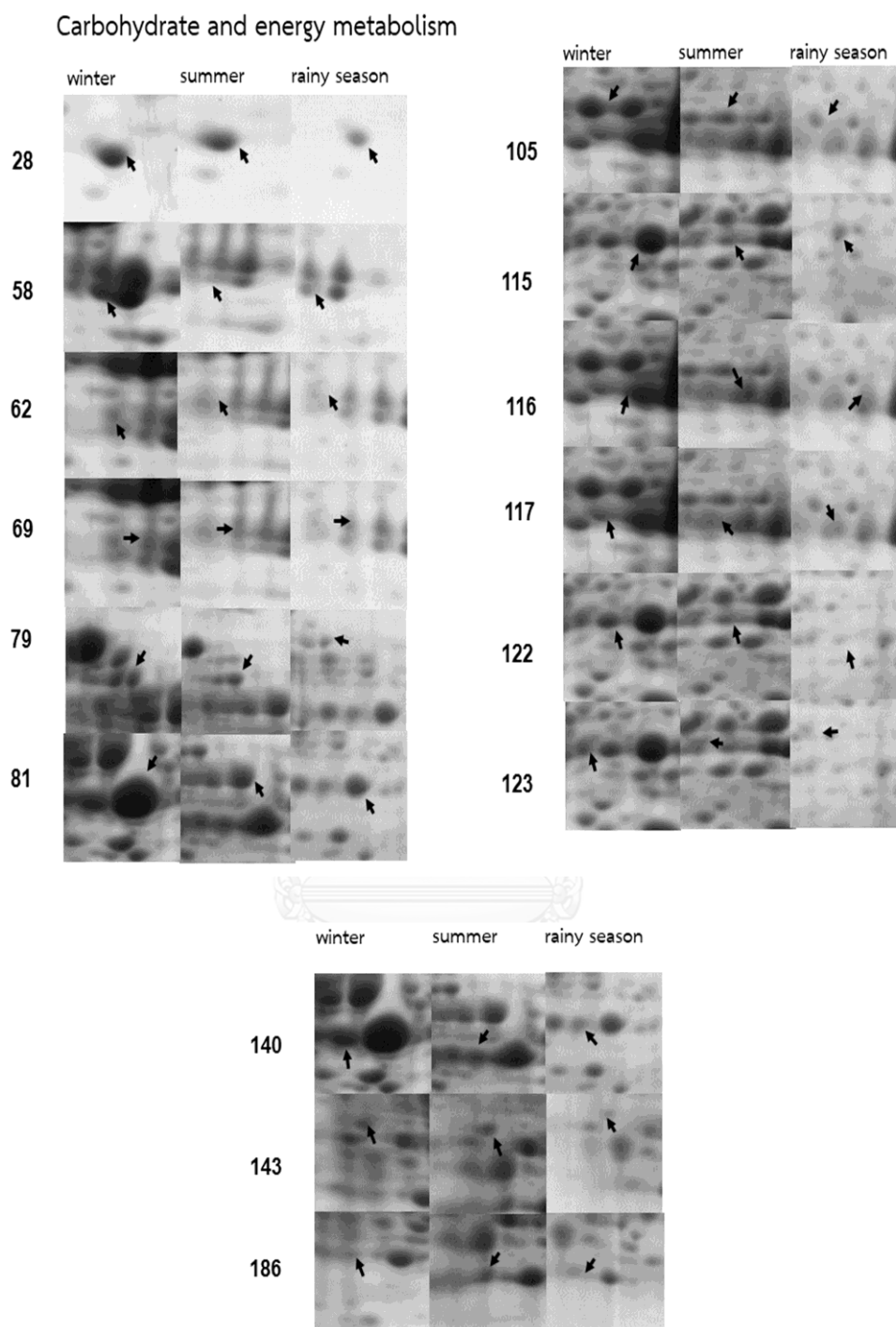


Figure 30 Gel spots of 15 proteins in carbohydrate and energy metabolism with differential abundances during summer-or rainy season- as compared with winter-harvested samples.

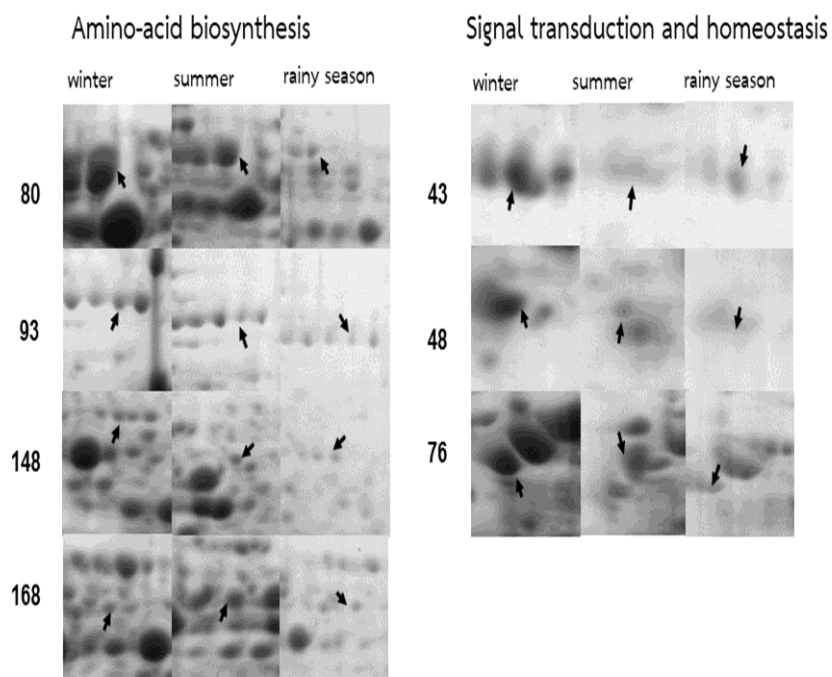


Figure 31 Gel spots of 7 proteins in amino-acid biosynthesis and signal transduction and homeostasis with differential abundances during summer or rainy season- as compared with winter-harvested samples.

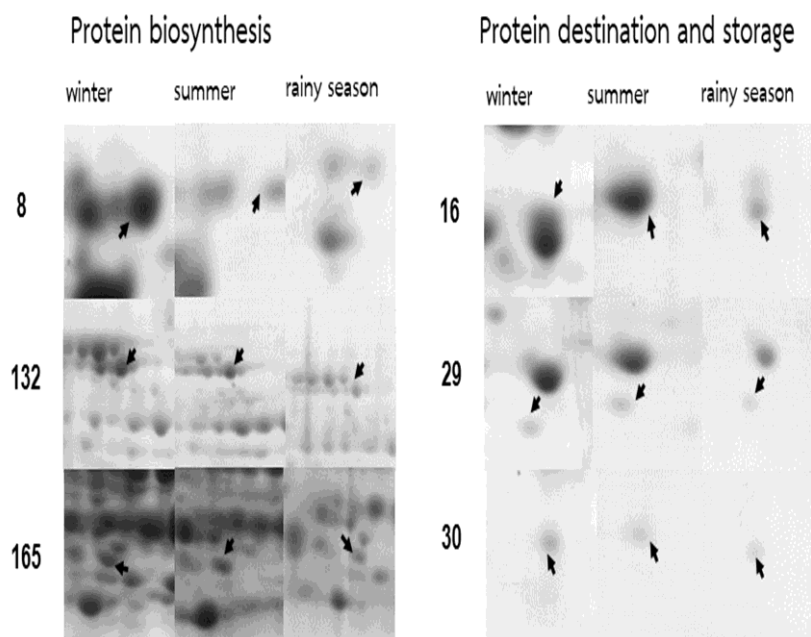


Figure 32 Gel spots of 6 proteins in protein biosynthesis and protein destination and storage with differential abundances during summer or rainy season- as compared with winter-harvested samples.

4.4.2 Proteins with differential levels in different seasons in leaves

To identify proteins with differential levels in different seasons, spot intensities on 2-DE gels were quantified using the Image Master program. The previous results revealed a variety of protein spots in winter-harvested samples originated from Lampang. Consequently, fold changes were calculated by comparing the intensities of each individual protein spot in summer- and rainy season- harvested samples with these of the corresponding spot in winter-harvested sample. The exhibited 3 and 4 protein spots were statistically-significantly increased, and 1 and 5 protein spots were statistically-significantly decreased in summer- and rainy season-harvested samples, respectively. Twelve proteins belonging to 5 functional groups were found involving in important metabolic pathways and therefore picked for further discussion (Table 9 and Figure 33-34).

Functional group 1: Carbohydrate and energy metabolism. Two protein groups including glyceraldehyde-3-phosphate dehydrogenase (GAPDH) and triosephosphate isomerase (API) were detected to have differential abundance levels. Glyceraldehyde-3-phosphate dehydrogenase (spot 109) converts D-glyceraldehyde-3-phosphate into 1,3-bisphosphoglycerate of the glycolysis (Mitprasat et al., 2011), which was statistically-significantly increased by 3.36 fold in rainy season- as compared with winter-harvested samples (Table 9 and Figure 33). Changes of glyceraldehyde-3-

phosphase dehydrogenase level might result from metabolic flexibility to facilitate plant response to environmental stresses (Ma et al., 2013), which tends to increase during rainy season.

The spots 25 and 28 of triosephosphate isomerase, they catalyzes the interconversion between D-glyceraldehyde-3-phosphate and dihydroacetone phosphate involving energy production. Their level were statistically-significantly decreased 2.44-fold and 1.33-fold in rainy season- as compared with winter-harvested samples, respectively (Table 9 and Figure 19). It might deteriorate in the photosynthetic activity resulted from the smaller amount of carbohydrate production for glycolysis in leaves (Li et al., 2011a). Notably, these proteins provided high scores in the protein identification process, suggesting the structural conservation of these key proteins in *B. superba* to green plants.

Functional group 2: Photosynthesis. The abundant photosynthetic enzymes in leaves are well known for their biological importance in energy harvesting, conversion and storage of photoassimilation (Rasineni et al., 2009). Two proteins in photosynthesis with altering relative abundances were oxygen-evolving enhancer protein 2 (spot 27) and ribulose-1,5-bisphosphate carboxylase/oxygenase (spot 41). Oxygen-evolving enhancer protein 2 is a key enzyme involving in maintenance of photosystem II core stability and regulation of the primary site in photosystem II

photoinhibition, including light reaction and response to bacterium, light intensity and abiotic stresses (Zhang et al., 2012). From densitometric analysis, oxygen-evolving enhancer protein 2 level was statistically-significantly increased by 1.81-fold in rainy season-as compared with winter-harvested samples (Table 9 and Figure 33). It was possible that an increase in oxygen-evolving enhancer protein 2 level during rainy season might present a mechanism of plant adaptation in response to abiotic stress and thermal stress (Janmohammadi et al., 2015).

Ribulose-1,5-bisphosphate carboxylase/oxygenase (RuBisCO) is the essential enzyme for photosynthetic induced carbon fixation in the Calvin cycle, catalyzing the carboxylation or oxygenation reactions (Ashida et al., 2008). The rate of RuBisCO activation is regulated by RuBisCO activase enzyme (Jensen, 2000). It was identified from spot 44 with sequence similarity to RuBisCO large subunit from *Touroulia guianensis* (% sequence coverage = 18; protein score = 371 to be statistically-significantly increased by 1.51-fold in summer-as compared with winter-harvested samples (Table 9 and Figure 33), while Ribulose-1,5-bisphosphate carboxylase (spot 41) was statistically-significantly increased by 2.14-fold in rainy season-as compared with winter-harvested samples (Table 9 and Figure 28). High temperature could lead to the reduction in the activation state of RuBisCo to affect a loss of RuBisCO activase activity (Han et al., 2009) and limited interactions between activase and RuBisCO necessary for CO₂ fixation during photosynthesis (Jensen, 2000); however, the decrease

in RuBisCO content might also be derived from reduction of photosynthesis as shown in *Triticum aestivum* L seedlings (Cheng et al., 2015). It might therefore be possible that the increases of RuBisCO levels during summer might be the high temperature stress response to compensate for the lower activity of RuBisCO (Jensen, 2000) so that the photosynthesis rate and activity remains sufficient for plant survival (Cheng et al., 2015). For increased Ribulose-1,5-bisphosphate carboxylase level, it might be required for production of adenosine triphosphate (ATP) and nicotinamide adenine dinucleotide phosphate-oxidase (NADPH), which involves in photophosphorylation and photosynthesis electron transport under low light intensity during rainy season including capability of carbon assimilation in leaves (Lee et al., 2013).

Functional group 3: Secondary metabolism. The protein with differential abundance level is the secondary metabolism group of isoflavone reductase which is involved in the (iso) flavone and lignin biosynthesis (Ma et al., 2013) via the phenylpropanoid pathway. The enzyme catalyzes the nicotinamide adenine dinucleotide phosphate (NADP)-dependent reduction of 2'-hydroxyformononetin to isoflavanone (3R)-vestitone in *Medicago sativa* (Veitch, 2013). Isoflavone reductase matched well with that from *Glycine max* with % sequence coverage of 16 and protein score of 206. Its level was statistically- significantly decreased by 2.44-fold and 3.13-fold in summer- and rainy season- as compared with winter-harvested samples, respectively (Table 9 and Figure 34). It is the one of the drought-responsive proteins

(Grimplet et al., 2009), is related in defense against numerous stresses and effectiveness of the antioxidant system (Komatsu and Hossain, 2013). Because the amount of water on average is lower in winter, the activities of isoflavone reductase might be increased in response to water stress (Komatsu and Hossain, 2013). The finding also suggests that *B. superba* leaf might exhibit antioxidant activity as found in the other tuberous plant, *Pueraria mirifica* (Cherdshewasart and Sutjit, 2008).

Functional group 4: Defense and Stress. One of the molecular chaperones to be identified was 20 kDa chaperonin, which can act as a co-chaperone of chaperonin-60 for discharging of the biologically active proteins from chaperonin-60 (Bertsch et al., 1992). The 20 kDa chaperonin (spot 36) level in stress group was decreased by 2.36-fold in rainy season -as compared with winter-harvested samples (Table 9 and Figure 34). It is possible that the increase in 20 kDa chaperonin level during winter supports the essential function of protective roles in chaperones for the prevention of protein misfolding and protein aggregation in response to low temperature (Wang et al., 2004) and drought stresses (Komatsu and Hossain, 2013).

Functional group 5: ROS scavenging and detoxifying. ROS's is a highly oxidative substance generated in high amount conditions during conditions to protect plants against oxidative damage (Ma et al., 2013). Two of the well-studied ROS-related enzymes involving in defense against abiotic and biotic stresses were superoxide

dismutase (SOD) and monodehydroascobate reductase (MDAR) in ROS scavenging and detoxifying group. Superoxide dismutase (SOD) catalyzes dismutation of superoxide anions by converting superoxide anion radicals (O_2^-) to hydrogen peroxide (H_2O_2) and oxygen (O_2). SODs are categorized by their metal cofactors. The copper/zinc of superoxide dismutase (Cu/Zn-SOD) is one of SOD-related metalloenzymes, which is found in chloroplast and cytosol. In the study, the spot 64 had sequence similarities to the copper/zinc of superoxide dismutase (Cu/Zn-SOD) from *Petunia hybrida* (% sequence coverage = 12; protein score = 139), and its level was statistically-significantly increased by 4.32-fold in summer- as compared with winter-harvested samples (Table 9 and Figure 34). It might be produced in correlation with levels of oxidative stress induced in drought and high light conditions (Gill and Tuteja, 2010) to scavenge the ROS (Ngamhui et al., 2012); therefore, its level is increased during summer.

For the second differential ROS-related enzyme was monodehydroascorbate reductase, it is the enzyme that catalyzes a reduction of monodehydroascorbate (MDHA) to its oxidized form, ascorbate, as a way to defend against stress (Gill and Tuteja, 2010). Monodehydroascorbate reductase-like isoform 1 (spot 66) was statistically-significantly increased by 1.85-fold in rainy season- as compared with winter-harvested samples, respectively (Table 9 and Figure 34). It was possible that waterlogging might combine with oxidative stress during rainy season resulting the increases of enzymes,

which related to the ascorbate dependent antioxidative system, as shown in roots of wheat (*Triticum aestivum*) and rice seedlings (Kumutha et al., 2009).

Functional group 6: RNA metabolism: glycine-rich RNA-binding protein is one of the ubiquitous cellular proteins in response to abiotic and biotic stress of plants to be linked to various independent physiological processes (Ciuzan et al., 2015), involved in regulation of gene expression, especially at the post-transcriptional level as well as mRNA stability, pre-mRNA splicing, translation, nucleocytoplasmic mRNA transport and deterioration (Kim et al., 2010). From the densitometric, the results demonstrated that glycine-rich RNA-binding protein GRP1A-like (spot 62) was statistically-significantly increased by 2.66-fold in summer- as compared with winter-harvested samples (Table 9 and Figure 34). It was possible that change of glycine-rich RNA-binding protein level due to the expression of GRP genes in response to abiotic stress (Ciuzan et al., 2015), which might be finely combined during summer. Moreover, the function of glycine-rich RNA-binding protein as RNA chaperones might play a prominent role in the process of cold adaptation both in monocotyledonous and dicotyledonous plants (Kim et al., 2010).

Functional group 7: Protein destination and storage. Proteasome subunits are multicatalytic proteinase complex related to ATP/ubiquitin-dependent proteolytic pathway (Huang et al., 2012) and degradation of proteins (Genschik et al., 1994). As

summer initiates and temperatures increases, this can lead to dehydration stress (de Oliveira et al., 2013). Proteasome subunit alpha type which was detected in spot 23 and was identified from the match with proteasome subunit alpha type from *Ricinus communis* with percent sequence coverage of 17 and protein score of 219. From densitometric analysis, proteasome subunit alpha type was statistically-significantly increased by 2.24-fold in summer- as compared with winter-harvested samples, respectively (Table 9 and Figure 34). It was increased during summer because protein degradation could be tightly controlled within cells in response to abiotic stresses (Huang et al., 2012).

In total, the proteomic analysis identified 12 proteins in leaves with statistically-significantly changing levels. Compared to detected levels in winter-harvested samples, proteins with the increased in summer-harvested samples were RuBisCO (spot 44), Cu/Zn-SOD (spot 64), glycine-rich RNA-binding protein GRPA-like (spot 62) and proteasome subunit alpha type, putative (spot 23), whereas one protein in secondary metabolism with the decreased levels was isoflavone-reductase homolog 2 (spot 30).

For rainy season-as compared with winter-harvested samples, proteins with the increased levels in rainy season-harvested samples were glyceraldehyde-3-phosphate dehydrogenase B subunit (spot 82), oxygen-evolving enhancer protein 2 (spot 27), ribulose-1,5-bisphosphate carboxylase (spot 41) and monodehydroascorbate

reductase-like isoform 1 (spot 66), while those proteins with the decreased levels were triphosphate isomerase (spot 25 and 28), isoflavone-reductase homolog 2 (spot 30) and 20 kDa chaperonin (spot 36).

One protein with altering levels was isoflavone-reductase homolog 2 (spot 30), which belongs to secondary metabolism to be statistically-significantly increased in winter- harvested samples.



Table 9 Identified proteins of leaves were analyzed for changes and differences using the Image Master 2-DE program

Spot no.	Protein name	Between				Score ^{d)}	% Coverage ^{e)}
		summer and winter	rainy season and winter	Fold change ^{b)}	Fold change ^{c)}		
		p-value ^{a)}	p-value ^{a)}				
Functional group 1: Carbohydrate and energy metabolism							
25	gi 57283985 Triosephosphate isomerase	0.14	0.02	0.68	↓ 2.44	146	8
28	gi 77540216 Triosephosphate isomerase	0.98	0.03	1.00	↓ 1.33	393	31
82	gi 351726690 Glyceraldehyde-3-phosphate dehydrogenase B subunit	0.67	0.00	1.25	↑ 3.36	394	15
Functional group 2: Photosynthesis							
27	gi 356501429 Oxygen-evolving enhancer protein 2	0.06	0.00	1.97	↑ 1.81	134	13
41	gi 2961268 Ribulose-1,5-bisphosphate carboxylase	0.67	0.04	0.93	↑ 2.14	234	7
44	gi 1771817 Ribulose-1,5-bisphosphate carboxylase /oxygenase large subunit	0.02	0.93	↑ 1.51	0.96	371	18
Functional group 3 Secondary metabolism							
30	gi 351726399 Isoflavone reductase homolog 2	0.02	0.01	↓ 2.44	↓ 3.13	206	16
Functional group 4: Defense and Stress							
Stress							
36	gi 356556406 20 kDa chaperonin	0.27	0.02	0.79	↓ 2.33	235	16
Functional group 5: ROS scavenging and detoxifying							
64	gi 134684 Superoxide dismutase [Cu-Zn]	0.02	0.77	↑ 4.35	0.92	139	12

Table 9 (Continued)

Spot no.	Protein name	Between					
		summer and winter		rainy season and winter		Fold	%
		p-value ^{a)}	Fold change ^{b)}	p-value ^{a)}	Fold change ^{c)}	Score ^{d)}	Coverage ^{e)}
Functional group 5: ROS scavenging and detoxifying							
66	g j356533631 Monodehydroascorbate reductase –like isoform	0.07	↑ 2.17	0.00	↑ 1.85	137	6
1							
Functional group 6: RNA metabolism							
62	g j359475330 Glycine-rich RNA-binding protein GRP1A-like	0.00	↑ 2.66	0.06	1.15	112	23
Functional group 6: Protein destination and storage							
23	g j255544626 Proteasome subunit alpha type, putative	0.01	↑ 2.24	0.11	1.21	219	17

a) p-value following Student's t-test of means of protein abundance in seasonal comparison

b) Fold change of the terms in the ratio summer/ winter of spot intensities in summer- as compared with winter-harvested samples

c) Fold change of the terms in the ratio rainy season/ winter of spot intensities in rainy season-as compared with winter-harvested samples

d) The protein scores from MS/MS ion-search

e) The percentage of the protein's sequence those peptide fragments

↑ A significant increase in fold changes, ↓ A significant decrease in fold change

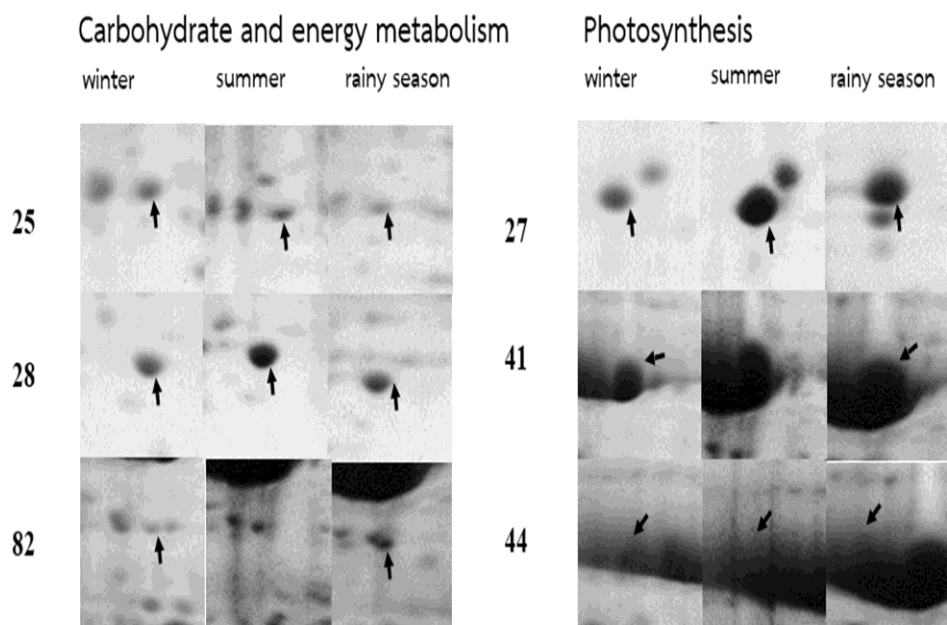


Figure 33 Gel spots of 6 proteins in carbohydrate and energy metabolism and photosynthesis with differential abundances in summer- or rainy season-as compared with winter-harvested samples.

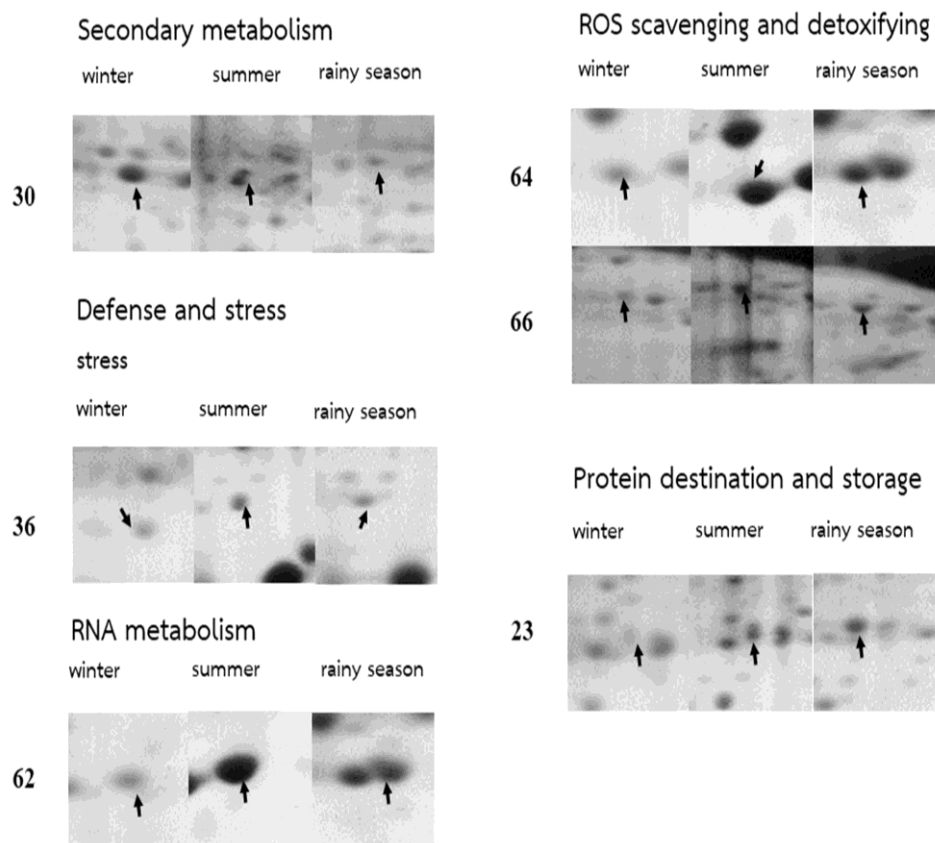


Figure 34 Gel spots of 6 proteins in defense and stress, ROS scavenging and detoxifying, RNA metabolism, protein destination and storage with differential abundances with differential abundances in summer- or rainy season- as compared with winter-harvested samples.

4.5 Proteins abundance in response to temperature stress and water stress

4.5.1 Proteins abundance in response to temperature stress and water stress in tubers

During summer, temperature stress can induce protein degradation, dehydration, and cell death (Waraich et al., 2012) and resulted in disruption of tuberous plant cells. High-temperature responsive proteins, namely, triosephosphate isomerase, alcohol dehydrogenase, alcohol dehydrogenase1, vacuolar ATP synthase subunit B, V-type proton ATPase catalytic subunit A, actin-101, α -tubulin-3 chain, methionine synthase, cytosolic ascorbate peroxidase, putative lactoylglutathione lyase-like, glutathione reductase, 5-methyltetrahydro pteroyltriglutamate-homocysteine methyltransferase, chloroplast acetohydroxy acid isomeroreductase, eukaryotic translation initiation factor 4A , proteasome subunit beta type-6-like, proteasome subunit beta type-1-like, 20S proteasome beta subunit 5 and ribulose 1,5-bisphosphate carboxylase-oxygenase large subunit were statistically-significantly increased in summer-harvested samples to aid plant survival under high temperature. On the contrary, glyceraldehyde -3-phosphate dehydrogenase, enolase, alcohol dehydrogenase, omega-amidase NIT2, cobalamine-independent methionine synthase, 5-methyltetrahydropteroyltriglutamate-homocysteine methyltransferase, class I small

heat shock protein 20.1, heat shock protein 70, D-3-phosphoglycerate dehydrogenase, ferritin, 14-3-3-like and translation initiation factor proteins were statistically-significantly decreased under high temperature (Figure 35).

The differential levels of proteins during temperature stress in summer might result from the differential expression of varied genes involved in replication and amendment of DNA in endoplasmic reticulum of plant cells, as previously shown in *Pyropia yezoensis* (Sun et al., 2015). Class I small heat shock protein 20.1 and heat shock protein 70 were statistically-significantly decreased under high temperature. This demonstrates that some common house-keeping genes might maintain levels of proteins to help plant survive under a wide range of environmental stress (Sun et al., 2015), especially thermal tolerance (Mahmood et al., 2010).

In addition, HSP synthesis and cellular localization could be correlated to the acquisition of thermal tolerance, stress conditions and tolerance in response to temperature stress in numerous cells (Simoes-Araujo et al., 2003). For sHSPs, the proteins might be accumulated in response to environmental stress (Mahmood et al., 2010).

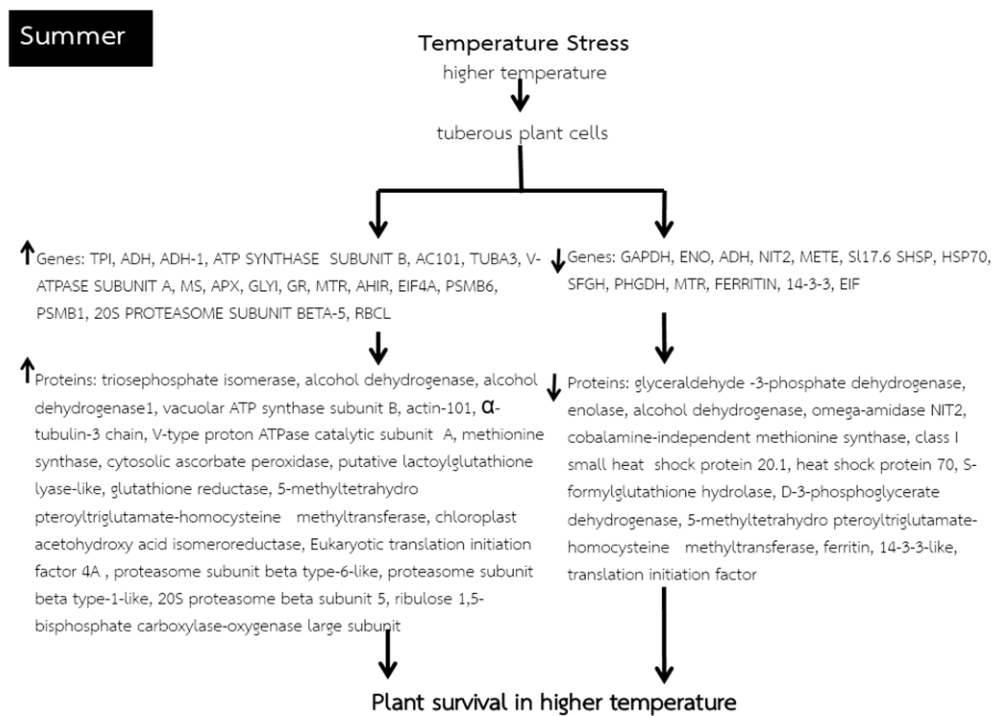


Figure 35 A model of proteins abundance in response to temperature stress during summer with analyzing from fold change of the terms in the ratio summer/ winter of spot intensities in summer- as compared with winter-harvested samples

During winter, water stress might initiate water deficit such as loss of water, drought and high soil salinity (de Oliveira et al., 2013). Low-temperature responsive proteins, namely, glyceraldehyde -3-phosphate dehydrogenase, enolase, alcohol dehydrogenase, omega-amidase NIT2, cobalamine-independent methionine synthase, D-3-phosphoglycerate dehydrogenase, class I small heat shock protein 20.1, 5-methyltetrahydropteroyltriglutamate-homocysteine methyltransferase, heat shock protein 70, ferritin, 14-3-3-like and translation initiation factor subunit were statistically-

significantly increased in winter-harvested samples to aid plant survival under low temperature, whereas the decreased proteins included triosephosphate isomerase, alcohol dehydrogenase, alcohol dehydrogenase1, vacuolar ATP synthase subunit B, V-type proton ATPase catalytic subunit A, V-type proton ATPase catalytic subunit A, cytosolic ascorbate peroxidase, putative lactoylglutathione lyase-like, glutathione reductase, actin-101, α -tubulin-3 chain, 5-methyltetrahydropteroyltriglutamate-homocysteine methyltransferase, methionine synthase, chloroplast acetohydroxy acid isomeroreductase, eukaryotic translation initiation factor 4A, proteasome subunit beta type-6-like, proteasome subunit beta type-1-like, 20S proteasome beta subunit 5 and ribulose 1,5-bisphosphate carboxylase-oxygenase large subunit (Figure 36).

The related proteins involved in growth, photosynthesis and protein synthesis were either decreased or increased in winter-harvested samples, because they might be sensitive to water deficit, as shown in grapevine (*Vitis vinifera* L.) (Cramer et al., 2013). Some proteins in carbohydrate and energy metabolism also had differential abundance levels during winter. This might be due to an effort to utilize energy more efficiently in response to water deficit. Thus, plants maintain a non-energy-conserving alternative oxidase pathway of respiration as an alternative pathway, which will be used in the periods of stress to control the power of a stress-signaling pathway from the mitochondrion to regulate metabolic plant responses (Cramer et al., 2013; Vanlerberghe et al., 2009).

Besides, water stress might result in decreased RuBisCO, thereby inhibiting photosynthesis (Cramer et al., 2013). Class I small heat shock protein 20.1 and heat shock protein 70 were active during winter, because they might be transferred from the leaves to store within tubers (Jungsukcharoen et al., 2016). For another decreased protein, the levels of proteins were effectively induced by higher temperature stresses.

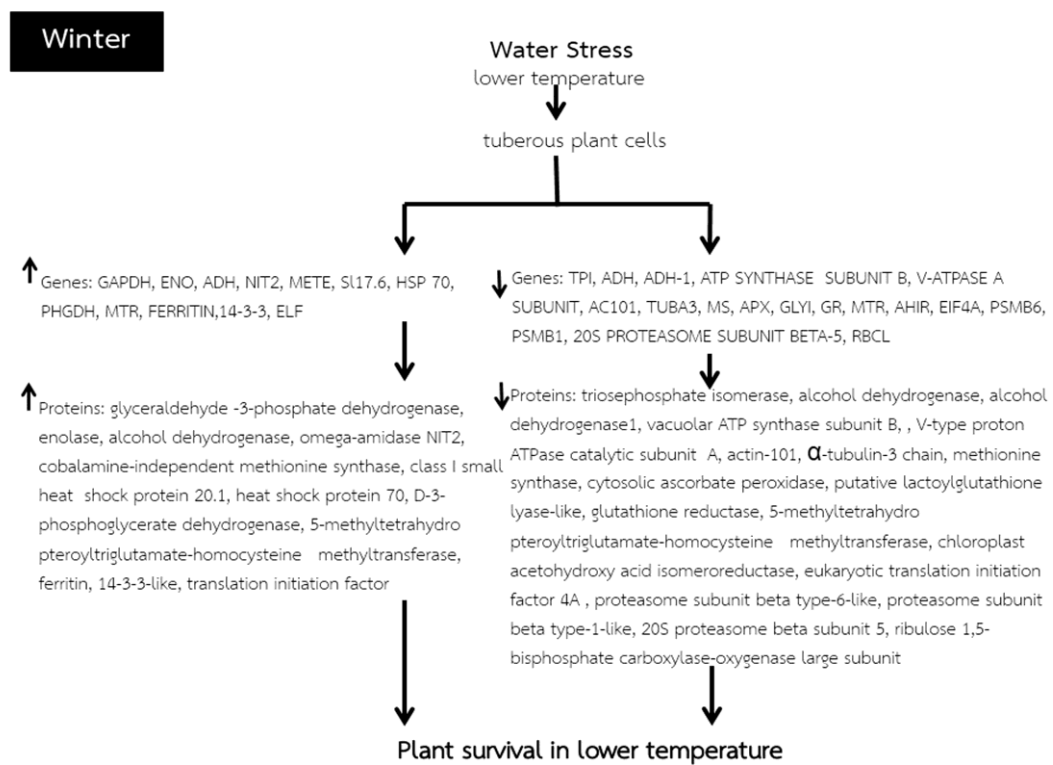


Figure 36 A model of proteins abundance in response to water stress during winter with analyzing from fold change of the terms in the ratio summer/ winter of spot intensities in summer- as compared with winter-harvested samples.

4.5.2 Proteins abundance in response to temperature stress and water stress in leaves

During summer, temperature stress can induce protein degradation, dehydration, and cell death (Waraich et al., 2012) and resulted in disruption of leaf plant cells. Ribulose 1,5 biphosphate carboxylase/oxygenase and the copper/zinc-of superoxide dismutase was statistically-significantly increased in the summer-harvested samples to aid plant survival under high temperature. Whereas, isoflavone reductase homolog 2 was statistically-significantly decreased under high temperature (Figure 37).

Elevated temperature might decline the activation state of RuBisCO by reducing the activation of RuBisCO activase (Yamori and von Caemmerer, 2009). For the copper/zinc-of superoxide dismutase, change of Cu/Zn-SOD level might depend on the susceptibility and tolerance of genotypes to be stimulated by overproduction of ROS under high temperature stress, as shown in wheat genotypes, (Almeselmani et al., 2006). High-temperature stress could influence the decreased expression of IFR2 gene involved in reduction of isoflavones concentration. Moreover, either the translocation of isoflavones or key metabolic precursors might be caused the decreased level of isoflavone reductase homolog 2, which was shown in *G. max* (L.) Merr. (Chennupati et al., 2012).

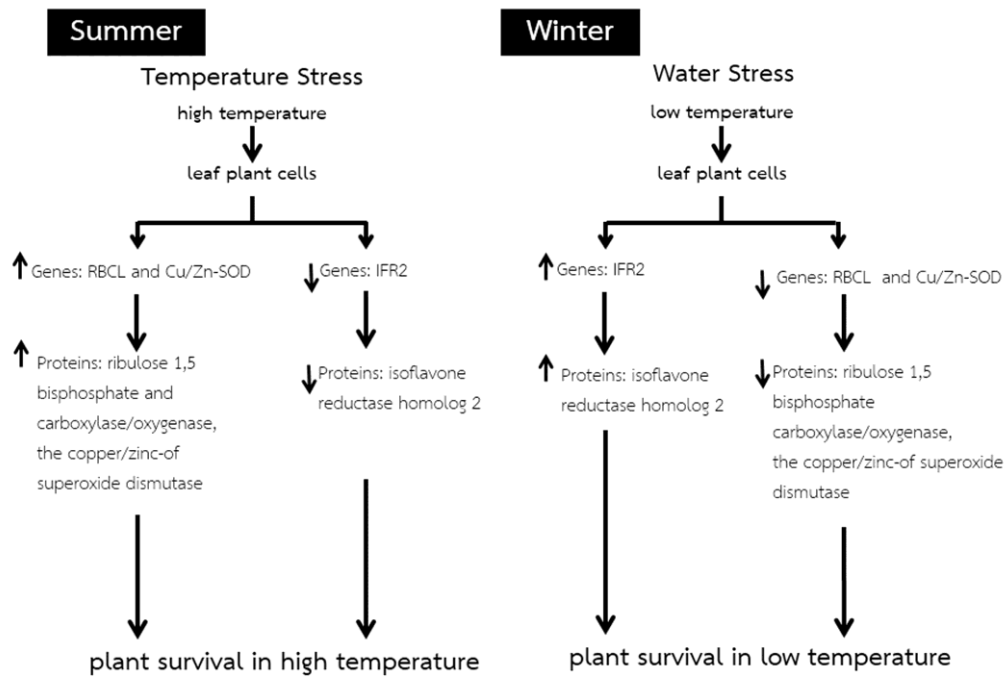


Figure 37 A model of proteins abundance in response to temperature stress during summer and water stress during winter with analyzing from fold change of the terms in the ratio summer/ winter of spot intensities in summer- as compared with winter-harvested samples.

During winter, water stress might initiate water deficit such as loss of water and drought (de Oliveira et al., 2013). Isoflavone reductase homolog 2 was statistically-significantly increased in winter-harvested samples, while ribulose 1,5 biphosphate carboxylase/oxygenase and the copper/zinc-of superoxide dismutase, monodehydroascorbate reductase -like isoform 1, proteasome subunit alpha type were statistically-significantly decreased in winter-harvested samples to aid plant survival under low temperature (Figure 37).

The increased IFR2 gene relating the increased isoflavone reductase homolog 2 proteins were induced under water stress because of the decrease of 2'-hydroxydaidzein to form 7,2'-dihydrodaidzein, which is one of the steps to involve in the aid of enhanced isoflavonoid biosynthesis in the elongation zone of roots, as shown in *G. max* (L.) Merr. (Yamaguchi et al., 2010). The other decreased proteins might result stress response and plant damage under long-lived drought condition, which was shown in barley (*Hordeum vulgare*) (Vitamvas et al., 2015).

CHAPTER V

CONCLUSION

B. superba tuber samples revealed the highest numbers of protein spots and a variety of proteins in winter-harvested samples from the 3 plant samples. The matched of 3 plant samples allowed identification of a total of 224 protein spots, whereas *B. superba* leave samples demonstrated more diverse protein spots in winter samples originated from Lampang. The matched of 3 plant samples allowed identification of a total of 112 protein spots.

The maximum protein appearance, forty-five differentially-abundant proteins were found in tubers originated from Chachoengsao, while twelve differentially-abundant proteins were found in leaves originated from Lampang. The differential proteins were found to be involved in the alternative physiological status within the tubers and leaves in response to seasonal changes and lead to changes in phenotype, allowing plant to survive during the severed seasonal changes.

In addition, the results demonstrated seasonal changes initiate an effect on temperature stress during summer and water stress during winter, which initiate

differential levels of carbohydrate and energy metabolism, cellular structure photosynthesis, secondary metabolism, protein destination and storage, signal transduction and homeostasis, amino-acid biosynthesis, protein biosynthesis, RNA and protein binding and stimulated defense and stress mechanisms and relative oxygen species catabolizing enzymes. The proteins might potentially be used as candidates for protein markers in differing seasons in other plants.

For harvesting period of *B. superba* tubers and leaves, the finding suggested both tubers and leaves in the winter-harvested samples were more diverse protein spots than the other seasons. The recommended harvesting season of the plant tuber and leaf materials might be in winter, not summer or rainy season. Moreover, this is the first report on discovery of isoflavone reductase homolog 2 proteins involving in enhanced isoflavonoid biosynthesis in *B. superba* leaves to be induced in response to water stress during winter. *B. superba* leaves might be an alternative material source for the commercial scale extraction for natural isoflavones and other phytochemicals to be used for anti-aging and alternative medicines to aid of rejuvenation, promotion of sexual vigor and treatment of male erectile dysfunction.

REFERENCES



REFERENCES

Agrawal, L., Chakraborty, S., Jaiswal, D.K., Gupta, S., Datta, A., and Chakraborty, N. Comparative proteomics of tuber induction, development and maturation reveal the complexity of tuberization process in potato (*Solanum tuberosum* L.). J. Proteome Res. 7(2008): 3803-3817.

Ahuja, I., Vos, R.C., Bones, A.M., and Hall, R.D. Plant molecular stress responses face climate change. Trends Plant Sci. 15(2010): 664-674.

Almeselmani, M., Deshmukh, P.S., Sairam, R.K., Kushwaha, S.R., and Singh, T.P. Protective role of antioxidant enzymes under high temperature stress. Plant Sci. 171(2006): 382-388.

Aman, S., Iqbal, M., Abbas, S., Banaras, S., Awais, M., Ahmad, I., Shinwari, Z.K., and Shakeel, S. Molecular and comparative analysis of newly isolated beta-tubulin partial gene sequences from selected medicinal plants. Pak. J. Bot. 45(2013): 507-512.

Apel, K., and Hirt, H. Reactive oxygen species: metabolism, oxidative stress, and signal transduction. Annu. Rev. Plant Biol. 55(2004): 373-399.

Arechaga, I., and Jones, P.C. The roter in the membrane of the ATP synthase and relatives. FEBS Lett. 494(2001): 1-5.

Ashida, H., Saito, Y., Nakano, T., Tandeau de Marsac, N., Sekowska, A., Danchin, A., and Yokota, A. RuBisCO-like proteins as the enolase enzyme in the methionine salvage pathway: functional and evolutionary relationships between RuBisCO-like proteins and photosynthetic RuBisCO. J. Exp. Bot. 59(2008): 1543-1554.

Ban, Y., Kobayashi, Y., Hara, T., Hamada, T., Hashimoto, T., Takeda, S., and Hattori, T. Tubulin is rapidly phosphorylated in response to hyperosmotic stress in rice and *Arabidopsis*. Plant Cell Physiol. 54(2013): 848-858.

Bertsch, U., Soll, J., Seetharam, R., and Viitanen, P.V. Identification, characterization, and DNA sequence of a functional "double" groES-like chaperonin from chloroplasts of higher plants. Proc. Natl. Acad. Sci. USA. 89(1992): 8696-8700.

Boonmee, A., Srisomsap, C., Chokchaichamnankit, D., Karnchanatat, A., and Sangvanich, P. A proteomic analysis of *Curcuma comosa* Roxb. rhizomes. Proteome Sci. 9(2011): 43-50.

Boutraa, T., Akhkha, A., Al-Shoaibi, A.A., and Alhejeli, A.M. Effect of water stress on growth and water use efficiency (WUE) of some wheat cultivars (*Triticum durum*) grown in Saudi Arabia. J. Taibah Univ. Sci. 3(2010): 39-48.

Bradford, M.M. A rapid and sensitive method for the quantitation of microgram quantities of protein utilizing the principle of protein dye binding. Anal. Chem. 72(1976): 248-254.

Briat, J.F., Duc, C., Ravet, K., and Gaymard, F. Ferritins and iron storage in plants. Biochim. Biophys. Acta. 1800(2010): 806-814.

Carpentier, S.C., Witters, E., Laukens, K., Deckers, P., Swennen, R., and Panis, B. Preparation of protein extracts from recalcitrant plant tissues: an evaluation of different methods for two-dimensional gel electrophoresis analysis. Proteomics. 5(2005): 2497-2507.

Chakraborty, U., and Pradhan, D. High temperature-induced oxidative stress in *Lens culinaris*, role of antioxidants and amelioration of stress by chemical pre-treatments. J. Plant Interact. 6(2011): 43-52.

Cheng, Z., Dong, K., Ge, P., Bian, Y., Dong, L., Deng, X., Li, X., and Yan, Y. Identification of leaf proteins differentially accumulated between wheat cultivars distinct in their levels of drought tolerance. PLoS One. 10(2015): e0125302.

Chennupati, P., Seguin, P., Chamoun, R., and Jabaji, S. Effects of high-temperature stress on soybean isoflavone concentration and expression of key genes involved in isoflavone synthesis. J. Agric. Food Chem. 60(2012): 12421–12427.

Cherdshewasart, W., Bhuntaku, P., Panriansaen, R., Dahlan, W., and Malaivijitnond, S. Androgen disruption and toxicity tests of *Butea superba* Roxb., a traditional herb used for treatment of erectile dysfunction, in male rats. Maturitas. 60(2008): 131-137.

Cherdshewasart, W., Cheewasopit, W., and Picha, P. The differential anti-proliferation effect of white (*Pueraria mirifica*), red (*Butea superba*), and black (*Mucuna collettii*) kwao krua plants on the growth of MCF-7 cells. J. Ethnopharmacol. 93(2004): 255-260.

Cherdshewasart, W., and Nimsakul, N. Clinical trial of *Butea superba*, an alternative herbal treatment for erectile dysfunction. Asian J. Androl. 5(2003): 243-246.

Cherdshewasart, W., and Sutjit, W. Correlation of antioxidant activity and major isoflavonoid contents of the phytoestrogen-rich *Pueraria mirifica* and *Pueraria lobata* tubers. Phytomedicine. 15(2008): 38-43.

Chokchaichamnankit, D., Subhasitanont, P., Paricharttanakul, N.M., Sangvanich, P., Svasti, J., and Srisomsap, C. Proteomic alteration during dormant period of *Curcuma longa* rhizomes. J. Proteom. Bioinform. 02(2009): 380-387.

Chukeatirote, E., and Saisavoey, T. Antimicrobial property and antioxidant composition of crude extracts of *Pueraria mirifica*, *Butea superba* and *Mucuna macrocarpa*. Maejo Int. J. Sci. Technol. 3(2009): 212-221.

Ciuzan, O., Lazar, S.L., Lung, M.L., Pop, O.L., and Pamfil, D. Involvement of the glycine-rich RNA-binding proteins (GRP) in osmotic stress response during seed germination: a comparison between GRP 2 and GRP 7. Med. Cluj-Napoca. Hortic. 72(2015): 61-67.

Cramer, G.R., Van Sluyter, S.C., Hopper, D.W., Pascovici, D., Keighley, T.a., and Haynes, P.A. Proteomic analysis indicates massive changes in metabolism prior to the inhibition of growth and photosynthesis of grapevine (*Vitis vinifera* L.) in response to water deficit. BMC Plant Biol.13(2013): 49.

Csiszar, J., Lantos, E., Tari, I., Madosa, E., Wodala, B., Vashegyi, A., Horvath, F., Pecsvaradi, A., Szabo, M., Bartha, B., et al. Antioxidant enzyme activities in *Allium* species and their cultivars under water stress. Plant Soil Environ. 53(2007): 517-523.

de Oliveira, A.B., Alencar, N.L.M., and Gomes-Filho, E. Comparison between the water and salt Stress effects on plant growth and development. InTech. (2013): 1-28.

Diaz, C., Kusano, M., Sulpice, R., Araki, M., Redestig, H., Saito, K., Stitt, M., and Shin, R. Determining novel functions of *Arabidopsis* 14-3-3 proteins in central metabolic processes. BMC Syst. Biol. 5(2011): 192.

Dietz, K.L., Tavakoli, N., Kluge, C., Mimura, T., Sharma, S.S., Harris, G.C., Chardonnens, A.N., and Golldack, D. Significance of the V-type ATPase for the adaptation to stressful growth conditions and its regulation on the molecular and biochemical level. J. Exp. Bot. 52(2001): 1969–1980.

Dixon, D.C., Seagull, R.W., and Triplett, B.A. Changes in the accumulation of α - and β -Tubulin isotypes during cotton fiber development. Plant Physiol. 105(1994): 1347-1353.

Donnelly, B.E., Madden, R.D., Ayoubi, P., Porter, D.R., and Dillwith, J.W. The wheat (*Triticum aestivum* L.) leaf proteome. Proteomics 5(2005): 1624-1633.

Du, H., Ding, M., Tang, D., and Huang, D. Analysis of differential protein expression during the early stage of in vitro tuberization in taro. Sci. Hort. 129(2011): 904-909.

Dumas, R., Biou, F., Halgand, F., Douce, R., and Duggleb, R.G. Enzymology, structure, and dynamics of acetoxy acid isomerase. Acc. Chem. Res. 34(2001): 399-408.

Farooq, M., Wahid, A., Kobayashi, N., Fujita, D., and Basra, S.M.A. Plant drought stress: effects, mechanisms and management. Agron. Sustain. Dev. 29(2009): 185-212.

Faurobert, M., Pelpoir, E., and Chaib, J. Phenol extraction of proteins for proteomic studies of recalcitrant plant tissues. Methods Mole. Biol. 355(2007): 9-14.

Feller, U., Crafts-Brandner, S.J., and Salvucci, M.E. moderately high temperatures inhibit Ribulose-1,5-Bisphosphate carboxylase/oxygenase (RuBisCO) activase-mediated activation of RubisCO. Plant Physiol. 116(1998): 539-546.

Fernando, D.D., Lazzaro, M.D., and Owens, J.N. Growth and development of conifer pollen tubes. Sex. Plant Reprod. 18(2005): 149-162.

Figeys, D. Proteomics: The basic overview In D. Figeys (ed.), Industrial proteomics: Applications for biotechnology and pharmaceuticals, pp. 1-61, Ottawa: John Wiley & Sons, Inc, 2005.

Funato, Y., and Miki, H. Nucleoredoxin, a novel thioredoxin family member involved in cell growth and differentiation. Antioxid. Redox. Signal. 9(2007): 1035-1057.

Galili, G., Amir, R., and Fernie, A.R. The regulation of essential amino acid synthesis and accumulation in plants. Annu. Rev. Plant Biol. 67(2016): 153-178.

Gallie, D.R., Le, H., Caldwell, C., and Browning, K.S. Analysis of translation elongation factors from wheat during development and following heat shock. Biochem. Biophys. Res. Commun. 245(1998): 295-300.

Gass, N., Glagotskaia, T., Mellema, S., Stuurman, J., Barone, M., Mandel, T., Tunalı, U.R., and Kuhlemeier, C. Pyruvate decarboxylase provides growing pollen tubes with a competitive advantage in petunia. Plant Cell. 17(2005): 2355-2368.

Genschik, P., Jamet, E., Philipps, G., Parmentier, Y., Gigot, C., and Fleck, J. Molecular characterization of a β -type proteasome subunit from *Arabidopsis thaliana* co-expressed at a high level with an α -type proteasome subunit early in the cell cycle. Plant J. 6(1994): 537-546.

Ghosh, D., and Xu, J. Abiotic stress responses in plant roots: a proteomics perspective. Front Plant Sci. 5(2014): 6.

Gill, S.S., Anjum, N.A., Hasanuzzaman, M., Gill, R., Trivedi, D.K., Ahmad, I., Pereira, E., and Tuteja, N. Glutathione and glutathione reductase: a boon in disguise for plant abiotic stress defense operations. Plant Physiol. Biochem. 70(2013): 204-212.

Gill, S.S., and Tuteja, N. Reactive oxygen species and antioxidant machinery in abiotic stress tolerance in crop plants. Plant Physiol. Biochem. 48(2010): 909-930.

Graves, P.R., and Haystead, T.A.J. Molecular Biologist's Guide to Proteomics. Microbiol. Mole. Biol. Rev. 66(2002): 39-63.

Grimplet, J., Wheatley, M.D., Jouira, H.B., Deluc, L.G., Cramer, G.R., and Cushman, J.C. Proteomic and selected metabolite analysis of grape berry tissues under well-watered and water-deficit stress conditions. Proteomics. 9(2009): 2503-2528.

Han, F., Chen, H., Li, X.-J., Yang, M.-F., Liu, G.-S., and Shen, S.-H. A comparative proteomic analysis of rice seedlings under various high-temperature stresses. BBA Proteins Proteom. 1794(2009): 1625-1634.

Hanschmann, E.M., Godoy, J.R., Berndt, C., Hudemann, C., and Lillig, C.H. Thioredoxins, glutaredoxins, and peroxiredoxins--molecular mechanisms and health significance: from cofactors to antioxidants to redox signaling. Antioxid. Redox Signal. 19(2013): 1539-1605.

Hashiguchi, A., Ahsan, N., and Komatsu, S. Proteomics application of crops in the context of climatic changes. Food Res. Int. 43(2010): 1803-1813.

Hauser, M., Egger, M., Wallner, M., Wopfner, N., Schmidt, G., and Ferreira, F. Molecular properties of food allergens: a current classification into protein families. Open Immunol. J. 1(2008): 1-12.

Hego, E., Bes, C.M., Bedon, F., Palagi, P.M., Chaumeil, P., Barre, A., Claverol, S., Dupuy, J.W., Bonneau, M., Lalanne, C., et al. Differential accumulation of soluble proteins in roots of metalicolous and nonmetalicolous populations of *Agrostis capillaris* L. exposed to Cu. Proteomics. 14(2014): 1746-1758.

Hernandez, G., and Vazquez-Pianzola, P. Functional diversity of the eukaryotic translation initiation factors belonging to eIF4 families. Mech. Dev. 122(2005): 865-876.

Hossain, Z., Nouri, M.Z., and Komatsu, S. Plant cell organelle proteomics in response to abiotic stress. J. Proteom. Res. 11(2012): 37-48.

Huang, Z., Hong, Q., Xue, P., Paul, G., Feng, Z., Wang, L., Mei, Y., Wu, L., Chen, X., and Wu, D. A proteome-wide screen identifies valosin-containing protein as an essential regulator of podocyte endoplasmic reticulum stress. Chinese Sci. Bull. 57(2012): 2493-2505.

Ingkaninan, K., Temkitthawon, P., Chuenchom, K., Yuyaem, T., and Thongnoi, W. Screening for acetylcholinesterase inhibitory activity in plants used in Thai traditional rejuvenating and neurotonic remedies. J. Ethnopharmacol. 89(2003): 261-264.

Jaenicke, R., Heber, U., Franks, F., Chapman, D., Griffin, M.C.A., Hvidt, A., and Cowan, D.A. Protein Structure and Function at Low Temperatures [and Discussion]. Philos. Trans. R. Soc. Lon. B. Biol. Sci. 326(1990): 535-553.

Janmohammadi, M., Zolla, L., and Rinalducci, S. Low temperature tolerance in plants: Changes at the protein level. Phytochemistry. 117(2015): 76-89.

Jensen, R.G. Activation of RuBisCO regulates photosynthesis at high temperature and CO₂. Proc. Natl. Acad. Sci. USA. 97(2000): 12937–12938.

Jin, S.H., Li, X.Q., Wang, G.G., and Zhu, X.T. Brassinosteroids alleviate high-temperature injury in *Ficus concinna* seedlings via maintaining higher antioxidant defence and glyoxalase systems. AoB Plants. 7(2015): 1-12.

Job, C., Rajjou, L., Lovigny, Y., Belghazi, M., and Job, D. Patterns of protein oxidation in *Arabidopsis* seeds and during germination. Plant Physiol. 138(2005): 790-802.

Jungsukcharoen, J., Chokchaichamnankit, D., Srisomsap, C., Cherdshewasart, W., and Sangvanich, P. Proteome analysis of *Pueraria mirifica* tubers collected in different seasons. Biosci. Biotechnol. Biochem. (2016): 1-11.

Kaewmuangmoon, J. Leaf morphometry, genetic variation, and phylogeny of red kwao krua. Master's thesis, Faculty of Science: Chulalongkorn University, 2006.

Kelish, A.E., Zhao, F., Heller, W., Durner, J., Winkler, J.B., Behrendt, H., Hoffmann, C.T., Horres, R., Pfeifer, F., Frank, U., et al. Ragweed (*Ambrosia artemisiifolia*) pollen allergenicity: SuperSAGE transcriptomic analysis upon elevated CO₂ and drought stress. BMC Plant Biol. 14(2014): 176.

Khan, S., Ul-Hasan, M., and Khan, M.A. Annual and seasonal distribution of sunshine in Pakistan 1931-1990. In Gâstescu, P., Jr.Lewis, W., Bretcan, P (eds.), Water resources and wetlands, pp. 354-360. Tulcea - Romania: Conference Proceedings, 14-16 September 2012, 2012.

Kim, J.Y., Kim, W.Y., Kwak, K.J., Oh, S.H., Han, Y.S., and Kang, H. Glycine-rich RNA-binding proteins are functionally conserved in *Arabidopsis thaliana* and *Oryza sativa* during cold adaptation process. J. Exp. Bot. 61(2010): 2317-2325.

Komatsu, S., and Hossain, Z. Organ-specific proteome analysis for identification of abiotic stress response mechanism in crop. Front. Plant Sci. 4(2013): 71.

Krasnikov, B.F., Chien, C.H., Nostramo, R., Pinto, J.T., Nieves, E., Callaway, M., Sun, J., Huebner, K., and Cooper, A.J. Identification of the putative tumor suppressor Nit2 as omega-amidase, an enzyme metabolically linked to glutamine and asparagine transamination. Biochimie. 91(2009): 1072-1080.

Kumutha, D., Ezhimathi, K., Sairam, R.K., Srivastava, G.C., Deshimukh, P.S., and Meena, R.C. Waterlogging induced oxidative stress and antioxidant activity in pigeonpea genotypes Biol. Plantarum. 53(2009): 75-84.

Laughner, B.J., Sehnke, P.C., and Ferl, R.J. A novel nuclear member of the thioredoxin superfamily. Plant Physiol. 118(1998): 987-996.

Lee, D.G., Ahsan, N., Lee, S.H., Kang, K.Y., Bahk, J.D., Lee, I.J., and Lee, B.H. A proteomic approach in analyzing heat-responsive proteins in rice leaves. Proteomics. 7(2007): 3369-3383.

Lee, J.J., Kim, Y.H., Kwak, Y.S., An, J.Y., Kim, P.J., Lee, B.H., Kumar, V., Park, K.W., Chang, E.S., Jeong, J.C., et al. A comparative study of proteomic differences between pencil and storage roots of sweetpotato (*Ipomoea batatas* (L.) Lam.). Plant Physiol. Biochem. 87(2015): 92-101.

Lee, K., Lee, S.H., and Woo, S.Y. RuBisCO activity and gene expression of tropical tree species under light stress. *Afr. J. Biotechnol.* 12(2013): 2764-2769.

Lehesranta, S.J., Davies, H.V., Shepherd, L.V., Koistinen, K.M., Massat, N., Nunan, N., McNicol, J.W., and Karenlampi, S.O. Proteomic analysis of the potato tuber life cycle. *Proteomics.* 6(2006): 6042-6052.

Leichert, L., and Jakob, U. Global methods to monitor the thiol–disulfide state of proteins in vivo. *Antioxid. Redox Signal.* 8(2006): 763-773.

Levine, J.M., McEachern, A.K., and Cowan, C. Rainfall effects on rare annual plants. *J. Ecol.* 96(2008): 795-806.

Li, Q., Huang, J., Liu, S., Li, J., Yang, X., Liu, Y., and Liu, Z. Proteomic analysis of young leaves at three developmental stages in an albino tea cultivar. *Proteome Sci.* 9(2011^a): 44.

Li, Q., Huang, J., Liu, S., Li, J., Yang, X., Liu, Y., and Liu, Z. Proteomic analysis of young leaves at three developmental stages in an albino tea cultivar. *Proteome Sci.* 9(2011^b): 44.

Loontaisong, A. Chemical constituents and biological activity of *Butea superba* Roxb.

Master, s thesis, Faculty of Science: Chulalongkorn University, 2005.

Lurie, S., and Sabehat, A. Prestorage temperature manipulations to reduce chilling injury in tomatoes. Postharvest Biol. Tech. 11(1997): 57-62.

Ma, K., Ishikawa, T., Seki, H., Furihata, K., Ueki, H., Narimatsu, S., Higuchi, Y., and Chaichantipyuth, C. Isolation of new isoflavonolignans, butesuperins A and B, from a Thai miracle herb. Heterocycles. 65(2005): 893-900.

Ma, R., Sun, L., Chen, X., Jiang, R., Sun, H., and Zhao, D. Proteomic changes in different growth periods of ginseng roots. Plant Physiol. Biochem. 67(2013): 20-32.

Mahajan, S., and Tuteja, N. Cold, salinity and drought stresses: an overview. Arch. Biochem. Biophys. 444(2005): 139-158.

Mahmood, T., Safdar, W., Abbasi, B.H., and Naqvi, S.M.S. An overview on the small heat shock proteins. Afr. J. Biotechnol. 9(2010): 927-949.

Malaivijitnond, S., Ketsuwan, A., Watanabe, G., Taya, K., and Cherdshewasart, W. Luteinizing hormone reduction by the male potency herb, *Butea superba* Roxb. Braz. J. Med. Biol. Res. 43(2010): 843-852.

Mccurdy, D.W., Kovar, D.R., and Staiger, C.J. Actin and actin-binding proteins in higher plants. Protoplasma. 215(2001): 89-104.

Mitprasat, M., Roytrakul, S., Jiemsup, S., Boonseng, O., and Yokthongwattana, K. Leaf proteomic analysis in cassava (*Manihot esculenta*, Crantz) during plant development, from planting of stem cutting to storage root formation. Planta. 233(2011): 1209-1221.

Mittler, R., Finka, A., and Goloubinoff, P. How do plants feel the heat? Trends Biochem. Sci. 37(2012): 118-125.



Mohamed, H., and Al-Whaibi. Plant heat-shock proteins: A mini review. J. King Saud Univ.Sci. 23(2011): 139-150.

Nakanishi-Matsui, M., Sekiya, M., Nakamoto, R.K., and Futai, M. The mechanism of rotating proton pumping ATPases. Biochim. Biophys. Acta. 1797(2010): 1343-1352.

Ngamhui, N., Akkasaeng, C., Zhu, Y.J., Tantisuwichwong, N., Roytrakul, S., and Sansayawichai, T. Differentially expressed proteins in sugarcane leaves in response to water deficit stress. Plant Omics J. 5(2012): 365-371.

Ngamrojanavanich, N., Loontaisong, A., Pengpreecha, S., Cherdshewasart, W., Pornpakakul, S., Pudhom, K., Roengsumran, S., and Petsom, A. Cytotoxic constituents from *Butea superba* Roxb. J. Ethnopharmacol. 109(2007): 354-358.

Noctor, G., Mhamdi, A., Chaouch, S., Han, Y., Neukermans, J., Garcia, B.M., Queval, G., and Foyer, C.H. Glutathione in plants: an integrated overview. Plant Cell Environ. 35(2012): 454-484.

Porter, J.R., and Semenov, M.A. Crop responses to climatic variation. Philos. Trans. of The R. Soc. B. 360(2005): 2021-2035.

Radauer, C., and Breiteneder, H. Evolutionary biology of plant food allergens. J. Allergy Clin. Immunol. 120(2007): 518-525.

Rampitsch, C., and Srinivasan, M. The application of proteomics to plant biology: a review. Can. J. Bot. 84(2006): 883-892.

Rasineni, G.K., Chinnaboina, M., and Reddy, A.R. Proteomic approach to study leaf proteins in a fast-growing tree species, *Gmelina arborea* Linn. Roxb. Trees. 24(2009): 129-138.

Ravanel, S., Gakiere, B., Job, D., and Douce, R. The specific features of methionine biosynthesis and metabolism in plants. Proc. Natl. Acad. Sci. USA. 95(1998): 7805-7812.

Roengsumran, S., Petsom, A., Ngamrojanavanich, N., Rugsilp, T., Sittiwicheanwong, P., Khorphueng, P., Cherdshewasart, W., and Chaichantipyuth, C. Flavonoid and flavonoid glycoside from *Butea superba* Roxb. and their cAMP phosphodiesterase inhibitory activity. J. Sci. Res. Chula. Univ. 25(2000): 169-176.

Rosignol, M., Peltier, J.B., Mock, H.P., Matros, A., Maldonado, A.M., and Jorin, J.V. Plant proteome analysis: a 2004-2006 update. Proteomics. 6(2006): 5529-5548.

Ruksilp, T. Chemical constituents of the tuberous roots of *Butea superba* Roxb. Master's thesis, Faculty of Science, Chulalongkorn University, 1995.

Sangkaong, W. Cytotoxicity tests of extracts from white kwao krua *Pueraria mirifica*, Red kwao krua, *Butea superba* and black kwao kroa, *Mucuna collettii* on Hep-G2 cells. Doctor's thesis, Faculty of Science, Chulalongkorn University, 2005.

Santos, A., and Van Ree, R. Profilins: mimickers of allergy or relevant allergens? Int. Arch. Allergy Immunol. 155(2011): 191-204.

Sawasdi-putsa, N. Proteomics of manila tamarind seeds *Pithecellobium dulce*. Doctor's thesis, Faculty of science, Chulalongkorn University, 2008.

Sebehat, A., Lurie, S., and Weiss, D. Expression of small heat-Shock proteins at low temperatures: A possible role in protecting against chilling injuries. Plant Physiol. 117(1998): 651-658.

Shinozaki, K., and Yamaguchi-Shinozaki, K. Molecular responses to dehydration and low temperature: differences and cross-talk between two stress signaling pathways. Curr. Opin. Plant Biol. 3(2000): 217-223.

Simoës-Araújo, J.L., Rumjanek, N.G., and Margis-Pinheiro, M. Small heat shock proteins genes are differentially expressed in distinct varieties of common bean. Braz. J. Plant Physiol. 15(2003): 33-41.

Sinha, M., Singh, R.P., Kushwaha, G.S., Iqbal, N., Singh, A., Kaushik, S., Kaur, P., Sharma, S., and Singh, T.P. Current overview of allergens of plant pathogenesis related protein families. Hindawi Publishing Corporation. 2014(2014): 1-19.

Somera, G.N. Proteins and temperature. Annu. Rev. Physiol. 57(1995): 43-68.

Song, Y., Chen, Q., Ci, D., Shao, X., and Zhang, D. Effects of high temperature on photosynthesis and related gene expression in poplar. BMC Plant Biol.14(2014): 111.

Songnuan, W. Wind-pollination and the roles of pollen allergenic proteins. Asian Pac. J. Allergy Immunol.31(2013): 261-270.

Srisomsap, C., Sawangareetrakul, P., Subhasitanont, P., Chokchaichamnankit, D., Chiablaem, K., Bhudhisawasdi, V., Wongkham, S., and Svasti, J. Proteomic studies of cholangiocarcinoma and hepatocellular carcinoma cell secretomes. J. Biomed. Biotechnol. 2010(2010): 1-18.

Sun, P., Mao, Y., Li, G., Cao, M., Kong, F., Wang, L., and Bi, G. Comparative transcriptome profiling of *Pyropia yezoensis* (Ueda) M.S. Hwang & H.G. Choi in response to temperature stresses. BMC Genomics. 16(2015): 463.

Suntara, A. The Remedy pamphlet of kwao krua tuber of Luang Anusarnsuntarakromkarnpiset, Chiang Mai: Upatipongsa Press,1931.

Timperio, A.M., Egidì, M.G., and Zolla, L. Proteomics applied on plant abiotic stresses:

Role of heat shock proteins (HSP). J. Proteomics. 71(2008): 391-411.

Tocharus, C., Smitasiri, Y., and Jeenapongsa, R. *Butea superba* Roxb. enhances penile

erection in rats. Phytothe. Res. 20(2006): 484-489.

Twyman, R.M. Principles of Proteomics, New York: Taylor and Francis Group, 2004.

Vanlerberghe, G.C., Cvetkovska, M., and Wang, J. Is the maintenance of homeostatic

mitochondrial signaling during stress a physiological role for alternative oxidase?

Physiol. Plant. 137(2009): 392-406.

Veitch, N.C. Isoflavonoids of the leguminosae. Nat. Prod. Rep. 30(2013): 988-1027.

Vera-Reyes, I., Huerta-Heredia, A.A., Ponce-Noyola, T., Rojas, C.G., M., C., Trejo-Tapia, G.,

and Ramos-Valdivia, A.C. Monoterpenoid indole alkaloids and phenols are required

antioxidants in glutathione depleted *Uncaria tomentosa* root cultures. Front. Environ.

Sci. 3(2015): 1-11.

Vitamvas, P., Urban, M.O., Skodacek, Z., Kosova, K., Pitelkova, I., Vitamvas, J., Renaut, J., and Prasil, I.T. Quantitative analysis of proteome extracted from barley crowns grown under different drought conditions. Front. Plant Sci. 6(2015): 1-18.

Wahid, A., Gelani, S., Ashraf, M., and Foolad, M. Heat tolerance in plants: An overview. Environ. Exp. Bot. 61(2007): 199-223.

Wang, W., Vinocur, B., Shoseyov, O., and Altman, A. Role of plant heat-shock proteins and molecular chaperones in the abiotic stress response. Trends Plant Sci. 9(2004): 244-252.

Waraich, E.A., Ahmad, R., Halim, A., and Aziz, T. Alleviation of temperature stress by nutrient management in crop plants: a review. J. Soil Sci. Plant Nutr. 12(2012): 221-244.

Wu, B., Niu, N., Li, J., and Li, S. Leaf:fruit ratio affects the proteomic profile of grape berry skins. J. Am. Soc. Hortic. Sci. 6(2013): 416-427.

Xu, C., Garrett, W.M., Sullivan, J., Caperna, T.J., and Natarajan, S. Separation and identification of soybean leaf proteins by two-dimensional gel electrophoresis and mass spectrometry. Phytochemistry. 67(2006): 2431-2440.

Xu, Y. Studies on gene structure, enzymatic activity and regulatory mechanism of acetoxy acid isomeroeductase from G2 pea. Sci. China Ser. C 46(2003): 389-398.

Yadav, S.K., Singla-Pareek, S.L., and Sopory, S.K. An overview on the role of methylglyoxal and glyoxalases in plants. Drug Metabol. Drug Interact. 23(2008): 51-68.

Yadava, R.N., and Reddy, K.I.S. A new bio-active flavonol glycoside from the stems of *Butea superba* Roxb. J. Asian Nat. Prod. Res. 1(1998): 139-145.

Yamaguchi, M., Valliyodan, B., Zhang, J., Lenoble, M.E., Yu, O., Rogers, E.E., Nguyen, H.T., and Sharp, R.E. Regulation of growth response to water stress in the soybean primary root. I. Proteomic analysis reveals region-specific regulation of phenylpropanoid metabolism and control of free iron in the elongation zone. Plant Cell Environ. 33(2010): 223-243.

Yamori, W., and von Caemmerer, S. Effect of RuBisCO activase deficiency on the temperature response of CO₂ assimilation rate and Rubisco activation state: Insights from transgenic tobacco with reduced amounts of RuBisCC Activase. Plant Physiol. 151(2009): 2073-2082.

Zhang, Y., Xu, L., Zhu, X., Gong, Y., Xiang, F., Sun, X., and Liu, L. Proteomic Analysis of Heat Stress Response in Leaves of Radish (*Raphanus sativus* L.). Plant Mole. Biol. Rep. 31(2012): 195-203.





APPENDIX A

จุฬาลงกรณ์มหาวิทยาลัย
CHULALONGKORN UNIVERSITY

Table 10 Solution for protein extraction

Solution	Chemical	Final concentration	Amount
Extraction buffer	Sucrose	0.7 M	49.92 g
	Tris (USB™)	0.5 M	12.14 g
	HCl	30 mM	523.50 µl
	EDTA-Fluka	50 mM	3.722 g
	KCl-Merck	0.1 M	1.491 g
	β-mecaptoethanol	2%	4 ml
	1 M PMSF (phenylmethylsulfonyl fluoride)	2 mM	400 µl
	Milli-Q water (cold water)		to 200 ml
1 M PMSF	PMSF	1 M	0.0696 g
	Double distilled H ₂ O		to 400 µl
Phenol solution	Phenol detached crystals-Merck	99+% (w/v)	500 g
	Double distilled H ₂ O		to 500 ml
Precipitation	Ammonium acetate	0.1 M	0.7708 g
	Methanol		to 100 ml
99.9% Acetone	Acetone (cold)	99.90%	to 100 ml

Table 11 Solution for 2D-PAGE

Solution	Chemical	Final concentration	Amount
Lysis buffer	Urea-Biorad	7 M	420 mg
	Thiourea	2 M	152.50 mg
	CHAPS (4°C)	4% (w/v)	40 mg
	DTT (dithiothreitol)	2% (w/v)	20 mg
	Ampholine (pH 3-10)	5% (v/v)	50 μ l
	Milli-Q water		to 1000 μ l
Rehydration buffer	Urea-Biorad	8 M	480 mg
	CHAPS	2% (w/v)	20 mg
	DTT(dithiothreitol)	0.28 % (w/v)	2.8 mg
	IPG buffer (pH 3-10)	0.5% (v/v)	5 μ l
	Milli-Q water		to 1000 μ l
	Bromophenol blue	0.002% (w/v)	400 μ l
Equilibration buffer I	0.5 M Tris-HCl,pH 6.8	50 mM	0.75 ml
	Urea	6 M	2.70 g
	Glycerol	30% (v/v)	2.25 ml
	SDS	2% (w/v)	75 mg
	Milli-Q water		to 7.5 ml
	DTT	1% (w/v)	75 mg
Equilibration buffer II	0.5 M Tris-HCl,pH 6.8	50 mM	0.75 ml
	Urea	6 M	2.70 g
	Glycerol	30% (v/v)	2.25 ml
	SDS	2% (w/v)	75 mg
	Milli-Q water		to 7.5 ml
	Iodoacetamide	2.5% (w/v)	187.5 mg
0.5 M Tris-HCl,pH 6.8	Tris base	0.5 M	15 g
			adjust to pH
	HCl		6.8
	Milli-Q water		to 250 ml

Table 11 (Continued)

Solution	Chemical	Final concentration	Amount
14% Separating gel solution	1.5 M Tris-HCl, pH 8.8	1.5 M	2250 μ l
	30% Acrylamide / 0.8% bis acrylamide		4545 μ l
	10% SDS	10% (v/v)	100 μ l
	10% Ammonium persulfate (APS)	10% (v/v)	50 μ l
	TEMED		5 μ l
	Milli-Q water		to 10 ml
1.5 M Tris-HCl (pH 8.8)	Tris base	1.5 M	45.38 g
	HCl		adjust to pH 8.8
	Milli-Q water		to 250 ml
30% Acrylamide / 0.8% bis acrylamide	30% Acrylamide	30% (w/v)	30 g
	0.8% bis acrylamide	0.8% (w/v)	0.8 g
	Milli-Q water		to 100 ml
10% SDS	SDS	10% (w/v)	10 g
	Milli-Q water		to 100 ml
10% APS	APS	10% (w/v)	0.1 g
	Milli-Q water		to 1 ml
4% Stacking gel solution	0.5M Tris-HCl ,pH 6.8	0.5 M	625 μ l
	30% Acrylamide/0.8% bis acrylamide		325 μ l
	10% (w/w) SDS	10% (v/v)	25 μ l
	10% APS	10% (w/v)	12.5 μ l
	TEMED		2.5 μ l
	Milli-Q water		to 2.5 ml
5X running buffer	Tris base		15 g
	Glycine		72 g
	SDS		5 g
	RO water		to 1000 ml
1X running buffer	5X running buffer		200 ml
	RO water		to 1000 ml
Agarose sealing solution	0.5% Agarose	0.50%	0.5 g
	5X running buffer		to 100 ml
	Coomassies Blue	0.002% (w/v)	200 μ l

Table 12 Coomassies gel stain and destain solution

Solution	Chemical	Amount
Coomassies Gel stain	Coomassies Blue R-250	0.1 g
	40% Methanol (AR)	40 ml
	10% Acetic acid	10 ml
	R.O water	to 100 ml
Coomassies Gel destain I	40% Methanol (AR)	40 ml
	10 % Acetic acid	10 ml
	R.O water	to 100 ml
Coomassies Gel destain II	10% Methanol (AR)	10 ml
	5 % Acetic acid	5 ml
	R.O water	to 100 ml

Table 13 Digestion solutions

Solution	Chemical	Final concentration	Amount
0.2 M Ammonium bicarbonate (NH ₄ HCO ₃)	NH ₄ HCO ₃	0.2 M	1.581 g
	Milli-Q water		to 100 ml
0.1 M Tris-HCl, pH 8.5	Tris base	0.1 M	1.211 g
	Milli-Q water		to 100 ml
	HCl		adjust to 8.5
10 mM Calcium chloride (CaCl ₂)	CaCl ₂	10 mM	14.70 mg
	Milli-Q water		to 10 ml
10 mM EDTA	EDTA	10 mM	37.22 mg
	Milli-Q water		to 10 ml
100 mM Dithiothreitol (DTT)	DTT	100 mM	3.085 mg
	Milli-Q water		to 200 µl
200 mM Iodoacetamide (IAA)	IAA	200 mM	7.398 mg
	Milli-Q water		to 200 µl
5 % Formic acid (HCOOH)	Formic acid	5% (v/v)	5 ml
	Milli-Q water		to 100 ml
Washing and Destaining Coomassie blue stained gels			
Solution 1			
0.1 M NH ₄ HCO ₃ / 50% ACN	0.2 M NH ₄ HCO ₃	0.1 M	500 µl
50 ul / sample	100% ACN	50% (v/v)	500 µl
Reduction and alkylation			
Solution 2			
0.1 M NH ₄ HCO ₃ / 10 mM DTT/	0.2 M NH ₄ HCO ₃	0.1 M	500 µl
10 mM EDTA to reduce	100 mM DTT	10 mM	100 µl
50 ul / sample	10 mM EDTA	10 mM	100 µl
	Milli-Q water		to 1000 µl
Solution 3			
100 mM IAA/0.1M NH ₄ HCO ₃	200 mM IAA	100 Mm	500 µl
50 ul / sample	0.2 M NH ₄ HCO ₃	0.1 M	500 µl
Washing			
Solution 4			
3x with 0.05 M Tris-HCl, pH 8.5/	0.1 M Tris-HCl	0.05 M	500 µl
50% ACN	50%ACN	50% (v/v)	500 µl
50 ul / sample			
(3 times)			

Table 13 (Continued)

Solution	Chemical	Final concentration	Amount
Digestion and extraction			
Solution 5.1			
One part trypsin:	Trypsin solution		40 μ l
5 μ l 0.2 mg / ml stock, 1 μ l 10 % acetic acid,	10 % acetic acid	10% (v/v)	8 μ l
4 μ l MiliQ-water of solution 1	Milli-Q water		to 80 μ l
Solution 5.2			
Nine parts buffer:	0.1 M Tris-HCl	0.05 M	500 μ l
90 μ l 0.05 M Tris-HCl, pH8.5 /	100%ACN	50 % (v/v)	100 μ l
10%ACN / 1 mM CaCl ₂ of solution2	10 mM CaCl ₂	1 mM	100 μ l
	Milli-Q water		to 1000 μ l
**Solution 5.1+5.2			
37 μ l / sample	Solution 5.1		80 μ l
	Solution 5.2		720 μ l
Solution 6			
2 % Trifluoroacetic acid (TFA)	TFA	2% (v/v)	12 μ l
	Milli-Q water		to 600 μ l
Solution 7			
0.05 Tris-HCl, pH8.5/ 1 mM CaCl ₂	0.1 M Tris-HCl	0.05 M	500 μ l
40 μ l / sample	10 mM CaCl ₂	1 mM	100 μ l
	Milli-Q water		to 1000 μ l
Solution 8			
100% Acetonitrile (ACN)	100%ACN	100% (v/v)	1000 μ l
40 μ l / sample			
Solution 9			
5% Formic acid/ 100%ACN	5% Formic acid	5% (v/v)	500 μ l
40 μ l / sample	100%ACN	100% (v/v)	500 μ l

APPENDIX B



Table 16 Identified protein and peptide sequences of *B.suberba* tubers originated from Lampang, Saraburi and Chachoengsao were identified by two-dimensional Polyacrylamide Gel electrophoresis (2D-PAGE) coupled with LC/MS/MS

Spot no.	Accession number	Protein name	Organism	Theoretical MW (Da)	pI	Score	Peptide match	% Coverage	Sequences
1	gi 3914435	Profilin-1	<i>Glycine max</i>	14091	4.58	46	13	16	K.YMVIQEGPGAVIR.G [6] K.YMVIQEGPGAVIR.G+ Oxidation (M) [6] K.GPGGVTVK.K
2	gi 13274150	Putative cytosolic CuZn-superoxide	<i>Populus tremula</i> x <i>Populus tremuloides</i>	15186	5.47	63	3	13	K.EHGAPEDENR.H R.VACGVIGLQG.-+ Carbamidomethyl (C) [2]
3	gi 225451120	SOD [Cu-Zn]-like isoform 2	<i>Vitis vinifera</i>	15272	5.49	159	7	26	K.EHGAPEDENR.H R.AVVVHADPDDLK.G [2] K.GGHELK.S
4	gi 134684	Superoxide Dismutase [Cu-Zn]	<i>Petunia hybrida</i>	22302	6.17	58	5	12	R.VACGVIGLQG.-+ Carbamidomethyl (C) [3] R.ALWHELEDDLK.G [4] K.GGHELK.LTTGNAGGR.L
5	gi 349591294	Class I small heat shock protein 20.1	<i>Solanum lycopersicum</i>	17628	5.82	123	5	17	K.ADLPGLK.K K.AAMENGVLTVPK.E + Oxidation (M) K.ASMENGVLTVPK.E K.ACMENGVLTVPK.E K.SIEISG.-

Table 16 (Continued)

Spot no.	Accession number	Protein name	Organism	Theoretical MW (Da)	pI	Score	Peptide match	% Coverage	Sequences
6	gj 33325131	Eukaryotic translation Initiation factor 5A isoform VIII	<i>Hevea brasiliensis</i>	17344	5.60	55	10	31	K.TYQQAGTIR.K [2] K.NGYIVIK.N K.WEVSTSK.T [2] R.LPTDENLLSOIK.D [3] K.DGFAEGK.D K.DIGPK.-
7	gj 351721881	18.5 kDa class I heat shock protein	<i>Glycine max</i>	18491	5.82	238	6	26	M.SLIPNFFGGR.R R.ENSAPVSTR.V K.VQIEDDK.V K.VQIEDDKVLSQISGER.N
8	gj 151347490	Translation initiation factor	<i>Carica papaya</i>	17421	5.60	159	5	17	K.VLSQISGER.N R.FRLPENAK.V R.KNGYIVIK.S K.NGYIVIK.S K.NGYIVIK.S K.WEVSTSK.T K.CHFVGIIDFTGK.K + Carbamidomethyl (C)

Table 16 (Continued)

Spot no.	Accession number	Protein name	Organism	Theoretical MW (Da)	pI	Score	Peptide match	% Coverage	Sequences
9	gij 351721881	18.5 kDa class I heat shock protein	<i>Glycine max</i>	18491	5.82	312	8	32	RENSAFVSTR.V K.VQIEDDK.V [2] K.VLQISGER.N R.FRLPENAK.V K.ASMENGLTIVTPK.E K.ASMENGLTIVTPK.E + Oxidation (M) K.AIEISG.-
10	gij 41059801	Small heat shock protein	<i>Prunus persica</i>	17380	5.98	55	1	5	K.VLHISGER.S
11	gij 123556	18.2 kDa class I heat shock protein	<i>Medicago sativa</i>	18154	5.81	132	3	15	RENSAFVSTR.V R.VLQISGER.S R.FRLPENAK.M
12	gij 356496106	18.2 kDa class I heat shock protein	<i>Glycine max</i>	16362	5.56	88	7	16	KADLPGLKIK [3] K.EEVKVEVEEGR.V K.VEEVEEGR.V K.TIEISG.- [2]

Table 16 (Continued)

Spot no.	Accession number	Protein name	Organism	Theoretical MW (Da)	pI	Score	Peptide match	% Coverage	Sequences
13	gi 38639431	17.5 kDa class I heat shock protein	<i>Carica papaya</i>	17471	5.31	76	6	12	R.ADLPLGLK.K [2] K.VLEDDR.V K.AIEISG.- [3]
14	gi 356559136	17.4 kDa class III heat shock protein	<i>Glycine max</i>	17959	6.17	97	2	14	R.RGPQNLLR.K K.FRLPENANVSATAK.C
15	gi 1675394	Alcohol dehydrogenase 3	<i>Oryza sativa</i>	40802	6.78	54	12	13	K.TNLGK.V + Carbamidomethyl (C) R.IIGIDSK.K [2] R.IIGIDSKK.F K.GTAFGGFK.S K.VDEVTHSMNLTIDINKA K.AFDLHEGGCLR.C + Carbamidomethyl (C) [6]
16	gi 502132065	Proteasome subunit beta type-6-like	<i>Cicer arietinum</i>	25110	5.12	207	4	16	R.TSTGVVANRA K.DEAELVK.K K.KAVSLAIR.D R.TVIINSEGVTR.N
17	gi 363808072	Allene oxide cyclase 4 chloroplastic-like	<i>Glycine max</i>	28394	8.75	68	2	6	K.LHQVYPFK.I K.ILYTFYLG.K

Table 16 (Continued)

Spot no.	Accession number	Protein name	Organism	Theoretical MW (Da)	pI	Score	Peptide match	% Sequences
18	gi 358345896	Allene-oxide cyclase	<i>Medicago truncatula</i>	27932	8.54	87	4	5 K.VQELSVYEINEKDR.G [4]
19	gi 255582541	Heat shock protein putative	<i>Ricinus communis</i>	26082	8.59	161	4	11 R.FDMPGLSK.E R.FDMPGLSK.E + Oxidation (M) K.VSVEDDVLVIK.G R.LKLPDNCEK.D + Carbamidomethyl (C)
20	gi 161291483	Heat shock protein	<i>Ammopiptanthus</i>	26082	7.66	165	3	12 R.FDMPGLSK.E K.VSVEDDVLVIK.G (M) K.NGVLYITIPK.T
21	gi 363807526	Uncharacterized protein LOC100798019 precursor	<i>Glycine max</i>	26013	7.77	70	13	17 R.IFEDTMTFPGR.N + Oxidation (M) [3] K.VSVEDDVLVIK.G [6] R.LKLPDNCEK.D + Carbamidomethyl (C) K.LLPDNCEK.D + Carbamidomethyl (C) K.NGVLYITIPK.T [2]
22	gi 15235282	Glyceraldehyde -3-phosphate dehydrogenase	<i>Solms-laubachia</i>	13267	6.81	41	5	23 R.AASFNIPSSSTGAAGA [2] R.VPTVDVSVWDLTVRL [3]

Table 16 (Continued)

Spot no.	Accession number	Protein name	Organism	Theoretical MW (Da)	pI	Score	Peptide match	% Sequences	% Coverage
23	gi 351723665	Uncharacterized protein LOC100306050 precursor	<i>Glycine max</i>	16723	5.16	54	1	7	K.GVEISPPDIAR.G
24	gi 351723665	Uncharacterized protein LOC100306050 precursor	<i>Glycine max</i>	16723	5.16	54	1	7	K.GVEISPPDIAR.G
25	gi 351726094	Uncharacterized protein LOC100527202 precursor	<i>Glycine max</i>	19331	4.73	33	1	5	K.TSCSSPSYTR.D + Carbamidomethyl (C)
26	gi 2746513	Alcohol dehydrogenase 1 partial	<i>Leavenworthia uniflora</i>	36520	6.01	78	2	5	K.KFVGTEFVNPKE K.TDIPGWVEK.Y
27	gi 26245395	Nucleoside diphosphate kinase	<i>Glycine max</i>	16344	6.91	114	2	12	R.GLIGEISRL R.GDFAIDIGR.N

Table 16 (Continued)

Spot no.	Accession number	Protein name	Organism	Theoretical MW (Da)	pI	Score	Peptide match	% Coverage	Sequences
28	gi 77540216	Triosephosphate isomerase	<i>Glycine max</i>	27187	5.87	206	15	23	K.CNGTTEEVKK.I + Carbamidomethyl (C) K.IVTTLNEAK.V K.IVTTLNEAK.V K.VIACIGETLEQR.E + Carbamidomethyl (C) [7] K.VATPAQAQEVHADLRK [2]
29	gi 356526807	Proteasome subunit beta type-1-like	<i>Glycine max</i>	24573	6.20	144	4	15	R.IYGGSVNGGCK.E+ Carbamidomethyl (C) [3] R.MSTGYNILTR.D + Oxidation (M) R.HLIYQHQNK.Q K.TVFASATER.D R.EYMDLRK + Oxidation (M)
30	gi 227937349	20S proteasome beta subunit 5	<i>Citrus maxima</i>	29244	5.89	166	5	13	K.GTTTLAFIFKE K.EGVMVAADSR.A K.EGVMVAADSR.A + Oxidation (M) K.LLANILYSYR.G R.AYHATFR.D R.SELTEIR.L
31	gi 84579412	9-cis-epoxycarotenoid dioxygenase 4	<i>Lactuca sativa</i>	64049	7.65	37	1	1	

Table 16 (Continued)

Spot no.	Accession number	Protein name	Organism	Theoretical MW (Da)	pl	Score	Peptide match	% Coverage	Sequences
32	gi 356526968	Glutathione S- transferase F10-like	<i>Glycine max</i>	25708	6.12	148	4	12	R.VIVCLIEK.E + Carbamidomethyl (C) K.YKNOGTDLLGKT K.NQGTDLLGKT K.VLDIYEER.L
33	gi 57283985	Triose-phosphate isomerase	<i>Phaseolus vulgaris</i> var. nanus	27183	5.87	144	3	10	K.FFVGGNWK.C K.IVTTLINEAK.V K.VAYALSOGLK.V
34	gi 225448353	Hydroxyglutathione hydrolase cytoplasmic	<i>Vitis vinifera</i>	28651	5.53	67	1	3	R.VDLPLOER.V
35	gi 300392456	SEC 13 family protein	<i>Lotus japonicus</i>	32598	5.59	130	3	9	R.LATASSDHTIK.I K.STIASASQDGK.V K.VIIVTVAKE
36	gi 357465811	Omega-amidase NIT2	<i>Medicago truncatula</i>	39012	7.11	77	5	9	R.LYNTCCVFGTDGK.L + 2 Carbamidomethyl (C) [2] R.FPELAMIYAAR.G + Oxidation (M) [2]

Table 16 (Continued)

Spot no.	Accession number	Protein name	Organism	Theoretical MW (Da)	pI	Score	Peptide match	% Coverage	Sequences
37	gi 120969450	Cytosolic ascorbate peroxidase	<i>Arachis hypogaea</i>	27034	5.52	47	9	28	K.SYPTVSADYQK.A R.GFIAEK.R R.LLEPIKE R.LPDATK.G K.AMGLSDQDIVALSGGHTLGAHKE + Oxidation (M) K.EGLLQLPSDK.A K.LSELGFADA- [3]
38	gi 356496249	Proteasome subunit alpha type-4-like isoform 1	<i>Glycine max</i>	27294	5.96	59	8	29	R.TTIFSEGR.L K.DGWLVLGEEK K.LLQTSTSTTEK.M K.AGAIGANNQAAQSILK.Q [2] K.QDYKDDITR.E R.EEAVQLALK.V K.TMDSTSLTSEK.L + Oxidation (M)

Table 16 (Continued)

Spot no.	Accession number	Protein name	Organism	Theoretical MW (Da)	pI	Score	Peptide match	% Coverage	Sequences
39	gi 255647220	Unknown	<i>Glycine max</i>	27162	5.60	300	38	54	R.VFQIEYAAKA [2] K.AVDNSGTVIGIK.C [2] K.CKDGWLGVEK.L + Carbamidomethyl (C) K.DGWLGVEK.L [2] K.MMLPGSNR.R + 2 Oxidation (M) R.HSGMAVAGLAADGR.Q [2] K.SEATNYDSVYGEPIPK.E [5] R.DGPQLYMVPEPSGVSYR.Y [3] R.DGPQLYMVPEPSGVSYR.Y + Oxidation (M) [4] R.YFGAAIGK.G [2] K.TEIEK.L K.LADMTCR.Q + Carbamidomethyl (C) ; Oxidation (M) K.IYGVHDEAK.D [2] K.VPELLEEAKA [9] K.AALEEMDAD.- + Oxidation (M)

Table 16 (Continued)

Spot no.	Accession number	Protein name	Organism	Theoretical MW (Da)	pI	Score	Peptide match	% Coverage	Sequences
40	gij356496096	Proteasome subunit alpha type-2-A-like	<i>Glycine max</i>	25608	5.51	266	6	23	K.AANGVVIATEK.K K.KLPSILVDETSVQK.I K.LPSILVDETSVQK.I K.EPIPVTLVLR.E K.EGFEQGJSGK.N K.NIEIGIIGADK.K
41	gij25091405	Thaumatococcus-like protein 1	<i>Prunus persica</i>	25748	8.29	64	1	4	K.GSDGSIACK.S + Carbamidomethyl (C)
42	gij255637227	Unknown	<i>Glycine max</i>	29152	5.94	57	12	11	K.ESSEEREHAEK.L K.LLHVHVSADR.N [6] K.IAEYVTQLR.L [5] K.GDALHAMELALSLEK.L + Oxidation (M)
43	gij1052778	Ferritin	<i>Pisum sativum</i>	28629	6.01	109	7	9	[4] K.ISEYVAQLR.R [3] K.ESSEEREHAEK.L K.GDALYAMELALSLEK.L + Oxidation (M) K.LLHVHVSADR.N K.IAEYVTQLR.L [9]
44	gij255637227	Unknown	<i>Glycine max</i>	29152	5.94	52	12	17	

Table 16 (Continued)

Spot no.	Accession number	Protein name	Organism	Theoretical MW (Da)	pI	Score	Peptide match	% Coverage	Sequences
45	gij3023194	14-3-3 like protein A	<i>Glycine max</i>	29031	4.72	160	4	15	R.EENVYMAK.L + Oxidation (M) R.NLLSVAYK.N R.IISSIEQKE
46	gij413916456	Cyclin superfamily protein, putative	<i>Zea mays</i>	44233	8.88	41	1	1	K.SAQDIALADLAPTHPIR.L K.LASYISR.L
47	gij15227376	S-formylglutathione hydrolase	<i>Arabidopsis thaliana</i>	31635	5.91	124	4	9	R.MYDYVVK.E K.AFTNYLGDNKA K.KVNAPLLLR.L K.VNAPLLLR.L
48	gij67107029	14-3-3 like	<i>Manihot esculenta</i>	29813	4.75	295	7	21	R.EENVYMAK.L + Oxidation (M) K.LAEQAER.Y R.NLLSVAYK.N R.IISSIEQKE K.SAQDIALADLAPTHPIR.L K.DSTLIMQLLR.D K.DSTLIMQLLR.D + Oxidation (M)

Table 16 (Continued)

Spot no.	Accession number	Protein name	Organism	Theoretical MW (Da)	pI	Score	Peptide match	% Coverage	Sequences
49	gi 225438420	Eukaryotic translation initiation factor 6-2 isoform 1	<i>Vitis vinifera</i>	26473	4.77	97	6	17	K.SLIDSYV.- [2] R.NSLPDQVWQR.I R.EAQPSAIVDEMR.K R.EAQPSAIVDEMR.K + Oxidation (M) R.LOFENSEVGVFSKL + Carbamidomethyl (C)
50	gi 15235282	D-3-phosphoglycerate dehydrogenase	<i>Arabidopsis thaliana</i>	63286	8.54	83	1	2	R.LAVQLVAGGSGVK.N
51	gi 974782	Cobalamine-independent methionine synthase (Vitamin-B12-independent methionine synthase isozyme)	<i>Solenostemon scutellarioides</i>	86717	6.17	121	2	3	K.YLFAGWDGR.N K.YGAGIGPGYDIHSR.I
52	gi 356538206	Isoflavone reductase homolog A622-like	<i>Glycine max</i>	33973	6.12	130	2	7	K.ILVGGTYIGK.F K.VVILGDGNVK.A

Table 16 (Continued)

Spot no.	Accession number	Protein name	Organism	Theoretical		Score	Peptide match	% Coverage	Sequences
				MW (Da)	pI				
53	gi 4255689399	Branched-chain-amino-acid aminotransferase, partial	<i>Glycine max</i>	35948	6.28	243	5	13	R.MQIGAER.M K.TIGNYA AVLK.A K.GTILPGITR.K R.KSIIDVAR.S R.SQGFQVEER.L R.DYVSGFPKE
54	gi 356504476	NADP-dependent alkenal double bond reductase P1	<i>Glycine max</i>	37905	5.81	170	4	11	K.LGFDEAFNYKE K.EESDLNATLKR K.TLDAVLPMIR.V + Oxidation (M)
55	gi 42568800	Branched-chain-amino-acid aminotransferase 5	<i>Arabidopsis thaliana</i>	45552	8.03	125	3	6	K.TIGNYA AVLK.A K.GTILPGITR.K R.SQGFQVEER.N

Table 16 (Continued)

Spot no.	Accession number	Protein name	Organism	Theoretical MW (Da)	pI	Score	Peptide match	% Coverage	Sequences
56	gi 356531939	Putative lactoylglutathione lyase-like	<i>Glycine max</i>	33451	6.14	263	6	18	R.FLHVYR.V K.FYTECFGMKL + Carbamidomethyl (C) K.FYTECFGMKL + Carbamidomethyl (C) ; Oxidation (M)
57	gi 1619903	Thiol protease isoform B, partial	<i>Glycine max</i>	34946	7.60	44	1	2	K.DPDGYAFELIQRS K.SAEWNIVTQELGGK.I K.TVLVDNQDFLK.E
58	gi 48508784	Glyceraldehyde -3-phosphate dehydrogenase	<i>Triticum aestivum</i>	36626	7.08	157	4	7	R.IGINGFGR.I K.KVIISAPSKD K.VIISAPSKD K.LTGMAFR.V + Oxidation (M)

Table 16 (Continued)

Spot no.	Accession number	Protein name	Organism	Theoretical MW (Da)	pI	Score	Peptide match	% Coverage	Sequences
59	gi 351723699	Glyceraldehyde -3-phosphate dehydrogenase C subunit	<i>Glycine max</i>	36701	6.72	224	6	14	R.IGINGFGR.I K.YDSVHGHWK.H K.KVIISAPSK.D K.VIISAPSK.D R.AASFNIIPSSTGAAGA K.LTGMAFR.V + Oxidation (M) K.AFAHPPEELNSPASYK.G K.VPEETLK.D K.VGSVFAALGSDGGVK.L
60	gi 356549751	Stern-specific protein TST1-like isoform 1	<i>Glycine max</i>	28029	6.30	136	3	14	
61	gi 225448353	Hydroxyacylglutathione hydrolase cytoplasmic	<i>Vitis vinifera</i>	28651	5.53	56	1	3	R.VDLPELQER.V
62	gi 307136111	Glyceraldehyde -3-phosphate dehydrogenase	<i>Cucumis melo</i>	36640	6.62	92	4	11	K.DAPMFWGVNEKE + Oxidation (M) K.AAIKEEGNLK.G R.SSIFDAK.A

Table 16 (Continued)

Spot no.	Accession number	Protein name	Organism	Theoretical MW (Da)	pI	Score	Peptide match	% Coverage	Sequences
63	gij211906450	Phosphoglycerate kinase	<i>Gossypium hirsutum</i>	42237	5.97	77	28	20	R.AAVPTIK.Y K.YSLKPLVPR.L [6] K.EEEKNDPEFAK.K K.NDPEFAK.K R.AHASTEGLVAK.Y [2] K.ELDYLVGAVANPK.K [7] K.FAAGTEAVAK.K [2] K.LAELSGK.G [2] K.GVTTIIGGGDSVAAVEK.A [6]
64	gij356514703	Omega-amidase, NIT2	<i>Glycine max</i>	38534	7.68	317	6	14	R.TAIQDAASK.G K.ITVGGSSIPER.S R.KIHLFDIDIPGK.I K.IHLFDIDIPGK.I K.ITFIESK.T R.FPELAMIYAAR.G + Oxidation (M)

Table 16 (Continued)

Spot no.	Accession number	Protein name	Organism	Theoretical MW (Da)	pI	Score	Peptide match	% Coverage	Sequences
65	gi 356525744	Phosphoglycerate kinase, cytosolic-like	<i>Glycine max</i>	42366	6.28	448	11	30	K.YSLKPLVPR.L K.LVAQLPEGGVLLLENVR.F K.EEEKNDPEFAK.K K.YLKPSVAGFLMQK.E K.YLKPSVAGFLMQK.E + Oxidation (M) K.RPFAAIVGGSK.V K.IGVESLLEK.V K.FAADANSK.T K.KLAELSGKG K.GVTTIIGGDSVAAYEK.V K.MSHISTGGASLELLEGGK.Q + Oxidation (M)
66	gi 3023847	Guanine nucleotide-binding protein subunit beta-like protein	<i>Medicago sativa</i>	35644	7.07	46	7	19	R.AHTDVTAIATPIDNSDMIVTASR.D R.AHTDVTAIATPIDNSDMIVTASR.D+ Oxidation (M) K.TYGVPR.R R.NTLAGHSGYNTVAVSPDGLCASGGK.D + Carbamidomethyl (C) [2] K.SIVEDLK.V [2]

Table 16 (Continued)

Spot no.	Accession number	Protein name	Organism	Theoretical MW (Da)	pI	Score	Peptide match	% Coverage	Sequences
67	gi 212292267	Rack (receptor for activated protein kinase C)	<i>Phaseolus vulgaris</i>	35580	7.60	53	16	36	R.AHTDVTAAATPIDNSDMIVTASR.D R.AHTDVTAAATPIDNSDMIVTASR.D + Oxidation (M) [2] R.LWDLAAGTSAR.R [2] K.DVLSVAFSIDNR.Q [3] K.LWNTLGECK.Y + Carbamidomethyl (C) K.YTIQSDAHSDDWSCVR.F + Carbamidomethyl (C) [2] R.FSPSTLQPTIVSASWDR.T [2] K.YWNLTNCKL + Carbamidomethyl (C) R.YWLCATEQSIK.I + Carbamidomethyl (C) K.IWDLESK.S
68	gi 356514703	Omega-amidase, NIT2	<i>Glycine max</i>	38534	7.68	226	6	10	R.TAIQDAASK.G [2] K.ITIVGGSIPER.S K.IHLFDIDIPGK.I [2] K.ITFLESK.T

Table 16 (Continued)

Spot no.	Accession number	Protein name	Organism	Theoretical MW (Da)	pI	Score	Peptide match	% Coverage	Sequences
69	gjl418731090	Glyceraldehyde -3-phosphate dehydrogenase	<i>Solanum tuberosum</i>	36701	7.03	155	11	15	R.IGINGFGR.I [2] K.KVIISAPSK.D [2] K.VIISAPSK.D [2] K.DAPMFVWGVNEKE + Oxidation (M) R.AASFNIIPSSSTGAAGA [2] R.SSIFDAK.A [2]
70	gjl356536156	D-3-phosphoglycerate dehydrogenase, chloplastic	<i>Glycine max</i>	63573	6.32	654	10	18	K.ISLCDALIVR.S + Carbamidomethyl (C) R.NVAQADASVK.A K.YVGYSLVGK.T K.TLAVLFGK.V K.GLGMNVIAHDPYAPADRA + Oxidation (M) R.GGVIEDALVR.A R.LAVQLVAGGSVK.T R.FASAI SDSGEIK.V K.DGIPHLTK.V

Table 16 (Continued)

Spot no.	Accession number	Protein name	Organism	Theoretical		Score	Peptide match	% Coverage	Sequences
				MW (Da)	pI				
71	gi 8894548	Hypothetical protein	<i>Cicer arietinum</i>	54901	4.87	89	6	5	K.YIAPEQVPVOYGGLSR.E [4] K.VLTIIDNQTSK.K [2]
72	gi 255561582	Patellin-3,putative	<i>Ricinus communis</i>	69576	4.76	108	3	3	K.ISQSVSFKE R.MISPFLLTOR.T
73	gi 358348031	Gene X-like protein	<i>Medicago truncatula</i>	77534	8.25	58	2	2	K.FVFAGPSK.S R.LELEARR.N K.ISDEMEK.A
74	gi 356500683	Heat shock protein 70 kDa protein	<i>Glycine max</i>	71582	5.20	343	38	24	R.VEIIANDOGNR.T R.TTPSYVAFTDTER.L [2] K.NQVAMNPTNTVFDK.R K.NQVAMNPTNTVFDK.R + Oxidation (M) [3] K.LWPFK.V R.EVAEAFLGHAVK.N [5] K.NAVITVPAYFNDSOR.Q [5] R.IINEPTAAAIAYGLDK.K [8] R.IINEPTAAAIAYGLDKK.A K.ATAGDTHLGGEDFDNR.M

Table 16 (Continued)

Spot no.	Accession number	Protein name	Organism	Theoretical MW (Da)	pI	Score	Peptide match	% Coverage	Sequences
74	g 356500683	Heat shock protein 70 kDa protein	<i>Glycine max</i>	71582	5.20	343	38	24	R.MVNHFYSEFR.R R.MVNHFYSEFR.R + Oxidation (M) K.VQQLLODFFNGK.E R.TKDNLLGK.F R.DNNLLGK.F K.NSLENYNMR.N + Oxidation (M) K.ELESICNPIAK.M + Carbamidomethyl (C) [4]
75	g 211906504	Heat shock protein 70	<i>Gossypium hirsutum</i>	70952	5.11	304	31	27	R.VEIIANDQGNR.T R.TTPSYVAFDTER.L K.NOVAMNPTNTVFDK.R K.NOVAMNPTNTVFDK.R + Oxidation (M) K.QFSAEEISSMVLMIK.M K.QFSAEEISSMVLMIK.M + 2 Oxidation (M) K.NAVTVPAYFNDSQR.Q [3] K.DAGVIAGLNVMR.I [2] K.DAGVIAGLNVMR.I + Oxidation (M) R.IINEPTAAAAYGLDK.K [4]

Table 16 (Continued)

Spot no.	Accession number	Protein name	Organism	Theoretical MW (Da)	pI	Score	Peptide match	% Coverage	Sequences
75	gi 211906504	Heat shock protein 70	Gossypium hirsutum	70952	5.11	304	31	27	K.ATAGDTHLGGEDFDNR.M R.MVNHVQEFK.R + Oxidation (M) R.FEELNMDLFR.K R.FEELNMDLFR.K + Oxidation (M) [2] K.VOQLLQDFFNGK.E [5] R.DNILLGK.F K.IITTTNDK.G K.NALENYAYNMR.N K.NALENYAYNMR.N + Oxidation (M) K.ELESICNPIIAK.M + Carbamidomethyl (C)
76	gi 356526803	Probable nucleoredoxin 1	Glycine max	64172	4.86	277	8	8	R.DFLLR.N R.SRLDELHFVR.G R.LDELHFVR.G [2] R.IQELR.D R.DFVISSDGK.K K.LLVEVYEK.L K.FAELDEILK.A

Table 16 (Continued)

Spot no.	Accession number	Protein name	Organism	Theoretical MW (Da)	pI	Score	Peptide match	% Coverage	Sequences
77	gjl186898205	Heat shock protein 70	<i>Hevea brasiliensis</i>	71694	5.27	52	14	16	R.VEIIANDQGNR.T R.TTSPSYVAFTDTER.L K.NQVAMNPTNTVFDAK.R K.NQVAMNPTNTVFDAK.R + Oxidation (M) K.NAWVTVPAYFNDSQR.Q [2] R.IINEPTAAAIAYGLDK.K [4] K.ATAGDTHLGGEDFNRL [2] K.IITITNDK.G R.NQLAEVEEFEDK.L
78	gjl356549495	Heat shock 70 kDa protein, mitochondrial-like	<i>Glycine max</i>	72983	5.68	317	7	9	K.VIENSEGAR.T K.ETAAYLGKS R.TESIDLSKD K.HLNITL.TR.S K.VQEVWSEFGKS K.EQQITIR.S K.EIEDAVSDLR.Q

Table 16 (Continued)

Spot no.	Accession number	Protein name	Organism	Theoretical MW (Da)	pI	Score	Peptide match	% Coverage	Sequences
79	gi 363806992	V-type proton ATPase catalytic subunit A	<i>Glycine max</i>	68736	5.41	476	11	17	K.ESEYGYVR.K R.SGDYYIPR.G K.IITYIAPPGQYSIK.D K.DTVLELEFQGVKK K.TVISQALS.KY R.TTLVANTSNMIPVAARE R.TTLVANTSNMIPVAARE + Oxidation (M) R.EDDLNEIVQLVGK.D K.FEDPAEGEAAALVAK.F K.LHEDLTNGFR.N R.NLEDETR.-
80	gi 356536156	D-3-phosphoglycerate dehydrogenase	<i>Glycine max</i>	62573	6.32	632	11	18	K.IISLCDALIVR.S + Carbamidomethyl (C) R.NVAQADASVK.A K.YYGVSVLYGK.T K.TLAVLGFQK.V

Table 16 (Continued)

Spot no.	Accession number	Protein name	Organism	Theoretical MW (Da)	pI	Score	Peptide match	% Coverage	Sequences
80	gi 356536156	D-3-phosphoglycerate dehydrogenase	<i>Glycine max</i>	62573	6.32	632	11	18	K:GLGMNVIADHPYAPADRA K:GLGMNVIADHPYAPADRA + Oxidation (M) R:GGVIDEDALVR.A R:FASAIISDSGEIK.V K:DGIPHLTKV
81	gi 356505318	Enolase-like	<i>Glycine max</i>	47628	5.92	350	10	18	K:AVDNVNTIAPALVGK.D K:MGVEYYHNLK.S K:MGVEYYHNLK.S + Oxidation (M)[2] K:VIGMDVAASEFYKEDK.T + Oxidation (M) K:TYDLNFK.E K:ACNALLK.V + Carbamidomethyl (C) K:AGWGMASHR.S + Oxidation (M) K:YNQLLR.I

Table 16 (Continued)

Spot no.	Accession number	Protein name	Organism	Theoretical MW (Da)	pI	Score	Peptide match	% Coverage	Sequences
82	gi 356513072	Phosphoglucomutase, cytoplasmic	<i>Glycine max</i>	63474	5.33	448	10	17	R.VETTPFDGQKPGTSGLR.K R.GATLVVSGDGR.Y R.SMPTSAALDVVAKH + Oxidation (M) K.LVTVEDIVR.Q K.ELMAYLVKL K.ELMAYLVKL + Oxidation (M) R.YLFEDGSR.L R.LSGTSGEGATIR.L R.LYIEQYEK.D R.LSNEALAPLVEVAKL
83	gi 357483399	Succinate dehydrogenase	<i>Medicago truncatula</i>	68879	6.10	314	4	6	K.YDAVVVGAGGAGLRA R.FQAASTILATGGYGRA K.VMQNNAVFR.T K.VMQNNAVFR.T + Oxidation (M)

Table 16 (Continued)

Spot no.	Accession number	Protein name	Organism	Theoretical MW (Da)	pI	Score	Peptide match	% Coverage	Sequences
84	gi 13467735	2,3-bisphosphoglycerate -independent phosphoglycerate mutase	<i>Ricinus communis</i>	60780	5.52	201	4	6	K.LVLDLALASGK.I K.IYEGEGFK.Y R.LDQLQLLLK.G R.VHVLTDGR.D
85	gi 356524354	Phosphoglucomutase, cytoplasmic	<i>Glycine max</i>	63351	5.35	522	10	15	R.GATLW5GDGR.Y K.EAIQITK.M R.SMPTSAALDWAK.H + Oxidation (M) K.LVTVEDIVR.Q R.YDYENVDAGAAKE K.ELMAYLVK.L K.ELMAYLVK.L + Oxidation (M) K.LOSSLSEVNQIVK.G R.YLFDGSR.L R.LYIEQYEK.D

Table 16 (Continued)

Spot no.	Accession number	Protein name	Organism	Theoretical MW (Da)	pI	Score	Peptide match	% Peptide	% Sequences
86	gi 22597178	Alcohol dehydrogenase 1	<i>Glycine max</i>	39981	6.19	212	4	9	R.ILFNSLCR.S + Carbamidomethyl (C) R.GVMLSDGK.T + Oxidation (M) R.IIGVDLLPNR.F R.TDIPGWEK.Y
87	gi 22597178	Alcohol dehydrogenase 1	<i>Glycine max</i>	39981	6.19	218	4	9	R.ILFNSLCR.S + Carbamidomethyl (C) R.GVMLSDGK.T + Oxidation (M) R.IIGVDLLPNR.F R.TDIPGWEK.Y
88	gi 22597178	Alcohol dehydrogenase 1	<i>Glycine max</i>	39981	6.19	227	6	11	R.ILFNSLCR.S + Carbamidomethyl (C) R.GVMLSDGK.T R.GVMLSDGK.T + Oxidation (M) R.VSGASRIIGVDLLPNR.F R.IIGVDLLPNR.F R.TDIPGWEK.Y

Table 16 (Continued)

Spot no.	Accession number	Protein name	Organism	Theoretical MW (Da)	pI	Score	Peptide match	% Coverage	Sequences
89	gij22597178	Alcohol dehydrogenase 1	<i>Glycine max</i>	39981	6.19	192	6	9	R.ILFNSLCR.S + Carbamidomethyl (C) R.GVMLSDGK.T R.GVMLSDGK.T + Oxidation (M) R.IIGVDLLPNR.F [2] R.TDIPGVVEK.Y
90	gij22597178	Alcohol dehydrogenase 1	<i>Glycine max</i>	39981	6.19	73	19	7	R.ILFNSLCR.S + Carbamidomethyl (C) [4] R.IIGVDLLPNR.F [14] R.TDIPGVVEK.Y
91	gij1351887	Alcohol dehydrogenase	<i>Malus x domestica</i>	41382	6.48	60	10	7	K.GONPLFPR.I [2] R.GVMLSDGK.S
92	gij351724907	Methionine synthase	<i>Glycine max</i>	84230	5.93	79	12	8	R.GVMLSDGK.S + Oxidation (M) K.KFGVTEFVNPKA [6] K.AGITVIQIDEAALR.E [4] R.EGLPLR.K K.YGAGIGPGVYDIHSPPR.I [2] R.IPPTEEIADR.I [2] K.YTEVKPALTNMVAAAK.L

Table 16 (Continued)

Spot no.	Accession number	Protein name	Organism	Theoretical MW (Da)	pI	Score	Peptide match	% Coverage	Sequences
92	gi 351724907	Methionine synthase	<i>Glycine max</i>	84230	5.93	79	12	8	K.YTEVKPALTNMVAALK + Oxidation (M) [2]
93	gi 356547867	5-methyltetrahydro pteroyltriglutamate -homocysteine methyltransferase	<i>Glycine max</i>	89014	6.33	473	9	11	K.SSAEELQK V K.SFSLLSLIDK.I K.AVTAYGFDIVR.G K.FLFGVVDGR.N K.WEVNALAK.A K.EEINNVK.L K.DEVEDELEK.A R.IPPTEEIADR.I
94	gi 356508448	5-methyltetrahydro pteroyltriglutamate -homocysteine methyltransferase	<i>Glycine max</i>	88609	6.41	420	7	10	K.YTEVKPALTNMVAALK + Oxidation (M) K.SFSLLSLIDK.I K.AVTAYGFDIVR.G K.FLFGVVDGR.N K.WEVNALAK.A K.YGAGIGPGVYDIHSPR.I R.IPPTEEIADR.I K.YTEVKPALTNMVAALK + Oxidation (M)

Table 16 (Continued)

Spot no.	Accession number	Protein name	Organism	Theoretical MW (Da)	pI	Score	Peptide match	% Coverage	Sequences
95	g 35608448	5-methyltetrahydro pteroyltriglutamate-homocysteine methyltransferase	<i>Glycine max</i>	88609	6.41	474	10	13	K.FALEFWDGK.S K.SFSLSLIDK.I K.FLFAGVVDGR.N K.SWLAFAAQK.V K.VVEVNALAK.A K.DEVEDLEK.A R.EGLPLRK.S K.YGAGIGGVYDIHSPR.I R.IPPTEEIADR.I K.YTEVKPALTNMVAALK.L
96	g 351724907	Methionine synthase	<i>Glycine max</i>	84230	5.93	297	5	8	K.SFSLSLLPK.V K.YLFAGVVDGR.N K.YGAGIGGVYDIHSPR.I R.IPPTEEIADR.I K.YTEVKPALTNMVAALK.L + Oxidation (M)

Table 16 (Continued)

Spot no.	Accession number	Protein name	Organism	Theoretical MW (Da)	pl	Score	Peptide match	% Coverage	Sequences
97	g 351724907	Methionine synthase	<i>Glycine max</i>	84230	5.93	331	6	9	K.SFSLLSLLPK.V K.YLFAAGVVDGR.N K.DEVEDLEKA K.YGAGIGPGVYDIHSPR.I R.IPPTTEEIADR.I K.YTEVKPALTNMVAALK.L + Oxidation (M)
98	g 351724907	Methionine synthase	<i>Glycine max</i>	84230	5.93	236	5	9	K.YLFAAGVVDGR.N K.DEVEDLEKA K.YGAGIGPGVYDIHSPR.I R.IPPTTEEIADR.I K.MLAVLEK.N R.IGINGFGR.I K.YDSVHGHWK.H K.KVIISAPSKD K.VIISAPSK.D R.AASFNIIPSTGAAGA K.LTGMAFR.V + Oxidation (M)
99	g 351723699	Glyceraldehyde -3-phosphate dehydrogenase C subunit	<i>Glycine max</i>	36701	6.72	220	6	14	

Table 16 (Continued)

Spot no.	Accession number	Protein name	Organism	Theoretical MW (Da)	pI	Score	Peptide match	% Coverage	Sequences
100	gij380746853	Glyceraldehyde -3-phosphate dehydrogenase	<i>Cuscuta pentagona</i>	32268	6.97	141	7	24	K.VVISAPSK.D K.VLPALNGK.L K.KWISAPSK.D [2] K.YDTVHGKWK.N K.DAPMFVVGVNEKE + Oxidation (M) R.AASFNIIPSSSTGAAK.A
101	gij48508784	Glyceraldehyde -3-phosphate dehydrogenase	<i>Triticum aestivum</i>	36626	7.08	182	6	10	R.IGINGFGR.I K.KVIISAPSK.D K.VIISAPSK.D [2] K.LLTGMAFR.V + Oxidation (M) K.AAIKEESEGNL.K.G K.LIICGGAYPR.D + Carbamidomethyl (C) R.AGMIFYR.K R.IGAPAMTSR.G R.IGAPAMTSR.G + Oxidation (M) K.DFEQIGFELHR.A

Table 16 (Continued)

Spot no.	Accession number	Protein name	Organism	Theoretical MW (Da)	pI	Score	Peptide match	% Coverage	Sequences
102	gi 134142075	Serine hydroxymethyltransferase	<i>Populus tremuloidea</i>	51944	7.18	228	5	8	K.LIICGGSAYPR.D + Carbamidomethyl (C) R.AGMIFYR.K R.IGAPAMTSR.G R.IGAPAMTSR.G + Oxidation (M) K.DFEQIGEFLLHRA
103	gi 356525790	Nitrite-specifier protein-5	<i>Glycine max</i>	35707	5.59	113	2	7	K.ELNELYSFDTR.A
104	gi 71793966	Alcohol dehydrogenase	<i>Alnus glutinosa</i>	40971	6.28	161	4	10	K.TWAQVETSGQKPTAR.S K.INPAAPLDKV K.KFGVTEFVNPKD R.TDIPGVVEK.Y
105	gi 255585914	Alcohol dehydrogenase, putative	<i>Ricinus communis</i>	40718	6.37	66	5	5	K.AFDLMLHGKSR.C R.IIGIDISK.K [2] R.IIGIDISK.K.Y
106	gi 342851387	Alcohol dehydrogenase, putative	<i>Malus rockii</i>	35862	6.21	87	2	5	R.SQVPWLVDKY [2] K.GQNPLFPR.I K.FGVTEFLNPK.E

Table 16 (Continued)

Spot no.	Accession number	Protein name	Organism	Theoretical MW (Da)	pI	Score	Peptide match	% Coverage	Sequences
107	gi 356577825	Monodehydroascorbate reductase	<i>Glycine max</i>	47011	5.49	202	4	9	K.AYLFPEPAR.L R.LTDFGVEGADAK.N R.EYDDADKLYEAIK.A K.EGLSFASK.I
108	gi 255636611	Unknown	<i>Glycine max</i>	47417	5.76	120	15	14	R.LYDL DASK.Y [2] K.CLADIVINHR.T + Carbamidomethyl (C) [5] R.GYCFEGGTPDAR.L + Carbamidomethyl (C) [3] K.IYMEQTRPDFAVGEK.W [2] K.IYMEQTRPDFAVGEK.W + Oxidation (M) [2] K.SVNILAAEADLLCCK.D
109	gi 356533631	Monodehydroascorbate reductase isoform 1	<i>Glycine max</i>	46822	5.73	159	4	10	K.AYLFPEPAR.L R.LPGFHYCVGGGER.L+ Carbamidomethyl (C) R.LTDFGVEGADAK.N K.EGLSFASK.I

Table 16 (Continued)

Spot no.	Accession number	Protein name	Organism	Theoretical MW (Da)	pI	Score	Peptide match	% Coverage	Sequences
110	gij356558578	Actin-101-like	<i>Glycine max</i>	41626	5.31	228	12	16	K.AGFAGDDAPRA R.HTGVVVGMGQK.D + 2 Oxidation (M) [2] R.LDLAGR.D R.GYSFSTSAEKE K.EISALAPSSMK.I [3] K.EISALAPSSMK.I + Oxidation (M) K.GEYDESGPAVHRK [3]
111	gij113781	Alpha-amylase	<i>Vigna mungo</i>	46859	5.45	73	6	5	R.LYDLASKY [3] K.CLADVINHR.T + Carbamidomethyl (C) R.FDFVK.G [2]
112	gij356509324	Alcohol dehydrogenase 1-like	<i>Glycine max</i>	40897	5.97	232	6	10	K.KFGVNEFVNP.KD K.FGVNEFVNP.KD K.THPVNF.LNER.T K.YMNGELELEK.F K.AFDYMLK.G K.AFDYMLK.G + Oxidation (M)

Table 16 (Continued)

Spot no.	Accession number	Protein name	Organism	Theoretical MW (Da)	pI	Score	Peptide match	% Coverage	Sequences
113	gij356525744	Phosphoglycerate kinase, cytosolic	<i>Glycine max</i>	42366	6.28	342	9	28	K.LVAQLPEGGVLLLENVR.F K.YLKPSVAGFLMQKE K.YLKPSVAGFLMQKE + Oxidation (M) K.RPFAAIVGGSK.V K.IGVIESLLEK.V K.KLAELSGK.G K.GVTTIIGGDSVAAVEK.V K.MSHISTGGGASLELLEKQ. + Oxidation (M)
114	gij356577825	Monodehydroascorbate reductase	<i>Glycine max</i>	47011	5.49	257	6	13	K.AYLPESPARG.L R.LLPEWYTEK.G R.L.TDFGVEGADAK.N K.NIFYLRE K.VQPPVADVQDLAKE K.EGLSFASK.I

Table 16 (Continued)

Spot no.	Accession number	Protein name	Organism	Theoretical MW (Da)	pI	Score	Peptide match	% Coverage	Sequences
115	gi 344190186	Enolase	<i>Corylus heterophylla</i>	49091	5.62	334	36	21	R.AAVPSGASTGYEALRLR.D [12] R.DGGSEYLGK.G [2] K.LAMQEFMILPYGASCFKE + Oxidation (M) K.MGVEVYHHLKA K.MGVEVYHHLKA + Oxidation (M) K.AGYTGK.V K.ACNALLK.V + Carbamidomethyl (C) [3] K.VNQIGSVTESIEAVR.M [12] R.AGWGVMASHR.S R.AGWGVMASHR.S + Oxidation (M) K.YNQLLR.I
116	gi 445589	Alcohol dehydrogenase	<i>Glycine max</i>	34404	6.14	277	5	12	K.INPAAPLDK.V R.IIGVDLV5AR.F K.KFGVNEFVNPKE.D K.FGVNEFVNPKE.D R.TDLPSVWEK.Y

Table 16 (Continued)

Spot no.	Accession number	Protein name	Organism	Theoretical MW (Da)	pI	Score	Peptide match	% Sequences Coverage
117	gi 445589	Alcohol dehydrogenase	<i>Glycine max</i>	34404	6.14	281	5	12
								K.INPAAPLDK.V R.IIGVDLVSAR.F K.KFGVNEFVNP.K.D K.FGVNEFVNP.K.D R.TDLPSWEK.Y
118	gi 445589	Alcohol dehydrogenase	<i>Glycine max</i>	34404	6.14	220	4	9
								R.IIGVDLLPNR.F K.KFGVNEFVNP.K.D K.FGVNEFVNP.K.D R.TDLPSWEK.Y
119	gi 445589	Alcohol dehydrogenase	<i>Glycine max</i>	34404	6.14	232	4	11
								K.INPAAPLDK.V R.IIGVDLLPNR.F K.FGVNEFVNP.K.D R.TDLPSWEK.Y
120	gi 22296818	Pyruvate kinase	<i>Glycine max</i>	55282	7.89	367	6	10
								Carbamidomethyl (C) R.KGSDLVNV.R.K K.GSDLVNV.R.K

Table 16 (Continued)

Spot no.	Accession number	Protein name	Organism	Theoretical MW (Da)	pI	Score	Peptide match	% Coverage	Sequences
120	g 22296818	Pyruvate kinase	<i>Glycine max</i>	55282	7.89	367	6	10	K.LIVLTR.G R.GLIPLGEGSAK.A R.GLCKPGDAVVALHR.I + Carbamidomethyl (C)
121	g 356521618	Pyruvate kinase	<i>Glycine max</i>	54251	7.53	408	8	11	K.IVCTLGPASR.S + Carbamidomethyl (C) K.IDMIALSFVR.K R.KGSDLVNV.R.K K.GSDLVNV.R.K K.NIMLMSK.V R.GDLGMEIEK.I
122	g 1169534	Enolase	<i>Ricinus communis</i>	47883	5.56	411	7	18	R.GDLGMEIEK.I + Oxidation (M) R.GLVPVLSAASAR.A K.HIANLAGNK.N K.LAMQEFMILPVGASSFKE K.EGLELLK.T K.TYDLNFKKEENNDGSOQK.I K.ACNALLK.V + Carbamidomethyl (C)

Table 16 (Continued)

Spot no.	Accession number	Protein name	Organism	Theoretical MW (Da)	pl	Score	Peptide match	% Coverage	Sequences
122	gi 1169534	Enolase	<i>Ricinus communis</i>	47883	5.56	411	7	18	K.VNQIGSVTESIEAVR.M R.AGWGVMASHR.S + Oxidation (M)
123	gi 356530953	Enolase	<i>Glycine max</i>	47989	5.92	295	7	16	R.AAVPSGASTGYEALRLR.D R.DGGSDYLGK.G K.HIANLAGNK.T K.VVIGMDVAASEFYDNK.D + Oxidation (M) K.TYDLNFK.E
124	gi 356509058	Peroxidase 52 Isoform 1	<i>Glycine max</i>	34503	9.14	46	3	7	K.ACNALLK.V + Carbamidomethyl (C) K.YNQLLR.I R.FSALGLSTK.D
125	gi 356496705	Peroxidase 72 Isoform 1	<i>Glycine max</i>	36417	9.23	66	3	7	K.DLVALSGGHTIGQARC [2] K.NLLANK.G K.NKVSADLVK.Q
126	gi 449457510	Peroxidase 72	<i>Cucumis sativus</i>	37424	9.18	208	4	11	K.MGNITPLTGSR.G + Oxidation (M) R.LHFHDCFVK.G + Carbamidomethyl (C) R.GFEVIDEIK.S K.GLLNSDEVLLTK.N

Table 16 (Continued)

Spot no.	Accession number	Protein name	Organism	Theoretical MW (Da)	pI	Score	Peptide match	% Coverage	Sequences
126	gi 449457510	Peroxidase 72	<i>Cucumis sativus</i>	37424	9.18	208	4	11	K.MGNITPLTGSRG + Oxidation (M)
127	gi 413916456	Cyclin superfamily protein, putative	<i>Zea mays</i>	44233	8.88	36	1	1	K.LASYISRL
128	gi 22597178	Alcohol dehydrogenase 1	<i>Glycine max</i>	39981	6.19	189	3	7	R.TDIPGVVEK.Y R.ILFNSLCR.S + Carbamidomethyl (C) R.IIGVDLVSAR.F
129	gi 22597178	Alcohol dehydrogenase 1	<i>Glycine max</i>	39981	6.19	197	4	9	R.ILFNSLCR.S + Carbamidomethyl (C) R.GWMLSDGK.T + Oxidation (M) R.IIGVDLVSAR.F
130	gi 470108526	Alcohol dehydrogenase 1	<i>Fragaria vesca</i>	41304	6.33	159	4	10	R.TDLPSWVEK.Y K.GONPLFPR.I K.INPAAPLDK.V R.TDLPGWVEK.Y K.FITHSVPFSEINK.A
131	gi 22597178	Alcohol dehydrogenase 1	<i>Glycine max</i>	39981	6.19	231	5	9	R.ILFNSLCR.S + Carbamidomethyl (C) R.GWMLSDGK.T R.GWMLSDGK.T + Oxidation (M)

Table 16 (Continued)

Spot no.	Accession number	Protein name	Organism	Theoretical MW (Da)	pI	Score	Peptide match	% Coverage	Sequences
131	gi 22597178	Alcohol dehydrogenase 1	<i>Glycine max</i>	39981	6.19	231	5	9	R.IIGDVLVSAR.F R.TDLPSSWEK.Y
132	gi 356525774	Elongation factor 2	<i>Glycine max</i>	93982	5.80	291	7	7	K.FTAEELR.R R.IRPVLTVNIK.M R.IIMGPNYVPEK.K + Oxidation (M) K.FSVSPWR.V K.GVOYLNEIK.D K.EGALAEENMR.A + Oxidation (M) R.GGGQIIP TAR.R
133	gi 356556977	Elongation factor 2	<i>Glycine max</i>	93996	5.80	316	9	9	K.FTAEELR.R R.NMSVAHVVDHGK.S R.IRPVLTVNIK.M R.IIMGPNYVPEK.K K.FSVSPWR.V K.GVOYLNEIK.D K.EGALAEENMR.A K.EGALAEENMR.A + Oxidation (M)

Table 16 (Continued)

Spot no.	Accession number	Protein name	Organism	Theoretical MW (Da)	pI	Score	Peptide match	% Sequences Coverage	Sequences
133	gi 356556977	Elongation factor 2	<i>Glycine max</i>	93996	5.80	316	9	9	R.GGGQIPTAR.R
134	gi 49439307	Chaperone protein ClpB1-like	<i>Cucumis sativus</i>	100877	5.99	182	5	4	R.ALWAAQLSSR.Y R.WTGIPVTR.L R.VGQNOQAVDAVAEAVLR.S R.VVTELSR.M [2]
135	gi 356519114	Chaperone protein ClpB1-like	<i>Glycine max</i>	84629	6.18	288	6	9	K.TAVVEGLAQR.I R.ALWAAQLSSR.Y R.MQLEVELHALEKE + Oxidation (M) R.WTGIPVTR.L R.VGQNOQAVDAVAEAVLR.S R.RPYSWLFDEVEK.A
136	gi 49439307	Chaperone protein ClpB1-like	<i>Cucumis sativus</i>	100877	5.99	182	5	5	R.GDVPSNLADVRL R.ALWAAQLSSR.Y K.AIDLVEACANVR.V + Carbamidomethyl (C) R.MQLEVELHALEKE + Oxidation (M) R.VVTELSR.M

Table 16 (Continued)

Spot no.	Accession number	Protein name	Organism	Theoretical MW (Da)	pI	Score	Peptide match	% Coverage	Sequences
137	gi 449439307	Chaperone protein ClpB1-like	<i>Cucumis sativus</i>	100877	5.99	104	2	1	R.ALVAAQLSSR.Y R.WTELSR.M
138	gi 255538186	D-3-phosphoglycerate dehydrogenase, putative	<i>Ricinus communis</i>	63396	5.81	140	3	4	K.YGVSLVGK.T K.TLAVIGFGK.V R.GGVIDEDALV.RA R.TIAMDATEGWR.G +
139	gi 356536246	ATP synthase subunit beta , mitochondrial	<i>Glycine max</i>	59799	5.80	50	5	6	Oxidation (M) R.VLNTGSPITVPVGRA [3]
140	gi 351724891	Enolase	<i>Glycine max</i>	47689	5.31	237	6	9	K.WDLLAPYQR.G K.HIANIAGNK.K K.MGVEVYHNLK.S + Oxidation (M) [2] K.TYDLNFK.E K.ACNALLK.V + Carbamidomethyl (C) K.YNQLLR.I

Table 16 (Continued)

Spot no.	Accession number	Protein name	Organism	Theoretical MW (Da)	pI	Score	Peptide match	% Coverage	Sequences
141	g 1169534	Enolase	<i>Ricinus communis</i>	47883	5.56	403	9	18	R.AAVPSGASTGIYEALRLR.D R.DGGS DYLGK.G K.AVENNSIIGPALIGK.D K.HIANLAGNK.N K.TYDLNFK.E [2] K.ACNALLLK.V + Carbamidomethyl (C) K.YNQLLR.I R.IEEELGAEVYAGAK.F
142	g 357520365	Protein tolB	<i>Medicago truncatula</i>	76488	6.52	191	4	5	R.IAYVEMPGVYVWNR.D + Oxidation (M) K.NNAFFSPSPDGK.W R.LDGSGLTR.L
143	g 226492645	Vacuolar ATP synthase subunit B	<i>Zea mays</i>	54028	5.07	422	11	13	K.YQEVNIR.L R.RGOVLEVDGEKA R.GOVLEVDGEKA K.TPVSLDMILGR.I

Table 16 (Continued)

Spot no.	Accession number	Protein name	Organism	Theoretical MW (Da)	pI	Score	Peptide match	% Coverage	Sequences
143	gi 226492645	Vacuolar ATP synthase subunit B	<i>Zea mays</i>	54028	5.07	422	11	13	K.TPVSLDMLGR.I + Oxidation (M) R.DFEENGSMER.V K.SAIGEGMTR.R K.SAIGEGMTR.R + Oxidation (M) R.KFVTOGAYDTR.N K.FVTOGAYDTR.N K.TLDQYYSR.D
144	gi 1351202	Tubulin beta chain (Beta-tubulin)	<i>Glycine max</i>	45721	5.63	533	12	28	R.EILHIQGGQCGNQIGAK.F + Carbamidomethyl (C) K.YSGDSEQLER.I R.INVYNEASGGR.Y R.EEYPDR.M R.FPQLNSDLR.K K.LAVNLIIPPR.L

Table 16 (Continued)

Spot no.	Accession number	Protein name	Organism	Theoretical MW (Da)	pI	Score	Peptide match	% Coverage	Sequences
144	gi 351202	Tubulin beta chain (Beta-tubulin)	<i>Glycine max</i>	45721	5.63	533	12	28	K.NMMCAADPR.H + Carbamidomethyl (C); Oxidation (M) [Z] R.YLTASAMFR.G + Oxidation (M) K.EVDEQMINVQNK.N + Oxidation (M) K.SSVCDIPPK.G + Carbamidomethyl (C) R.VSEQFTAMFR.R + Oxidation (M)
145	gi 356508699	Cell division cycle protein 48 homolog	<i>Glycine max</i>	90826	5.11	311	8	7	R.LGDWVSHQCPDVK.Y + Carbamidomethyl (C) R.KGDLFLVR.G K.GDLFLVR.G K.LAGESESNLR.K K.AFEAEK.N K.LSDNVDLEK.V R.SVSDADIR.K R.GFGSEFRF
146	gi 341958461	Chloroplast acetoxy acid isomeroreductase	<i>Glycine max</i>	63569	7.14	170	3	4	K.NISVIACPK.G + Carbamidomethyl (C) R.SDIFGER.G K.NTVESITGIISK.T

Table 16 (Continued)

Spot no.	Accession number	Protein name	Organism	Theoretical MW (Da)	pI	Score	Peptide match	% Sequences	Coverage
147	gi 341958461	Chloroplast acetohydroxy acid isomeroreductase	<i>Glycine max</i>	63569	7.14	204	4	6	K.INLAGHDEYIVK.G K.NISVAVCPK.G + Carbamidomethyl (C) R.SDIFGER.G K.NTVESITGIISK.T K.NISVAVCPK.G +
148	gi 341958461	Chloroplast acetohydroxy acid isomeroreductase	<i>Glycine max</i>	63569	7.14	189	3	6	Carbamidomethyl (C) K.NTVESITGIISK.T
149	gi 341958461	Chloroplast acetohydroxy acid isomeroreductase	<i>Glycine max</i>	63569	7.14	209	5	8	R.GILLGAVHGVVESLFR.R K.INLAGHDEYIVK.G K.NISVAVCPK.G + Carbamidomethyl (C) R.RLYVOGKE R.SDIFGER.G K.NTVESITGIISK.T

Table 16 (Continued)

Spot no.	Accession number	Protein name	Organism	Theoretical MW (Da)	pl	Score	Peptide match	% Coverage	Sequences
150	gi 6714837	Glutathione reductase, cytosolic	<i>Glycine max</i>	58703	8.12	274	7	14	K.KLLVYASK.F K.NILNNAGVK.L K.IIDPHTVDVNGK.L R.GIEFHTEESPQAITKS K.SADGSFSLK.T K.GTYDGFSHMFATGR.R + Oxidation (M) K.ATLSGLPDR.V
151	gi 224133228	Glutathione reductase	<i>Populus trichocarpa</i>	60545	7.69	205	4	6	K.KLLVYASK.Y R.DFVAEQMSLR.G + Oxidation (M) K.NLGLES LGVK.IM K.ATLSGLPDR.V
152	gi 356539207	Apoptosis-inducing factor homolog A	<i>Glycine max</i>	39271	9.43	81	2	4	R.IKVDEHLR.V K.SGDLFVGK.T

Table 16 (Continued)

Spot no.	Accession number	Protein name	Organism	Theoretical MW (Da)	pI	Score	Peptide match	% Coverage	Sequences
153	gi 223469633	S18 ribosomal protein	<i>Jatropha curcas</i>	17599	10.46	178	4	21	R.VLNTNVDGK.Q K.IMFALTSIK.G + Oxidation (M) K.IPDWFLNR.Q K.LRDDLER.L
154	gi 356559573	Glutathione reductase	<i>Glycine max</i>	53958	5.63	141	4	6	K.HILIATGSR.A R.GFDDMR.A + Oxidation (M)
155	gi 357520365	Protein tolB	<i>Medicago truncatula</i>	76488	6.52	191	4	5	R.TNLTQLIK.T K.LVVDAETDK.V R.TYFHR.R R.IAYVEMPGVVVNR.D + Oxidation (M) K.NNAFFSPSPDGK.W R.LDGSGLTRL

Table 16 (Continued)

Spot no.	Accession number	Protein name	Organism	Theoretical MW (Da)	pI	Score	Peptide match	Peptide %	Coverage	Sequences
156	g 3556496197	Proliferation-associated protein 2G4-like	<i>Glycine max</i>	42946	6.30	290	6	15		K.SAAEIVNIK.A K.DVTEAIQK.V K.VAAAYDCK.I + Carbamidomethyl (C) K.IVEGL-SHOMKQ + Oxidation (M) K.WLSVSNPDTR.V R.VTSHPLQELQPTK.T
157	g 18157251	Ribulose 1,5-bisphosphate carboxylase-oxygenase large subunit	<i>Butea minor</i>	51578	6.04	470	10	20		K.DTDILAAFR.V R.IPISYIK.T K.YGRPLLGCTIKPK.L + Carbamidomethyl (C) R.AVYECLR.G + Carbamidomethyl (C) R.FVFCAEAYK.A + Carbamidomethyl (C) K.AQAETGEIK.G R.AMHAVIDR.Q R.LSGGDVHAGTWGK.L R.EITLGFVDLLR.D R.EGNEIIR.E

Table 16 (Continued)

Spot no.	Accession number	Protein name	Organism	Theoretical MW (Da)	pi	Score	Peptide match	% Sequences Coverage
158	gi 229464442	Ribulose-1,5-bisphosphate carboxylase/oxygenase large subunit	<i>Hylomecon japonica</i>	51502	6.00	370	8	18
								R:AVYECLR.G + Carbamidomethyl (C) K:AOAETGEIK.G K:GHYLNATAGTCEEMMK.R + Carbamidomethyl (C); Oxidation (M) R:AMHVIDR.Q R:LSGGDHHAGTVVGK.L R:EITLGFVDLLR.D
159	gi 229464442	Ribulose-1,5-bisphosphate carboxylase/oxygenase large subunit	<i>Hylomecon japonica</i>	51502	6.00	316	6	13
								R:VALEACVKAR.N + Carbamidomethyl (C) K:AOAETGEIK.G R:LSGGDHHAGTVVGK.L R:EITLGFVDLLR.D R:VALEACVKAR.N + Carbamidomethyl (C)

Table 16 (Continued)

Spot no.	Accession number	Protein name	Organism	Theoretical MW (Da)	pI	Score	Peptide match	%	Sequences
160	gi 255580564	Nutrient reservoir, putative	<i>Ricinus communis</i>	38947	6.97	102	2	5	R.VQVWVGDGR.R K.AGNLFVPR.F
161	gi 50058096	Glutathione reductase	<i>Zinnia violacea</i>	60947	8.75	185	4	6	K.KLLVYASKY K.NILNNAGVKL K.NLGLETVGVKL K.ATLSGLPDR.V
162	gi 356536156	D-3-phosphoglycerate dehydrogenase	<i>Glycine max</i>	62573	6.32	765	12	21	K.LGDAGLKLK.D K.ISLCDALIVR.S + Carbamidomethyl (C) R.NVAQADASVK.A K.YGVSLVGK.T K.TLAVLGFVK.V K.GLGMNVIHDPYAPADR.A + Oxidation (M) R.GGVIDEALV.R.A

Table 16 (Continued)

Spot no.	Accession number	Protein name	Organism	Theoretical MW (Da)	pl	Score	Peptide match	% Coverage	Sequences
162	gi 356536156	D-3-phosphoglycerate dehydrogenase	<i>Glycine max</i>	62573	6.32	765	12	21	R.LAVQLVAGGSGVK.T R.FASAISDSGEIK.V R.FASAISDSGEIKVEGR.V K.DGIPHLTK.V R.KQAVMAIGVDEQPSKE
163	gi 356536156	D-3-phosphoglycerate dehydrogenase	<i>Glycine max</i>	62573	6.32	539	8	14	K.LGDAGLKLK.D K.ISLCDALIVR.S + Carbamidomethyl (C) R.NVAQADASVK.A K.YYGVSLVGK.T K.GLGMNVAHDPYAPADRA + Oxidation (M) R.GGVIEDALVR.A R.FASAISDSGEIK.V K.DGIPHLTK.V

Table 16 (Continued)

Spot no.	Accession number	Protein name	Organism	Theoretical MW (Da)	pI	Score	Peptide match	% Coverage	Sequences
164	gi 356536156	D-3-phosphoglycerate dehydrogenase	<i>Glycine max</i>	62573	6.32	705	12	20	K.LGDAGLKLK.D K.ISLCDALIVR.S + Carbamidomethyl (C) R.NVAOADASVK.A K.YYGVSLVGK.T K.TLAVILGFQK.V K.GLGMNVIHDPYAPADR.A K.GLGMNVIHDPYAPADR.A + Oxidation (M) R.GGVDEDALVR.A R.LAVQLVAGGGVK.T R.FASAIQDSGEIK.V K.DGIPHLTK.V R.KQAVMAGVDEQPSK.E + Oxidation (M) R.GIYAYGFEKPSAIQQR.G K.GLDVIOQAQSGTGK.T R.ELAAQIEK.V R.ALGDYILGVK.V K.FMINKPVR.I
165	gi 1170509	Eukaryotic translation initiation factor 4A (ATP-dependent RNA helicase eIF4A)	<i>Hevea brasiliensis</i>	46898	5.31	553	12	23	

Table 16 (Continued)

Spot no.	Accession number	Protein name	Organism	Theoretical MW (Da)	pI	Score	Peptide match	% Coverage	Sequences
165	gi 1170509	Eukaryotic translation initiation factor 4A (ATP-dependent RNA helicase eIF4A)	<i>Hevea brasiliensis</i>	46898	5.31	553	12	23	K.RDELTLEGIK.Q R.DELTLEGIK.Q K.QFYVNVKE.E R.VLITTTDLLAR.G K.GVAINFVTR.E R.MLFDIQK.F R.MLFDIQK.F + Oxidation (M) R.EPVPFSLSPR.M
166	gi 33149681	Pyruvate decarboxylase	<i>Dianthus caryophyllus</i>	65401	5.99	196	6	9	K.MGLEAAVEAAAEFLNK.A + Oxidation (M) K.AILVQPDV.V [2] R.VNVLFQHIQK.M R.VSAANSRPPNPQ.-
167	gi 341958461	Chloroplast acetohydroxy acid isomereductase	<i>Glycine max</i>	63569	7.14	234	5	8	K.INLAGHDEYVK.G K.NISVAVCPK.G + Carbamidomethyl (C) R.RLYVQGKE R.SDIFGER.G K.NTVESITGIISK.T

Table 16 (Continued)

Spot no.	Accession number	Protein name	Organism	Theoretical MW (Da)	pI	Score	Peptide match	% Coverage	Sequences
168	gi 341958461	Chloroplast acetohydroxy acid isomeroreductase	<i>Glycine max</i>	63569	7.14	205	4	7	K.INLAGHDEYVK.G K.NISVIACPK.G + Carbamidomethyl (C) R.RLYVQGKE R.GILLGAVHGWESLFR.R
169	gi 6225542	Chloroplast acetohydroxy acid isomeroreductase	<i>Glycine max</i>	62812	6.62	162	5	5	K.NFSVIACPK.G + Carbamidomethyl (C) R.RLYVQGKE K.SDIFGER.G K.EGLPAFPMGKI
170	gi 356536156	D-3-phosphoglycerate dehydrogenase	<i>Glycine max</i>	62573	6.32	387	6	10	K.EGLPAFPMGK.I + Oxidation (M) K.LGDAGLKLLK.D R.NVAQADASVK.A K.YYGVSLVGK.T K.TLAVLGFVK.V K.GLGMNVIAHDPYAPADR.A + Oxidation (M) R.GGVIEDALV.R.A R.LAVQLVAGGSGVK.T

Table 16 (Continued)

Spot no.	Accession number	Protein name	Organism	Theoretical MW (Da)	pI	Score	Peptide match	% Coverage	Sequences
171	gi 22597178	Alcohol dehydrogenase 1	<i>Glycine max</i>	39981	6.19	180	4	9	R.ILFNSLCR.S + Carbamidomethyl (C) R.GVMLSDGKT + Oxidation (M) R.IIGVDLYSAR.F R.TDIPGWEEK.Y
172	gi 125662890	Glyceraldehyde -3-phosphate dehydrogenase	<i>Beta vulgaris</i>	36650	6.77	70	3	11	R.AASFNIIPSSSTGAAKA R.VPTVDVSWDLTVR.L K.AGIALNDHFAK.L
173	gi 75110834	UDP- sugar pyrophosphorylase	<i>Pisum sativum</i>	66136	5.87	219	4	6	K.VACLEDNDAR.L + Carbamidomethyl (C) R.LALDPQNR.Y K.EAIGGITR.L K.TGGAIQEFVNP.K.Y
174	gi 351727947	UDP- sugar pyrophosphorylase 1	<i>Glycine max</i>	66085	5.70	215	5	7	K.VACLEDNDAR.L + Carbamidomethyl (C) K.EAIGGITR.L K.TGGAIQEFVNP.K.Y K.DASEPEVLR.I K.IEQLETK.Y

Table 16 (Continued)

Spot no.	Accession number	Protein name	Organism	Theoretical MW (Da)	pI	Score	Peptide match	% Coverage	Sequences
175	gi 3023814	Glyceraldehyde -3-phosphate dehydrogenase,cytosolic	<i>Craterostigma plantagineum</i>	36454	7.06	147	4	7	R.IGINGFGR.I K.KVISAPSK.D K.VISAPSK.D
176	gi 120666	Glyceraldehyde -3-phosphate dehydrogenase,cytosolic	<i>Antirrhinum majur</i>	36662	8.30	111	3	5	K.LTGMAFR.V + Oxidation (M) R.IGINGFGR.I K.KVISAPSK.D
177	gi 356516495	Chaperone protein ClpC, chloroplastic	<i>Glycine max</i>	102434	6.09	588	13	11	R.VLELSLEEAR.Q K.TAIAEGLAQR.I K.AIDLIDEAGSR.V K.AQISTLVEK.G R.VIGODEAVK.A R.RPYTWLFDIEI.KA K.SLVTEELK.Q R.LDEMIVFR.Q

Table 16 (Continued)

Spot no.	Accession number	Protein name	Organism	Theoretical MW (Da)	pI	Score	Peptide match	% Coverage	Sequences
177	gi 356516495	Chaperone protein ClpC, chloroplastic	<i>Glycine max</i>	102434	6.09	588	13	11	R.LDEMIMFR.Q + Oxidation (M) K.EIADIMLKE K.EIADIMLKE + Oxidation (M) K.VKDIEIQVTER.F R.LLEDSMAEK.M
178	gi 356508861	Chaperone protein ClpC, chloroplastic	<i>Glycine max</i>	102490	6.16	108	4	4	R.LOHAQLPEEAR.E K.SLVTEELK.Q K.QYFRPEFLNR.L K.EIADIMLKE
179	gi 356501703	Heat shock protein 90	<i>Glycine max</i>	89661	5.25	290	8	8	K.DAVDFDIR.I K.EEYNEFYK.K K.DDIINPK.T R.EILOESR.V K.LGCIEDR.E + Carbamidomethyl (C) K.DIYYAADSVTSAK.N K.EDLDLGDK.N K.VASVQISNR.L

Table 16 (Continued)

Spot no.	Accession number	Protein name	Organism	Theoretical MW (Da)	pI	Score	Peptide match	% Coverage	Sequences
180	g 356558578	Actin-101	<i>Glycine max</i>	41626	5.31	189	5	12	K.AGFAGDDAPRA R.VAPEEHPVLLTEAPLNPK.A R.DLTEYLVKJ K.EISALAPSSMKI K.EISALAPSSMKI + Oxidation (M)
181	g 20559	Heat shock protein 70 (AA 6-651)	<i>Petunia x hybrida</i>	70738	5.07	103	3	6	R.IINEPTAAAAYGLDKK R.MVNHVQEFK.R + Oxidation (M)
182	g 356501703	Heat shock protein 90	<i>Glycine max</i>	89661	5.25	275	7	7	K.SSVHVDVLYGGSTRJ R.YEYQAEVSR.L K.DAVDFDIRJ K.EEYNEFYK.K K.DDIINPK.T R.EILOESR.V K.EDLDLGKNEEKE K.VASVQISNRL

Table 16 (Continued)

Spot no.	Accession number	Protein name	Organism	Theoretical MW (Da)	pI	Score	Peptide match	% Coverage	Sequences
183	gi 356536246	ATP synthase subunit beta , mitochondrial	<i>Glycine max</i>	59799	5.80	50	5	6	R.TIAMDATEGWVR.G + Oxidation (M)
184	gi 460378451	Luminal-binding protein 5	<i>Solanum lycopersicum</i>	73444	5.07	188	4	5	R.VLNTGSPITVPVGRA [3] K.WDLLAPYQR.G K.ETAFLGK.T K.DAGVAGLNVAR.I R.VMEYFIKL + Oxidation (M) R.LSQEEIER.M
185	gi 113204693	Homocystein S-methyltransferase	<i>Medicago sativa</i>	32607	4.97	53	1	3	R.FIHGLISSIKK
186	gi 22597178	Alcohol dehydrogenase 1	<i>Glycine max</i>	39981	6.19	187	3	7	R.ILFNSLCR.S + Carbamidomethyl (C) R.IIGVDLLPNR.F R.TDIPGVVEK.Y K.AITACSMK.A + Oxidation (M)
187	gi 168001673	Predicted protein	<i>Physcomitrella patens</i>	82960	9.08	19	1	1	(M)
188	gi 302791918	Hypothetical protein SELIMODRAFT_176503	<i>Selaginella moellendorffii</i>	40392	6.78	18	1	3	R.SCFVGTSEGYK.I

Table 16 (Continued)

Spot no.	Accession number	Protein name	Organism	Theoretical MW (Da)	pI	Score	Peptide match	% Coverage	Sequences
189	g 21807	Heat shock protein 17.3	<i>Triticum aestivum</i>	17342	5.58	49	1	6	R.AMAATPADVKE + Oxidation (M)
190	g 351721881	18.5 kDa class I heat shock protein	<i>Glycine max</i>	18491	5.82	146	4	19	R.ENSAFVSTR.V K.VQIEDDK.V K.VLQISGER.N R.FRLPENAK.V
191	g 99033689	Chaperone	<i>Agave tequilana</i>	18325	6.19	150	4	16	K.EEVKVEVEDGR.V K.VEVEDGR.V
192	g 356519335	26.5 kDa heat shock protein, mitochondrial	<i>Glycine max</i>	24584	9.11	142	3	11	R.VLOISGER.S R.FRLPENAK.T K.ITIDDGVLTIK.G K.AELKDGVLTVTIPR.T
193	g 1052778	Ferritin-3, chloroplastic	<i>Vigna unguiculata</i>	28426	5.54	84	1	3	K.IAEVLTQLR.L

Table 16 (Continued)

Spot no.	Accession number	Protein name	Organism	Theoretical MW (Da)	pI	Score	Peptide match	% Coverage	Sequences
194	gi 67107029	14-3-3 protein	<i>Manihot esculenta</i>	29813	4.75	240	7	18	R.EENVYMAKL R.EENVYMAKL + Oxidation (M) K.LAEQAER.Y R.NLLSVAYK.N K.SAQDIALADLAPTHPIR.L KDSTLIMQLLR.D KDSTLIMQLLR.D + Oxidation (M)
195	gi 359807014	Desiccation-related protein At2g46140-like	<i>Glycine max</i>	34343	4.74	172	7	16	K.GGFLDTVK.D K.DFIQDIGEK.I R.LTLPLEK.T [2] R.FSFEETVAILHLK.L K.GHIDVDTFFGAMK.L K.GHIDVDTFFGAMK.L + Oxidation (M)
196	gi 149391151	Glyceraldehyde -3-phosphate dehydrogenase	<i>Oryza sativa</i> Indica Group	28297	8.62	370	9	23	K.IGINGFGR.I K.TLLFGEKE K.KVISAPSK.D K.VVISAPSK.D

Table 16 (Continued)

Spot no.	Accession number	Protein name	Organism	Theoretical		Score	Peptide match	% Sequences
				MW (Da)	pI			
196	gi 149391151	Glyceraldehyde -3-phosphate dehydrogenase	<i>Oryza sativa</i> Indica Group	28297	8.62	370	9	23
								K.DAPMFVGVNEKE K.DAPMFVGVNEKE + Oxidation (M) R.FGIVEGLMITYVHAITATQK.T R.FGIVEGLMITYVHAITATQK.T + Oxidation (M) K.VLPALNGKL K.THINIWIGHVDSGKS K.STTTGHLIYK.L
197	gi 399414	Elongation factor 1- alpha	<i>Triticum aestivum</i>	49138	9.20	257	6	12
								K.YYCTIDAPGHR.D + Carbamidomethyl (C) R.LPLODVYK.I K.IGGIGTPVGR.V [2]
198	gi 359807022	Uncharacterized protein LOC100813980	<i>Glycine max</i>	39118	9.39	79	2	4
								K.SGDLFVGK.T K.ELGVEPNVK.K
199	gi 62909961	Peroxidase	<i>Pisum sativum</i>	38032	5.84	188	5	9
								R.MLASLVR.L + Oxidation (M) R.GLDVWNKIK.T K.NYYSNLQYK.K K.MGNIGVLTGK.Q K.MGNIGVLTGK.Q + Oxidation (M)

Table 16 (Continued)

Spot no.	Accession number	Protein name	Organism	Theoretical MW (Da)	pI	Score	Peptide match	% Coverage	Sequences
200	gi 22296818	Pyruvate kinase	<i>Glycine max</i>	55282	7.89	692	16	24	K.IVCTLGPASR.S + Carbamidomethyl (C) K.DGKPIQLK.E K.IDMIALSFVR.K K.IDMIALSFVR.K + Oxidation (M) R.KGSDLVNR.K K.GSDLVNR.K [2] R.ETDAFMVAR.G R.ETDAFMVAR.G + Oxidation (M) R.GDLGMEIPVEK.I R.GDLGMEIPVEK.I + Oxidation (M) R.STPLPMSPLESLASSAVR.T K.LLIVLTR.G R.GLIPILGESSAKA K.ATDAESTEVIIEALK.S R.GLCKPGDAVVALHR.I + Carbamidomethyl (C)

Table 16 (Continued)

Spot no.	Accession number	Protein name	Organism	Theoretical MW (Da)	pI	Score	Peptide match	% Coverage	Sequences
201	gi 389548688	Serine hydroxymethyl-transferase	<i>Glycine max</i>	51733	7.59	418	9	17	K.YSEGMPGNR.Y + Oxidation (M) K.LJCGGSAYPR.D + Carbamidomethyl (C) R.AGMIFYR.K K.LCDLNCNITVKN.N + 2 Carbamidomethyl (C) K.NAVFGDSSALAPGGV.R.I R.IGAPAMTSR.G R.IGAPAMTSR.G + Oxidation (M) K.DFEQJGEFLH.R.A R.AVTLTLEIQKE
202	gi 22597178	Alcohol dehydrogenase 1	<i>Glycine max</i>	39981	6.19	189	3	7	R.IIFNSLCSR.S + Carbamidomethyl (C) [6] R.IIGVDLLPNR.F R.TDIPGVVEK.Y
203	gi 502117964	Enolase-phosphatase E1 26.5 kDa heat shock	<i>Cicer arietinum</i>	53391	4.38	41	1	1	K.DSDIEVVK.E
204	gi 356519335	protein, mitochondrial-like	<i>Glycine max</i>	24584	9.11	166	4	11	K.ITIDDGVLTIK.G K.AELKDGVLTVTIPR.T K.DGVLTVTIPR.T K.DGVLTVTIPR.T

Table 16 (Continued)

Spot no.	Accession number	Protein name	Organism	Theoretical MW (Da)	pI	Score	Peptide match	% Coverage	Sequences
205	g 1169534	Enolase	<i>Ricinus communis</i>	47883	5.56	112	3	5	K.HIANLAGNIK.N K.ACNALLLK.V + Carbamidomethyl (C) K.YNQLLR.I
206	g 159470791	Exostosin-like glycosyltransferase	<i>Chlamydomonas reinhardtii</i>	56018	8.95	41	1	1	R.VAEADIPRL
207	g 1169534	Enolase	<i>Glycine max</i>	47883	5.56	257	6	10	R.DGGSDYLKG.G K.HIANLAGNIK.N K.EGLELLK.T K.TYDLNFKE K.ACNALLLK.V + Carbamidomethyl (C) K.YNQLLR.I
208	g 3556560917	Tubulin alpha-3 chain-like	<i>Glycine max</i>	49053	5.10	209	5	11	R.QLFHPPEQLISGKE K.EDAANNFAR.G R.SLDIERPTYTNLNR.L K.DVNAAVSNIK.T R.EDLAALEKD

Table 16 (Continued)

Spot no.	Accession number	Protein name	Organism	Theoretical MW (Da)	pI	Score	Peptide match	% Coverage	Sequences
209	gi 26245395	Nucleoside diphosphate kinase	<i>Glycine max</i>	16344	6.91	105	2	12	R.GLIGEISR.L R.GDFAIDIGR.N
210	gi 302847713	Acetylglucosaminyltransferase	<i>Volvox carteri</i> f. <i>nagariensis</i>	29019	4.74	54	1	2	R.LAEADIPR.M
211	gi 356536246	ATP synthase subunit beta	<i>Glycine max</i>	59799	5.80	423	9	15	K.ITDEFTGK.G R.TIAMDATEGVVR.G R.TIAMDATEGVVR.G + Oxidation (M) R.VLNTGSPTTPVGR.A K.VVDLLAPYQR.G K.IGLFGGAGVGK.T K.TVLIMELINNAK.A + Oxidation (M) K.AHGGFSVFAGVGER.T R.EGNDLYR.E
212	gi 502082432	Ketol-acid reductoisomerase	<i>Cicer arietinum</i>	63532	6.18	170	4	5	K.NISVIACPK.G + Carbamidomethyl (C) K.NTVESITGIISK.T K.EGLPAPFMGKI K.EGLPAPFMGKI + Oxidation (M)

Table 16 (Continued)

Spot no.	Accession number	Protein name	Organism	Theoretical MW (Da)	pI	Score	Peptide match	% Coverage	Sequences
213	gij502120564	Uncharacterized protein	<i>Cicer arietinum</i>	120841	5.79	543	11	10	R.TIAMDATEGVVR.G + R.TIAMDATEGVVR.G + Oxidation (M) K.WYDLLAPYQR.G K.IGLFGAGVGK.T K.TVLIMELINNVAK.A K.TVLIMELINNVAK.A + Oxidation (M) R.EGNDLYR.E R.FIQANSEVSALLGR.I K.GAIGHVCOVIGAVVDVR.F + Carbamidomethyl (C) R.LVLEVAQHLGEGEVR.T R.VLNTGSPITVPVGR.A
		LOC101500213							
214	gij35561923	Glucan endo-1,3-beta-glucosidase 5-like	<i>Glycine max</i>	84337	5.61	95	2	2	R.NANLQYAQR.F K.YQLNIGSR.A

Table 16 (Continued)

Spot no.	Accession number	Protein name	Organism	Theoretical MW (Da)	pI	Score	Peptide match	% Coverage	Sequences
215	gi 1498330	Actin,partial	<i>Glycine max</i>	37150	5.38	243	5	18	-AGFAGDDAPRA K.DAYVGDEAOSK.R K.IWHHTFYNELR.V R.VAPEEHPVLLTEAPLNPK.A
216	gi 543176666	Alcohol dehydrogenase 1	<i>Phaseolus vulgaris</i>	41328	6.39	94	2	4	KEISALAPSSMKI + Oxidation (M) K.ILFNSLCR.T + Carbamidomethyl (C) K.GQNPLFPR.I
217	gi 502140113	Lipoxygenase homology domain-containing protein 1	<i>Cicer arietinum</i>	21310	6.05	112	2	8	K.YGYIYIK.N R.GNLDIFSGR.G
218	gi 356536156	D-3-phosphoglycerate dehydrogenase	<i>Glycine max</i>	62573	6.32	644	10	19	K.LGDAGLKLKD R.INVAQADASVKA K.YYGVSLVGK.T K.TLAVLGFVK.V K.GLGMNVIHDPYAPADR.A + Oxidation (M) R.GGVDEDELVR.A R.LAVQLVAGGGVK.T R.FASAI SDSGEIK.V

Table 16 (Continued)

Spot no.	Accession number	Protein name	Organism	Theoretical MW (Da)	pI	Score	Peptide match	% Sequences Coverage
218	gi 356536156	D-3-phosphoglycerate dehydrogenase	<i>Glycine max</i>	62573	6.32	644	10	19 K.DGIPHLTK.V R.KQAVMAIGVDEQPSK.E + Oxidation (M)
219	gi 71793966	Alcohol dehydrogenase	<i>Alnus glutinosa</i>	40971	6.28	149	4	11 K.INPAAPLDK.V K.KFGVTEFVNP.K.D R.TDIPGW.EK.Y K.FITHSVPFSEINK.A
220	gi 356552857	Pyruvate dehydrogenase E1 component subunit beta, mitochondrial-like	<i>Glycine max</i>	38751	5.80	144	3	8 K.VLSPYSSSEDAR.G R.STINTSVR.K
221	gi 356559136	17.4 kDa class III heat shock protein-like	<i>Glycine max</i>	17959	6.17	155	3	14 R.MAVPQVEDIVR.A + Oxidation (M) R.RGPQNLLR.K K.FRLPENANVSATAK.C R.LPENANVSATAK.C
222	gi 16930753	Small heat shock protein	<i>Retama raetam</i>	17880	5.82	161	4	18 K.EEVKVEVEEGR.V K.VEEVEGR.V R.FRLPENAK.V K.KPDVKPVQITG.-

Table 16 (Continued)

Spot no.	Accession number	Protein name	Organism	Theoretical MW (Da)	pl	Score	Peptide match	% Coverage	Sequences
223	gi 543177195	CHP-rich zinc finger protein	<i>Phaseolus vulgaris</i>	26411	5.81	165	4	12	R:KLEDDFDFAFTASKA R:LCLEVER.L + Carbamidomethyl (C) R:LGSAVIMGSR.G R:LGSAVIMGSR.G + Oxidation (M)
224	gi 508712741	Chloroplast heat shock protein 70 isoform 3	<i>Theobroma cacao</i>	75464	5.40	465	10	15	K:IMSEVDEESKQ K:LECPAIGKQ + Carbamidomethyl (C) K:QFAAEESAQVLR.K R:IAGLEVLR.I R:IINEPTAASLAYGFEEK.K K:HIETTLTR.V R:VKFEELCSDLLDR.L + Carbamidomethyl (C) K:TPVENSLR.D K:DIDEVILVGGSTR.M K:INQADSVVYQTEKQ

Table 17 Protein sequences of leaves were identified by two-dimensional Polyacrylamide Gel electrophoresis (2D-PAGE) coupled with LC/MS/MS

Spot no.	Accession number	Protein name	Organism	Theoretical MW (Da)	pl	Score	Peptide match	% Coverage	Sequences
1	gi 3980231	Ribulose 1,5 bisphosphate carboxylase/oxygenase large subunit	<i>Stewartia pseudocamellia</i>	51268	6.46	400	9	20	K.LTYTDPDYETK.D K.DTDILAAFR.V R.IPISYIK.T K.DDENVNSQPFMR.W + Oxidation (M) R.AVVECLR.G + Carbamidomethyl (C) R.FVFCAEAIYK.A + Carbamidomethyl (C) R.DNGLLLHIHR.A K.WSPELAAACEWKE + Carbamidomethyl (C) R.EITLGFVLLR.D R.VALEACYKAR.N + Carbamidomethyl (C) R.IQIDYIQ.-
2	gi 527200637	Hypothetical protein M569_06763	<i>Genlisea aurea</i>	13163	4.60	48	1	5	R.IQIDYIQ.-
3	gi 527200637	Hypothetical protein M569_06763	<i>Genlisea aurea</i>	13163	4.60	37	1	5	R.IQIDYIQ.-

Table 17 (Continued)

Spot no.	Accession number	Protein name	Organism	Theoretical MW (Da)	pI	Score	Peptide match	% Sequences	Coverage
4	gij55584320	ATPase beta subunit	<i>Thamnochoortus erectus</i>	1362	9.62	32	1	100	-MIRINPTTSSSSSA.- + Oxidation (M)
5	gij225448341	Cytochrome P450 734A1	<i>Vitis vinifera</i>	59649	9.08	28	1	1	R.VCFGSSYGK.G
6	gij15236014	Lipase/lipooxygenase, PLAT/LH2 family protein	<i>Arabidopsis thaliana</i>	20123	4.97	61	1	4	R.GNLDIFSGR.A
7	gij120005	Ferredoxin	<i>Leucaena leucocephala</i>	10581	4.01	33	1	9	R.SDWMETHKE
8	gij3980231	Ribulose 1,5 biphosphate carboxylase-oxygenase large subunit	<i>Stewartia pseudocamellia</i>	51268	6.46	400	9	20	K.LTTYTPDYETK.D K.DTDILAAFR.V R.IPISYIK.T K.DDENVNSQPFMR.W + Oxidation (M) R.AVYECLR.G + Carbamidomethyl (C) R.FVFCAEAIYKA + Carbamidomethyl (C) R.DNGLLLHIHR.A K.WSPELAAACEVWKE + Carbamidomethyl (C)

Table 17 (Continued)

Spot no.	Accession number	Protein name	Organism	Theoretical MW (Da)	pI	Score	Peptide match	% Coverage	Sequences
9	gi 2921320	Beta-1,3- β glucanase 5	<i>Glycine max</i>	25522	8.42	47	1	7	R.EITLGFVDLLR.D R.VALEACVKARN + Carbamidomethyl (C) K.VSTAITDTLLGNSYPPK.D
10	gi 21309	28kD RNA binding protein	<i>Spinacia oleracea</i>	24498	4.42	90	2	8	R.LEQLFSEHGK.V R.VNVAEERPR.R
11	gi 21309	28kD RNA binding protein	<i>Spinacia oleracea</i>	24498	4.42	92	2	8	R.LEQLFSEHGK.V R.VNVAEERPR.R K.GSDGVIACKS +
12	gi 25091405	Thaumatococcus-like protein 1	<i>Prunus persica</i>	25748	8.29	62	1	4	Carbamidomethyl (C)
13	gi 357507859	Phosphoglycolate phosphatase	<i>Medicago truncatula</i>	40307	6.90	178	5	10	R.LVFTNNSTKS K.VYVIGEDGILKE K.SQICMVGDR.L + Carbamidomethyl (C) K.SQICMVGDR.L + Carbamidomethyl (C) ; Oxidation (M) K.ISDFLSLKA

Table 17 (Continued)

Spot no.	Accession number	Protein name	Organism	Theoretical MW (Da)	pI	Score	Peptide match	% Coverage	Sequences
14	g 357507859	Phosphoglycolate phosphatase	<i>Medicago truncatula</i>	40307	6.90	195	5	10	R.LVFVTNNSTK.S K.VYVIGEDGILKE K.SQICMVGDR.L + Carbamidomethyl (C) K.SQICMVGDR.L + Carbamidomethyl (C) ; Oxidation (M) K.ISDFLSLKA
15	g 152143640	Chloroplast photosynthetic water oxidation complex 33kDa subunit precursor	<i>Morus nigra</i>	28249	5.48	173	4	10	K.RLTYDEIQSK.T R.LTYDEIQSK.T K.LCLEPTSFVTKA + Carbamidomethyl (C) R.VPFLFTIK.Q
16	g 152143640	Chloroplast photosynthetic water oxidation complex 33kDa subunit precursor	<i>Morus nigra</i>	28249	5.48	74	6	10	R.LTYDEIQSK.T R.VPFLFTIK.Q
17	g 1079736	Ribulose 1,5-bisphosphate carboxylase small subunit	<i>Glycine soja</i>	19962	8.80	87	2	8	R.SPGYYDGR.C R.IIGFDNVR.Q

Table 17 (Continued)

Spot no.	Accession number	Protein name	Organism	Theoretical MW (Da)	pI	Score	Peptide match	% Coverage	Sequences
18	gi 302122828	14-3-3g protein	<i>Gossypium hirsutum</i>	29405	4.70	332	9	23	R.EENVYMAKL + Oxidation (M) K.LAEQAERY R.NLLSVAYKN R.IISSIEQKE R.GNEDHVATIKE K.EAAESTLLAYK.S K.DSTLIMQLLR.D K.DSTLIMQLLR.D + Oxidation (M)
19	gi 1345588	14-3-3-like protein GF14-12	<i>Zea mays</i>	29618	4.75	122	3	9	R.EENVYMAKL + Oxidation (M)
20	gi 508777952	NAD(P)-binding Rossmann-fold superfamily protein isoform 1	<i>Theobroma cacao</i>	31979	7.62	151	3	6	R.EENVYMAKL + Oxidation (M) R.NLLSVAYKN R.IISSIEQKE K.GIEVISLSR.S R.KAESEVLSKY K.AESEVLSKY

Table 17 (Continued)

Spot no.	Accession number	Protein name	Organism	Theoretical MW (Da)	pI	Score	Peptide match	% Coverage	Sequences
21	gi 502079139	Putative lactoylglutathione lyase-like isoform X1	<i>Cicer arietinum</i>	37148	6.04	153	4	10	K:FYTECFGMK.L + Carbamidomethyl (C) K:FYTECFGMK.L + Carbamidomethyl (C); Oxidation (M) R:ASTPEPLCQVMLR.V + Carbamidomethyl (C); Oxidation (M) K:TVLVDNQDFLKE
22	gi 557532497	Hypothetical protein	<i>Citrus clementina</i>	27352	6.11	111	2	7	R:VFOIEYAAK.A K:VPDELLLEEAK.A
23	gi 255544626	CICLE_v10012559mg Proteasome subunit alpha type, putative	<i>Ricinus communis</i>	25582	5.73	219	4	17	K:AAANGWIATEK.K K:EPVPVQLVR.E K:EGFEGQISGK.N K:NIEIGIGADK.K
24	gi 15226479	Triosephosphate isomerase	<i>Arabidopsis thaliana</i>	33325	7.67	47	1	4	K:GPEFATVNSVTSK.K

Table 17 (Continued)

Spot no.	Accession number	Protein name	Organism	Theoretical MW (Da)	pI	Score	Peptide match	% Coverage	Sequences
25	g 57283985	Triose-phosphate isomerase	<i>Phaseolus vulgaris</i>	27183	5.87	146	2	8	K.VAYALSQGLK.V K.VIACIGETLEQRE + Carbamidomethyl (C)
26	g 129320	Protein P21	<i>var. nanus</i> <i>Glycine max</i>	21449	7.68	125	2	10	K.TQGGNNPCTVFK.T + 2 Carbamidomethyl (C)
27	g 356501429	Oxygen-evolving enhancer protein 2 chloroplastic-like	<i>Glycine max</i>	28000	7.68	134	5	13	R.CPDAYSYPK.D + Carbamidomethyl (C) K.TDIDFLPYNGDGFKL K.SITDYGSPPEEFLSK.V [3] K.VDYLLGKQ
28	g 77540216	Triosephosphate isomerase	<i>Glycine max</i>	27187	7.67	393	8	31	K.FFVGGNWK.C K.KIVTTLNEAK.V K.IVTTLNEAK.V K.VIACIGETLEQRE + Carbamidomethyl (C) K.ISNWDNVVLAYEPVWAIGTGK.V K.VATPAQAEVHADLR.K R.IIYGGSVNGGNCKE + Carbamidomethyl (C) [2]

Table 17 (Continued)

Spot no.	Accession number	Protein name	Organism	Theoretical MW (Da)	pI	Score	Peptide match	% Coverage	Sequences
29	gi 351726399	Isoflavone reductase homolog 2	<i>Glycine max</i>	33919	5.60	190	4	12	K.ILFIGGTGYIGKF K.FIVEASAKA K.AGHPTFLLYRE R.ESTLSNPAK.S K.FIVEASAKA
30	gi 351726399	Isoflavone reductase homolog 2	<i>Glycine max</i>	33919	5.60	206	5	16	K.AGHPTFLLYRE R.ESTLSNPAK.S K.FIVEASAKA K.AGHPTFLLYRE R.ESTLSNPAK.S K.KFYPSEFGNDVDR.T R.IYVPEEQLLKQ
31	gi 83283965	Malate dehydrogenase-like protein	<i>Solanum tuberosum</i>	35463	5.74	176	4	9	K.EFAPSIPEK.N K.NITCLTRL + Carbamidomethyl (C) R.ALGQISER.L R.LSVQVSDVK.N

Table 17 (Continued)

Spot no.	Accession number	Protein name	Organism	Theoretical MW (Da)	pI	Score	Peptide match	% Coverage	Sequences
32	gi 351726399	Isoflavone reductase homolog 2	<i>Glycine max</i>	33919	5.60	171	4	11	K.FIVEASAK.A R.ESTLSNPAK.S R.VIIIGDGNPK.A R.IYVPEEQLLK.Q
33	gi 356518030	Isoflavone reductase homolog	<i>Glycine max</i>	43079	6.10	239	5	12	K.IIIGGTGYIGK.H K.VIIIGDGNPK.A K.EEDIGTYTIR.A K.ILYLRPPK.N
34	gi 77540216	Triosephosphate isomerase	<i>Glycine max</i>	27187	5.87	126	4	13	K.IVTTLNEAK.V K.VIACIGETLEQRE + Carbamidomethyl [2] R.IYGGSVNGGNCKE + Carbamidomethyl (C)

Table 17 (Continued)

Spot no.	Accession number	Protein name	Organism	Theoretical MW (Da)	pl	Score	Peptide match	% Sequences Coverage
35	gij356526968	Glutathione S-transferase F10-like	<i>Glycine max</i>	25708	6.15	277	7	16 K.RVIVCLIEK.E + Carbamidomethyl (C) R.VIVCLIEK.E + Carbamidomethyl (C) K.YKNOGTDLLGK.T [2] K.NQGTDLLGK.T K.VLDIYEER.L K.KVLQLYK.D
36	gij356556406	20 kDa chaperonin, chloroplastic-like	<i>Glycine max</i>	26653	7..79	235	5	16 K.YTAIKPLGDR.V K.TGAQWYSK.Y K.DLKLPLNDR.V K.YAGNDFK.G
37	gij356526942	Oxygen-evolving enhancer protein 2 chloroplastic-like	<i>Glycine max</i>	28212	6.96	126	3	8 K.DGSDYITLR.V K.EVEYPGQVLR.Y R.RFVESTASSFSVA.- R.FVESTASSFSVA.-
38	gij502158725	Disease resistance response protein 206-like	<i>Cicer arietinum</i>	20849	5.10	127	2	11 R.AQGMFGLASLEDR.G + Oxidation (M) R.NPVQDTR.E

Table 17 (Continued)

Spot no.	Accession number	Protein name	Organism	Theoretical MW (Da)	pl	Score	Peptide match	% Coverage	Sequences
39	gij1079736	Ribulose 1,5-bisphosphate carboxylase small subunit precursor	<i>Glycine soja</i>	19962	8.80	120	3	12	K.EVEYLLR.K R.SPGYYDGR.C R.IIGFDNVR.Q
40	gij1079736	Ribulose 1,5-bisphosphate carboxylase small subunit precursor	<i>Glycine soja</i>	19962	8.80	98	2	8	R.SPGYYDGR.C R.IIGFDNVR.Q
41	gij2961268	Ribulose-1,5-bisphosphate carboxylase	<i>Iseritia pittieri</i>	52641	6.10	234	5	7	K.DTDILAAFR.V R.IPISYIK.T [2] K.AQAETGEIKG R.VALEACVKAR.N + Carbamidomethyl (C)

Table 17 (Continued)

Spot no.	Accession number	Protein name	Organism	Theoretical MW (Da)	pI	Score	Peptide match	% Coverage	Sequences
42	g 1881501	Ribulose-1,5-bisphosphate carboxylase/oxygenase large subunit	<i>Psychotria peteri</i>	52000	6.32	364	8	15	K.DTDILAAFR.V R.IPSYIK.T K.YGRPLLGCTIKPKL + Carbamidomethyl (C) R.AVYECLR.G + Carbamidomethyl (C) K.AQAETGEIK.G K.GHYLNATAGTCEEMMK.R + Carbamidomethyl ; Oxidation (M) R.VALEACVKAR.N + Carbamidomethyl [2]
43	g 2808617	Ribulose-1,5-bisphosphate carboxylase/oxygenase large subunit	<i>Phylloglossum drummondii</i>	50190	6.90	335	8	12	K.DTDILAAFR.M K.DEDILAAFR.M K.YGRPLLGCTIKPKL + Carbamidomethyl (C) R.AVYECLR.G + Carbamidomethyl (C)

Table 17 (Continued)

Spot no.	Accession number	Protein name	Organism	Theoretical MW (Da)	pI	Score	Peptide match	% Coverage	Sequences
44	g 1771817	Ribulose-1,5-bisphosphate carboxylase/oxygenase large subunit	<i>Touroulia guianensis</i>	51662	6.13	371	8	18	K.AQAETGEIK.G R.AMHAVIDR.Q R.AMHAVIDR.Q + Oxidation (M) R.VALEACVKAR.N + Carbamidomethyl (C) K.LTYTPDYETKD K.YGRPLLGGTIKPKL + Carbamidomethyl (C) R.FVFAEAYKA + Carbamidomethyl (C) K.AQAETGEIK.G K.GHYLNATAGTCEEMMK.R + Carbamidomethyl (C); Oxidation (M) R.AMHAVIDR.Q R.EITLGFVDLLR.D R.VALEACVKAR.N + Carbamidomethyl (C)

Table 17 (Continued)

Spot no.	Accession number	Protein name	Organism	Theoretical MW (Da)	pI	Score	Peptide match	% Coverage	Sequences
45	gi 1769935	Ribulose-1,5-bisphosphate carboxylase/oxygenase large subunit	<i>Burcheilia bubalina</i>	51911	6.12	312	6	12	K.LTYTPDYETK.D K.YGRPLLGCTIKPK.L + Carbamidomethyl (C) R.AVYECLR.G + Carbamidomethyl (C) R.FVFCAEALYK.A + Carbamidomethyl (C) K.AQETGEIKG R.VALEACVKAR.N + Carbamidomethyl (C)
46	gi 904085	Adenosine triphosphatase, partial (chloroplast)	<i>Boquila trifoliolata</i>	53577	4.97	370	7	16	R.IAQIIGPVLDAFPPGK.M K.MPNINYALWK.G + Oxidation (M) R.AVAMSATDGLMR.G + 2 Oxidation (M) K.LSIFETGIK.V K.WDLLAPYR.R K.IGLFGGAGVGK.T K.AHGGVSVFGVGGER.T

Table 17 (Continued)

Spot no.	Accession number	Protein name	Organism	Theoretical MW (Da)	pI	Score	Peptide match	% Coverage	Sequences
47	g 91214148	ATP synthase CF1 alpha subunit	<i>Glycine max</i>	55719	5.15	265	6	10	R.ERIEQYNTEVKI R. IEQYNTEVKI K.IVNTGTVLQVGDGIAR.I R.GEISASESR.L R.LIESPAPGIISR.R R.ELIIGDR.Q
48	g 11990290	Ribulose-1,5-bisphosphate carboxylase/oxygenase large subunit	<i>Prismatomeris beccariana</i>	51742	6.04	201	4	8	R.IPISYIK.T K.YGRPLLGGCTIKPKL + Carbamidomethyl (C) R.EITLGFVDLLR.D R.VALEACVKAR.N + Carbamidomethyl (C)

Table 17 (Continued)

Spot	Accession	Protein	Organism	Theoretical MW	Score	Peptide match	% Sequences
no.	number	name		(Da)	pl		Coverage
50	gi 132150	Ribulose biphosphate carboxylase small chain	<i>Pinus thunbergii</i>	19300	8.80	65 2	8 K.EVEYLLR.N R.SPGYYDGR.Y
51	gi 1079736	Ribulose 1,5-biphosphate carboxylase small subunit precursor	<i>Glycine soja</i>	19962	8.80	193 4	20 K.EVEYLLR.K R.SPGYYDGR.C K.LPMFGCTDASQVLK.E + Carbamidomethyl (C); Oxidation (M) R.IIGFDNVR.Q
52	gi 131772	40S ribosomal protein S14	<i>Zea mays</i>	16248	10.70	57 1	7 K.TPGFGAQSALR.A

Table 17 (Continued)

Spot no.	Accession number	Protein name	Organism	Theoretical MW (Da)	pI	Score	Peptide match	% Sequences	Coverage
53	gi 561036976	Hypothetical protein	<i>Phaseolus vulgaris</i>	41634	5.94	367	6	15	R.LLVSMGEALR.T + Oxidation (M) R.DQVAAAAMGVMGPR.T + 2 Oxidation (M) K.ETTEGEGK.L K.LIDYYVNEK.Y K.GIFTNVASPSAKA R.FEETLYGK.S
		PHAVU_001G240200g							
54	gi 357484753	Phosphoribulokinase	<i>Medicago truncatula</i>	45661	6.68	165	5	12	R.LTSVFGGAAEPPK.G K.GVTALDPR.A R.GHSLESIAK.A R.KPDFEAYIDPQK.Q R.AETPYGAAK.A

Table 17 (Continued)

Spot no.	Accession number	Protein name	Organism	Theoretical MW (Da)	pI	Score	Peptide match	% Coverage	Sequences
55	gi 356544404	Photosynthesis II stability/assembly factor HCF136, chloroplastic-like	<i>Oryza sativa</i> subsp. <i>japonica</i>	43281	6.79	655	16	37	R.QTILETK.N K.DGGNTWAPR.S R.FNSISFKG R.IPLSAELPGDMVYIK.A R.IPLSAQLPGNMVYIK.A + Oxidation (M) K.SAEMVTDEGAIYVTANR.G K.SAEMVTDEGAIYVTANR.G+Oxidation (M) [2] K.AAVOETVSATLNR.T R.TVSSGISGASYTGTFTNTVNR.S [2] R.GNFYL TWEFGPFWOPHNR.A R.IQNIMGWR.A + Oxidation (M) R.ADGGLWLLYR.G R.GFGILDVGYR.S K.AADNIAANLYSVK.F

Table 17 (Continued)

Spot no.	Accession number	Protein name	Organism	Theoretical MW (Da)	pI	Score	Peptide match	% Coverage	Sequences
56	gij356559803	Stromal 70 kDa heat shock-related protein, chloroplastic	<i>Glycine max</i>	73709	5.20	267	5	6	K.LDCPAIGK.Q + Carbamidomethyl (C) R.IAGLEVLR.I R.DEGIDLLK.D R.TPVENSLR.D
57	gij171854980	Protein disulfide isomerase	<i>Glycine max</i>	58554	5.13	191	5	10	K.DAISGGSTQAIK.D K.AASILSSHDPVVLAK.I K.DLASQYDVR.G K.QSGPASTEIK.S K.FFNPNNAK.A R.TKEDIIEFIEK.N K.SFOCELVFAK.M +
58	gij508726180	Ribulose biphosphate carboxylase/oxygenase activase, chloroplastic isoform 1	<i>Theobroma cacao</i>	48338	5.56	137	3	6	Carbamidomethyl (C) R.TDNVPDDDDVKK.L R.VYDDEVK.K

Table 17 (Continued)

Spot no.	Accession number	Protein name	Organism	Theoretical MW (Da)	pI	Score	Peptide match	% Coverage	Sequences
59	gi 351724777	Alanine aminotransferase 3	<i>Glycine max</i>	53390	5.52	239	5	10	K.VLMDLGPPIK.E + Oxidation (M) K.GYYGECGQR.G + Carbamidomethyl (C) R.ESTGILES.LR R.LMTDGFNSCR.N + Carbamidomethyl (C); Oxidation (M) K.VPDPVYCLK.L + Carbamidomethyl (C) R.VVDLADIVANWK.-

Table 17 (Continued)

Spot no.	Accession number	Protein name	Organism	Theoretical MW (Da)	pI	Score	Peptide match	% Coverage	Sequences
60	gij255543455	Glyceraldehyde -3-phosphate dehydrogenase	<i>Ricinus communis</i>	43087	8.14	495	10	25	K.VAINGFGR.I K.DSPLDVIINDTGGVK.Q R.NPANLPWK.D K.KVLITAPGK.G K.VLITAPGK.G R.AAALNIVPTSTGAAGA K.AVALVLPTLK.G K.TFAEEVNAAFR.E K.VIAWYDNEWGYSQR.V R.VVDLADIVANNWK.-

Table 17 (Continued)

Spot no.	Accession number	Protein name	Organism	Theoretical MW (Da)	pI	Score	Peptide match	% Coverage	Sequences
61	gi 356525742	Phosphoglycerate kinase, chloroplastic-like	<i>Glycine max</i>	50236	7.79	454	8	18	K.SVGDLSAADLKG K.YSLAPLVPR.L K.ELDYLVGAVSNPK.R K.IGVIESLLEK.V K.LDLATSLAK.A K.FAPDANSK.V K.FAVGTEAIKK
62	gi 359475330	Glycine-rich RNA -binding protein GRP1A-like	<i>Vitis vinifera</i>	16319	6.32	112	3	23	K.GVTTIIGGGDSVAAVEK.V R.GFGFVTFSSSEOSMR.D R.DAIEGMNGONLDGR.N + Oxidation (M) R.NITYNEAOSR.G

Table 17 (Continued)

Spot no.	Accession number	Protein name	Organism	Theoretical MW (Da)	pI	Score	Peptide match	% Sequences	Coverage
63	gi 62734702	Retrotransposon protein	<i>Pseudotsuga menziesii</i>	138642	8.77	40	1	0	R.LTFVKNMRA + Oxidation (M)
64	gi 134684	Superoxide dismutase [Cu-Zn], chloroplastic	<i>Petunia x hybrida</i>	22302	6.17	139	4	12	R.ALVWHELEDDLK.G [3] K.GGHELSTTGNAGGR.L
65	gi 356577825	Monodehydroascorbate reductase	<i>Glycine max</i>	47011	5.49	192	3	8	K.AYLFPEPAR.L R.LTDFGVEGADAKN
66	gi 356533631	Monodehydroascorbate reductase -like isoform 1	<i>Glycine max</i>	46822	5.73	137	3	6	R.LTDFGVEGADAKN K.NIFYLRE K.EGLSFASK.I

Table 17 (Continued)

Spot no.	Accession number	Protein name	Organism	Theoretical MW (Da)	pI	Score	Peptide match	% Sequences	% Coverage
67	gi 38123356	Pathogenesis-related class 10 protein SPE-16	<i>Pachyrhizus erosus</i>	15798	5.02	58	1	6	K.GDAPLSDAVR.D
68	gi 124230	Eukaryotic translation initiation factor 5A-1	<i>Medicago sativa</i>	17648	5.48	73	2	9	K.NGYIVIK.N K.WEVSTSK.T
69	gi 159470791	Exostosin-like glycosyltransferase	<i>Chlamydomonas reinhardtii</i>	56018	8.95	52	2	1	R.VAEADIPR.L [2]
70	gi 217072770	Unknown	<i>Medicago truncatula</i>	28143	7.66	80	2	6	K.VDYLLGKQ
71	gi 356502736	Proteasome subunit alpha type-7-like isoform 1	<i>Glycine max</i>	27085	5.82	242	4	15	R.GTDNVLGVVEK.K R.YIAGLQQK.Y R.ALLEVESGGK.N K.NIEVAVMTKE + Oxidation (M)

Table 17 (Continued)

Spot no.	Accession number	Protein name	Organism	Theoretical MW (Da)	pI	Score	Peptide match	% Coverage	Sequences
72	gij351727433	Guanine nucleotide -binding protein subunit beta-like protein	<i>Glycine max</i>	35586	7.62	156	6	20	R.SILWHLTK.E R.LWDLAAGTSAR.R K.LWNLTGGECK.Y + Carbamidomethyl (C) R.FSPSTLQPTVSASWDR.T
73	gij356526942	Oxygen-evolving enhancer protein 1	<i>Litchi chinensis</i>	35165	6.96	132	3	7	K.YVMNLTNCKL + Carbamidomethyl (C) R.YWLCAAATEQSIK.I + Carbamidomethyl (C) R.LTYDEIQSK.T R.VPFLFTIK.Q R.GDEEELAKE
74	gij326467059	Oxygen-evolving enhancer protein 1	<i>Litchi chinensis</i>	35165	5.86	175	4	7	K.RLTYDEIQSK.T R.LTYDEIQSK.T R.VPFLFTIK.Q R.GDEEELAKE
75	gij326467059	Oxygen-evolving enhancer protein 1	<i>Litchi chinensis</i>	35165	5.86	98	5	7	R.LTYDEIQSK.T R.GDEEELAKE

Table 17 (Continued)

Spot no.	Accession number	Protein name	Organism	Theoretical MW (Da)	pI	Score	Peptide match	% Coverage	Sequences
76	gi 357507859	Phosphoglycolate phosphatase	<i>Medicago truncatula</i>	40307	5.15	199	6	10	K.RLVFVTNNSTK.S R.LLVFVTNNSTK.S R.ENPGCLFIATNR.D + Carbamidomethyl (C) K.SQICMVGDR.L + Carbamidomethyl (C) K.SQICMVGDR.L + Carbamidomethyl (C) ; Oxidation (M) K.IIDFSLK.A
77	gi 351726214	Calreticulin I precursor	<i>Glycine max</i>	48114	4.43	79	2	7	R.FYAISAEYPEFSNK.D K.SGTLFDNVLITDDPEYAKQ

Table 17 (Continued)

Spot no.	Accession number	Protein name	Organism	Theoretical MW (Da)	pI	Score	Peptide match	% Coverage	Sequences
78	gij356544363	Uncharacterized protein LOC100792883	<i>Glycine max</i>	149573	4.69	421	10	6	K.VISEVSYTK.V R.FLEAQEKI KIQELEVELQR.L R.FIAAEQR.N R.LEDLIQSSHK.L K.ENLLEILR.D K.LQSTESDLR.E R.KILEAESK.S K.LEDYAQKF K.LELEAALK.N K.ILFNSLCR.T +
79	gij543176666	Alcohol dehydrogenase 1	<i>Phaseolus vulgaris</i>	41328	6.39	250	5	11	Carbamidomethyl (C) K.GQNPLFPR.I K.SSESNLCEVLR.I + Carbamidomethyl (C) R.GVMLSDGK.T KINPAAPLDK.V

Table 17 (Continued)

Spot no.	Accession number	Protein name	Organism	Theoretical MW (Da)	pI	Score	Peptide match	% Coverage	Sequences
80	gi 671611	Ribulose-1,5-bisphosphate carboxylase/oxygenase large subunit	<i>Prostanthera nivea</i>	52365	6.33	283	5	9	K.DTDILAAFR.V R.AVYECLR.G + Carbamidomethyl (C) K.AQAETGEIK.G R.EITLGFVDLLR.D R.VALEACVKAR.N + Carbamidomethyl (C)
81	gi 5881134	Phosphoribulokinase	<i>Beta vulgaris</i>	30596	5.15	189	4	11	R.RLTSVFGGAAEPPK.G R.LTSVFGGAAEPPK.G K.GVTALDPR.A R.GHSLESIK.A

Table 17 (Continued)

Spot no.	Accession number	Protein name	Organism	Theoretical MW (Da)	pI	Score	Peptide match	Peptide % Coverage	Sequences
82	gi 351726690	Glyceraldehyde-3-phosphate dehydrogenase B subunit	<i>Glycine max</i>	48199	7.10	394	7	15	K.YDSMLGTFK.A + Oxidation (M) K.ILDNETITVDGKPIK.V K.KVIITAPAK.G K.VIITAPAK.G K.ILDEEFGMK.G R.AAALNIVPTSTGAAK.A K.GLTAEDVNAEFR.K K.QSAEEISSMVLK.M + 2 Oxidation (M) K.MKEAEAYLGSTVK.N + Oxidation (M) K.NAVWTVPAYFNDSQR.Q K.DAGVISGLNVMRI + Oxidation (M) R.IVNHVQEFK.R + Oxidation (M) R.ARFEELNMDLFRK + Oxidation (M)
83	gi 502145084	Heat shock cognate 70 kDa protein 2-like	<i>Cicer arietinum</i>	71128	5.11	445	10	15	

Table 17 (Continued)

Spot no.	Accession number	Protein name	Organism	Theoretical MW (Da)	pI	Score	Peptide match	% Coverage	Sequences
84	gi 356549495	Heat shock 70 kDa protein, mitochondrial-like	<i>Glycine max</i>	72383	5.68	370	8	10	K.VIENSEGAR.T K.IMKETAAYLGK.S + Oxidation (M) R.IAGLDVQR.I R.TESIDLSKD K.HLNITLTR.S K.VQEVWSEIFGK.S K.EQQITIR.S K.EIEDAVSDLR.Q

Table 17 (Continued)

Spot no.	Accession number	Protein name	Organism	Theoretical MW (Da)	pI	Score	Peptide match	% Coverage	Sequences
85	gi 294095	Ferredoxin NADP+ reductase, partial	<i>Pisum sativum</i>	10721	4.99	151	3	27	R.LDFAVSR.E K.MYIQR.M + Oxidation (M) K.GIDDIMVSLAAK.D + Oxidation (M)
86	gi 356504476	NADP-dependent alkenal double bond reductase P1-like	<i>Glycine max</i>	37905	5.81	261	6	17	R.DYVSGFPE K.VLESGHPDYK.K K.LTDCYVVGSAKSE K.LGFDEFNYKE K.EESDLNATL.R
87	gi 120661	Glyceraldehyde -3-phosphate dehydrogenase A	<i>Nicotiana tabacum</i>	41837	6.60	91	3	10	K.TLDAVLPNMR.V + Oxidation (M) K.DSPLDVIINDTGGVK.Q R.AAALNIVPTSTGAAK.A K.TFAEEVNAAF.R

Table 17 (Continued)

Spot no.	Accession number	Protein name	Organism	Theoretical MW (Da)	pI	Score	Peptide match	% Coverage	Sequences
88	gi 356549501	Probable cinnamyl alcohol dehydrogenase 1-like	<i>Glycine max</i>	38616	6.88	148	4	7	R.DASGVLSPYK.F R.YCFMIPK.S + Carbamidomethyl (C) R.YCFMIPK.S + Carbamidomethyl (C) ; Oxidation (M) K.EEALSLLGADK.F
89	gi 120658	Glyceraldehyde -3-phosphate dehydrogenase A	<i>Pisum sativum</i>	43312	8.80	72	2	6	R.AAALNIVPTSTGAAK.A K.AVALVPLTLK.G
90	gi 84453208	Putative cytosolic factor	<i>Trifolium pretense</i>	67827	4.72	130	4	7	R.OATNKALLOLDNYPEFVAK.Q K.ALQLLDNYPEFVAK.Q K.FVFAGPSK.S K.YIAPEQVPVQYGGLSR.E

Table 17 (Continued)

Spot no.	Accession number	Protein name	Organism	Theoretical MW (Da)	pI	Score	Peptide match	% Coverage	Sequences
91	gi 12230569	Superoxide dismutase [Cu-Zn], chloroplast	<i>Medicago sativa</i>	20813	6.02	38	1	6	R.ALVHELEDDLK.G
92	gi 302845553	Minichromosome maintenance protein 4	<i>Volvox carteri</i>	108095	6.11	23	1	2	R.MAQGASTGASGVSRTMLLTALR.Q
93	gi 632736	Pathogen- and wound-inducible antifungal protein	<i>f. nagariensis</i> <i>Nicotiana tabacum</i>	21907	8.40	54	1	6	+ 2 Oxidation (M) R.VTNTGTGAQTTVRI
94	gi 20341	CBP20 precursor Ribulose biphosphate carboxylase	<i>Oryza sativa</i>	19456	8.26	49	1	4	R.IIGFDNVR.Q

Table 17 (Continued)

Spot no.	Accession number	Protein name	Organism	Theoretical MW (Da)	pI	Score	Peptide match	% Coverage	Sequences
95	gi 28380082	Maturase K	<i>Adesmia lanata</i>	60976	9.04	52	1	3	R:QFISLEDAETIKSFNLR.S
96	gi 255543455	Glyceraldehyde -3-phosphate dehydrogenase	<i>Ricinus communis</i>	43087	8.14	621	15	31	K:VAINGFGR.I R:KDSPLDVIAINDTGGVK.Q [2] K:DSPLDVIAINDTGGVK.Q [2] R:NPANLPWK.D K:KVLITAPGK.G K:VLITAPGK.G R:AAALNIVPTSTGAAK.A [2] K:AVLVLPCLK.G K:TFEEVNAAFRE R:CTDVSSTVDSSLTMVMGDDMVK.V + Carbamidomethyl (C); 3 Oxidation (M) K:VIAWYDNEWGYSOR.V R:VVDLADIVANNWK.-

Table 17 (Continued)

Spot no.	Accession number	Protein name	Organism	Theoretical MW (Da)	pI	Score	Peptide match	% Coverage	Sequences
97	gi 255543455	Glyceraldehyde -3-phosphate dehydrogenase	<i>Ricinus communis</i>	43087	8.14	541	16	32	R:KDSPLDVIANDTGGVK.Q [3] K:DSPLDVIANDTGGVK.Q [2] R:NPANLPWK.D K:KVLITAPGK.G [2] K:VLITAPGK.G K:GTMTHSYTGDQR.L R:AAALNIVPTSTGAAK.A [2] K:AVALVLP.TLK.G K:TFEEVNAAFR.E R:CTDVSSTVSSSLTMVMGGDDMK.V + Carbamidomethyl (C); 3 Oxidation (M) K:VIAWYDNEWGYSQR.V R:VVDLADIVANINWK.-

Table 17 (Continued)

Spot no.	Accession number	Protein name	Organism	Theoretical		Score	Peptide match	% Coverage	Sequences
				MW (Da)	pI				
98	gi 5817720	Maturase -like protein	<i>Adesmia volckmannii</i>	61146	8.98	34	1	3	R.QFISSLEDAETIKSFNNLR.S
99	gi 1771248	Ribulose 1,5 biphosphate carboxylase large subunit	<i>Maackia amurensis</i>	50367	6.33	101	3	5	R.IPISYIK.T R.AVYECLR.G + Carbamidomethyl (C) R.EITLGFVDLLR.D
100	gi 75207006	Ferric leghemoglobin reductase	<i>Vigna unguiculata</i>	55745	8.08	81	2	4	K.IVSSSTGALALTEIPK.K R.TPFTAGLGLDKI
101	gi 75207006	Ferric leghemoglobin reductase	<i>Vigna unguiculata</i>	55745	8.08	164	5	10	K.FVSPSEYSVDTIDGGNTWK.G [2] K.IVSSSTGALALTEIPK.K R.TPFTAGLGLDKI K.AIDNAEGLVKI

Table 17 (Continued)

Spot no.	Accession number	Protein name	Organism	Theoretical MW (Da)	pI	Score	Peptide match	% Coverage	Sequences
102	gi 356500643	NADP-dependent glyceralddehyde-3-phosphate dehydrogenase	<i>Glycine max</i>	53217	6.76	167	5	11	K-SVSIINPTTR.K K.FLYSDSFPGNER.T K.GLINCVTGK.G + Carbamidomethyl (C) R.IAWEEPFPGVLPVIR.I R.GPDHFFPQGIK.D
103	gi 147797552	Hydrothetical protein VITISV_037210	<i>Vitis vinifera</i>	78877	6.01	36	1	1	R.IAYVEFFGVVWNR.D
104	gi 363807510	Uncharacterized protein LOC100775490	<i>Glycine max</i>	44109	6.57	157	5	12	R.AAVAWAEGKPLSLETIEVAPPQK.G K.ILFNSLCR.T + Carbamidomethyl (C) R.TDVVWMDAK.G R.TDIPGVVEK.Y [2]

Table 17 (Continued)

Spot no.	Accession number	Protein name	Organism	Theoretical MW (Da)	pI	Score	Peptide match	% Coverage	Sequences
105	g 363807510	Uncharacterized protein	<i>Glycine max</i>	44109	6.57	189	4	12	R.AAVAVEAGKPLSIETIEVAPPQK.G K.ILFNSLCR.T + Carbamidomethyl (C) R.TDVYWWDAK.G R.TDIPGWEEK.Y
		LOC100775490							
106	g 363807510	Uncharacterized protein	<i>Glycine max</i>	44109	6.57	81	3	10	R.AAVAVEAGKPLSIETIEVAPPQK.G K.ILFNSLCR.T + Carbamidomethyl (C) R.TDIPGWEEK.Y
		LOC100775490							
107	g 255585914	Alcohol dehydrogenase, putative	<i>Ricinus communis</i>	40718	6.37	93	2	4	R.IIGIDISK.K R.SQVPWLVDK.Y
108	g 255544626	Proteasome subunit alpha type, putative	<i>Ricinus communis</i>	25582	5.73	219	4	17	K.AANGVVIATEK.K K.EPIPVTQLVRE K.EGFEQISGK.N K.NIEIGIGADK.K

Table 17 (Continued)

Spot no.	Accession number	Protein name	Organism	Theoretical MW (Da)	pI	Score	Peptide match	% Coverage	Sequences
109	gi 255543455	Glyceraldehyde -3-phosphate dehydrogenase	<i>Ricinus communis</i>	43087	8.14	677	16	35	K.VAINGFGR.I R.KDSPLDVIAINDTGGVK.Q [2] K.DSPLDVIAINDTGGVK.Q [2] R.NPANLPWK.D K.KVLTAPGK.G K.VLITAPGK.G R.AALNIVPTSTGAAK.A K.AVALVPLTK.G K.TFAEEVNAAFRE K.GILSVCEPLVSVDFR.C + Carbamidomethyl (C); R.CTDVSSSTVDSSLTMVMGDDMWK.V + Carbamidomethyl (C); 3 Oxidation (M) K.VIAWYDNEWGYSQR.V R.WDLADIVANNWK- [2]

Table 17 (Continued)

Spot no.	Accession number	Protein name	Organism	Theoretical MW (Da)	pI	Score	Peptide match	% Coverage	Sequences
110	gi 255543455	Glyceraldehyde -3-phosphate dehydrogenase	<i>Ricinus communis</i>	43087	8.14	495	10	25	K.VAINGFGR.I K.DSPLDVIAINDTGGVK.Q R.NPANLPWK.D K.KVLITAPGK.G K.VLITAPGK.G R.AAALNIVPTSTGAAK.A K.AVALVPLTLK.G K.TFAEEVNAAFR.E K.VIAWYDNEWGYSOR.V R.VVDLADIVANINWK.-
111	gi 255543455	Glyceraldehyde -3-phosphate dehydrogenase	<i>Ricinus communis</i>	43087	8.14	677	16	35	K.VAINGFGR.I R.KDSPLDVIAINDTGGVK.Q [2] K.DSPLDVIAINDTGGVK.Q [2] R.NPANLPWK.D K.KVLITAPGK.G K.VLITAPGK.G R.AAALNIVPTSTGAAK.A

Table 17 (Continued)

Spot no.	Accession number	Protein name	Organism	Theoretical MW (Da)	pI	Score	Peptide match	% Coverage	Sequences
111	gij255543455	Glyceraldehyde -3-phosphate dehydrogenase	<i>Ricinus communis</i>	43087	8.14	677	16	35	K.AVALVLP TLK.G K.TFAEEVNAAFRE K.GILSVCEPLVSVDFR.C+ Carbamidomethyl (C); R.CTDVSSSTVDSSLTMVMGDDMVK.V+ Carbamidomethyl (C); 3 Oxidation (M) K.VIAWYDNEWGYSQR.V R.VVDLADIVANNWK.- [2]
112	gij3023814	Glyceraldehyde -3-phosphate dehydrogenase	<i>Craterostigma plantagineum</i>	36454	7.06	93	1	4	K.IVAWYDNEWGYSR.V
113	gij255543455	Glyceraldehyde -3-phosphate dehydrogenase	<i>Ricinus communis</i>	43087	8.14	395	9	25	K.VAINGFGR.I K.DSPLDVAINDTGGVK.Q R.IPANLPWK.D K.IKVLITAPGK.G R.AAALNIVTSTGAAK.A K.AVALVLP TLK.G

Table 17 (Continued)

Spot no.	Accession number	Protein name	Organism	Theoretical MW (Da)	pI	Score	Peptide match	% Coverage	Sequences
113	gi 255543455	Glyceraldehyde -3-phosphate dehydrogenase	<i>Ricinus communis</i>	43087	8.14	395	9	25	K.TFAEEVNAAFRE K.VIAWYDNEWGYSQR.V R.VVDLADIVANNWK.-
114	gi 56796254	Glyceraldehyde -3-phosphate dehydrogenase	<i>Phaseolus vulgaris</i>	5668	4.31	58	1	39	K.GILGFTDEDVSTDFVGD5RS
115	gi 357437219	NADP-dependent glyceraldehyde-3- phosphate dehydrogenase	<i>Medicago truncatula</i>	53275	8.12	256	8	15	K.APIAECLVK.E + Carbamidomethyl (C) K.DAVTEVVR.S R.SGDLYSYCAEEGVR.I + Carbamidomethyl (C) K.FLVSDSFFPNER.T [2] K.GGFSYSGQR.C K.GATFCQEYR.R + Carbamidomethyl (C) K.DSGIGSOGITNSINMMTK.I + 2 Oxidation (M)

Table 17 (Continued)

Spot no.	Accession number	Protein name	Organism	Theoretical MW (Da)	pI	Score	Peptide match	% Coverage	Sequences
116	gi 356531939	Putative lactoylglutathione lyase-like	<i>Glycine max</i>	33451	6.14	259	7	23	R.FLHVYR.V K.FYTECFGMK.L + Carbamidomethyl (C) K.FYTECFGMK.L + Carbamidomethyl (C) ; Oxidation (M) K.DPDGYAFELIQR.S K.GNAYAOVAIGTDDVYK.S K.SAEVNVITQELGGK.I K.TVLVDNQDFLKE
117	gi 557532497	Hypothetical protein CICLE_v10012559mg	<i>Citrus clementina</i>	27352	6.11	111	2	7	R.VFQIEYAAK.A K.VPDELLEAK.A

Table 18 Changes and differences in tubers by Image Master 2-DE program

Protein ID	The terms in the ratio of summer/winter		The terms in the ratio of rainy season/winter	
	<i>p</i> -value	Fold	<i>p</i> -value	Fold
1	0.69	1.08	0.04	1.31
3	0.40	0.87	0.02	0.62
5	0.04	0.72	0.54	0.91
7	0.18	1.54	0.02	2.86
8	0.02	0.44	0.19	0.71
16	0.01	1.89	0.54	0.84
28	0.01	1.89	0.69	1.09
29	0.00	2.32	0.07	2.00
30	0.03	1.93	0.06	2.49
32	0.11	1.18	0.00	1.50
36	0.01	0.66	0.97	1.01
37	0.00	1.88	0.07	1.61
39	0.28	1.63	0.01	1.50
42	0.02	0.41	0.23	1.24
43	0.01	0.55	0.50	1.08
44	0.03	0.70	0.15	0.67
45	0.09	0.42	0.98	1.01
47	0.05	0.71	0.28	1.13
48	0.04	0.54	0.26	1.31
51	0.01	0.44	0.08	1.36
53	0.21	0.63	0.22	0.65
55	0.16	0.50	0.13	0.44
56	0.00	2.13	0.11	2.05
58	0.02	0.61	0.27	1.29
59	0.10	0.70	0.29	1.23
62	0.45	1.33	0.02	1.77
65	0.68	0.95	0.54	0.89
66	0.16	1.48	0.23	1.47
69	0.70	0.94	0.01	1.88
71	0.12	0.48	0.85	0.95
74	0.01	0.57	0.44	0.80
75	0.17	0.81	0.13	1.78

Table 18 (Continued)

Protein ID	The terms in the ratio of summer/winter		The terms in the ratio of rainy season/ winter	
	p-value	Fold	p-value	Fold
76	0.15	1.36	0.01	1.94
77	0.00	0.21	0.01	0.56
78	0.06	0.53	0.06	2.21
82	0.67	0.91	0.66	1.08
83	0.44	1.17	0.06	1.46
90	0.09	0.63	0.08	0.60
91	0.26	0.77	0.12	0.65
93	0.04	0.57	0.96	0.98
94	0.05	1.93	0.09	1.77
95	0.22	1.35	0.39	1.34
96	0.01	3.22	0.12	2.53
99	0.67	0.91	0.77	1.08
100	0.27	0.69	0.50	0.78
101	0.80	1.13	0.44	1.44
102	0.43	0.84	0.35	1.49
104	0.09	0.50	0.09	0.50
105	0.02	0.58	0.02	0.61
106	0.13	0.78	0.17	0.72
107	0.83	1.05	0.12	2.43
110	0.00	2.07	0.08	2.17
115	0.01	0.54	0.00	0.45
116	0.04	0.66	0.11	0.76
117	0.01	1.92	0.04	2.72
122	0.58	1.12	0.02	0.72
123	0.94	1.02	0.04	1.68
139	0.13	0.56	0.23	2.29
140	0.27	0.86	0.04	2.06
141	0.07	1.53	0.14	1.90
143	0.02	2.02	0.01	3.11
148	0.00	10.78	0.74	0.87
157	0.01	5.02	0.50	1.23
158	0.01	1.62	0.05	0.62
159	0.45	0.67	0.16	1.82

Table 18 (Continued)

Protein ID	The terms in the ratio of summer/winter		The terms in the ratio of rainy season/winter	
	<i>p</i> -value	Fold	<i>p</i> -value	Fold
168	0.01	8.07	0.01	2.06
169	0.05	5.18	0.15	1.80
172	0.57	1.24	0.98	0.99
186	0.01	1.99	0.01	4.88
127	0.05	0.45	0.23	1.28
132	0.06	0.71	0.03	0.72
133	0.27	0.75	0.34	0.76
144	0.40	1.27	0.12	1.85
145	0.16	0.73	0.13	1.32
150	0.00	1.88	0.01	1.32
165	0.01	1.86	0.01	2.12
208	0.00	5.05	0.14	4.39
134	0.07	0.27	0.14	0.54
135	0.96	1.02	0.87	0.93
185	0.91	0.97	0.89	0.94

Table 19 Changes and differences in leaves by Image Master 2-DE program

Protein ID	The terms in the ratio of summer/winter		The terms in the ratio of rainy season/winter	
	<i>p</i> -value	Fold	<i>p</i> -value	Fold
1	0.19	0.66	0.49	1.15
8	0.37	2.25	0.13	3.66
23	0.01	2.24	0.11	1.21
25	0.14	0.68	0.02	0.41
27	0.06	1.97	0.00	1.81
28	0.98	1.00	0.03	0.75
29	0.91	0.97	0.18	0.64
30	0.02	0.41	0.01	0.32
36	0.27	0.79	0.02	0.43
37	0.19	1.62	0.01	0.56
41	0.67	0.93	0.04	2.14
42	0.90	1.03	0.60	0.84
43	0.27	1.53	0.15	0.57
44	0.02	1.51	0.93	0.96
45	0.01	2.36	0.32	2.66
47	0.10	3.40	0.14	1.83
48	0.20	1.45	0.37	1.44
55	0.57	1.76	0.28	1.40
60	0.95	1.03	0.00	2.98
61	0.39	0.79	0.17	0.72
62	0.00	2.66	0.60	1.15
63	0.02	2.37	0.69	0.93
64	0.02	4.35	0.77	0.92
66	0.07	2.17	0.00	1.85
71	0.67	1.14	0.15	1.41
82	0.67	1.25	0.00	3.36
87	0.04	3.73	0.29	1.90
109	0.93	1.03	0.00	3.90
112	0.94	1.03	0.05	0.40

VITA

Miss Chonchanok Leelahawong was born on October 22th, 1984 in Bangkok, Thailand. She graduated with a Bachelor of Science in Microbiology, Faculty of Science, Silpakorn University in 2005. Also, she received a Master's degree of Science in 2009. She has studied in the Graduate school, Faculty of Science, Chulalongkorn University to the Doctor of Philosophy program in Biotechnology during 2010-2016. She was supported by a research grants for her doctoral thesis from National Research University, the Science for Local Project under the Chulalongkorn University Centenary Academic Development Plan (2008-2012) and the 90th Anniversary of Chulalongkorn University fund (Rathadaphiseksomphot Endowment Fund) (1/2014). She had coordinated research with the laboratory of Biochemistry, Chulabhorn Research Institute.



